GAS HOLD-UP AND MIXING IN BUBBLE COLUMNS CONTAINING TWO OR MORE PHASES

by

MOHAMMAD JAMIALAHMADI

Being a Thesis Submitted in Support of an Application for the Degree of Doctor of Philosophy

The University of Aston
in Birmingham

March 1982

Gas Hold-up and Mixing in Bubble Columns Containing Two or More Phases

M. Jamialahmadi Ph.D. Thesis 1982

SUMMARY

The bubble column is a device in which gas is bubbled through a column of liquid: it can be used to promote the chemical or biochemical transformation of matter through the action of catalysts or micro-organisms suspended in the liquid phase. The motion of such "solid" phases often has a strong influence on the performance of a bubble column, and in particular, on mass transfer, diffusion and reaction steps. Following a comprehensive literature review that highlighted the need for a systematic study of such systems, experiments were carried out in two and three dimensional bubble columns. The experimental programme has been developed by considering what happens on the molecular level in gas-liquid and gas-liquid-solid systems. This approach has also been used when discussing the experimental data.

(a) Air-Water Systems

The effect of superficial gas and liquid velocity, liquid phase temperature and liquid phase agitation on gas hold-up, bubble coalescence and break-up have been analysed. Gas and liquid phase flow patterns have been examined and, from these, the effect of column height and column diameter on gas hold-up have been more fully understood. A new kind of gas distributor for minimising bubble coalescence has been developed.

(b) The Gas Phase

The effect of the physical properties of the gas phase on gas hold-up have also been examined using the following gases: N_2, O_2, CO_2, NH_3 and air; the results have been analysed by considering phase properties at the molecular level.

(c) Air-Water Systems with Various Additives

The effect of soluble alcohols (C_1-C_3), non-soluble alcohols (C_4-C_8), inorganic salts (in particular KCl, NaCl and KI) and liquid phase viscosity on gas hold-up and bubble coalescence have been experimentally observed, and the results have been analysed by considering molecular behaviour in the bulk phases and at interfaces between phases.

(d) Three-Phase Systems

The effects of particle size, density, wettability and concentration on gas hold-up and bubble coalescence have been studied. Variations in the solid phase concentrations in both the axial and radial directions and liquid and solid phase dispersion coefficients have been measured. As a result of these measurements, we now have a better understanding of the behaviour of the solid phase in bubble columns.

(e) Four-Phase Systems

Some experiments have been carried out in four-phase systems, and the effects of superficial gas velocity and solids concentration on gas hold-up have been determined.

(f) Single Slug Velocity Measurements

Finally, in order to find out how different liquids and solid suspensions affect the rise velocity of bubbles, the velocities of single slugs in different systems have been studied.

Keywords: Gas-Holdup Liquid-mixing Solids-mixing Bubble-column

List of Contents

List of Figures

Acknowledgements

The author of this thesis wishes to express his thanks to:

(1) Dr. E.L. Smith for all the invaluable help and guidance received, as well as for the patience and enthusiasm shown at times of difficulty.

(2) Dr. M. Fidgett for his invaluable advice.

(3) Ms. K.A. Murphy for her assistance in presenting the diagrams.

1 Introduction

1.1 Background to the Project

A research group at the University of Aston in Birmingham has been concerned with what may be termed "biotechnology" for a number of years. The group is composed of chemical engineers headed by Dr. E.L. Smith and microbiologists supervised by Dr. R.N. Greenshields. The microbiologists in the group are mostly concerned with the applications of bubble columns, in particular for beer and alcohol fermentations, and biomass - and metabolite - production using moulds and bacteria. The engineering aspects of the research, that is to say design, scale-up and operation of tower fermenters for both aerobic and anaerobic processes, have been carried out mainly in the author's department.

The overall engineering research programme has been divided into the following sub-projects:

1. Properties of suspensions of micro-organisms;
2. behaviour of single bubbles in suspensions of micro-organisms;
3. behaviour of bubble swarms in tower fermenters;
4. properties of microbial aggregates and their behaviour in tower fermenters;
5. mass-and heat-transfer studies in gas-liquid systems in towers, and
6. development of mathematical models to aid in the design, scale up and operation of tower fermenters.

The author's research has been concerned with meeting some of the objectives of sub-project 4. The behaviour of microbial aggregates in a gas-liquid system has a strong influence on the performance of a bubble column fermenter, and, in particular, mass-transfer, diffusion and reaction steps are greatly affected by microbial hydrodynamics. The original objective of this work was to study the effect of microbial aggregates on fermenter behaviour using small and light plastic particles to simulate the solid (microbial) phase.

It is well known that the study of two - or more - phase systems in bubble columns is very complicated because different phases with different properties and flow patterns exist. Therefore, in order to avoid doing experiments based only on a trial and error approach the author, as in the case of many scientific and engineering studies, developed the programme in the following way. Firstly, a period of time was spent in making general observations and accumulating facts relevant to each individual phase before attempting to predict what would happen when the different phases came into contact. This was followed by a period of analysis of actual flow mechanisms and developments in theoretical understanding. The third stage, that of empirical correlation, was to have been started after a good understanding of the effect of different parameters and physical properties on the behaviour of the system had been acquired: however,

because of the complexity of the system, this was not completed.

At the outset, it was intended that initial studies with air-water systems (it should be noted that the studies in this area have previously been undertaken by Downie (1) and Shayegan Salek (2) in this University) would be followed by research with air-water-solid suspensions. After completing a series of gas hold-up measurements over a wide range of superficial gas and liquid velocities (which was accompanied by a literature review on gas-liquid systems) it became clear that the behaviour of the apparently simple air-water system was not easy to understand. In addition, an extensive literature survey indicated that most investigators, before fully understanding the effects of different parameters and the physical properties of each phase on the performance of the system had attempted to present empirical correlations. Consequently, in spite of the large number of such correlations to be found in the literature, there was still a lack of consistent information about the effects of the nature of the gas phase, dissolved salts (which are usually part of a fermentation culture medium), alcohols (which are metabolic products), the physical properties of the liquid phase and the column geometry on the performance of bubble columns. Therefore, the original experimental programme was expanded to include a systematic study of (i) gas-liquid systems with and without liquid phase additives (ii) the effect of the gas phase on gas hold-up, and (iii) gas-liquid-solid systems (some containing

two liquid phases).

1.2 Scope of the Present Work

1.2.1 Air-Water Systems

In the first part of the work we analysed each individual phase - air and water - on the molecular scale and then we considered what happens when these phases come into close contact. From these analyses we found that heating, agitation and vibration are among the main parameters which affect gas hold-up. The effect of a wide range of water temperatures on gas hold-up has been studied, and the effect of liquid-phase agitation on gas hold-up has been elucidated by some simple experiments and by analysing the results of other researchers. The effect of vibration has also been analysed using the findings of other researchers; the author himself has not done any experiments in this area.

In order to get some idea about the liquid - and gas - phase flow patterns, some mixing studies using an unsteady-state tracer technique have been performed in the liquid phase, and, for the gas phase qualitative results were obtained from visual observations and high-speed photography.

Finally, the effect of column diameter and column height have been analysed. Based on the above results, different methods for suppressing bubble coalescence have

been proposed. A new kind of gas distributor which makes it possible to operate in the bubbly -flow regime at superficial gas velocities up to 9 cm/s has been developed.

1.2.2 The Effect of the Nature of the Gas Phase on Gas Hold-up

In this part of the research programme, we considered the interface between the gas and liquid phases from the gas-side; different gases with different levels of polarity have been used in experiments to show the importance of the "compatability" of the gas and liquid phases. Finally, the liquid phase (i.e. water) was replaced by kerosine (which is totally non-polar), and the effects of different gases on gas hold-up in this new system were analysed.

1.2.3 The Effect of Additives in the Liquid Phase

After completing work with gas-liquid systems, a comprehensive study was carried out to find out how organic materials with different physical properties (i.e. solubility in water, polarity, surface tension and viscosity) affect gas hold-up. Ionic salt solutions were also used to clarify how the formation of strong adhesive

forces in the bulk of the liquid phase affects gas hold-up. Finally, gas hold-up was measured in concentrated solutions of potassium chloride in order to see how the bubble size, and consequently gas hold-up, varies if the surface tension at the interface between air and water increases significantly above 72 dynes/cm (the figure for pure water).

1.2.4 Three-Phase Systems

Three-phase fluidisation is a method in which gas, liquid and solid phases can be brought into contact by the upward cocurrent flow of the fluid phases through a bed of solid particles. This operation, although of recent origin, has found many industrial applications, such as the H-coal process (3) for the conversion of coal to liquid fuels, the Fischer-Tropsh synthesis (as described by Benson et al. (4)), effluent treatment and fermentation (5,6) and processes in the petroleum industry (7,8,9). A literature survey (see section 2.1) revealed that despite a large number of theoretical and experimental studies made in this area important aspects of the gas-liquid fluidisation of solids are not fully understood.

The objective of this section in the thesis is to look in more detail at different aspects of three-phase systems (especially those with light particles) and more

emphasis than hitherto is given to solid-phase properties. Investigations have been carried out with three-phase systems in which the surface properties, densities and sizes of the solid phase have been varied and using a range of operational conditions.

1.2.5 Radial Non-Uniformity of the Solid Phase and Mixing in Three Phase Systems

Researchers have generally assumed that solids are uniformly distributed over the cross-section of a column, and, in view of this, the author decided to assess the relative magnitude of the solids concentration gradient over the column cross-section prior to any study of mixing. The unsteady state tracer technique was employed to study mixing of the liquid and solid phases. We obtained both qualitative results (based on visual observations) and quantitative results evaluated from the residence time distribution (RTD) of tracers.

1.2.6 Four-Phase Systems Study

In most fermentation processes, four phases are present, these being gas, an organic liquid, an aqueous solution, and micro-organisms. Although the study of four-phase systems is much more complex than of two-and

three-phase systems, the author has carried out some systematic investigations with four-phase systems containing completely miscible, partly miscible, or non-miscible liquids.

1.2.7 Single Slug Velocity Measurements

In order to determine how different liquids or solids with different physical properties affect the rising velocity of a single slug, measurements have been made with a variety of systems. The results are related to those in earlier sections.

1.3 Thesis Outline

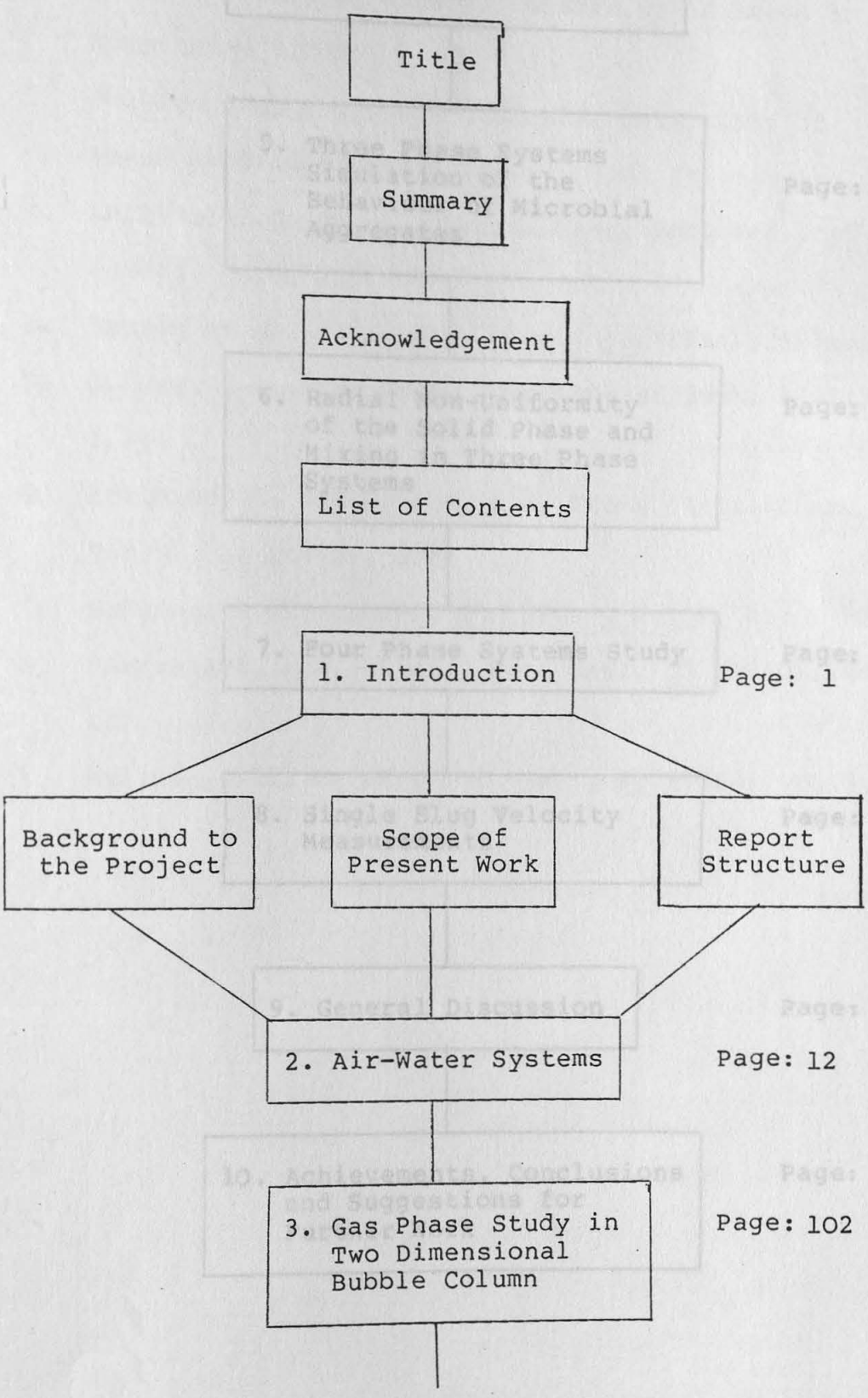

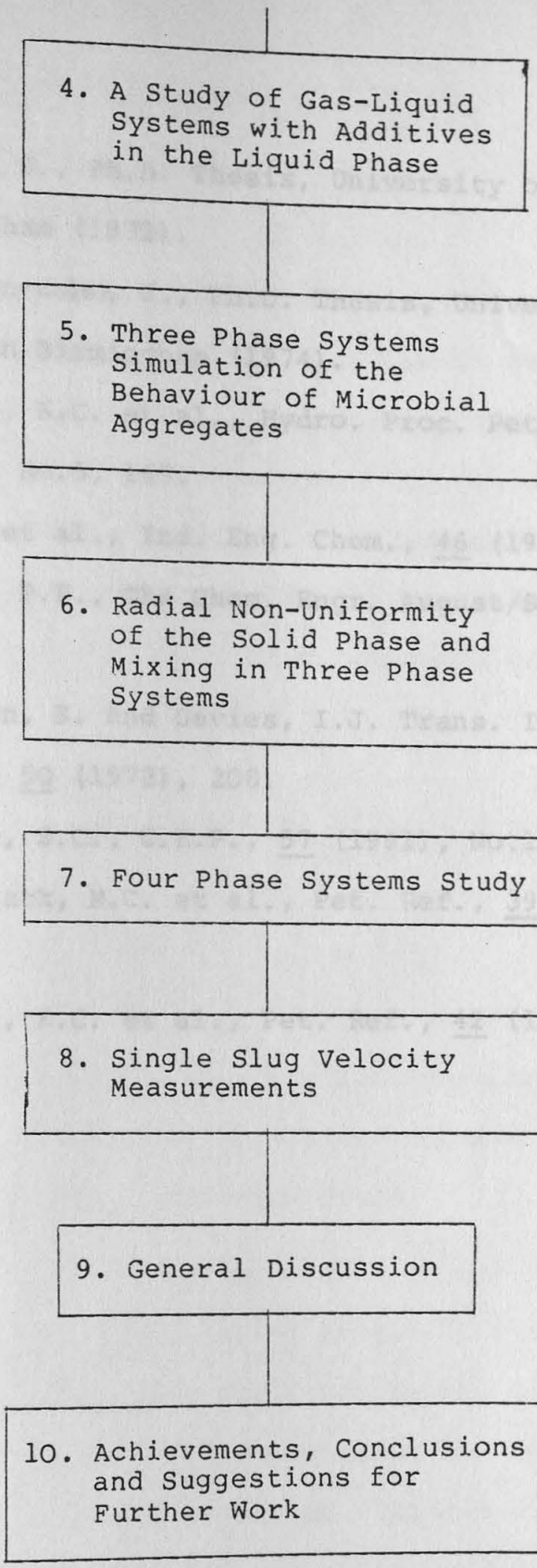
4. A Study of Gas-Liquid Systems with Additives in the Liquid Phase
Page: 121
5. Three Phase Systems Simulation of the Behaviour of Microbial Aggregates
Page: 169
6. Radial Non-Uniformity of the Solid Phase and Mixing in Three Phase Systems
Page: 223
7. Four Phase Systems Study
Page: 249
8. Single Slug Velocity Measurements
Page: 263
9. General Discussion
Page: 273
10. Achievements, Conclusions and Suggestions for Further Work
Page: 289

References

1. Downie, J., Ph.D. Thesis, University of Aston in Birmingham (1972).
2. Shayegan-Salek, J., Ph.D. Thesis, University of Aston in Birmingham (1974).
3. Hellwig, K.C. et al., Hydro. Proc. Pet. Ref., 45 (1966), No.5, 165.
4. Benson et al., Ind. Eng. Chem., 46 (1954), 2278.
5. Cooper, P.F., The Chem. Engr. August/Sept. 1981, p.343.
6. Atkinson, B. and Davies, I.J. Trans. Inst. Chem. Engrs., 50 (1972), 208.
7. Schuman, S.C., C.E.P., 57 (1961), No.12, 49.
8. Chervenack, M.C. et al., Pet. Ref., 39 (1960), No.10, 151.
9. Hellwig, K.C. et al., Pet. Ref., 42 (1963), No.5, 121.

2 Air-Water Systems

2.1 Literature Survey

2.1.1 Introduction

The volume of bubbles retained within the gas-liquid dispersion in a bubble column is referred to as the gas hold-up: it is an important parameter because it is used with other parameters for calculating mixing coefficients, mass transfer coefficients and chemical reaction rates. Average gas hold-up is obtained as the volume fraction of gas within the total volume of the system;

$$\varepsilon = \frac{(\text{Total volume}) - (\text{Liquid volume at rest})}{(\text{Total volume})}$$

$$= \frac{(V_{Tot} - V_L)}{V_{Tot}} \quad ;$$

The point or local volumetric gas fraction is also used, and this can be viewed as a time-averaged value at a particular point in the flow field.

Because of the importance of gas hold-up in bubble columns, an extensive amount of work by different investigators has been published in the literature. The aim of this chapter is to summarise the work on gas hold-up and bubble coalescence. To aid understanding, information is presented under the headings: effect of operational parameters, effect of column geometry, empirical correlations, bubble coalescence and liquid phase mixing.

2.1.2 Effect of Operational Parameters

In this section the effect of superficial gas and liquid velocity will be surveyed.

Effect of Superficial Gas Velocity, U_{sg}

One of the correlations which is presented by most investigators is that of gas hold-up as a function of superficial gas velocity. In spite of the fact that the results of various researchers are not always in good agreement, it is well known that a swarm of bubbles rises uniformly within a bubble column when the superficial gas velocity is low (usually less than 3 to 4 cm/s) and when bubbles of uniform size are generated at the gas distributor; this is the so called "bubbly-flow regime". When the gas velocity is increased (above 3-4 cm/s) bubbly flow ceases to be uniform and so called "turbulent flow" commences. In the bubbly flow regime gas hold-up increases almost linearly with superficial gas velocity and then tends to level off at higher velocities as turbulent flow sets in. Yamashita and Inoue (1) are some of the few workers to show that the gas hold-up may pass through a maximum with increasing gas flow rate: this peak, which appears to correspond to the transition point from bubbly to turbulent flow, has also been detected by Aoyama et al. (2) and Deckwer et al. (3) for air-water systems.

Gas hold-ups have been measured by different investigators under widely different conditions: these are summarised in Table 2.1.

Table 2.1 - Experimental Data Available in the Literature for Air-Water Systems.

Reference	Type of Flow	Superficial Velocities cm/s	Column Diameter cm	Column Height cm
Fair et al. (3)	Cocurrent	U_{sg} 10 U_{sl} 0.5	45.7 & 10.67	305
Niklin et al. (4)	Cocurrent & Countercurrent	U_{sg} 1100 U_{sl} 200	2.6	579
Braulick et al. (5)	Batchwise	U_{sg} 22 U_{sl} = 0	15;10 30.1;60	152
Akita and Yoshida (6)	Batchwise	U_{sg} 25 U_{sl} = 0	7.7;15.2; 30.1;60	90 to 350
Towell et al. (7)	Cocurrent	U_{sg} 30 U_{sl} 1.5	40.6;10.5	152;275
Hughmark (8)	Cocurrent	U_{sg} 30 U_{sl} 12	2.5;5.1;10	-
Reith et al. (9)	Cocurrent & Countercurrent	U_{sg} 45 U_{l} 2	14;29;50.8	152 to 380
Van Dierendonck et al. (10)	Cocurrent	U_{sg} 40 U_{sl} 3	14;60	
Aoyama et al. (2)	Cocurrent	U_{sg} 8 U_{sl} .623	5;10	
Voyer and Miller (11)	Cocurrent	10 U_{sg} 83 0.5 U_{sl} 3	140	20.5 to 238
Freedman and Davidson (12)	Batchwise & Cocurrent	U_{sg} 11 U_{sl} variable	23,61	305;427
Kunugita et al. (13)	Batchwise	0.76 U_{sg} 8 U_{sl} = 0	5	100
Kato & Nishiwaki (14)		U_{sg} 30 0.5 U_{sl} 1.5	21.4;12.2; 6.6	405;200;201

Akita & Yoshida (15)	Cocurrent & Countercurrent	0.5	U_{sg}	42	15.2;30.1; 60	400
		U_{sl}	4.5			
Deckwer et al. (16)	Cocurrent	U_{sg}	15		15;20	440;723
		U_{sl}	10			
Stanley et al. (17)	Batchwise	U_{sg}	30		4	11
		U_{sl} = 0				
Kastanek et al. (18)	Batchwise	U_{sg}	30		15;30	60 to 120
		U_{sl} = 0				
Yamashita et al. (1)	Batchwise	U_{sg}	30		30 x 1	107
		U_{sl} = 0				
Fissa and Schugerl (19)	Cocurrent & Countercurrent	U_{sg}	6		15.9	390
		U_{sl}	1.4			
Pexidr and Charpentier (20)	Countercurrent	U_{sg}	4		10	175
		U_{sl}	1.8			
Kawagoe et al. (21)	Cocurrent	U_{sg}	50		10.5	
		U_{sl}	3.9			
Koetsier et al. (22)	Batchwise	U_{sg}	10		5	60
		U_{sl} = 0				
Kumar et al. (23)	Batchwise	U_{sg}	14		5;7.5;10	
		U_{sl} = 0				
Todt et al. (24)	Cocurrent & Countercurrent	0.7	U_{sg}	10.7	14	380;440
		0.7	U_{sl}	2.4		
Schugerl & Lugke (25)	Cocurrent	U_{sg}	8		14	400
		U_{sl}	2.2			
Hsu et al. (26)	Cocurrent	.349	U_{sg}	3.46	7.6	
		.06	U_{sl}	0.476		
Hills (27)	Cocurrent	7	U_{sg}	350	15	1050
		U_{sl}	27			
Koide et al. (28)	Batchwise	U_{sg}	13		550	700
		U_{sl} = 0				
Hikita et al. (29)	Batchwise	4.2	U_{sg}	38	10	150
		U_{sl} = 0				
Botton, R. and Cosserat (98)	Cocurrent	U_{sg}	1400		2,7.5,25, 48	320
		U_{sl}	5			

Effect of Superficial Liquid Velocity, U_{sl}

Wide discrepancies surround the experimental results on the effect of liquid flow rate on gas hold-up. Several workers (6,9,14,15,23,25,30,31) claim to have found no effect of liquid flow rate on gas hold-up, while Towell et al. (7), Todt et al. (24), Kim et al. (32) and Kasturi and Stepanek (34) found gas hold-up increased with increasing liquid velocity. Shayegan Salek (33) suggested that increases in liquid-phase velocity cause a quicker wash-out of the gas phase with a consequent reduction in gas hold-up: Ostergaard and Michelsen (35), Hills (27) and Downie (38) also reported that an increase in liquid velocity caused a reduction in gas hold-up.

2.1.3 Effect of Column Geometry

Column Diameter

There are extensively reported studies in the literature on the determination of gas hold-up in columns ranging from 2.5 cm to 550 cm in diameter. This parameter was included in the projects of Shayegan Salek (33) and Downie (38) of this University; literature surveys and references are fully detailed in their works. They studied the effect of column diameter on gas hold-up in four different columns (7.6, 15.2, 30.5 and 61 cm) and concluded that as the column diameter increases the gas hold-up decreases at a fixed value of superficial gas velocity.

The data reported by Ellis (36) indicated that wall effects increase gas hold-up at diameters up to 7.5 cm and for diameters greater than 7.5 cm gas hold-up is independent of the diameter; this has been confirmed by Freedman and Davidson (12), but Fair et al. (3) and Yoshida (6) found no effect of column diameter when this exceeded 15 cm.

Reith et al. (9) observed much lower hold-ups for larger columns, and Hills (27) also concluded that the gas hold-up is dependent on the column diameter. Recently, Koide et al. (28) have studied gas hold-up in a large bubble column (550 cm): they concluded that the influence of column diameter on average gas hold-up was almost the same as that in a small sized bubble column; this view has been confirmed by Kumar et al. (23) and more recently by Hikita et al. (29).

The interested reader might also consult the papers of Kato and Nishiwaki (14), Shulman and Molstad (37), Argo and Cova (31) and Oki and Inoue (39). It is clear that there is some confusion about the effect of column diameter, and this highlights the need for a deeper understanding of fluid flow and mixing within bubble columns.

Effect of Column Height

Bridge et al. (40) reported a 12% increase in gas hold-up at the top of a column operated counter-currently, but Sideman et al. (41) observed no difference when operating co-currently.

Yoshida and Akita (6) found that column height does not have a marked effect on gas hold-up. However, they suggested that for heights of less than 100 cm end-effects might have an important influence on results. This view is supported by Towell et al. (7), who reported that columns of different lengths exhibited the same effects at the ends of the column but with an extended middle section.

Fair et al. (3) concluded that, although the local value of gas hold-up can vary somewhat with height, the dependence of average gas hold-up on height is not marked. This was confirmed by Bhaga and Weber (57).

Deckwer et al. (16), who carried out experimental work on two tall columns (440 and 723 cm in height), concluded that liquid height does not effect the hold-up.

The effect of the initial heights of clear liquid on gas hold-up was also studied by Kawagoe et al. (21): they observed gas hold-up to decrease when the initial liquid height increased.

2.1.4 Empirical Correlations

Let us now consider some of the empirical correlations and models which have been developed for air-water systems. Prior to 1973, these were summarised by Shayegan Salek (33) and Downie (38) of this University: consequently, the following section is mainly restricted to a review of work in the intervening period.

Bhaga and Weber (42) in the case of gas and liquid flow derived the following equation:

$$\frac{\langle U_{sg} \rangle}{\langle \varepsilon_g \rangle \langle 1-\varepsilon_g \rangle^{n+1}} = C_2 \frac{\langle U_{sg} + U_{sl} \rangle}{\langle 1 - \varepsilon_g \rangle^{n+1}} + K_2 U_\infty \qquad (2.1)$$

where:

C_2 = distribution parameter $= \dfrac{\langle \varepsilon_g (U_{sg}+U_{sl}) \rangle}{\langle \varepsilon_g \rangle \langle U_{sg}+U_{sl} \rangle}$

K_2 = terminal velocity coefficient =

$$\frac{\langle \varepsilon_g (1-\varepsilon)^{n+1} \rangle}{\langle \varepsilon_g \rangle \langle 1-\varepsilon_g \rangle^{n+1}}$$

$\langle\rangle$ = average value

n = exponent which depends on the bubble size and flow regime and can be determined experimentally.

The equation of Bhaga and Weber is in a generalised form and can be reduced to those of previous investigators by

neglecting the effect of non-uniform flow and concentration profiles or assuming different values for n or both.

Lockett and Kirkpatrick (43) correlated their results in terms of the Richardson-Zaki equation for solid particles (44) multiplied by an empirical correlation factor, $f(\varepsilon)$, to take account of bubble deformation: the latter was assumed to increase with bubble concentration. They reported that

$$U_{cg} = U_{bo}\ \varepsilon_g\ (1-\varepsilon_g)^n . f(\varepsilon) \qquad (2.2)$$

where

$$f(\varepsilon) = 1 + 2.55\ \varepsilon_g^3 \qquad (2.3)$$

Yamashita and Inoue (1) have given the following relationships between εg and U_{sg} for three and two-dimensional bubble columns:

For three-dimensional columns

$$\varepsilon_g = U_{sg}/(2.2\ U_{sg} + 0.3\ \sqrt{g\ d}), \qquad (2.4)$$

and for two-dimensional columns:

$$\varepsilon_g = U_{sg}/(2.2\ U_{sg} + 0.4\ (\sqrt{g\ d_e}) \qquad (2.5)$$

Here, d_e is the equivalent column diameter.

Hills (27) measured gas hold-up in a bubble column 15 cm in diameter and 1050 cm in height at superficial gas velocities of 7-350 cm/s and superficial liquid velocities of 0-27 cm/s. After excluding end-effects and correcting for liquid inertia and wall friction, his results were correlated by the following equations:

$$U_{sg}/\varepsilon_g = 0.24 + 1.35\ U_T^{0.93} \quad \text{for } U_{sl} > 30 \text{ cm/s} \tag{2.6}$$

and

$$U_s = 0.24 + 4\ \varepsilon_g^{1.72} \quad \text{for } U_{sl} < 30 \text{ cm/s} \tag{2.7}$$

where $U_T = U_{sg} + U_{sl}$ is total flow velocity.

Ueyama and Miyauchi (45) recently extended the work of Nicklin (99) and Yoshitome (68) for uniformly rising bubbles to the turbulent or recirculating flow regime and derived the following equation:

$$\varepsilon_g = \frac{1}{2}\left(\frac{1+\alpha}{1-\beta}\right)\left(1 - \sqrt{1-4\left(\frac{\alpha}{1+\beta}\right)\left(\frac{1-\alpha}{1+\beta}\right)}\right) \tag{2.8}$$

where $\alpha = \dfrac{U_{sg}}{U_s}$, $\beta = \dfrac{d^2 g}{192 V_t U_s}$ with $U_{sl} = 0$.

2.1.5 Bubble Coalescence

The loss of interfacial area caused by bubble coalescence is important in mass transfer equipment

such as bubble columns, whilst the coalescence-dependent transition between the bubbly and turbulent flow regimes is important in two-phase flow in pipes. In spite of considerable research, however, the mechanism of bubble coalescence is still unclear.

Most previous studies can be classified into the following broad categories.

(1) Coalescence in bubble columns where the gas distributor has a dominant influence on coalescence, large bubbles originating at the gas distributor.

The formation of large bubbles at the distributor can occur by more than one mechanism. An increase in gas flow rate, while the bubbles are forming in the constant frequency regime, causes the bubble size to increase (46). If the gas flow becomes turbulent through the holes in the distributor, large bubbles have been observed which break up into a range of bubble sizes just above the distributor.

Shulman and Molstad (37) found that, except at low gas flowrates, there was no dependence of bubble diameter on pore diameter when operating with both coarse and fine carbon distributors. They found that d_b increased from 0.3 to 0.5 cm as the superficial gas velocity increased to 9 cm/s, at which point some slugging was noted: as superficial gas velocity was increased further, considerable slugging was observed

at the bottom of the column. Braulick et al. (47), when working with large orifices (0.5 cm diameter) reported an increase in bubble diameter as the gas flowrate was increased, but Reith et al. (9) after examining several types of air distributor - single tubes, fine gauzes and perforated plates with different numbers of holes of various diameters - reached the conclusion that the gas hold-up remained unaffected by changes in orifice geometry. Yoshida and Akita (6) also expressed the view that fractional gas hold-up is not effected by nozzle diameter.

(2) Coalescence in bubble clouds in the main part of of the column

Little is known about the formation of large bubbles in the main part of a bubble column, well away from the distributor, and, indeed, it is not clear whether they form there at all. Moissis and Griffith (48) observed that the agglomeration of small bubbles to form larger ones in slug-flow occurs in two stages. First, the small bubbles come together and form a group of bubbles whose shape is that of a large one, and then the separate bubble interfaces collapse and a single large bubble is formed.

Kozokide et al. (49) found that bubbles which have been generated from a porous plate are small and equally sized, but sometimes (especially at higher gas

velocities) these small bubbles coalesce at a point slightly removed from the gas distributor in pure water and solvent. Marrucci et al. (50) also observed that bubbles on detaching from porous plates are very small, but since strong convective currents bring all the streams very close to each other in a narrow and confused region a few centimetres above the distributor, much larger bubbles come out from this region. Towell et al. (7) used high-speed cine films which were taken at the wall of the column and also at a depth of 12.7 cm: coalescence and break-up were observed from these films and the coalescence involved all sizes of bubbles and occurred in about 0.005s from the time of contact until noticeable oscillations of the combined bubble disappeared.

(3) Bubble wake coalescence

Crabtree and Bridgwater (51) concluded from their coalescence experiments that the bubble wake plays a vital part both in capturing non-aligned bubbles and in the subsequent possible coalescence. Using vertically aligned bubble pairs, each having volumes from 10 to 40 cm^3, in a 67% solution of sucrose in water, they demonstrated that bubbles up to initially 70 cm apart can coalesce. They also concluded that more detailed information about wake structure and the motion of bubbles in such wakes is required before a full explanation is possible.

Hills (52) has shown that coalescence does not normally occur by direct collision of a bubble cap with a bubble but by absorption of bubbles into the wake following a cap or by formation of satellite caps in the region of high voidage surrounding the main one.

(4) Theoretical descriptions of coalescence

These have been given by Lee and Hodgson (53), Marrucci (54), and recently by Darton et al. (55) and also in many papers listed above.

(5) Coalescence in agitated tanks

(6) Coalescence due to the effect of vibration

Parts (5) and (6) will be discussed and surveyed in Section (2.6.2).

2.1.6 Liquid Phase Mixing

Liquid circulation can occur in a bubble column with or without liquid flow. The work to create the circulation is supplied by expansion of the gas as it rises through the liquid. The circulation generally consists of an upward-flow region, where liquid relatively rich in entrained bubbles moves upwards, and a compensating region, where liquid with a lower gas hold-up moves downwards. Due to this, backmixing is usually detrimental to the performance of a gas-liquid reactor.

Several models are used to characterise mixing effects and non-ideal flow patterns in process vessels. Among these models, the axially dispersed plug-flow model is perhaps the most widely used one.

The Axially Dispersed Plug-Flow Model

This can be presented as a diffusion-type equation in which a dispersion coefficient replaces the ordinary molecular diffusivity. Levenspiel and Bischoff (76), when reviewing the patterns of flow in chemical process vessels, gave the following differential equation for the general dispersion model including chemical reaction and source terms:

$$\frac{\partial C}{\partial t} + U\nabla C = \nabla . \ (D.\nabla C) + s + r_c \qquad (2.9)$$

Because of the difficulties of specifying velocity profiles and limitations in experimental methods, the above equation is often simplified by assuming that:

(a) bulk flow occurs in the axial direction only, with radial symmetry;

(b) the dispersion coefficient is independent of position;

(c) fluid flows at the mean velocity (plug-flow);

(d) there is no variation in properties in the radial direction.

Then equation (2.9) can be written as:

$$\frac{\partial C}{\partial t} + U\frac{\partial C}{\partial x} = D_l \frac{\partial^2 C}{\partial_x{}^2} + s + r_c \qquad (2.10)$$

Equation (2.10) is the model used by many investigators when studying mixing in bubble columns and evaluating dispersion coefficients.

The usual method of finding the dispersion coefficient is to inject a suitable tracer at a point or plane in the system and monitor the changes in tracer concentration at one or more points; the dispersion coefficient may then be found from an analysis of the concentration data. In such stimulus-response experiments chemical reactions do not occur and $r_c = 0$ in equation (2.9). When the injection point for the tracer and the measuring points are sufficiently far apart and when there is no flow of liquid through the column equation (2.10) reduces to:

$$\frac{\partial C}{\partial t} = D_l \frac{\partial^2 C}{\partial x^2} \qquad (2.11)$$

Ohki and Inoue (39) assumed the following boundary conditions:

$$\frac{\partial C}{\partial x} = 0 \quad \text{at } x = 0 \text{ and } x = 1 ,$$

and the initial conditions

$$C(x,0) = C_o \text{ for } 0 \leqslant x \leqslant \lambda$$
$$C(x,0) = 0 \text{ for } x \geqslant \lambda$$

where λ is the height filled with tracer. They obtained the following solution for the set of equations:

$$\frac{C_{(t)}}{C_{(\infty)}} = 1 + 2 \sum_{n=1}^{\infty} \text{Cos}\left(\frac{n\pi}{L}x\right) . \exp\left[-\left(\frac{n\pi}{L}\right)^2 . D_1 . t\right] \qquad (2.12)$$

The graphical solution of equation (2.12) is shown in Figure (2.1) as $\left(\frac{C_{(t)}}{C_{(\infty)}}\right)$ plotted against $\left(\frac{\pi}{L}\right)^2 . D_1 . t$, with x/L as a parameter.

For steady-state conditions equation (2.10) reduces to:

$$U \frac{\partial C}{\partial x} = +D_1 \frac{\partial^2 C}{\partial x^2} \qquad (2.13)$$

Integration of this equation with the boundary conditions:

$$C = C_o \text{ at } x = 0 \text{ and } C = 0 \text{ at } x = +\infty$$

leads to:

$$\ln \frac{C}{C_o} = - \frac{U}{D_1} x \qquad (2.14)$$

where $U = \frac{U_{s1}}{1-\varepsilon}$

If $\frac{U}{D_1}$ is constant, a plot of $\ln (C/C_o)$ Vs.x gives a straight line of slope $-\frac{U}{D_1}$.

Previous Studies on Liquid Phase Mixing

The mixing of a liquid by a rising bubble current has been studied by numerous investigators over the last few decades. Most of these investigations have been carried out by using simple air-water systems.

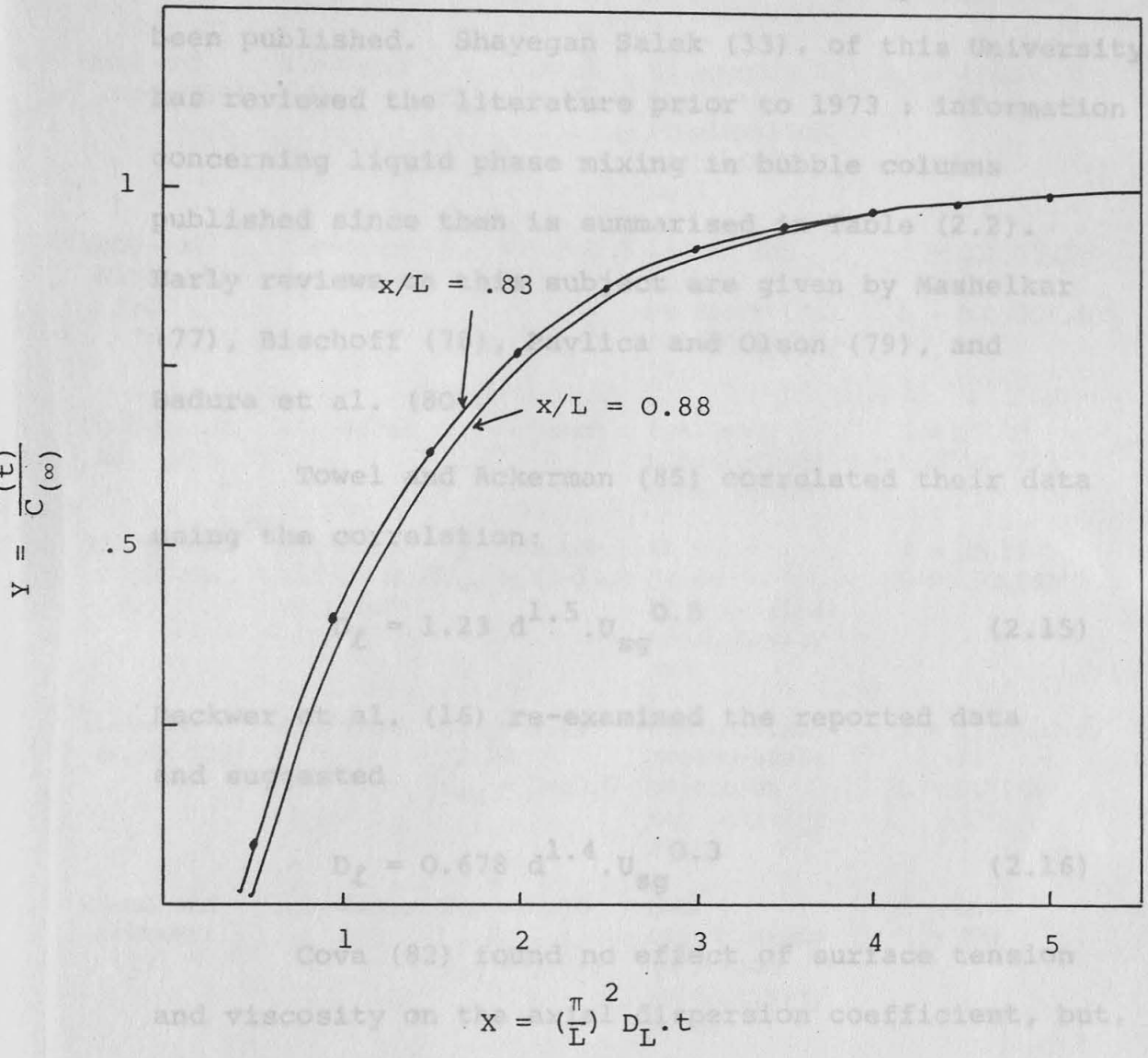

Figure 2.1 - Graphical Solution to the Dispersion Model (batch system)

As a result, a lot of experimental and theoretical work on liquid-phase mixing in two-phase flow systems has been published. Shayegan Salek (33), of this University, has reviewed the literature prior to 1973 : information concerning liquid phase mixing in bubble columns published since then is summarised in Table (2.2). Early reviews on this subject are given by Mashelkar (77), Bischoff (78), Pavlica and Olson (79), and Badura et al. (80).

Towel and Ackerman (85) correlated their data using the correlation:

$$D_\ell = 1.23\ d^{1.5}.U_{sg}^{0.5} \qquad (2.15)$$

Deckwer et al. (16) re-examined the reported data and suggested

$$D_\ell = 0.678\ d^{1.4}.U_{sg}^{0.3} \qquad (2.16)$$

Cova (82) found no effect of surface tension and viscosity on the axial dispersion coefficient, but, in small diameter columns, an increase in density increased the dispersion coefficient. For a single orifice, he proposed the relationship

$$D_\ell = 0.334\ U_{sg}^{0.32}\ \rho_L^{0.07} \qquad (2.17)$$

Hikita and Kikuawa (81) found the dispersion coefficient to be dependent upon the fluid viscosity and proposed the equation

Table 2.2 - Summary of Liquid-Phase Mixing Studies in Bubble Columns Since 1973.

Reference	System	Flow Rate cm/s	Tracer System	Column Characteristics cm	Dispersion Studies
Ohki and Inoue (39)	Air-Water	U_{sp} = batch U_{sg} = 0-25	UN aqueous Kcl pulse Pt electrical conducitivty cell	d = 4,8,16 L = 20,25,30	Axial
Kato and Nishiwaki (14)	Air-Water Concurrent	U_{sl} = 0.5-1.5	1-1.5N KCl pulse Pt electrical conducitivity cell	d = 6.6,12.2, 21.4 L = 200,201,405	Axial
Deckwer et al. (16)	Air-Water	U_{sl} = batch	Dye,heat, electrolytes Dirac pulse	d = 15,20 L = 440,723	Axial
Hikita and Kikukawa (81)	Air-Water Air-Aq MeOH solutions	U_{sl} = batch U_{sg} = 43-33.8	Aq KCl pulse Pt electrical conductivity cell	d = 10,19 L = 150,240	Axial
Shayegan Salek (33)	Air-Water	U_{sl} = 0.41-2.28 U_{sg} = 0-10.5	KCl solution steady-state injection conductivity meter	d = 15.2,30.5, 61 L = 247,247, 189	Axial and Radial
Eissa and Schugerl (19)	Air-Water	U_{sl} = 0.35-1.4 U_{sg} = 0.2-6	NaCl steady state injection conductivity meter	d = 15.9 L = 390	Axial
Cova (82)	N_2-Water N_2-Acetone	U_{sl} = 0.2-0.87 U_{sg} = 5.1-17.3	Heat steady state thermocouples	d = 1.9,4.57 L = 116,122	Axial
Alexander and Shah (83)	Air-aq. glycerol solutions Air-aq. triton DF 12 solutions	U_{sl} = batch U_{sg} = 0.7	H_2SO_4, Pulse Electrical conductivity	d = 6,15.2, 7.6x22.9 rectangular L = 124,308,112	Axial
Ostergaard (75)	Air-Water	U_{sl} = 1.9-13.5 U_{sg} = 0.5-20	gamma-ray-emitting ammonium bromide solution	d = 21.6 L = 700	Axial
Field and Davidson (84)	Air-Water	U_{sl} = 3-3.5 U_{sg} = 4-5.5	Radioactive tracer detectors	d = 320 L = 1890	Axial

$$D_\ell = (0.114 + 0.523\, U_{sg}^{0.77})\, d^{1.25} \left(\frac{1}{\mu_L}\right)^{0.12} \qquad (2.18)$$

Alexander and Shah (83) reported that the axial dispersion coefficient is independent of the surface tension and viscosity of liquid.

Theoretical analyses of the backmixing coefficient in a cylindrical, vertical bubble-column are given by Baird and Rice (86), and, recently, by Ueyama and Miyauchi (87) who measured backmixing in bubble columns with diameters up to 60 cm and superficial gas velocities up to 93 cm/s; the equation of motion for two-phase flow within a bubble column, operated within the circulation flow regime, has been solved and the liquid velocity profile determined by Ueyama and Miyauchi (45).

Although most of the data indicate that the liquid phase axial dispersion coefficient is independent of liquid flowrate, this is not the case for rectangular bubble columns. Stiegel and Shah (88) showed that the liquid phase dispersion coefficient in a rectangular bubble column depends on the liquid flowrate: Alexander and Shah (83) and Stiegel and Shah (88) also showed that for a given gas velocity, dispersion is greater in a rectangular bubble column than in a cylindrical column of equivalent diameter.

Whalley and Davidson (89) have considered various aspects of liquid circulation in bubble columns. Joshi and Sharma (90) have subsequently correlated liquid-phase axial dispersion coefficient data using the average liquid circulation velocity, calculated on the premise that multiple circulation cells exist within the column. Most recently, Field and Davidson (84) have measured both liquid and gas phase axial dispersion coefficients for a 320 cm i.d. industrial bubble column using radioactive tracers. They reported that, when U_{sg} is much greater than U_{sl}, the preferred correlation for D_ℓ in vertical bubble column is

$$D_\ell = 0.9\ d^{1.5}\ (L(U_{sg} - \varepsilon_g U_s))^{1/3} \qquad (2.19)$$

For the gas-phase axial dispersion coefficient, they give

$$D_g = 56.4\ d^{1.33}\ \left(\frac{U_{sg}}{\varepsilon_g}\right)^{3.56} \qquad (2.20)$$

2.2 Experimental Programme

When examining gas hold-up and bubble coalescence, all parameters which may have an effect should be carefully considered. The most important factors affecting gas hold-up and bubble coalescence may be divided into the following categories:

(1) Operational conditions, i.e. liquid and gas velocities.

(2) Liquid phase temperature.

(3) Mechanical agitation.

(4) Excitation of the water molecules by vibration.

(5) Liquid phase mixing.

(6) Column geometry.

Each of these parameters will now be described further.

2.2.1 Operational Conditions

Gas Flow-Rate

A high gas flow rate is not desirable in many fermentation processes. Outside the bubbly flow regime, coalescence occurs leading to a reduction in the gas-liquid interfacial area and the formation of slugs, which cause violent motion in the column. As was confirmed by the author, in some cases the wild movement of bubbles or slugs at higher air flows may break up microbial flocs during fermentation and lead to "wash-out" problems. Economy in the use of compressed air is also an important factor in process design, and this means that air flow-rates during fermentation must be kept to a minimum. For these reasons, attention has been concentrated on the bubbly-flow regime, and efforts

have been directed towards the design of gas distributors which give maximum "bubbly flow" in the required range of gas velocities. In the case of air-water systems, the literature survey reveals that departure from the bubbly flow regime usually happens at superficial gas velocities greater than 4 cm/s. However, in order to reveal general trends and irregularities in bubble column behaviour the author has studied superficial gas velocities up to 16 cm/s and 12 cm/s in two-and three-dimensional bubble columns respectively.

Liquid Flow Rate

Liquid flow rate directly controls the output of the column and so it is a very important parameter; as such, it is desirable to cover as wide a range of flow rates as possible. However, there are certain constraints which must be borne in mind. System behaviour at low liquid flow rates (corresponding to superficial liquid velocities < 1 cm/s) is of most interest as many biochemical reactions are relatively slow; in a "once through" process, long residence times may be involved. At relatively high liquid flow rates, micro-organisms are readily elutriated and thus it is difficult to maintain high microbial concentrations inside the column. For these reasons, liquid velocities were limited to a maximum figure of around 1 cm/s.

2.2.2 The Effect of Liquid Temperature

Liquid phase temperature is an important parameter having a significant effect on gas hold-up and bubble coalescence; up until now the effect of liquid phase temperature on gas hold-up has not been fully explored. A wide range of liquid phase temperatures and superficial gas velocities was used in order to determine trends and the effect of this important parameter on gas hold-up.

2.2.3 The Effect of Mechanical Agitation

Agitation, which is a mechanical method for transferring liquid from one part of a column to another, has a significant effect on gas hold-up and the rate of bubble coalescence and break-up. Numerous attempts have been made to see how bubble coalescence and break-up is affected by mechanical agitation and stirrer speed in agitated tanks. Some work has also been published about the effect of stirrer speed on gas hold-up in multi-stage continuous fermenters. In order to find out how mechanical agitation effects gas hold-up and bubble coalescence, some of these works have been critically surveyed and discussed; furthermore, some runs have been performed by the author during which a simple agitator was inserted in a bubble column.

2.2.4 Effect of Vibration

Another factor which has a significant effect on bubble coalescence is vibration. The use of pulsed columns in liquid-liquid extraction has become an established chemical engineering operation. It is, therefore, understandable that a similar technique has been tried in bubble columns. Despite the fact that the use of vibration is not yet well developed in the bubble column, there are some important reports, based on work on a pilot plant scale, of the effect of vibration on bubble coalescence. The author has attempted to collect together such information and relate the results to other work on bubble coalescence.

2.2.5 Liquid Phase Mixing

The gas bubbles, which are produced at the bottom of the column by a distributing device, agitate the liquid phase and, especially at higher superficial gas velocities, produce almost complete mixing. To characterise the degree of mixing, the author has made use of the axially dispersed plug-flow model (see Section 2.1.6).

2.2.6 Column Geometry

The effect of column geometry on gas hold-up and

liquid phase mixing for air water systems has already been studied in depth by Shayegan Salek (33) of this University. He determined how the geometry of the column, particularly column diameter and gas distributor design, affected gas hold-up and liquid phase mixing; in the author's research programme, a more detailed study has been made of the effect of column height on gas hold-up since this parameter was largely ignored by Shayegan Salek.

2.3 Measurement Techniques

2.3.1 Gas Hold-Up Measurements

The methods available for the measurement of gas hold-up in bubble columns have been documented by Shayegan-Salek (33). These techniques fall into four categories, which may be summarised as follows:-

(1) bed expansion techniques

(2) manometric techniques

(3) measurements of bed resistivity

(4) radiation attenuation methods.

(1) Bed Expansion Techniques

This is the most common and simple of the techniques mentioned above and has been widely used. The method relies on the instantaneous isolation of the experimental system for both liquid and gaseous feeds.

This is achieved by the use of quick-action isolation values on both inlets. The gas hold-up may be determined by noting the volume of both phases after they have separated. Figure (2.2) illustrates the different stages of separation of the two phases.

(2) Manometric Techniques

This is another popular technique in which the gas hold-up is determined by measuring the pressure at one or several points in the column using a manometric system. A and B in Figure (2.3) represent two manometers positioned at arbitrary distances along the length of the column. The difference in the manometer levels, h, gives a direct indication of the hold-up in the section contained between the two tappings. This is also true for the case where more than two manometers are used.

By definition,

$$\text{Average gas hold-up} = \varepsilon_g = \frac{LS - L_o S}{LS} = 1 - \frac{L_o}{L} \qquad (2.21)$$

where L_o = height of liquid in the tower if the gas were excluded, L = height of areated liquid and S = cross-sectional area.

The density of the gas/liquid mixture may also be defined by:

$$\rho = \frac{L_o S \rho_L + S(L - L_o)\rho_G}{LS}$$

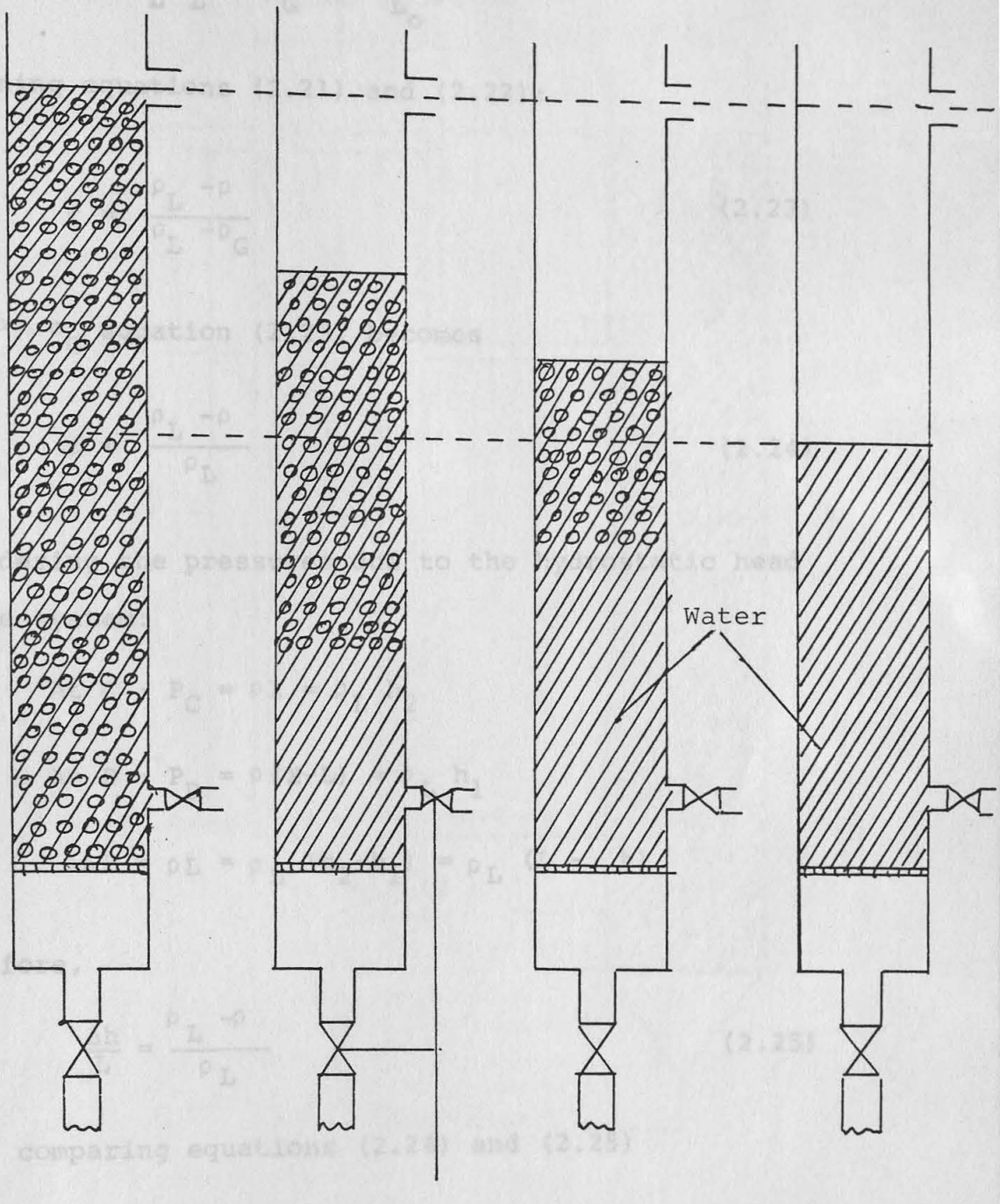

Figure 2.2 - Stages in the collapse of a Bed of Bubbles

or $$\rho = \rho_L - (\rho_L - \rho_G)\ (1 - \frac{L_o}{L}) \qquad (2.22)$$

$$\equiv \rho_L \frac{L_o}{L} + \rho_G\ (1 - \frac{L}{L_o})$$

Combining equations (2.21) and (2.22):

$$\varepsilon = \frac{\rho_L - \rho}{\rho_L - \rho_G} \qquad (2.23)$$

As $\rho_L >> \rho_G$ equation (2.23) becomes

$$\varepsilon = \frac{\rho_L - \rho}{\rho_L} \qquad (2.24)$$

Considering the pressures due to the hydrostatic head in the system:

$$\text{At C} : P_C = \rho X = \rho_L\ h_2$$

$$\text{At D} : P_D = \rho\,(X-L) = \rho_L\ h_1$$

and $$\Delta P = \rho L = \rho_L\ (h_2 - h_1) = \rho_L\ (L - h)$$

Therefore,

$$\frac{\Delta h}{L} = \frac{\rho_L - \rho}{\rho_L} \qquad (2.25)$$

Thus, comparing equations (2.24) and (2.25)

$$\varepsilon = \frac{\Delta h}{L}\ .$$

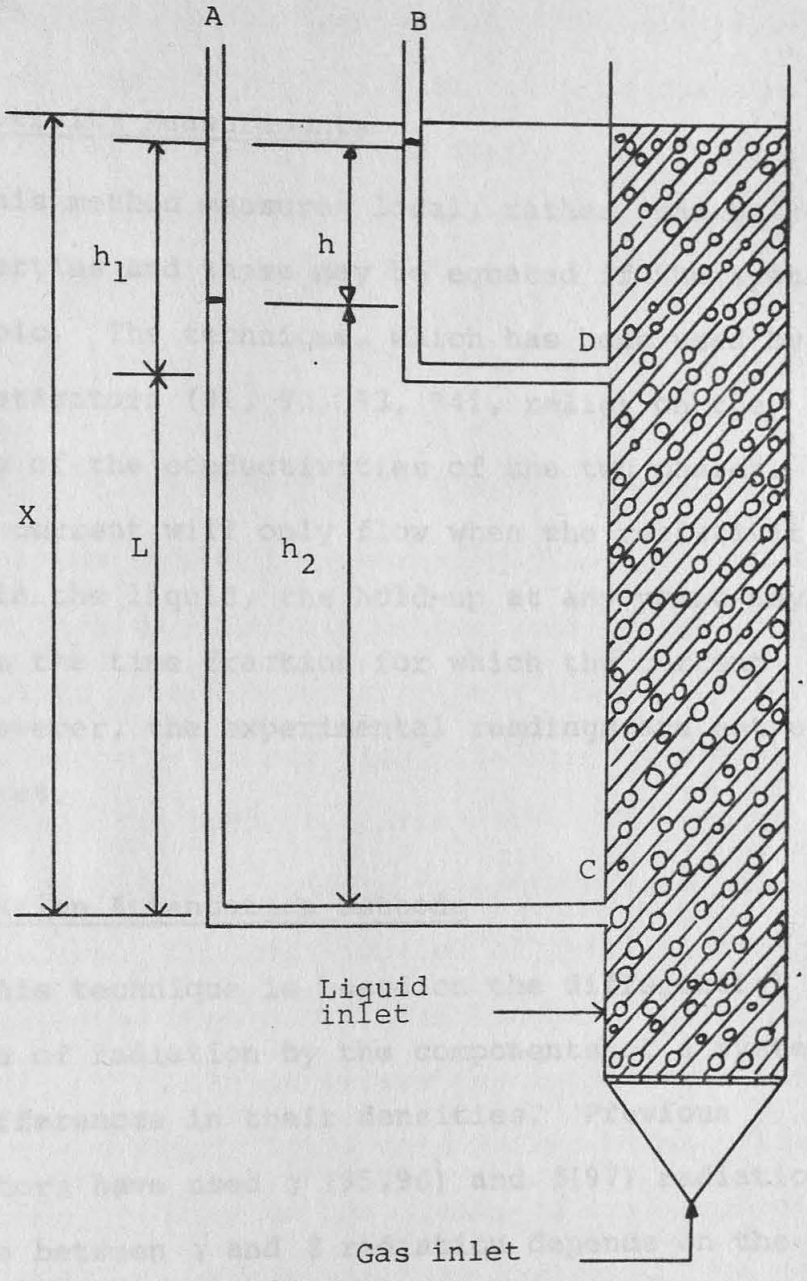

Figure 2.3 - Diagrammatic representation of the system for measurement of gas hold-up

With this simple technique gas hold-up can be measured for any section as well as the whole length of the column, provided there are a sufficient number of manometers.

(3) Resistivity Measurements

This method measures local, rather than bulk, void properties and these may be equated if the system is isotropic. The technique, which has been used by many investigators (91, 92, 93, 94), relies on the difference of the conductivities of the two phases. Since the current will only flow when the resistivity probe is in the liquid, the hold-up at any point may be found from the time fraction for which the current flows. However, the experimental readings are not easy to interpret.

(4) Radiation Attenuation Methods

This technique is based on the differential absorption of radiation by the components of a system due to differences in their densities. Previous investigators have used γ (95,96) and β(97) radiation. The choice between γ and β radiation depends on the sensitivity required and the distance to be traversed by the radiation, although in a system containing living organisms the possibility of cell mutation (and even death) must also be considered. Both γ and β radiation

may cause mutation but this is a function of the dose and the complexity of the organism. β radiation is absorbed more readily than the γ radiation, and so small density differences can be detected using β rays: for the same reason β radiation can only be used to traverse a short distance. This distance, or range, depends on the material through which the radiation must pass and the initial energy.

2.3.2 Methods for Measuring Axial Dispersion Coefficients

Various types of tracer inputs may be used to find the effective axial dispersion coefficient using unsteady-state injection of a tracer: the common inputs are the pulse or delta function, the step function, and periodic functions such as a sine wave. The tracer concentration is then measured downstream from the injection point. The modification of this input signal by the system can then be related to the dispersion coefficient, which characterises the intensity of axial mixing in the system. Pulse methods are often preferable from the point of view of simplicity of experimental equipment and ease of mathematical analysis.

If a pulse of tracer is injected into a flowing stream, this discontinuously spreads out as it moves with the fluid past a downstream measurement point. For a fixed distance between the injection point and

measurement point, the amount of spreading depends on the intensity of dispersion in the system and can be used to characterise quantitatively the dispersion phenomenon.

Steady-State Methods

The principle of the method is simple, a steady stream of tracer is usually injected at the top of the column. The tracer travels downwards due to the liquid circulation patterns and eventually the system reaches a steady state, the concentration of tracer over the length of the column remaining unchanged. Samples can then be taken at different points over the length of the column and analysed for tracer; alternatively, in-line detectors can be used. Dispersion coefficients are then evaluated using equation (2.14).

2.4 Experimental Equipment and Experimental Procedure

The experimental studies were conducted in a two-dimensional bubble column of dimensions 1.3 cm x 15.3 cm x 134 cm and a three-dimensional bubble column 15.2 cm in diameter and of variable height.

2.4.1 The Two-Dimensional Bubble Column

To allow clear visual and photographic observations to be made, it is convenient to use two-dimensional beds. For this work, the two-dimensional bed was constructed from perspex, and the opposite faces were glued and bolted together. The distributor section and bed section were bolted together using flanges. A support screen was placed between these inside a rubber gasket. The arrangement is shown in Figure (2.4) and (2.5). The following distributor arrangements were adopted:

(a) a 0.2 cm thick copper plate drilled with 0.1 cm holes on a 0.6 cm square pitch,

and (b) a 100 mesh wire gauze.

During preliminary work, it was found that a combination of (a) and (b) gave excellent gas distribution.

A mains water supply (1) was available from a nearby rig and this was tapped using a suitable valve switching arrangement along with a bank of on-line water rotameters (2). The water was pumped into the column using a DCL micropump arrangement (3): for some tests the liquid was obtained directly from the mains water supply. The liquid entered the column through a 0.9 cm diameter pipe drilled with 0.2 cm holes.

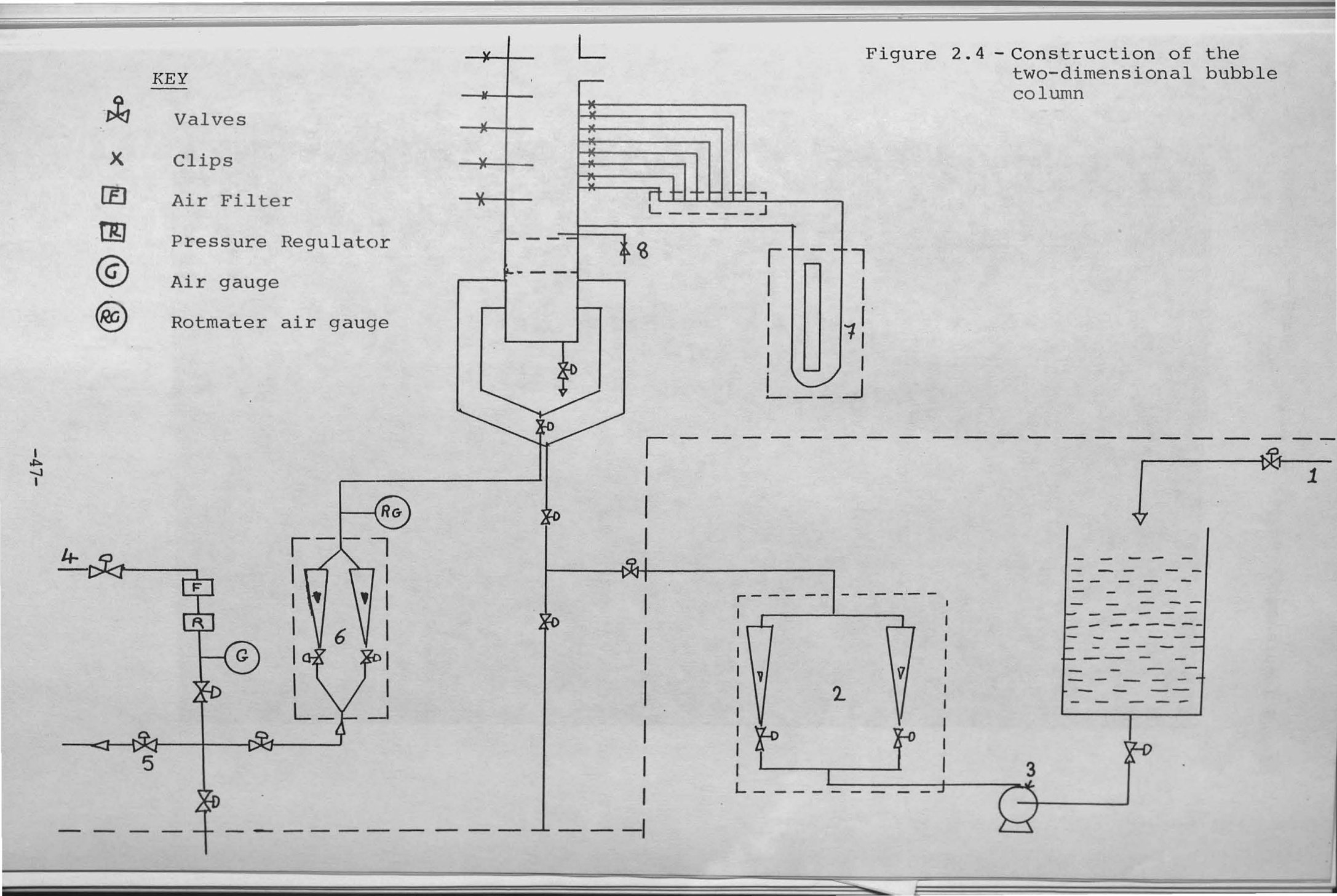

Figure 2.4 - Construction of the two-dimensional bubble column

Figure 2.5 - General View of the Two-Dimensional Bubble Column

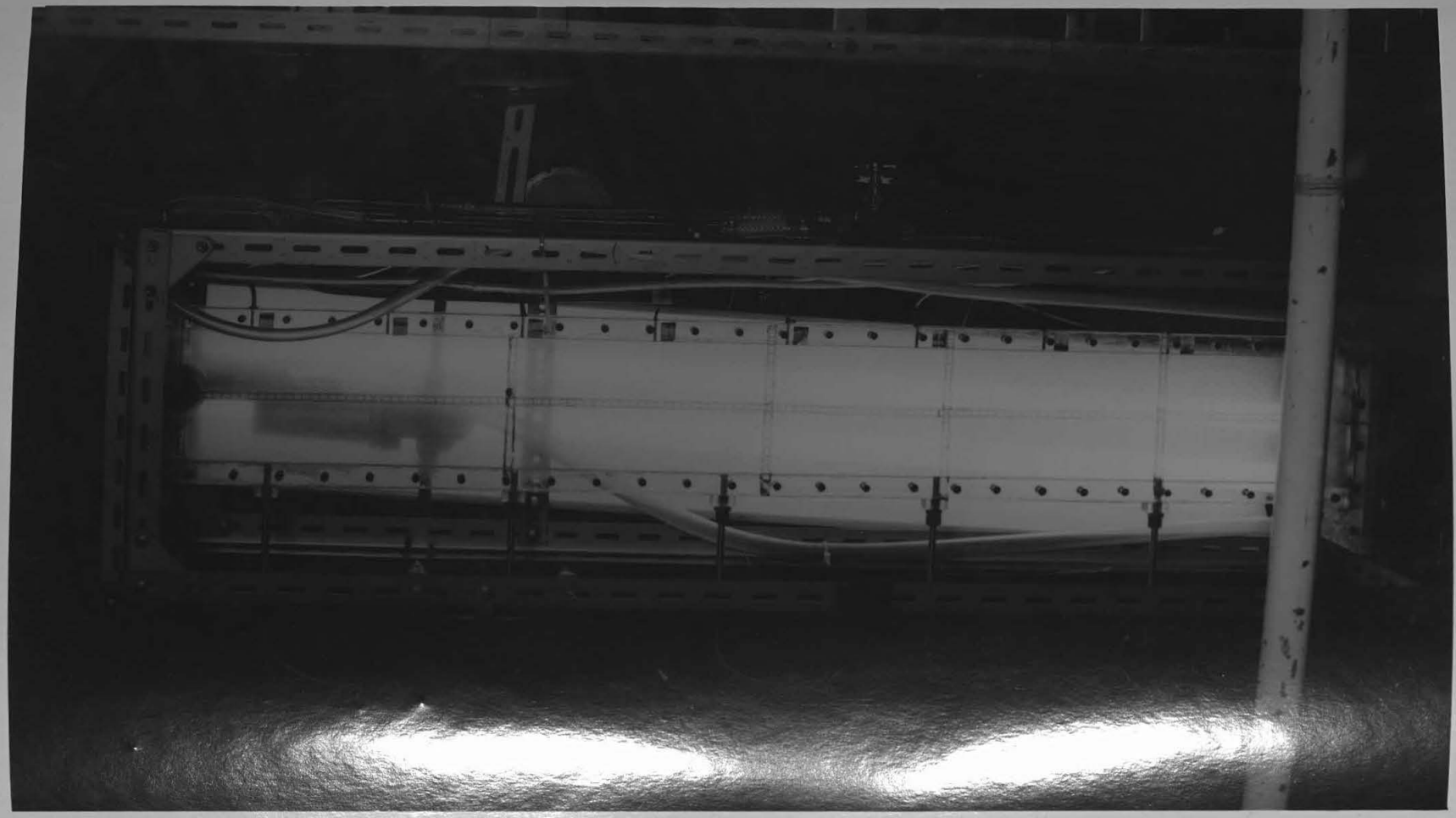

Mains compressed air (4) was available at 50 psig. This was far too high a working pressure for the P.V.C. air line to the rig, and so the supply was reduced using a pressure regulator, adjusted to 15 psig; a safety valve (5) was also incorporated into the system. The air supply diverged into two separately valved air rotameters (6) (7A and 10A), before converging again, and passing into the equipment, as Figure (2.4) shows.

An arrangement to measure pressure drop was also available (7). Eight tappings were located in the sides of the column and these were connected to a common junction unit. Tappings were isolated using clips, such that only one could be monitored at any one time. A tapping just above the support screen constituted the other arm of the manometer. In addition, in order to measure solid composition inside the column, five sampling points were drilled along the length of the column. A hole was also drilled near to the gas distributor (8) for washing out and removing solids from the column.

2.4.2 The Three-Dimensional Bubble Column

Experimental studies were also carried out in a vertical column of variable height, and of 15.2 cm diameter. The general layout of the rig is shown in Figure (2.6).

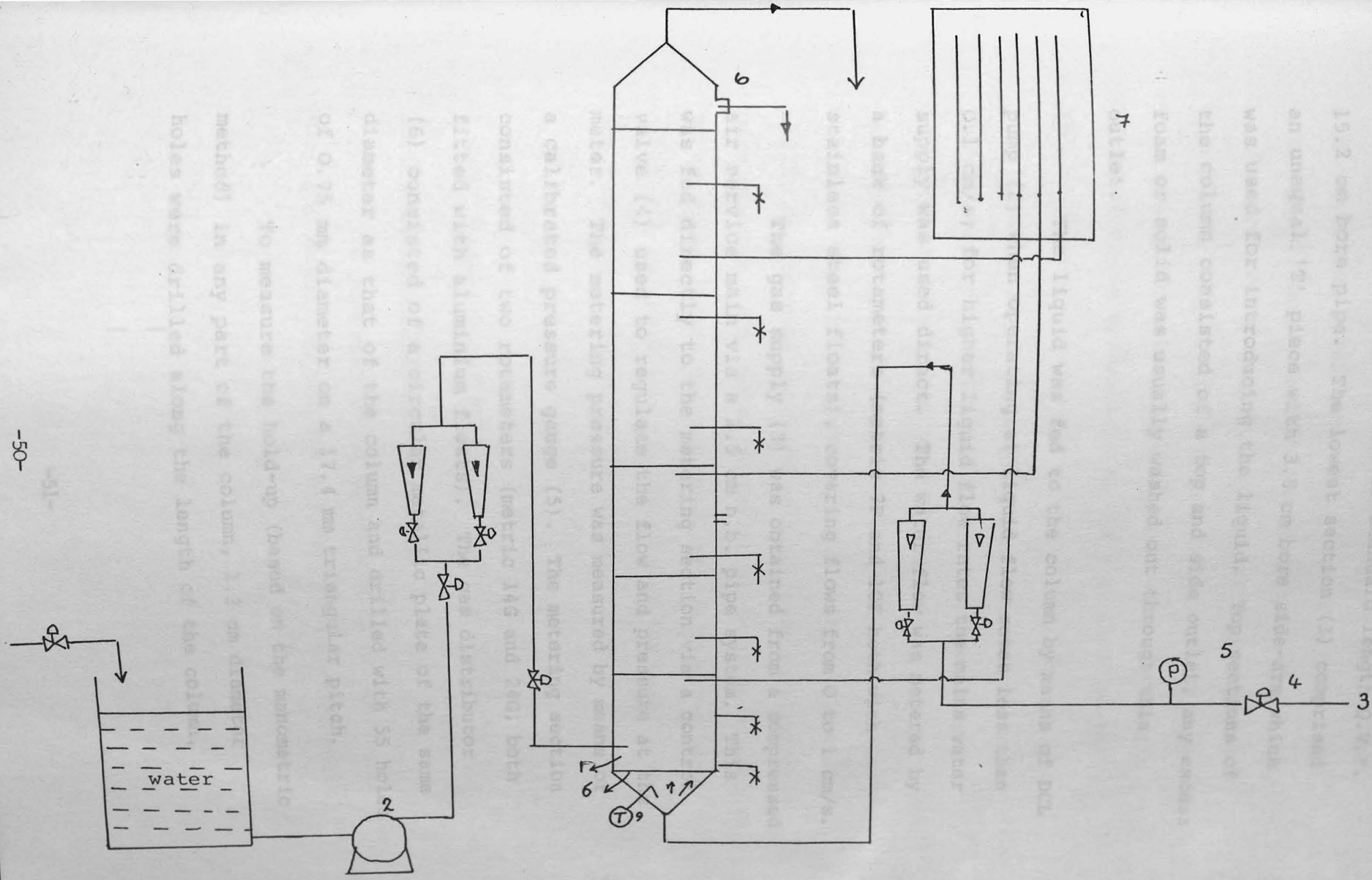

Figure 2.6 - Construction of the 15.2 cm diameter column

The column was made of standard length Q.V.F. 15.2 cm bore pipe. The lowest section (1) comprised an unequal 'T' piece with 3.8 cm bore side-arm which was used for introducing the liquid. Top sections of the column consisted of a top and side outlet, any excess foam or solid was usually washed out through this outlet.

The liquid was fed to the column by means of DCL pump (2) when operating at liquid flow rates less than 0.1 cm/s; for higher liquid flow rates the mains water supply was used direct. The water flow was metered by a bank of rotameters (metric 7F and 10F both with stainless steel floats), covering flows from 0 to 1 cm/s.

The gas supply (3) was obtained from a compressed air service main via a 2.5 cm n.b. pipe system. This was fed directly to the metering section via a control valve (4) used to regulate the flow and pressure at the meter. The metering pressure was measured by means of a calibrated pressure gauge (5). The metering section consisted of two rotameters (metric 14G and 24G, both fitted with aluminium floats). The gas distributor (6) consisted of a circular metallic plate of the same diameter as that of the column and drilled with 55 holes of 0.75 mm diameter on a 17.4 mm triangular pitch.

To measure the hold-up (based on the manometric method) in any part of the column, 1.3 cm diameter holes were drilled along the length of the column.

The holes were supplied with fittings so that 3.2 mm o.d. stainless steel tubes could easily be inserted into the column; these tubes were connected by means of flexible P.V.C. tubing to vertical glass tubes mounted at the top of the column (7). Besides each glass tube a self-adhesive downward scale was affixed: the zeros of these scales were at the same level as the water outlet.

In order to determine solid composition in any part of the column 1.8 cm diameter holes were drilled along the length on the wall of the column, and these holes were supplied with suitable fittings and rubber washers 1 cm i.d. so that stainless steel tubes could easily be inserted into the column; these sampling tubes were movable in a radial direction, thus allowing samples to be taken at any desired position. A hole was also drilled 1 cm above the gas distributor for washing out and removing solids from the column.

2.4.3 Experimental Procedure

Measurement of Average Gas Hold-up

The manometric and bed expansion methods were used for measuring the gas hold-up, as described below.

The Manometric Method

Two manometers were used to provide an indication of the overall gas hold-up in air-water systems. These were each positioned about two column diameters away from the top and bottom of the column to avoid end-effects. It was found that the fluctuations of the liquid levels in the manometers could be reduced markedly by using a 1 mm diameter stainless steel sampling tube.

The Bed Expansion Method

This method was the main one used for measuring gas hold-up, particularly at higher temperatures or when using three-or four-phase systems. This method was preferred because the manometers tended to become blocked by the solid phase when studying multi-phase systems.

Dispersion Coefficient Measurement

The backmixing of the liquid phase in air-water systems was evaluated by the unsteady-state tracer technique. This involved the injection of a 1% methylene blue solution at the top of the column and the monitoring of dye concentration as a function of time at the bottom of the column. Air and tap water were used throughout the mixing studies as the gas and liquid phases.

For each experiment, after setting the appropriate gas flow rate, an automatic timer was switched on simultaneously with the introduction of the

liquid tracer at the top of the column. Samples were then taken from the bottom of the column and the time at which samples were taken was recorded: the dye concentration was measured by means of a spectrophotometer.

Randomisation and Replication

The experimental plan for each column was carried out in a completely random fashion, and each experiment was repeated at least twice.

2.5 Experimental Results

2.5.1 Effect of Operating Temperature

The effect of water temperature on gas hold-up was studied using tap water as the liquid phase. A range of temperatures from 20 ^{o}C to 70 ^{o}C was chosen because this covers temperatures frequently used in fermentation processes. Figure (2.7) shows the shape of slugs formed at different temperatures between 35 ^{o}C to 60 ^{o}C; these pictures were taken using high-speed photography in the two-dimensional bubble column. Figures (2.8) and (2.9) show how the temperature affected gas hold-up for $U_{s\ell}=0$ in the two-and three-dimensional bubble columns respectively. Detailed information is presented in Tables (1) and (2) of Appendix (A).

Figure 2.7 - Shape of Slugs at Higher Temperature

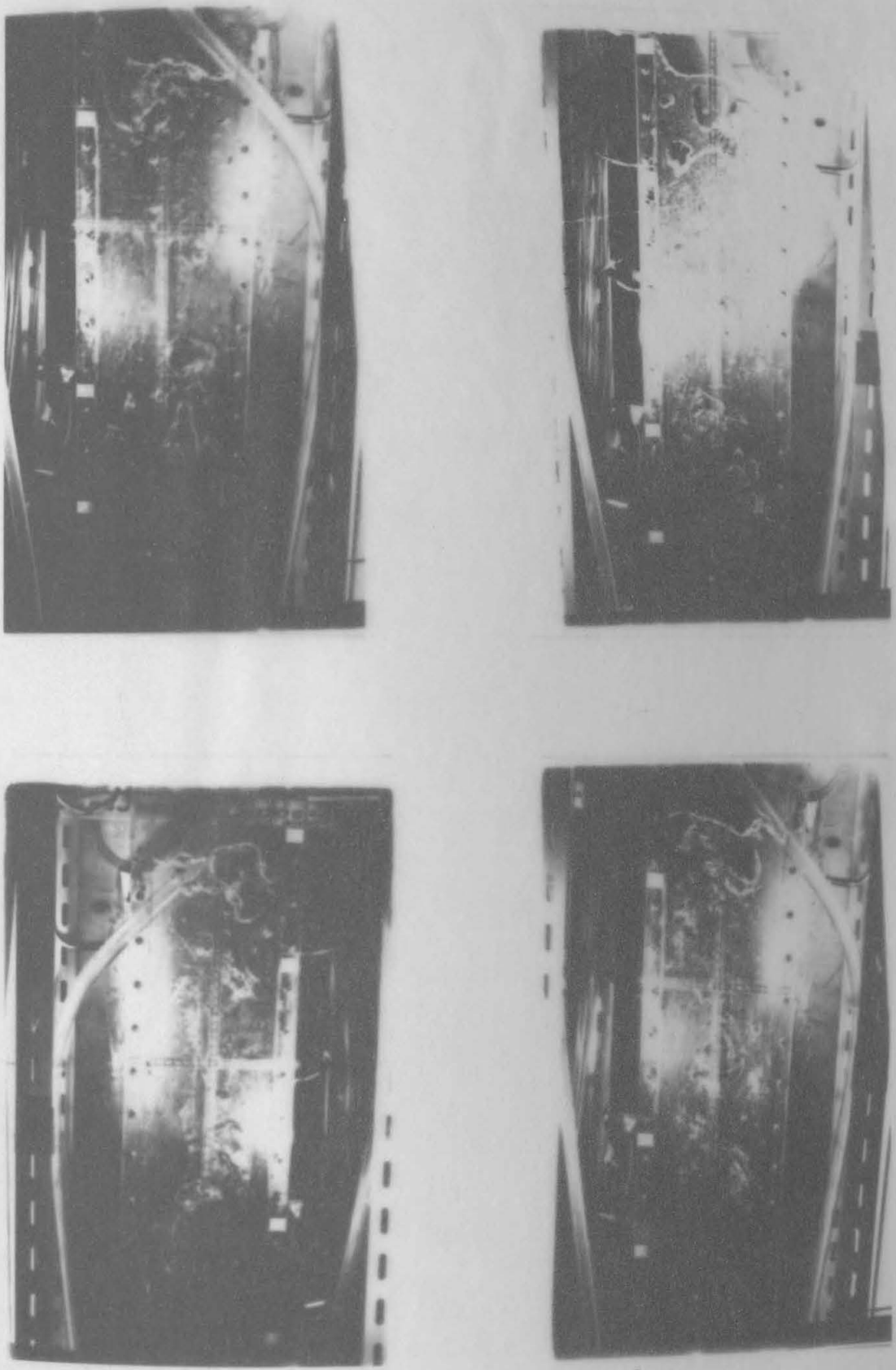

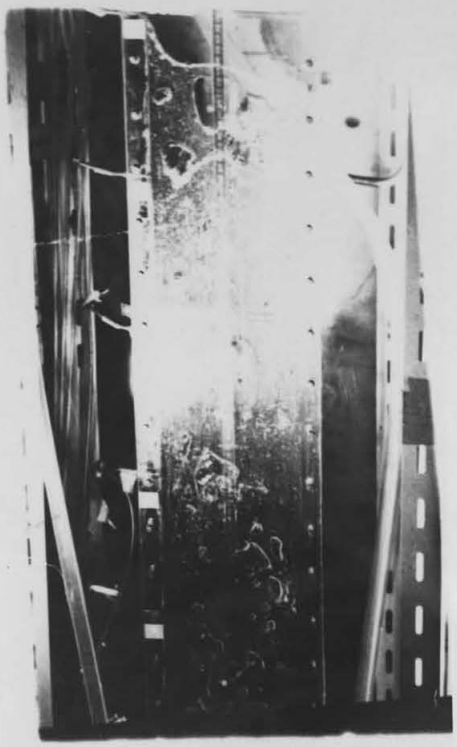

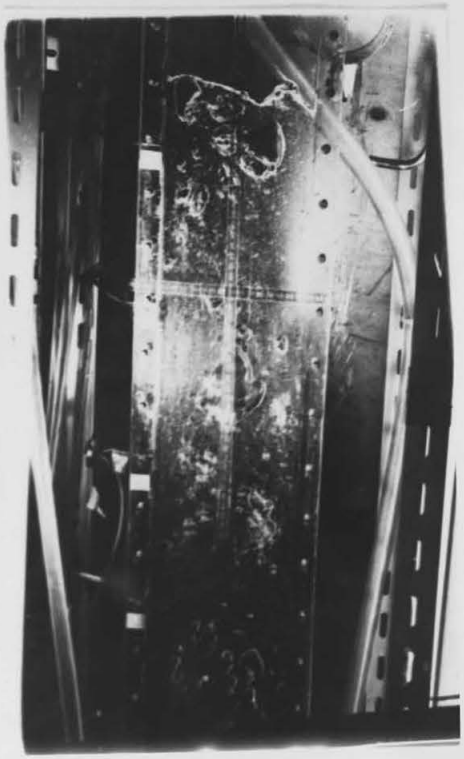

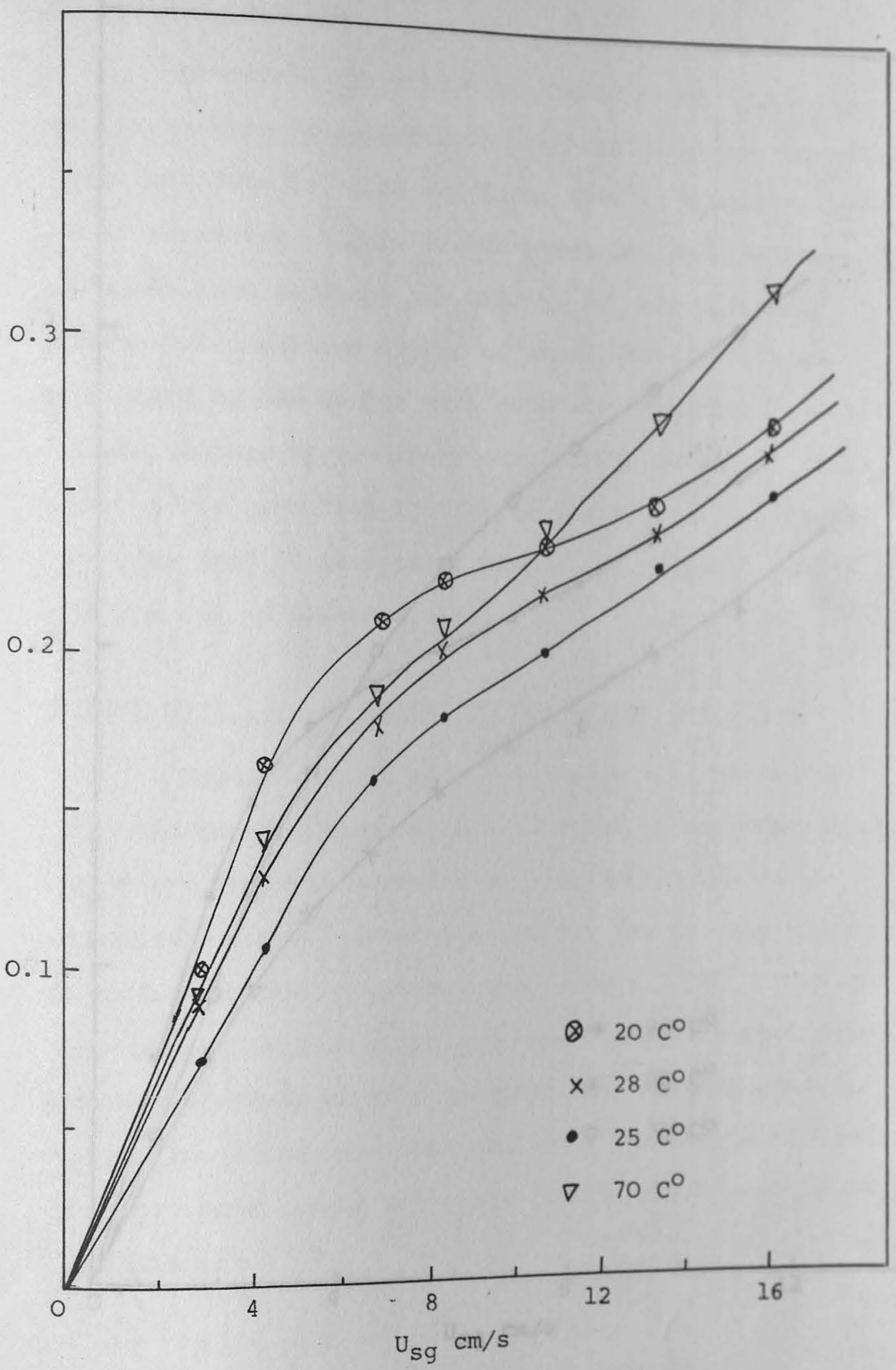

Figure 2.8 - Typical influence of water temperature on gas hold-up in two dimensional bubble column and for $U_{s\ell}$=o.

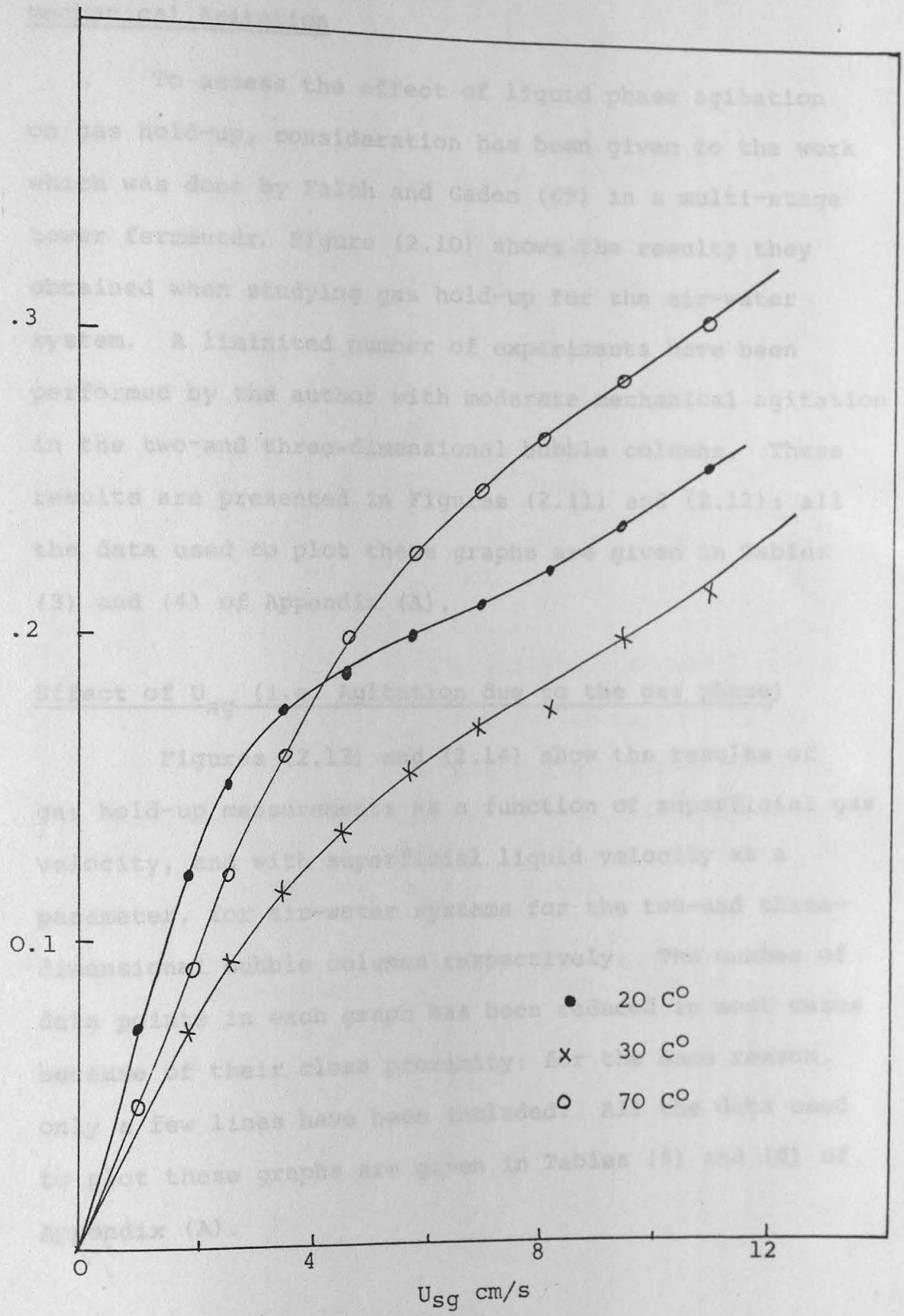

Figure 2.9 Typical influence of water temperature on gas hold-up in three dimensional bubble column and for $U_{s\ell}$=0.

2.5.2 Effect of Liquid Phase Agitation

Mechanical Agitation

To assess the effect of liquid phase agitation on gas hold-up, consideration has been given to the work which was done by Falch and Gaden (69) in a multi-stage tower fermenter. Figure (2.10) shows the results they obtained when studying gas hold-up for the air-water system. A liminited number of experiments have been performed by the author with moderate mechanical agitation in the two-and three-dimensional bubble columns. These results are presented in Figures (2.11) and (2.12): all the data used to plot these graphs are given in Tables (3) and (4) of Appendix (A).

Effect of U_{sg} (i.e. Agitation due to the gas phase)

Figures (2.13) and (2.14) show the results of gas hold-up measurements as a function of superficial gas velocity, and with superficial liquid velocity as a parameter, for air-water systems for the two-and three-dimensional bubble columns respectively. The number of data points in each graph has been reduced in most cases because of their close proximity: for the same reason, only a few lines have been included. All the data used to plot these graphs are given in Tables (5) and (6) of Appendix (A).

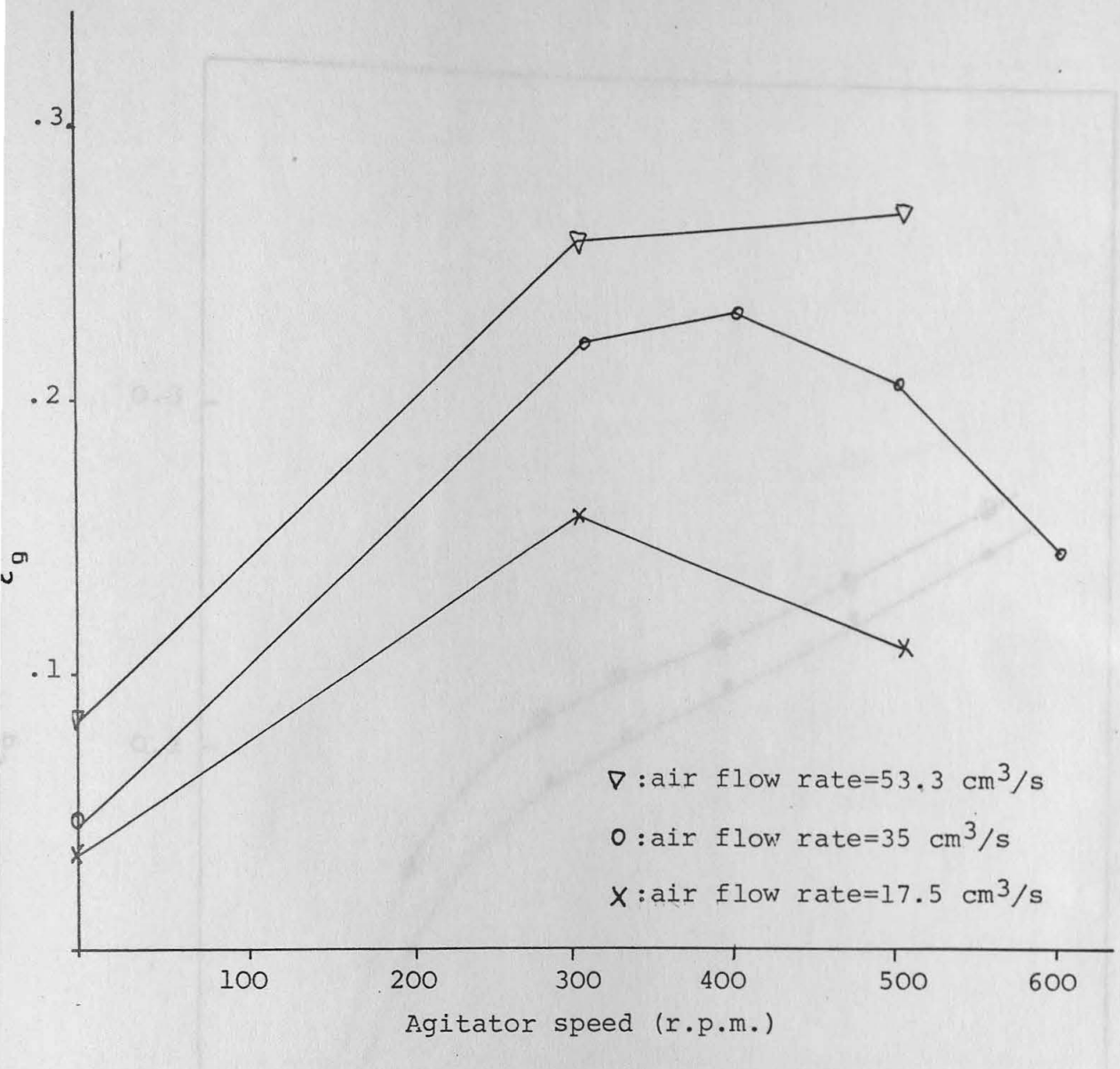

Figure 2.1 O - Effect of agitator speed on gas hold-up in air-water system (Flach and Gaden (69))

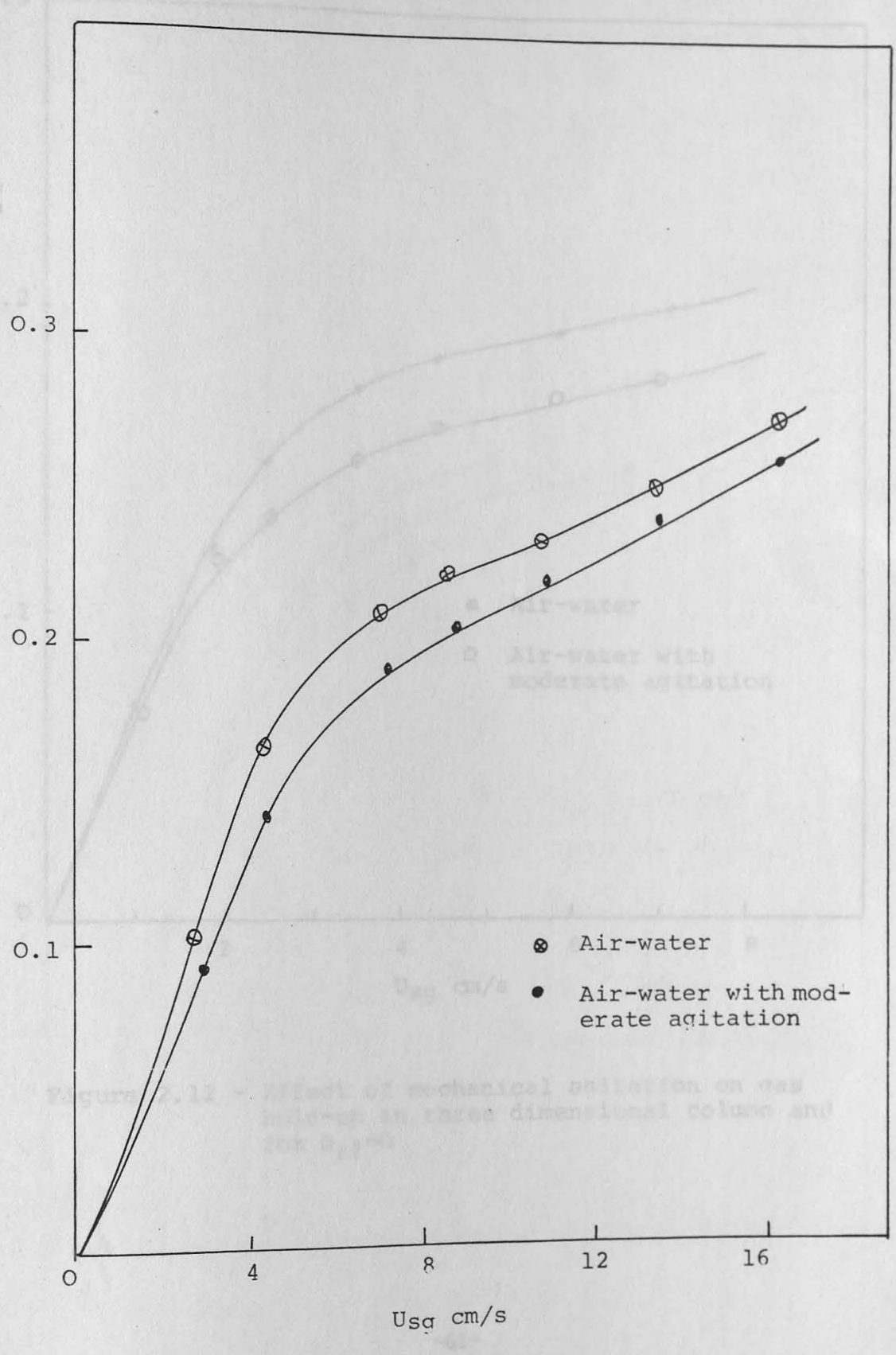

Figure 2.11 - Typical influence of mechanical agitation on gas hold-up in two dimensional bubble column & for $U_{s\ell}=0$.

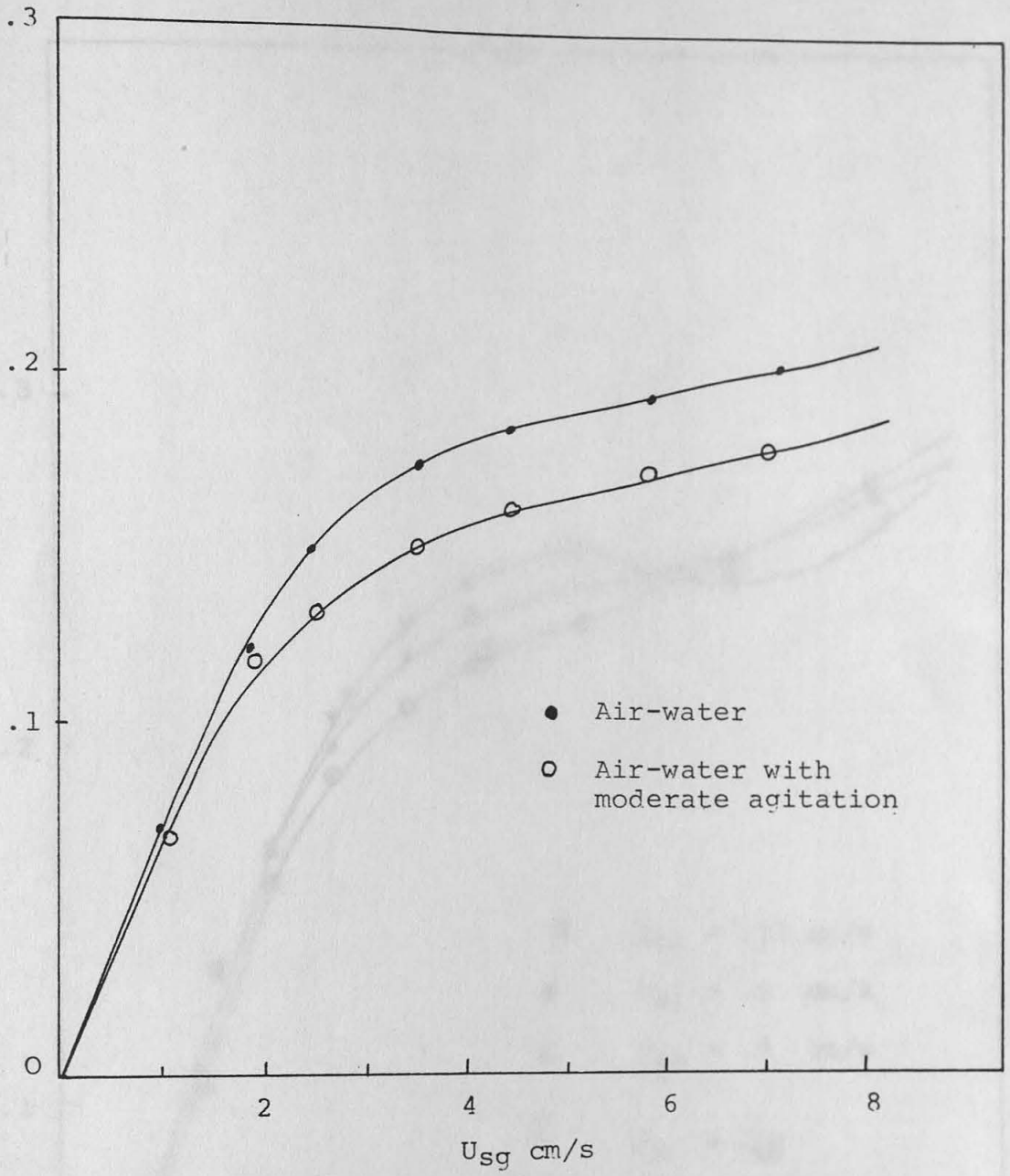

Figure 2.12 - Effect of mechanical agitation on gas hold-up in three dimensional column and for $U_{s\ell}=0$

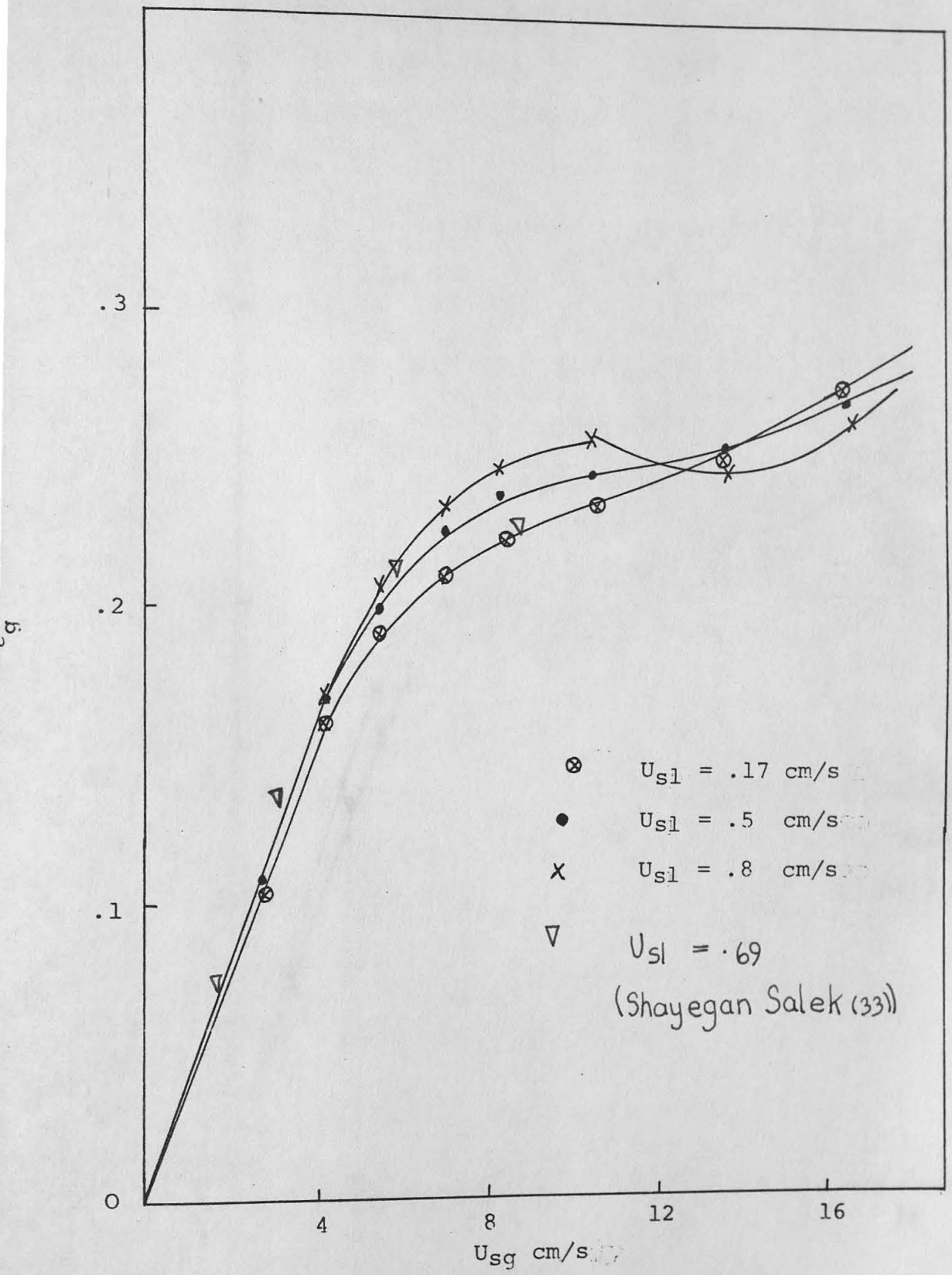

Figure 2.13 - Typical influence of U_{sg} and $U_{s\ell}$ on gas hold-up in two dimensional bubble column

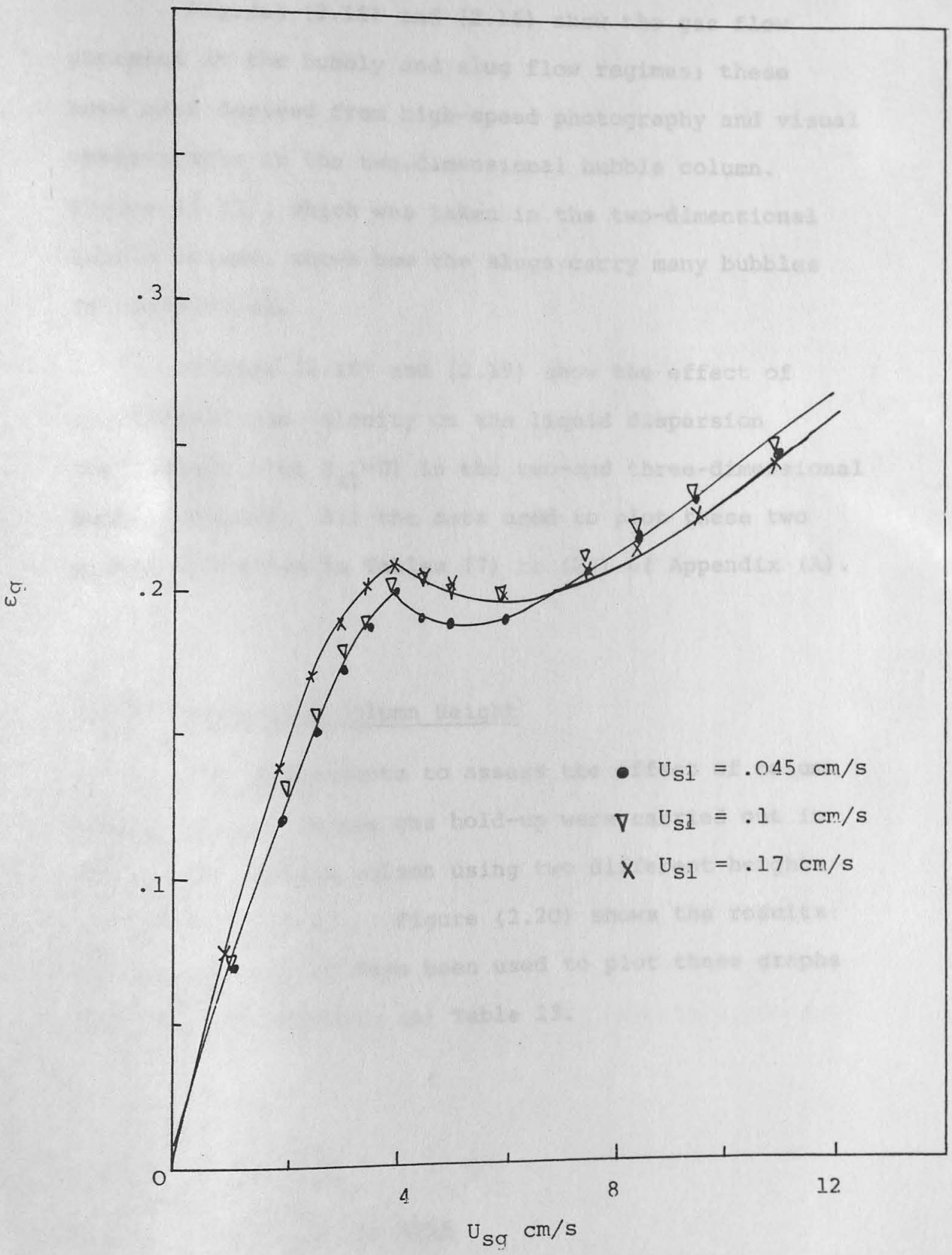

Figure 2.14 - Effect of U_{sg} and U_{sl} on gas hold-up in three dimensional bubble column

2.5.3 Gas and Liquid Flow Patterns

Figures (2.15) and (2.16) show the gas flow patterns in the bubbly and slug flow regimes; these have been derived from high-speed photography and visual observations in the two-dimensional bubble column. Figure (2.17), which was taken in the two-dimensional bubble column, shows how the slugs carry many bubbles in their wakes.

Figure (2.18) and (2.19) show the effect of superficial gas velocity on the liquid dispersion coefficient (for $U_{sl}=0$) in the two-and three-dimensional bubble columns. All the data used to plot these two graphs are given in Tables (7) to (22) of Appendix (A).

2.5.4 Effect of Column Height

The experiments to assess the effect of column height on the average gas hold-up were carried out in the tubular bubble column using two different heights (110 cm and 175 cm). Figure (2.20) shows the results: all the data which have been used to plot these graphs are given in Appendix (A) Table 23.

2.6 Discussion

2.6.1 Bubble Coalescence

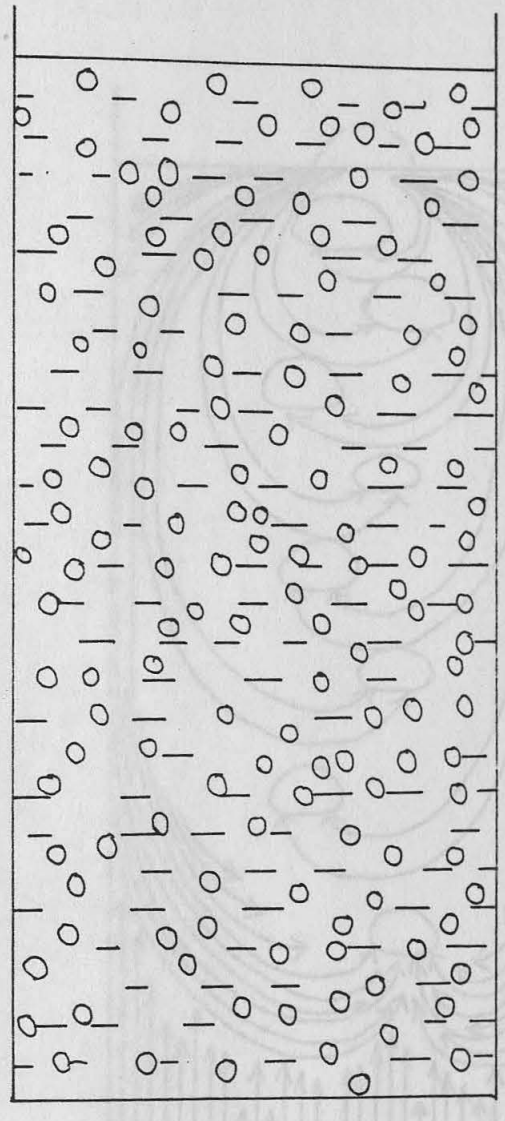

Figure 2.15 - Gas flow pattern in bubbly flow regimes

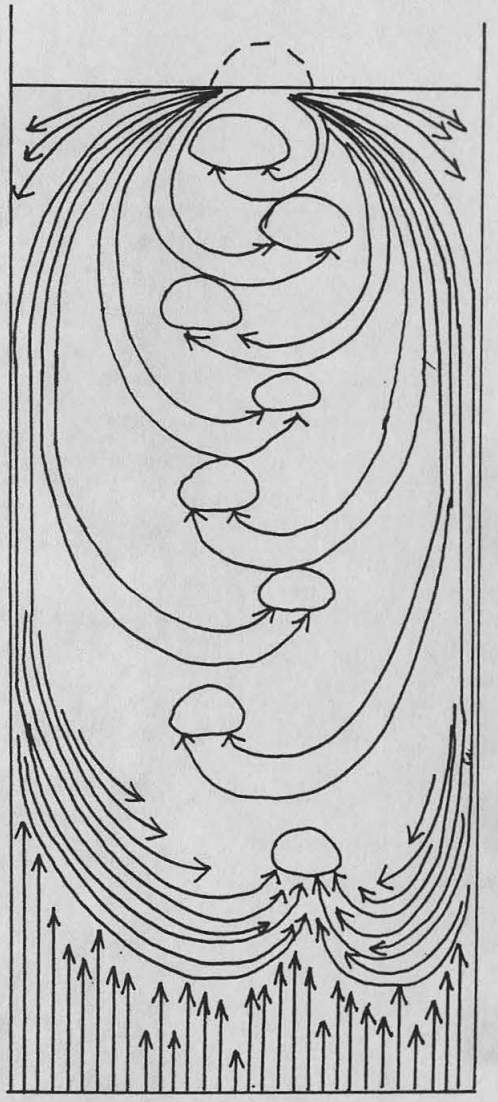

Figure 2.16 - Gas flow pattern in slug flow regime

Figure 2.17 - Slugs with small bubbles in their wakes.

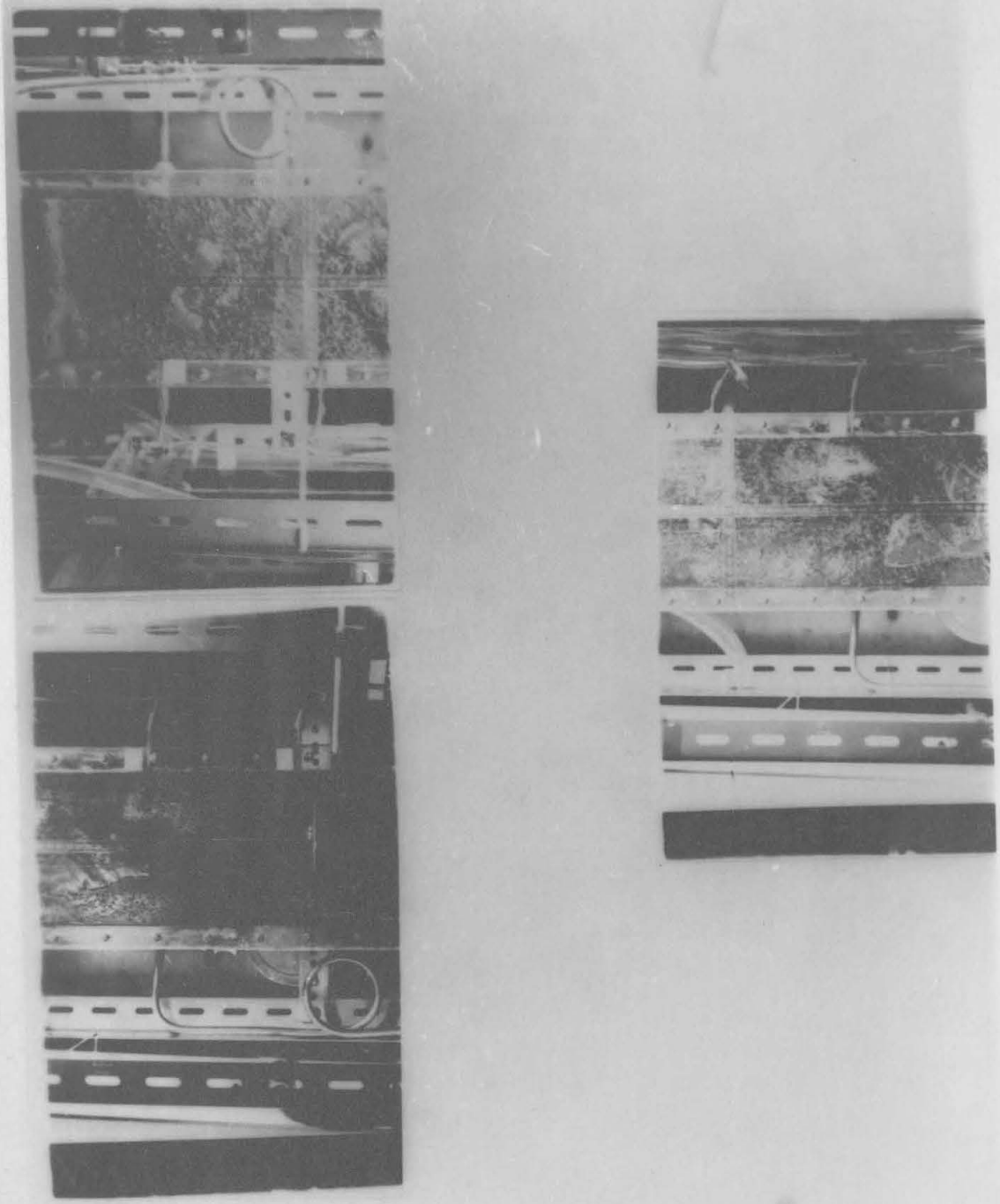

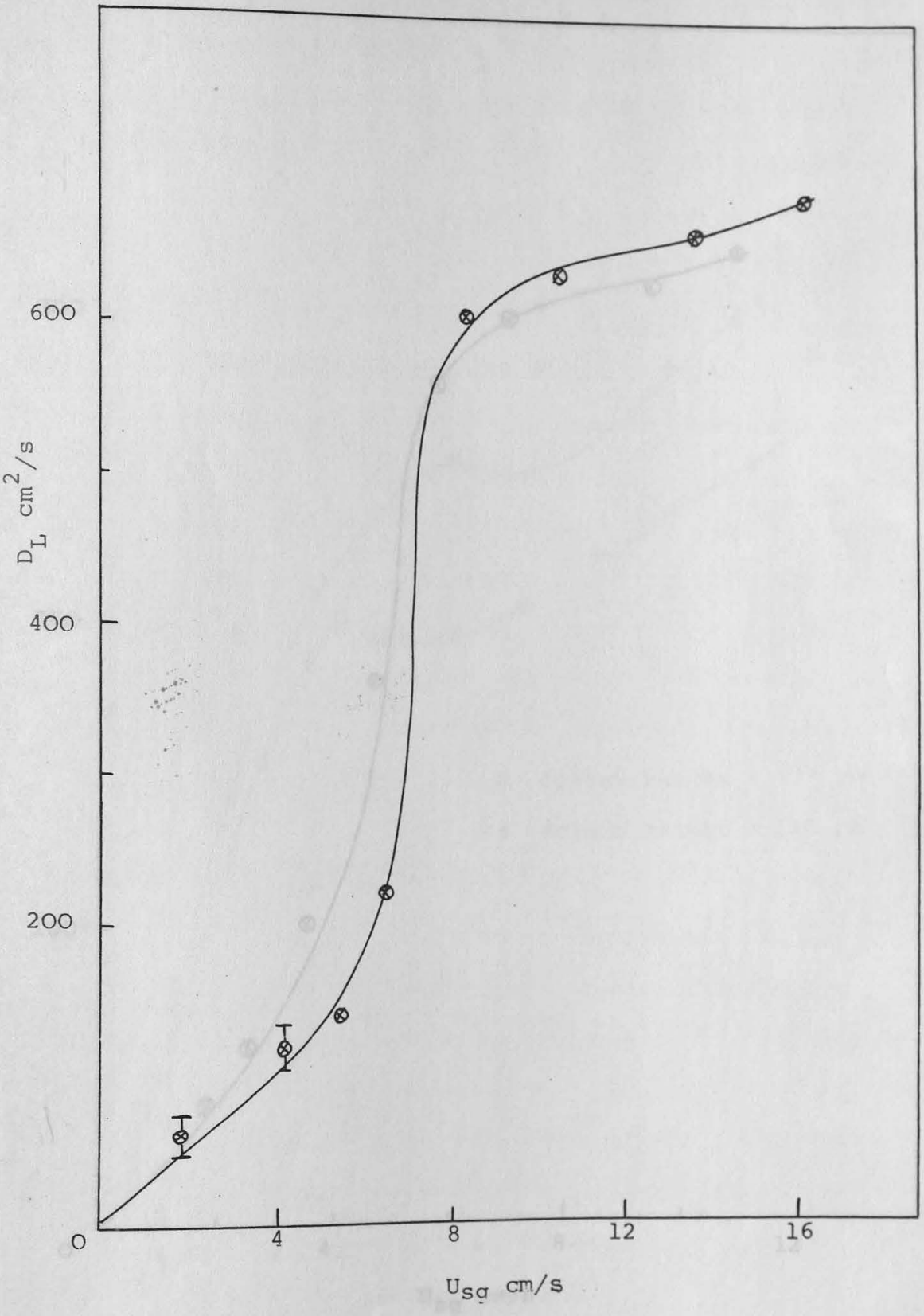

Figure 2.18 - Typical influence of superficial gas velocity on liquid dispersion coefficient in two-dimensional bubble column and for $U_{s\ell}=0$

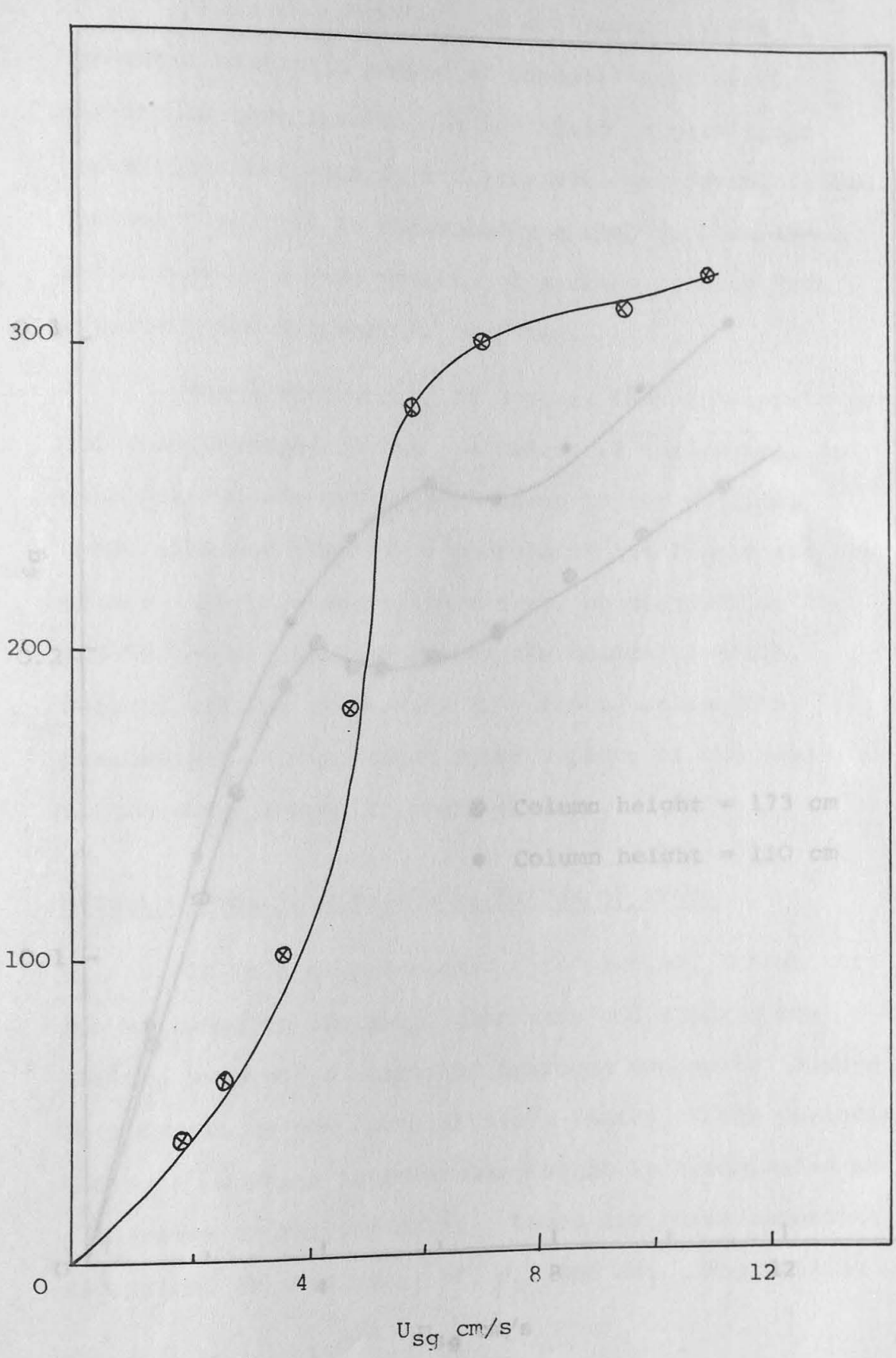

Figure 2.19 - Effect of superficial gas velocity on liquid dispersion coefficient in three dimensional bubble column and for $Us_\ell = 0$

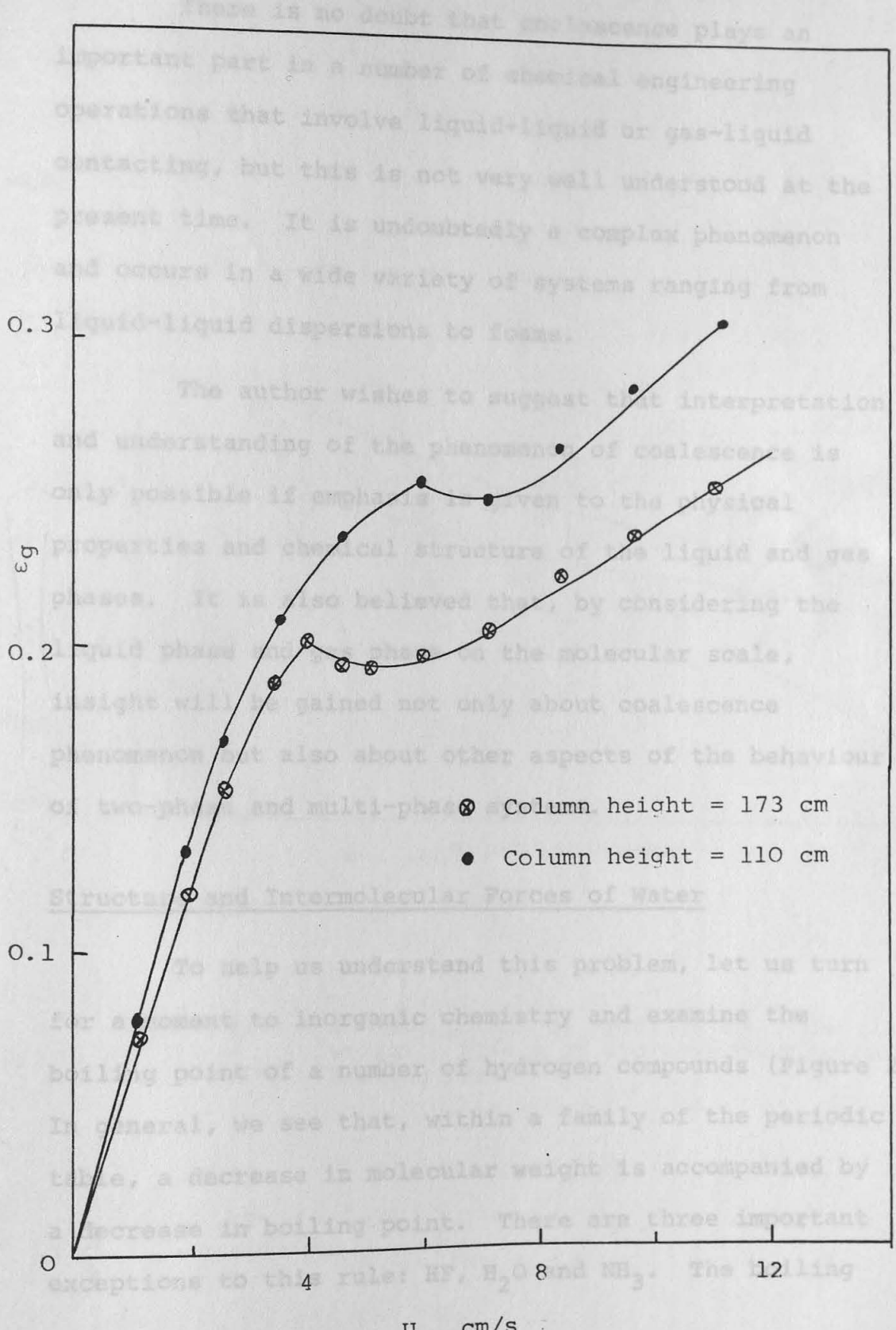

Figure 2.20 - Typical influence of column height on gas hold-up in three dimensional bubble column & for U_s = 0.045 cm/s

Introductory Comments

There is no doubt that coalescence plays an important part in a number of chemical engineering operations that involve liquid-liquid or gas-liquid contacting, but this is not very well understood at the present time. It is undoubtedly a complex phenomenon and occurs in a wide variety of systems ranging from liquid-liquid dispersions to foams.

The author wishes to suggest that interpretation and understanding of the phenomenon of coalescence is only possible if emphasis is given to the physical properties and chemical structure of the liquid and gas phases. It is also believed that, by considering the liquid phase and gas phase on the molecular scale, insight will be gained not only about coalescence phenomenon but also about other aspects of the behaviour of two-phase and multi-phase systems.

Structure and Intermolecular Forces of Water

To help us understand this problem, let us turn for a moment to inorganic chemistry and examine the boiling point of a number of hydrogen compounds (Figure 2.21). In general, we see that, within a family of the periodic table, a decrease in molecular weight is accompanied by a decrease in boiling point. There are three important exceptions to this rule: HF, H_2O and NH_3. The boiling

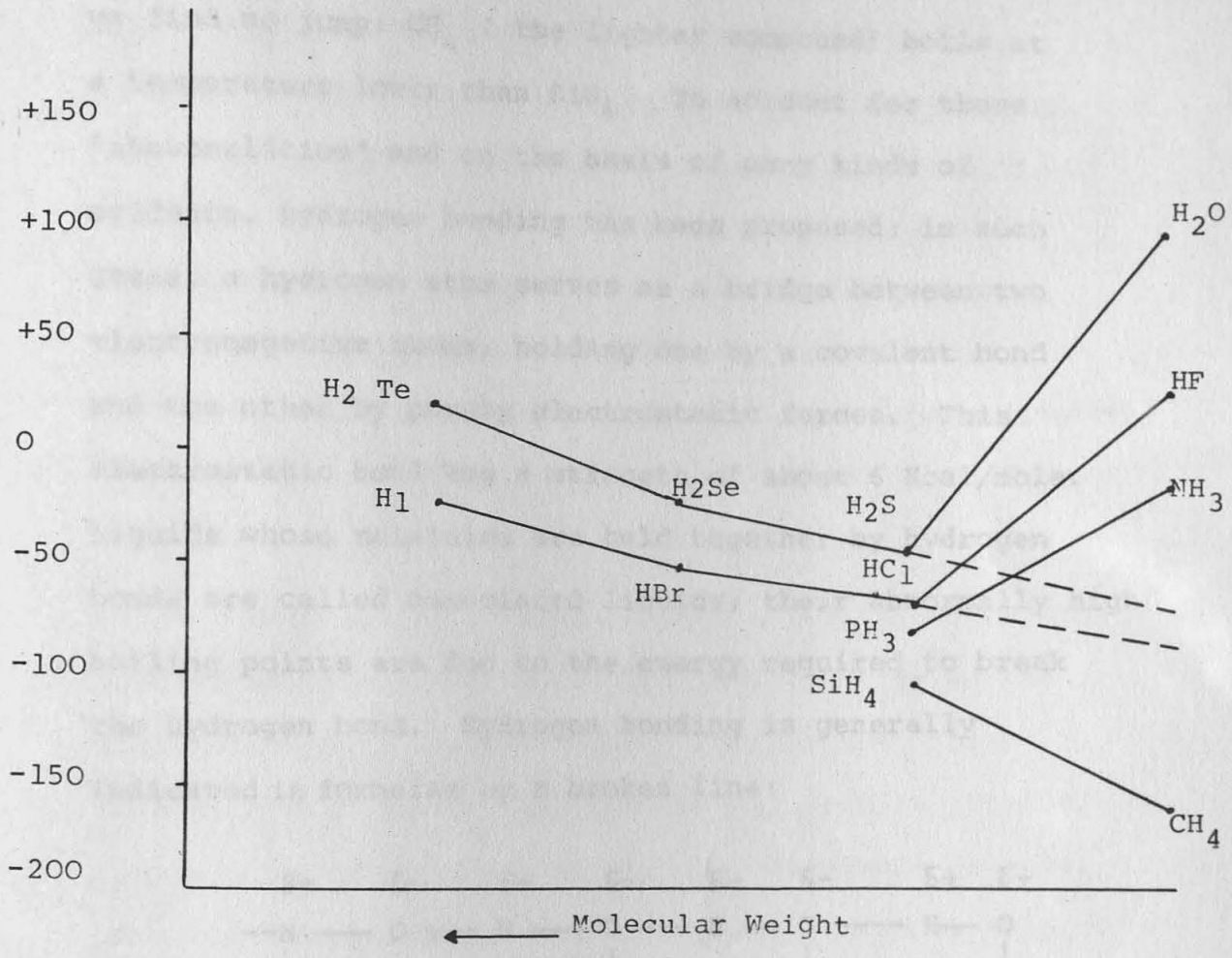

Figure 2.21 - Boiling points of hydrides vs. molecular weight. Effect of hydrogen bonding on boiling point

point decreases as we proceed from H_2Te to H_2Se to H_2S but at H_2O, which we might expect to boil at about $-80^{\circ}C$, there is a jump to $100^{\circ}C$. In the fourth family, however, we find no jump: CH_4 (the lighter compound) boils at a temperature lower than SiH_4. To account for these "abnormalities" and on the basis of many kinds of evidence, hydrogen bonding has been proposed: in such cases, a hydrogen atom serves as a bridge between two electronegative atoms, holding one by a covalent bond and the other by purely electrostatic forces. This electrostatic bond has a strength of about 6 Kcal/mole. Liquids whose molecules are held together by hydrogen bonds are called associated liquids; their abnormally high boiling points are due to the energy required to break the hydrogen bond. Hydrogen bonding is generally indicated in formulae by a broken line:

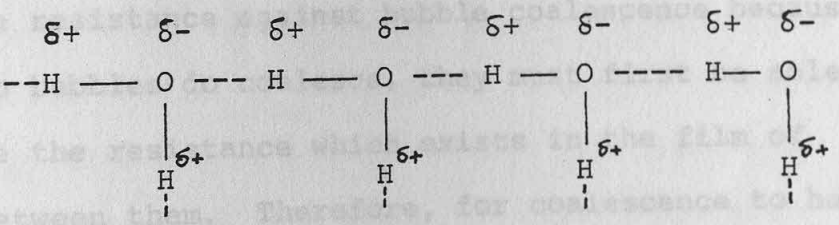

For hydrogen bonding to be important, electronegative atoms must come from the group: F, O, N. Only hydrogen bonded to one of these three elements is positive enough, and only these three elements are negative enough for the necessary attraction to exist. These three elements owe their special effectiveness to the concentrated negative charge on their small atoms.

Structure of the Gas Phase

Air is a combination of 21% oxygen and 79% nitrogen. The polarity of gas molecules such as oxygen and nitrogen is zero; therefore, they cannot make any kind of physical bond with polar liquids such as water. As a result, at the interface between water and air, the molecules of water which are at the surface can only form bonds (hydrogen bonds) with the interior water molecules whilst their exterior sides are free and unbonded. Thus the liquid surface behaves like a stretched elastic skin, and this leads to the concept of surface tension.

When air is bubbled through a pool of water, the bubbles ascend to the top of the pool by overcoming the intermolecular forces of water. Furthermore, these intermolecular forces (hydrogen bonds) seem to provide the main resistance against bubble coalescence because, when two bubbles do coalesce, they must first be able to overcome the resistance which exists in the film of water between them. Therefore, for coalescence to happen bubbles should have enough energy to break the barrier between themselves; alternatively if the resistance which exists between bubbles in some way becomes weak, the chance of bubble coalescence occurring should increase. Furthermore, as mentioned above, the main resistance to the inter-mixing of water molecules and air molecules arises from the attraction between water molecules since this effectively limits contact between water and air molecules.

2.6.2 Methods for Promoting Coalescence

It would seem that if the hydrogen bond between water molecules becomes relatively weak, then bubble coalescence should increase; it should also be possible to reach a higher level of inter-mixing between air and water molecules by partially destroying these bridges between water molecules. There are three main methods which can be used to weaken or break bonds: these can be classified under the following headings:

(1) heating the liquid;

(2) mechanical agitation;

(3) exciting the water molecules by vibration.

Effect of Heating

It is instructive to observe what happens when the temperature of the fluids in a bubble column, operating in the bubbly flow regime at low superficial gas velocities (i.e. U_{sg} = 2 cm/s) is slowly increased. The bubbly flow regime slowly becomes turbulent and bubbles coalesce and form slugs. When the temperature reaches about 60-70^{o}C (with low gas velocity) the degree of turbulence and back-mixing becomes very intense: some bubbles appear to be almost stationary just above the gas distributor whilst slugs appear to be very floppy (see Figure (2.7)) and slow moving. It is worth noting here that in a small diameter tube the rise velocity of slugs of about the same size decreases from about 32 cm/s

at 20°C to 26 cm/s at 35°C and 22 cm/s at about 65°C.

With a greater energy input to the system, for example by using a gas velocity of more than 10 cm/s, we have found that the slugs disappear and fewer visible bubbles exist or form: these observations suggest that water and air are mixed to some extent on the molecular scale.

The effect of liquid-phase temperature on gas hold-up in the two-dimensional column is shown in Figure (2.8). Figure (2.9) also shows the effect of liquid phase temperature on gas hold-up in the three-dimensional bubble column. These figures show that by using a moderate energy input to water the intermolecular forces between water molecules become weaker, and, therefore, bubbles can easily coalesce resulting in a reduction in gas hold-up.

Weakening the intermolecular forces (i.e. hydrogen bonds) of water also causes a reduction in surface tension and viscosity, because, as we mentioned in the introduction, water (in contrast to H_2S) is in the liquid state at room temperature because of its intermolecular forces. So, if we continue to increase the temperature of water, the intermolecular forces of water become weaker and weaker; therefore, the similarity or compatability between water molecules and the gas phase molecules increases. When the temperature of water

reaches about 70°C the column looks blurred, due in part to the evaporation of water molecules into the gas bubbles. At this stage, if we provide more energy to the system, for example by increasing gas velocity, the slugs disappear altogether and only small bubbles are seen.

Liquid Agitation

(1) Mechanical Agitation

The purpose of agitation is the transfer of liquid particles from one part of the system to another. Looked at another way, agitation is a mechanical method for breaking bonds. The idea is further illustrated by considering what happens in a mechano-chemical reaction: if a viscous solution of polymer, say a 1% solution of natural rubber, is stirred vigorously, the molecular weight of polymer will decrease, since the energy input leads to the rupturing of bonds between polymer units.

Let us consider now the effect of mechanical agitation on the behaviour of gas-liquid dispersions. Although there is a lot of literature about gas hold-up, interfacial areas and mass transfer coefficients in stirred tank reactors, most of it refers to experiments carried out at relatively low superficial gas velocities ($U_{sg} \leq 1$ cm/s). However, it is necessary to study the research carried out at superficial gas velocities comparable with those used in bubble column reactors ($1 \leq U_{sg} \leq 5$ cm/s) in order to discover the effect of agitation.

Reith and Beek (66), who studied bubble coalescence in a stirred tank reactor in the range of $1 \leqslant U_{sg} \leqslant 3$ cm/s, found that at low stirrer speed ($<$10 revs/s), there was no coalescence but, at higher stirrer speeds, more bubbles were entrained and recirculated before they left the vessel. Under these later conditions, they observed bubble coalescence, and for stirrer speeds $>$15 revs/s coalescence was complete.

Preen (67) concluded that practically all gas disintegration takes place in the neighbourhood of the impeller while in parts of the vessel away from the agitator coalescence occurs.

Figure (2.10), based on the work of Falch and Gaden (69), shows the effect of agitator speed on gas hold-up. It illustrates how the bubble coalescence increases when the agitator speed exceeds 300 rpm.

Figures (2.11) and (2.12) show the average gas hold-up for two-and three-dimensional bubble columns using moderate mechanical agitation. It appears that coalescence is higher when agitation is employed.

(2) Agitation due to the Gas Phase: The effect of Superficial Gas Velocity

When a gas is bubbled into a liquid through a series of orifices, such as a perforated plate, the pressure energy contained in the gas serves two purposes:

it is used in creating gas bubbles and, at the same time, in agitating the liquid as the bubbles force their way to the top of the column by overcoming the intermolecular forces in the liquid. The amount of agitation of the liquid phase caused by bubbles depends on the superficial gas velocity. In the bubbly flow regime, the bubbles are able to clear a way in an axial direction without any collisions or coalescence occurring. Therefore, the column is uniform in appearance, and the extent of liquid phase agitation is not significant. On increasing the gas velocity, eventually a point will be reached when the bubbles are able to overcome surface tension forces and coalesce. Increasing the gas velocity above this transition point leads to the formation of many large bubbles which ascend at the centre of the column following a snake-like path: this is often referred to as the slug flow or turbulent regime. At very high gas velocities, the slugs will become unstable and break-up resulting in higher gas hold-ups.

The Effect of Vibration

The intensity, or loudness, of a sound depends upon the extent, or amplitude, of the vibration set up, and its pitch upon the frequency, or number of vibrations per second. Disturbances of the same type as sound waves may be inaudible either because the intensity (loudness) is insufficient or because the ear is deaf to

those particular frequencies. The normal range of hearing extends approximately from 20 to 20,000 vibrations per second; sounds of higher frequency than 20,000 are called supersonic or ultrasonic. Ultrasonic excitation is a second method of changing the level of molecular energy. There are a number of reports on the effect of ultrasonic energy on the behaviour of air-water systems and some are considered below: the author, himself, has not carried out any work using this method of energy input.

Gaines (56) showed that, if intense audible sound is introduced into a vessel containing water cloudy with tiny air bubbles, these immediately coalesce to form large bubbles which rise to the surface, the water becoming clear in a few seconds. A similar effect of ultrasonic sound has been reported by Harvey (57).

Buchanan et al. (58) showed that at low vibration frequencies the surface of the liquid exhibits various modes of surface wave whose configuration depends on the frequency of vibration: when they increased the vibration the surface lost definition becoming a turbulent zone of droplets and bubbles.

Blake (59) has found that extremeley small bubbles can appear at the pressure antinodes; these then coalesce to form bubbles up to a millimetre or so in diameter, and bubbles of this order of size, or slightly larger, are also observed streaming away from the major pressure antinodes.

Goldman and Ringo (60) subjected water super-saturated with carbon dioxide to a moderately intense standing wave field of 60 KC/s: they observed formation of bubbles of all sizes.

Boyle (61) in his work produced stationary waves by placing a generator above a vertical column of liquid, the air-liquid surface serving as a reflector: he found that it is possible to adjust the operating conditions so as to produce either large or small bubbles in the liquid. When large bubbles were produced they rose rapidly through the liquid, but the small bubbles, especially at very high frequencies, could be made to stay almost stationary.

Minnaert (62) has given the following formula for predicting the average diameter of bubbles in a vibrated bed:

$$F = \frac{656}{d_b} ,$$

where "f" is the frequency in cycles/s and d_b is the bubble diameter in cm. The diameter corresponding to 840 cycles/s is 7.8 mm; this is a much larger diameter than that usually found under similar conditions in the absence of sound (63).

The above results clearly indicate that sound, like heat, may cause coalescence at moderate frequencies and break up large bubbles to create a uniform dispersion

of air in water at high frequencies. These phenomenon have been clearly described by Lloyd Hopwood (64) following his studies of the effect of ultra-sonic vibration over a wide frequency range on the behaviour of gas-liquid mixtures. He observed that with moderate intensities of vibration, the bubbles formed slowly and, as they grew in size (due to coalescence), they oscillated and tended to rise to the surface in an irregular zigzag manner. For high intensities, he found that no gas bubbles were even visible. Therefore, as explained before, if in some way the inter-molecular forces of water (i.e. the H-bonds) are weakened, the chance of bubble coalescence occurring will increase. However, if the water molecules are excited to such an extent that the inter-molecular forces are almost destroyed, then mixing between water and air molecules will occur on a molecular scale; consequently, few bubbles will exist.

2.6.3 Gas Flow Patterns

In the bubbly flow regime, visual observations and high-speed photography show that the bubbles detaching from the gas distributor are about 5 mm in diameter and ascend through the liquid phase without colliding or coalescing; the degree of bubble backmixing at the sides of the column is also very low (see Figure (2.15)).

At higher superficial gas velocities, the bubbles coalesce within a few centimetres of the gas distributor and large bubbles form; these ascend at the centre of the column along a wave-like path, as Figure (2.16) shows. The slugs carry a considerable amount of liquid in their wakes: in addition, high-speed photography shows that when a slug is rising a large number of small bubbles also rise in its wake (see Figure (2.17)). Later, when the slugs leave the system, the small bubbles in the wake cannot overcome the downwards liquid flow and so, they get dragged downwards with the liquid at the sides of the column. These small bubbles near the wall of the column can move downwards as far as the gas distributor; for this reason, the density of bubbles (i.e. gas hold-up) at the bottom of the column often appears to be high.

Visual observations and high-speed photography also show that liquid and gas circulate rapidly in "mixing" cells created by the snake-like movement of the slugs. At the centre of each cell large bubbles form due to the relatively high density of gas; these large bubbles also tend to coalesce with the slugs which are ascending at the centre of the column.

2.6.4 Liquid Flow Patterns and Liquid Phase Mixing

Liquid mixing in bubble columns is a process in which adjacent components of a volume of liquid move away

from each other at a certain time. Depending upon the size of the components, the finest mixing evidently is that in which the molecules represent the components which change location. The displacement of these components (or molecules) from each other in bubble columns is caused by rising bubbles, and the intensity of these movements depends on the gas velocity (i.e. the energy input).

Figures (2.18) and (2.19) show the effect of superficial gas velocity on the liquid dispersion coefficient measured at the side of the column using the unsteady-state calorimetric method described in Section (2.3.2). Studies of mixing in the liquid phase of bubble columns have been carried out by numerous investigators over the years, and the trends from the author's work are in good agreement with the findings of others (70, 71, 72, 73, 74, 75).

Three regions(bubbly flow, a transition region and slug-flow) can clearly be recognised in the above figures. These regimes correspond with regimes identified by means of visual observations. In the bubbly-flow regime, the bubbles do not transport a large volume of liquid upwards and so the extent of liquid backmixing at the side of the column is low. By comparison, in the slug (or turbulent) flow regime, liquid transport is greatly enhanced and strong circulation patterns are set up.

2.6.5 The Effect of Liquid Flow-Rate

The author's results showing the effect of superficial liquid velocity are summarised in Figures (2.13) and (2.14) for the two-and three-dimensional bubble columns respectively. The plots indicate that as the liquid flowrate increases gas hold-up slightly increases in the bubbly flow regime but decreases in the turbulent flow regime: the effect on the transition point should also be noted. These trends can be explained as follows: as U_{sl} increases, liquid circulation in the bubbly-flow regime is reduced and gas hold-up increases; however, when slugs form, it would seem that the intensity of liquid circulation increases with U_{sl} leading to a decrease in gas hold-up.

2.6.6 The Effect of Column Height and Diameter

The effect of column height on average gas hold-up is illustrated by the results plotted in Figure (2.20) (see also (72)). Many investigators, in particular Siemes et al. (71), have shown that the mixing in bubble columns increases significantly with bed height and column diameter. In other words, as column height or diameter increases the intensity of liquid agitation increases; consequently a lower hold-up is to be expected.

2.7 Methods for Suppressing Bubble Coalescence

2.7.1 Introduction

In section (2.6), factors which cause coalescence phenomena were discussed. Two important parameters which assist bubble coalescence are (1) liquid-phase backmixing (which becomes significant at $U_{sg} > 4$ cm/s in the three-dimensional bubble column) and (2) the bubble rise velocity. Therefore, it appears that if, in some way, it is possible to inhibit liquid circulation or decrease bubble velocity, bubble coalescence will to some extent be suppressed and gas hold-up increased.

2.7.2 The Suppression of Circulatory Flows

It is apparent that the liquid-phase backmixing in bubble columns has a detrimental effect on gas hold-up. Unfortunately, this circulation flow is intensified on scaling up bubble columns, and the only practical way of reducing it is to fit radial baffles. This type of modified bubble column would appear to be better than other types of multistage tower fermenter. To date the design of such baffles and the effect they have on the performance of bubble columns have received very little attention. As far as the author can ascertain, Fair et al. (3) are the only researchers to have carried out any experiments on a commercial scale, sparged contactor using the air-water system. They used a column 45.7 cm

in diameter, 320 cm high and constructed of plexi-glass. For some experiments, an assembly of 20 perforated-plate baffles spaced 14 cm apart was suspended in the vessel: in some of the tests, the baffles were subjected to a rapid (17.5 cycles/s) reciprocating motion. Data were collected on gas hold-up for air-water with and without the baffles. Figure (2.22), presented by these authors, shows how the baffles increased gas hold-up by some 40 to 50% (by reducing liquid backmixing). Movement of the baffles further increased the hold-up by some 25 to 30% over the stationary case, as is shown in Figure (2.23).

2.7.3 The Reduction of Bubble Velocity

As mentioned before, in the bubbly-flow regime, the bubbles leaving the gas distributor were relatively small and uniform in size and ascended through the liquid-phase without coalescence. At higher superficial gas velocities (U_{sg} > 4 cm/s in the three-dimensional bubble column) the bubbles were seen to coalesce at a point a few centimetres above the gas distributor. This phenomena has also been observed by Koide et al. (49) who found that bubbles generated from porous plates are small and of equal size at low gas velocities but coalesce at a point slightly removed from the gas distributor in pure water and solvents at high gas velocities. Marrucci et al. (50) also observed that the

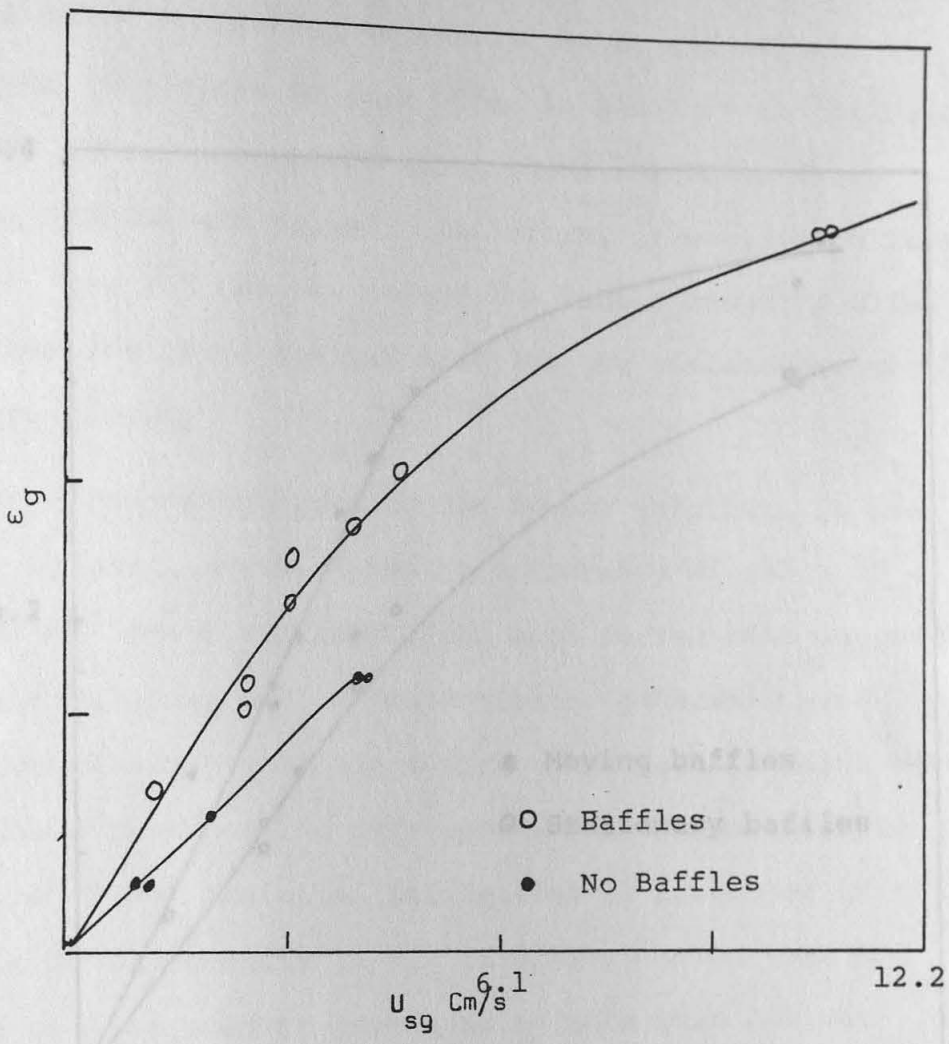

Figure 2.22 - Effect of close-fitting perforated baffles on gas hold-up

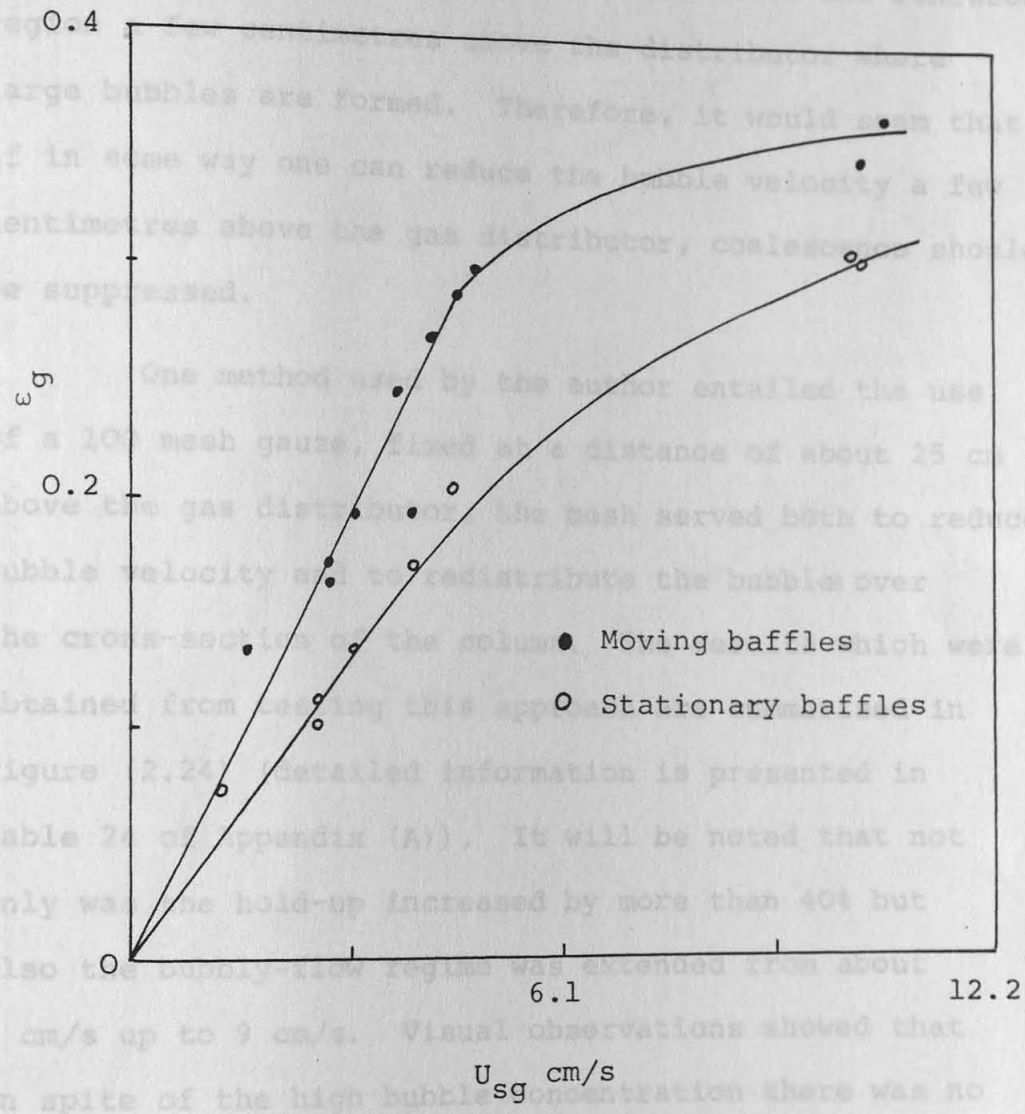

Figure 2.23 - Effect of moving baffles on gas hold-up

bubbles detaching from a porous plate are very small and uniform but strong convective motions bring all the streams very close to each other in a narrow and confused region a few centimetres above the distributor where large bubbles are formed. Therefore, it would seem that if in some way one can reduce the bubble velocity a few centimetres above the gas distributor, coalescence should be suppressed.

One method used by the author entailed the use of a 100 mesh gauze, fixed at a distance of about 25 cm above the gas distributor; the mesh served both to reduce bubble velocity and to redistribute the bubbles over the cross-section of the column. The results which were obtained from testing this approach are summarised in Figure (2.24) (detailed information is presented in Table 24 of Appendix (A)). It will be noted that not only was the hold-up increased by more than 40% but also the bubbly-flow regime was extended from about 4 cm/s up to 9 cm/s. Visual observations showed that in spite of the high bubble concentration there was no sign of coalescence.

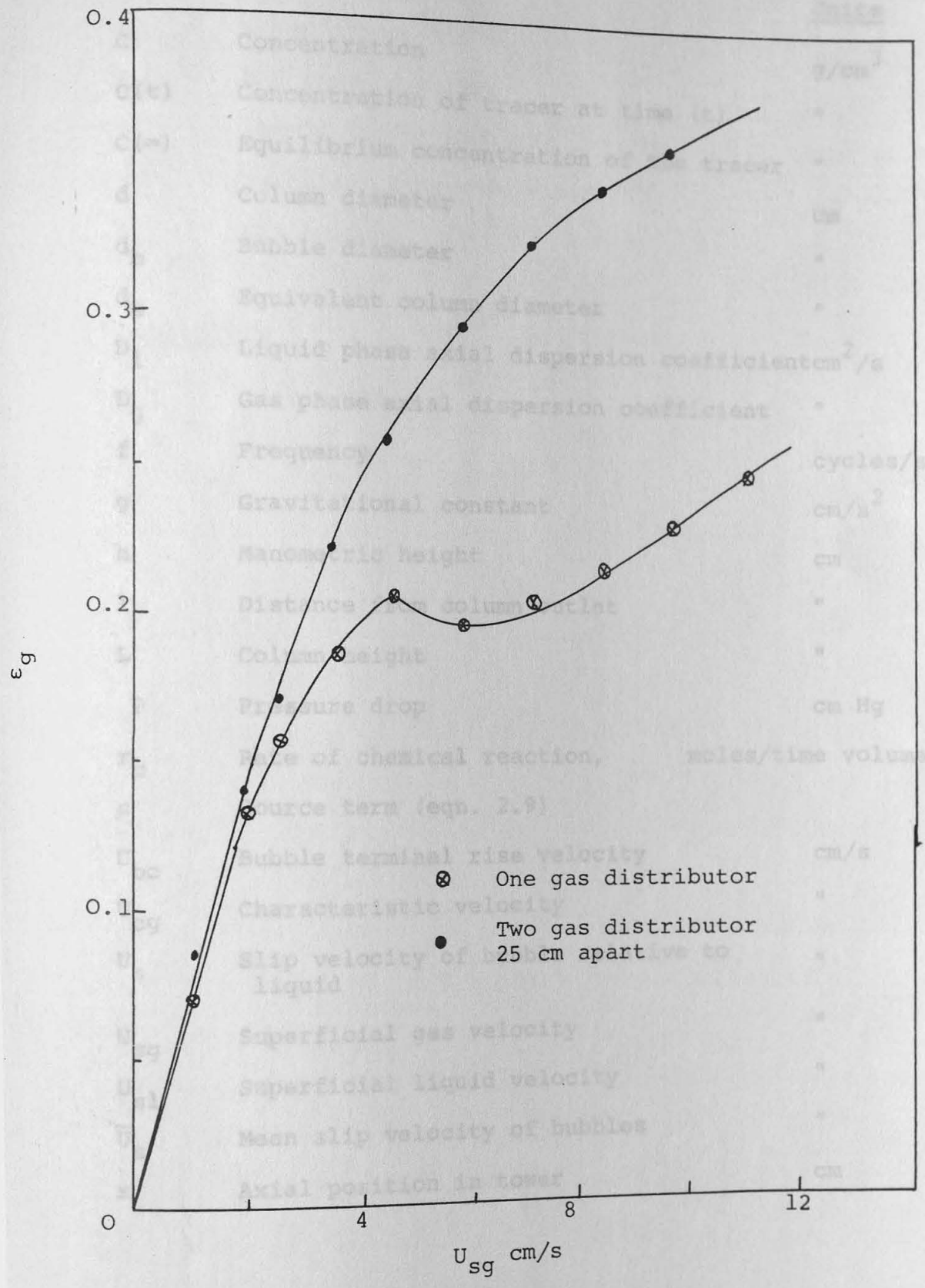

Figure 2.24 - Effect of _____ second gas distributor on gas hold-up, in three dimensional bubble column & for $U_{s\ell}$=0.17 cm/sec

Nomenclature

		Units
C	Concentration	g/cm^3
$C(t)$	Concentration of tracer at time (t)	"
$C(\infty)$	Equilibrium concentration of the tracer	"
d	Column diameter	cm
d_b	Bubble diameter	"
d_e	Equivalent column diameter	"
D_l	Liquid phase axial dispersion coefficient	cm^2/s
D_g	Gas phase axial dispersion coefficient	"
f	Frequency	cycles/s
g	Gravitational constant	cm/s^2
h	Manometric height	cm
l	Distance from column outlet	"
L	Column height	"
P	Pressure drop	cm Hg
r_c	Rate of chemical reaction,	moles/time volume
s	Source term (eqn. 2.9)	
U_{bo}	Bubble terminal rise velocity	cm/s
U_{cg}	Characteristic velocity	"
U_s	Slip velocity of bubble relative to liquid	"
U_{sg}	Superficial gas velocity	"
U_{sl}	Superficial liquid velocity	"
$\overline{U}_s$	Mean slip velocity of bubbles	"
x	Axial position in tower	cm

Greek Letters

ρ_L	Liquid phase density	g/cm^3
ρ_G	Gas phase density	"
μ_L	Liquid phase viscosity	g/cms or cP
ν_t	Turbulent kinematic viscosity	cm^2/s
ε_g	Gas hold-up	

Subscripts

l,L	Liquid phase
g,G	Gas phase

References

1. Yamashita and Inoue. J. of Chem. Eng. of Japan, 8, 334 (1975).
2. Aoyama, Y., Ogushi, K., Koide, K., and Kubota, H. J. of Chem. Eng. of Japan, 1, 158 (1968).
3. Fair, J.R., Lambright, A.J., and Andersen, J.W. Ind. Eng. Chem. Process Des. Dev., 1, 33 (1962).
4. Nicklin, D.J., Wilkes, J.O. and Davidson, J.F. Trans. Inst. Chem. Eng., 40, 61 (1962).
5. Braulick, W.J., Fair, J.R. and Lerney, B.J. A.I.Ch.E. Journal, 11, 73 (1965).
6. Akita, K. and Yoshida, F. A.I.Ch.E. Journal, 11, 9 (1965).
7. Towell, G.D., Strand, C.P. and Ackerman, G.H. A.I.Ch.E. Symp. Ser. 10, 97, (1965).
8. Hughmark, G.A. Ind. Eng. Chem. Process Des. Dev., 6, 218 (1967).
9. Reith, T., Renken, S. and Israel, B.A. Chem. Eng. Sci., 23, 619 (1968).
10. Van Dierendonck, L.L., Fortuin, J.M. and Venderbos, D. European Symp. on Chemical Reaction Engineering, Brussels, Sept. 1968, Pergamon, Oxford, 1971, p.105.
11. Voyer, R.D. and Miller, A.I. Can. J. Chem. Eng., 48, 335 (1968).
12. Freedman, W. and Davidson, J.F. Trans. Inst. Chem. Eng., 47, 335 (1968).

13. Kunugita, E., Ikura, E. and Otake, T. J. of Chem. Eng. Japan, 3, 24 (1970).

14. Kato, Y. and Nishiwaki, A. International Chem. Eng., 12, 182 (1972).

15. Akita, K. and Yoshida, F. Ind. Eng. Chem. Process Des. Dev., 12, 76 (1973).

16. Deckwer, W.D., Burckhart, R. and Zoll, G. Chem. Eng. Sci. 29, 2177 (1974).

17. Hobbs, S.Y., Pratt, C.F. A.I.Ch.E. Journal, 20, 1978 (1974).

18. Kastanek, F., Nyvlt, V. and Rylek, M. Collect. Czech. Chem. Commun, 39, 528 (1974).

19. Essa, S. Schugerl, K. Chem. Eng. Sci., 30, 1251 (1975).

20. Pexidr, V. and Charpentier, J.C. Collect. Czech. Chem. Commun., 40, 3130 (1975).

21. Kawagoe, K., Inoue, T., Nakao, K. and Otake, T. Int. Chem. Eng., 16, 176 (1976).

22. Koetster, W.T., Vanswaaij, W.P.M. and Vandermost, M. J. of Chem. Eng. of Japan, 9, 332 (1976).

23. Kumar, A., Degaleesan, T.E., Laddha, G.S. and Hoselscher, H.E. Can. J. Chem. Eng., 54, 503 (1976).

24. Todt, J. Lucke, J., Schugerl, K. and Renken, A. Chem. Eng. Sci., 32, 369 (1977).

25. Schugerl, K. and Lucke. J. Advances in Biochemical Eng., 7 (1977), 1.

26. Hsu, H.H., Erickson, L.E. and Fan, L.T. Biotechol. Bioeng. 19, 247 (1977).

27. Hills, J.H. Chem. Eng. J., 12, 89 (1976).

28. Koide, K., Morooka, S., Ueyama, K., Matsuura, A., Yamashita, F., Iwamoto, S., Kato, Y., Inoue, H., Shigeta, M., Suzuki, S. J. of Chem. Eng. of Japan, 12, 98 (1979).

29. Hikita, H., Asai, S., Tanigawa, K., Segawa, K. and Kitao, M. Chem. Eng. J., 20, 59 (1980).

30. Bischoff, K.B. and Phillips, J.B., Ind. Engng. Chem. Process Design Develop., 5, 416 (1966).

31. Argo, W.B. and Cova, D.R. Ind. Engng. Chem. Process Design Develop, 4, 352, (1965).

32. Kim, D.S., Baker, C.G.J. and Bergougnon, M.A., Can. J. Chem. Engng., 50, 695, (1972).

33. Shayegan-Salek, J., Ph.D. Thesis, University of Aston in Birmingham (1974).

34. Kasturi, G. and Stepanek, J.Chem. Eng. Sci. 29, 713 (1974).

35. Ostergaard, K. and Michelsen, M.L. Symp. on Fundamental and Applied Fluidisation, Tampa, Florida, May (1968).

36. Ellis, J.E. and Jones, E.L. Two-Phase Flow Symp., Exeter, 2,-B102 (1965).

37. Shulman, H.L. and Molstad, M.C. Ind. Engng. Chem., 42, 1058 (1950).

38. Downie, J. Ph.D. Thesis, University of Aston in Birmingham (1972).

39. Ohki, Y. and Inoue, H. Chem. Eng. Sci, 25, 1 (1970).

40. Bridge, A.G., Lapidus, L. and Elgin, J.C. A.I.Ch.E. Journal, 10 (1964), 819.

41. Sideman, S., Hortescg, O., and Fulton, J.W. Ind. Eng. Chem. 58 (7), 32, (1966).

42. Bahga, D. and Weber, M.E. Can. J. Chem. Eng., 50 (1972), 323.

43. Lockett, M.J. and Kirkpatrick, R.D. Trans. Inst. Chem. Engrs. 53 (1975), 267.

44. Richardson, J.F. and Zaki, W.N. Trans. Inst. Chem. Engrs., 32 (1954), 35.

45. Ueyama, K. and Miyauchi, T. A.I.Ch.E. Journal, 25 (1979), 258.

46. Leibson, I., Holcomb, E.G., Cocoso, A.G. and Jacmic, J. A.I.Ch.E. Journal, 2 (1965), 296.

47. Braulick, W.J., Fair, J.R. and Lerner, B.J. A.I.Ch.E. Journal, 11 (1965), 73.

48. Moissis, R. and Griffith, P. U.S. Office of Naval Research No. NR 1814 (39) DSR Project No. 7-7673 Tech. Rept. No.18, June (1960).

49. Koide, K., Kato, S., Tanak, Y. and Kubota, H. J. of Chem. Eng. of Japan, 1 (1968), 51.

50. Marrucci, G. and Nicodemo, L. Chem. Eng. Sci., 22 (1967), 1257.

51. Crabtree, J.R. and Bridgwater, J. Chem. Eng. Sci. 26 (1971) 839.

52. Hills, J.H., Trans. Inst. Chem. Engrs, 53 (1975), 224.

53. Lee, J.C. and Hodgson, T.D. Chem. Eng. Sci. 23 (1968), 1375.

54. Marrucci, C. Chem. Eng. Sci. 24 (1969), 975.

55. Darton, R.C., Nauze, R.D., Davidson, J.F. and Harrison, D. Trans. Inst. Chem. Engrs. 55 (1977), 274.

56. Gaines, N. Physics, 3 (1932), 209.

57. Harvey, Biol. Bull. 59 (1930), 306.

58. Buchanan, R.H., Jameson, G. and Oedjoe, D. I. and E.C. Fundamentals, 1 (1962), 82.

59. Baird, M.H.I. Chem. Eng. Sci. 17 (1962), 87.

60. Goldman, D.E. and Ringo, G.R. J. Acoust. Soc. Amer., 21 (1949), 270.

61. Boyle, R.W. Nature, 120 (1927), 476.

62. Minnaert, M. Phil. Mag., 16 (1933), 235.

63. Houghton, G. Mclean, A.M. and Ritchie, P.D. Chem. Eng. Sci., 7 (1957), 26.

64. Prof. F. Lloyd Hopwood. Nature, 128 (1931), 748.

65. Towell, G.D., Strand, C.P. and Ackermann, B.S. in Rottenburg, P.A. (Ed.) "Mixing:Theory related to Practice" 1965, (London:-I.Chem.E.).

66. Reith, T. Jr., and Professor Beek, W.J. Trans. Inst. Chem. Engrs, 48 (1970), T63.

67. Preen, B.V. Ph.D. Thesis, University of Durban, South Africa, 1961.

68. Yoshitome, H., Kagaku Kogaku. 27 (1963), 27.

69. Falch, E. and Gaden, E. Biotec.and Bioeng. XI (1969), 927.

70. Argo, W.B. and Cova, D.R. Ind. Eng. Chem. Process Design and Develop., 4 (1965), 352.

71. Siemes, W. and Weiss, W., Chemie-Ingr-Tech., 29 (1957), 727.

72. Habil, F. Chemie. Ing. Techn, 44, (1972), 697.

73. Kunugita, E., Ikur, M. and Otake, T. J. of Chem. Eng. of Japan, 3 (1970), 24.

74. Tadaki, T. and Maeda, S. Chem. Eng. Tokyo, 2 (1964), 195.

75. Ostergaard, K. A.I.Ch.E. Symp. Series, 74 (1978), 82.

76. Levenspiel, O. and Bischoff, K.B. Adv. Chem. Eng., 4 (1963), 95.

77. Mashelkar, R.A. Brit. Chem. Eng., 15 No.10, 1297 (1970).

78. Bischoff, K.B., Ind. Eng. Chem., 58, No.11, 18 (1966).

79. Pavlica, R.T. and Olson, J.H. Ind. Eng. Chem. 62, No.12, 45 (1970).

80. Badura, R., Deckwer, W.D., Warnecke, H.J. and Langermann, H. Chemie Ing. Techn., 46 No.9, 399 (1974).

81. Hikita, H. and Kikuawa, H. Chem. Eng. J., 8 (1974), 191.

82. Cova, D.R. Ind. Eng. Chem. Process Design Develop, 13 No. 3, 292 (1974).

83. Alexander, B.F. and Shah, Y.T. Chem. Eng. J., 11 (1976), 153.

84. Field, R.W. and Davidson, J.F. Trans. Inst. Chem. Eng., 58 (1980), 228.

85. Towell, G.D. and Ackerman, G.H. Proceedings of the Fifth European Second International Symp. on Chemical Reaction Engineering, p.B3-1, Amsterdam (1972).

86. Baird, M.H.I., and Rice, R.G. Chem. Eng. J., 9 (1975), 17.

87. Ueyama, T. and Miyauchi, T. Kagaku Kagaku Ronbunshu, 2 (1977), 155.

88. Stiegel, G.J., and Shah, Y.T. Can. J. Chem. Eng. 55 (1977), 3.

89. Whalley, P.B. and Davidson, J.F. Proceedings of the Symp. on Multi-phase Flow Systems, Symp. Series. No. 38 (1975).

90. Joshi, J.B., and Sharma, M.M. Trans. Inst. Chem. Engrs. 54 (1976), 42.

91. Neal, L.G. and Bankoff, S.G. A.I.Ch.E. Journal, 9, (1963), 490.

92. Hills, J.H. Trans. Inst. Chem. Engrs., 52 (1974), 1.

93. Rigby, G.R., G.P. Van Blockland., Park, W.H. and Capes, C.E. Chem. Eng. Sci., 25 (1970), 1729.

94. Darton, R.C. and Harrison D. Some Properties of Gas Bubbles in Three-Phase Fluidised Bed. Symp. on Multiphase Flow Systems, Strathclyde 1974.

95. Marchaterre, J.F. and Petrick, J. Nucl. Sci. Eng. 7 (1960), 525.

96. Isbin, H.S., Rodriguez, H.A., Larson, H.C. and Pattie, B.D. A.I.Ch.E. Journal, 5 (1959), 427.

97. Perkins, N.C. Yusuf, M. and Leppert, G. Nucl. Sci. Eng. 11 (1961), 304.

98. Botton, R. and Cosserat, D. The Chem. Eng. J., 16 (1978), 107.

99. Nicklin, D.J. Chem. Eng. Sci. 17 (1962), 693.

3 Gas-Phase Study in the Two-Dimensional Bubble Column

3.1 Introduction

Data showing the influence of gas properties on the gas hold-up in bubble columns are scarce and lead to conflicting conclusions. Bhaga et al. (1) and Koetsier et al. (2) concluded from the results of their experiments that an increase in the gas density results in increasing gas hold-up, while Akita and Yoshida (3) and Shulman and Moslstad (4) reported that the nature of the gas had no effect. Recently, Hikita et al. (5) mentioned that the effects of gas density and the gas viscosity on the gas hold-up are not so great. Since industrial processes, in which a liquid is contacted with a gas, are numerous, it is essential to clarify the effect of the nature of gases on gas hold-up; as an introduction, it is instructive to start with the parameters which have most effect on the solubilities of gases in polar and non-polar liquids.

3.2 Solubilities of Gases in Liquids

Solubilities in water of many gases have been reported in the literature; they range in terms of solute mole fraction from about 0.000007 for helium to about 0.3 for ammonia at 25^{o}C. Whereas for non-polar

solvents a considerable degree of success has been achieved in explaining the order of gas solubilities and the variation with temperature, such success has largely eluded workers dealing with aqueous and similar solutions.

Solubilities are not the same for a particular gas in all non-polar solvents, and there appears to be a dependence on the solvent internal pressure or solubility parameter. On the other hand, solubilities in water and other polar and associating solvents are usually much lower than the ideal solubilities, except in a few cases. The reduction in solubility has been attributed to hydrogen bonding or association (Garrett (6)), which appears to have the effect of "excluding" solute molecules. Solubilities above ideal solubilities may be considered to involve some degree of chemical association or solvation, for example when NH_3 dissolves in water.

For non-polar and even slightly polar solvents it has been found that solubilities of all gases appear to approach a constant molar concentration as the solvent critical temperature is approached (7,8).

Gas solubilities in water (9) and chlorobenzene (a non-associated solvent) (8,10,11,12) are shown in Figures (3.1) and (3.2) respectively. It is readily apparent that the solubilities are usually much lower in water, and, in some cases such as paraffin gases, the

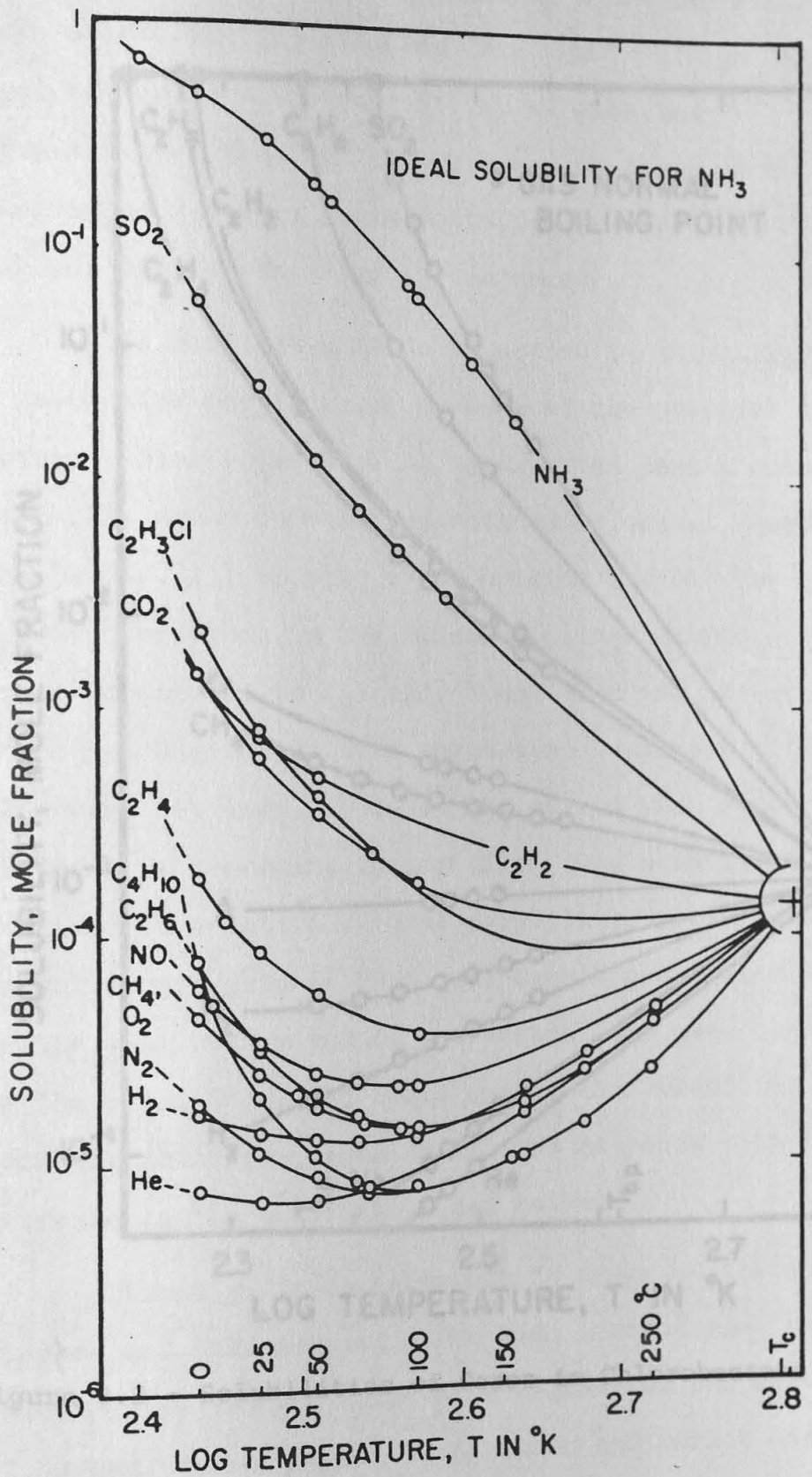

Figure 3.1 - Solubilities of Gases in Water

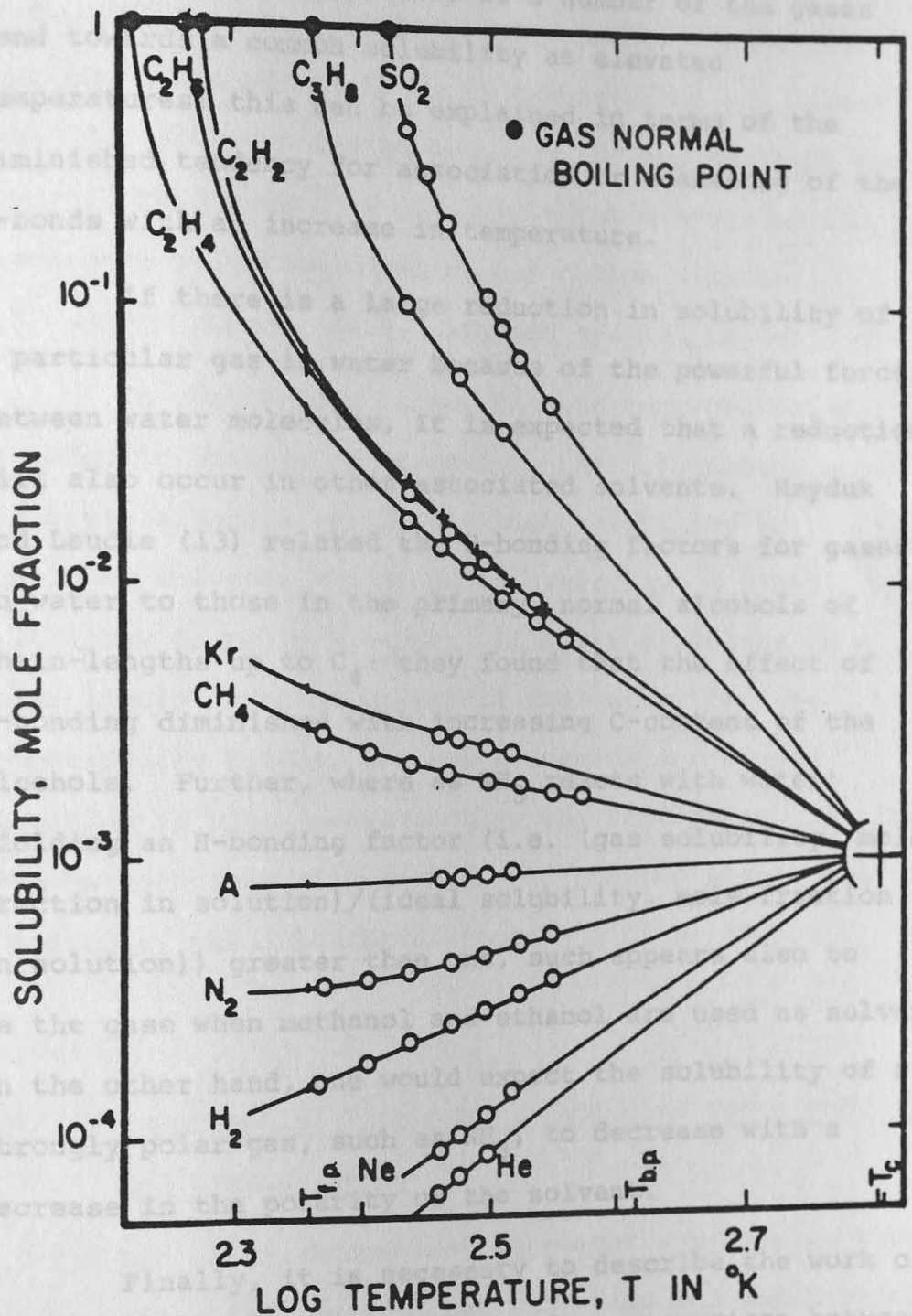

Figure 3.2 - Solubilities of Gases in Chlorobenzene

solubilities are reduced by factors of thousands. It is also clear that even in a highly H-bonding solvent, like water, the solubilities of a number of the gases tend towards a common solubility at elevated temperatures; this can be explained in terms of the diminished tendency for association or weakening of the H-bonds with an increase in temperature.

If there is a large reduction in solubility of a particular gas in water because of the powerful forces between water molecules, it is expected that a reduction will also occur in other associated solvents. Hayduk and Laudie (13) related the H-bonding factors for gases in water to those in the primary, normal alcohols of chain-lengths up to C_4: they found that the effect of H-bonding diminished with increasing C-content of the alcohols. Further, where as NH_3 reacts with water yielding an H-bonding factor (i.e. (gas solubility, mole fraction in solution)/(ideal solubility, mole fraction in solution)) greater than one, such appears also to be the case when methanol and ethanol are used as solvents. On the other hand, one would expect the solubility of a strongly polar gas, such as NH_3, to decrease with a decrease in the polarity of the solvent.

Finally, it is necessary to describe the work of Gjalbek and Anderson (11), who made a comparison between the experimental and calculated values for the solubility of oxygen, carbon monoxide, nitrogen and carbon dioxide

in solvents with different polarities. They plotted the difference between experimental and calculated values of the solubilities of these gases against the dipole moments of the solvents (see Figure (3.3)). This figure shows that the slope of the lines is greatest for CO_2, almost equal for nitrogen and carbon monoxide and smallest for oxygen. This result is possibly related again to the electronic polarisation which for carbon dioxide is 6.6, carbon monoxide 4.9, nitrogen 4.4 and oxygen 4 ml.

In conclusion, it may be said that the solubility of gases is chiefly determined by their polarity; non-polar gases have a relatively high solubility in non-polar solvents whilst polar gases have a high solubility in polar liquids. If a gas dissolves in a polar liquid (such as water) it indicates that the compatability between the gas molecules and liquid molecules is high; consequently, the tension at the interface between them will be low. If the two phases are not compatible, the interfacial tension will be high.

3.3 Experimental Programme : Choice of Gases and and Liquid Phases

Let us first consider air-water systems, as they are very familiar, easy to use and cheap and about which

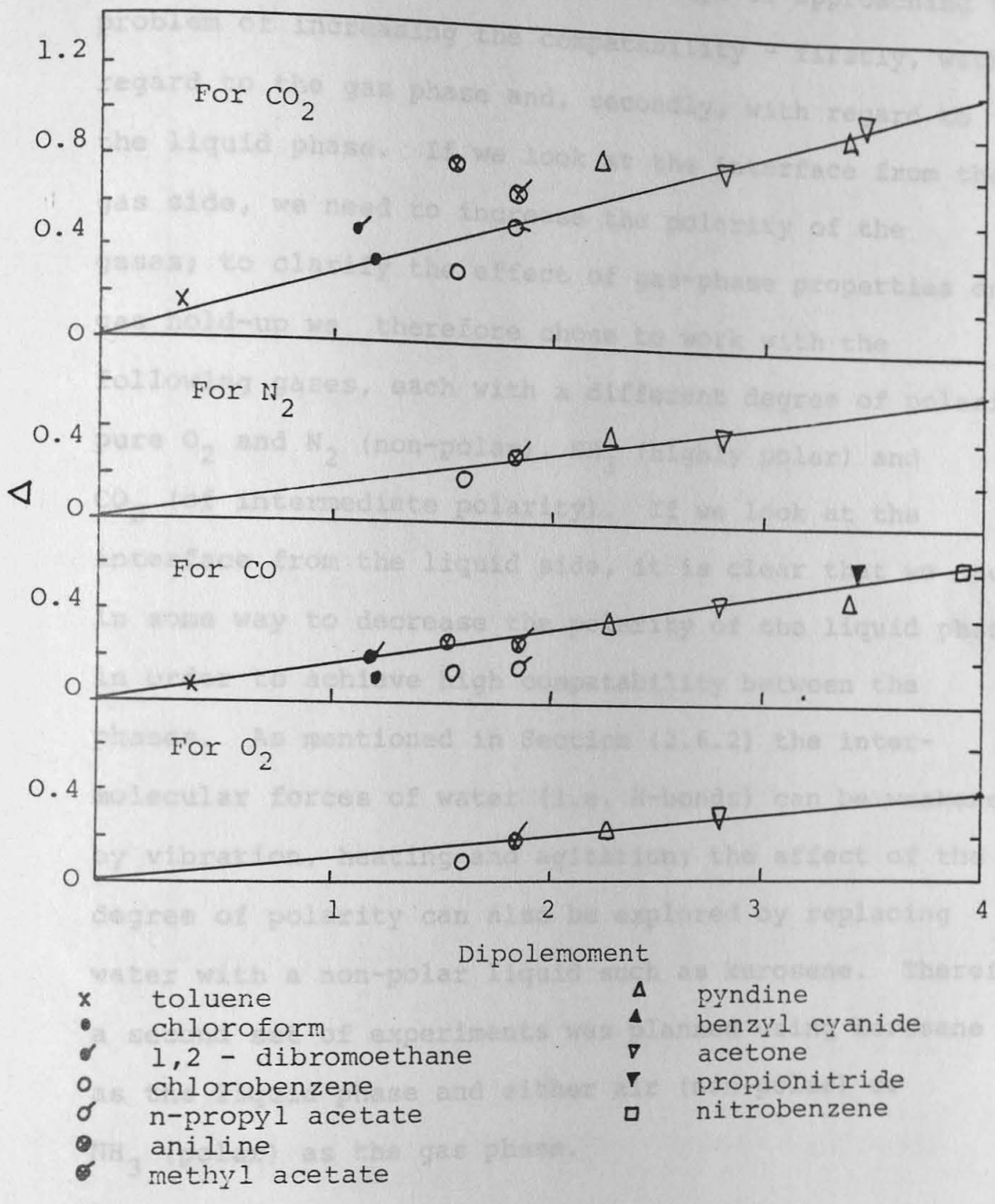

Figure 3.3 - Difference in solubility between experimental and calculated values (Δ) of CO_2, N_2, CO and O_2 in polar solvents against the dipolemoments of the solvents.

much data have been published. Looking at the interface (see Figure (3.4)), there are two ways of approaching the problem of increasing the compatability - firstly, with regard to the gas phase and, secondly, with regard to the liquid phase. If we look at the interface from the gas side, we need to increase the polarity of the gases; to clarify the effect of gas-phase properties on gas hold-up we therefore chose to work with the following gases, each with a different degree of polarity: pure O_2 and N_2 (non-polar), NH_3 (highly polar) and CO_2 (of intermediate polarity). If we look at the interface from the liquid side, it is clear that we need in some way to decrease the polarity of the liquid phase in order to achieve high compatability between the phases. As mentioned in Section (2.6.2) the inter-molecular forces of water (i.e. H-bonds) can be weakened by vibration, heating and agitation; the effect of the degree of polarity can also be explored by replacing water with a non-polar liquid such as kerosene. Therefore, a second set of experiments was planned using kerosene as the liquid phase and either air (non-polar) or NH_3 (polar) as the gas phase.

3.4 Results and Discussion

The two-dimensional bubble column, which has been described in Section (2.4.1), was used in determining the effect of the gas phase on gas hold-up. The bubble

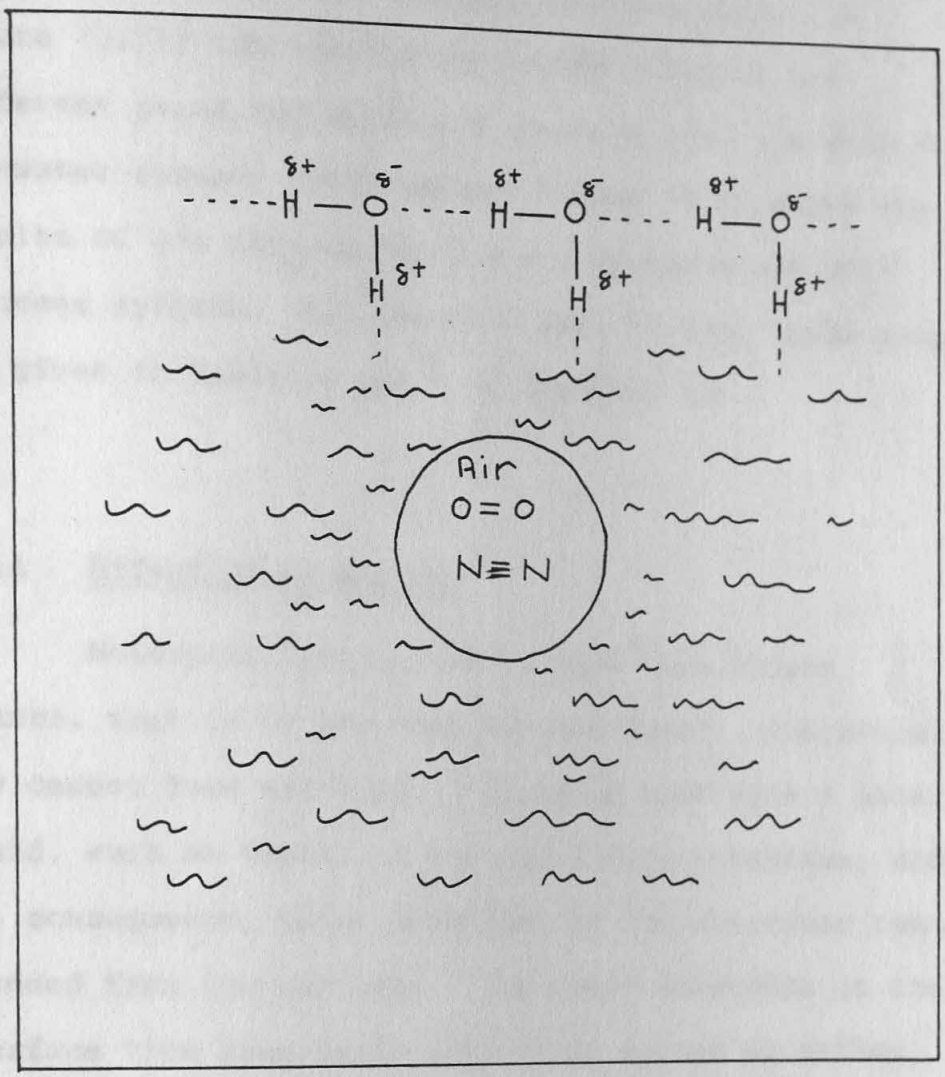

Figure 3.4 - Diagram showing air bubble surrounded by water

column was operated continuously with respect to gas flow and batchwise with respect to the liquid. In Figure (3.5)) the results which were obtained for different gases and water are compared with the data for air-water system. Furthermore, Figure (3.6) shows the results of gas hold-up for the air-kerosene and NH_3-kerosene systems. All the data used to plot these graphs are given in Tables 1 and 2 of Appendix (B).

3.4.1 Effect of N_2 and O_2

Molecules like O_2 and N_2 have zero dipole moments, that is to say they are non-polar. Therefore, they cannot form any kind of physical bond with a polar liquid, such as water, at the gas-liquid interface, and, as a consequence, water molecules at the interface remain unbonded from the gas side. The water molecules at the interface thus experience attractive forces on either side due to their neighbours and from within the bulk of the liquid, and these put them in a state of tension. The water interface with O_2 and N_2, therefore, behaves like the air-water interface as a stretched elastic skin; consequently, we should expect the same bubble size and hold-up as is shown in Figure (3.5).

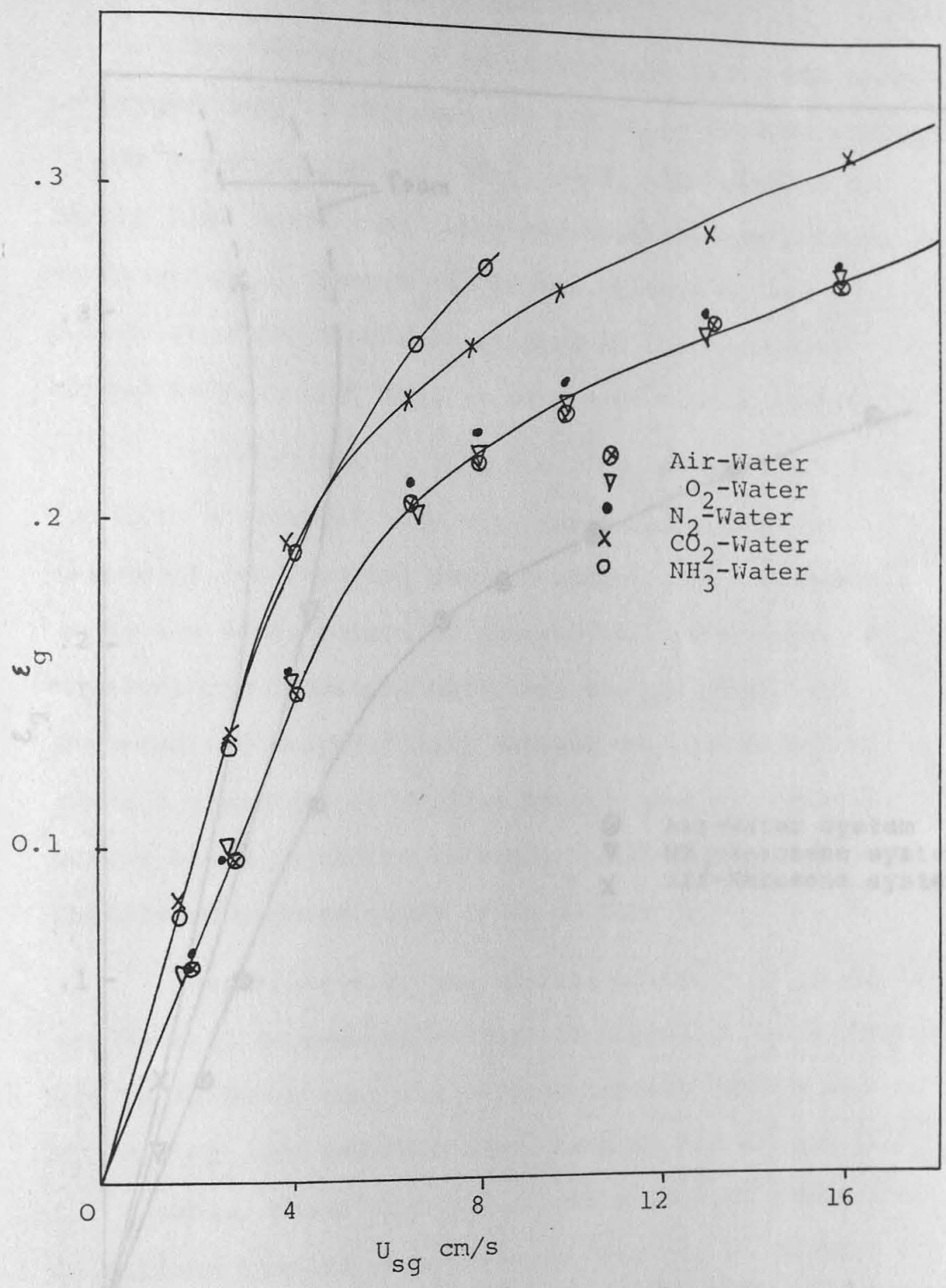

Figure 3.5 - Effect of the nature of the gas on gas hold-up for $U_{sl} = 0$

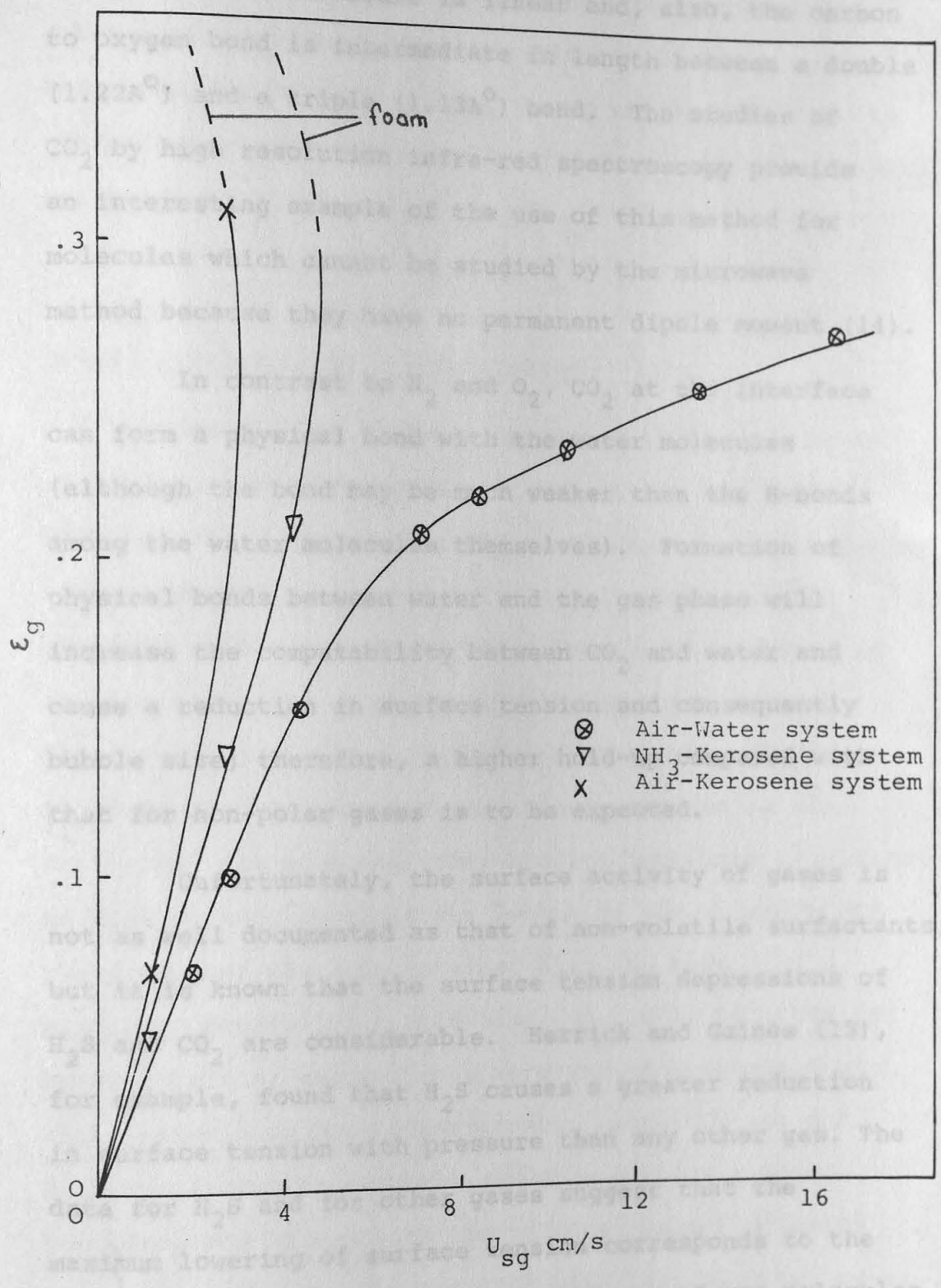

Figure 3.6 - Effect of the nature of the liquid on gas hold-up for $U_{sl} = 0$

3.4.2 Effect of CO_2 on Gas Hold-up

The OCO molecule is linear and, also, the carbon to oxygen bond is intermediate in length between a double ($1.22A^{o}$) and a triple ($1.13A^{o}$) bond. The studies of CO_2 by high resolution infra-red spectroscopy provide an interesting example of the use of this method for molecules which cannot be studied by the microwave method because they have no permanent dipole moment (14).

In contrast to N_2 and O_2, CO_2 at the interface can form a physical bond with the water molecules (although the bond may be much weaker than the H-bonds among the water molecules themselves). Formation of physical bonds between water and the gas phase will increase the compatability between CO_2 and water and cause a reduction in surface tension and consequently bubble size; therefore, a higher hold-up compared with that for non-polar gases is to be expected.

Unfortunately, the surface activity of gases is not as well documented as that of non-volatile surfactants, but it is known that the surface tension depressions of H_2S and CO_2 are considerable. Herrick and Gaines (15), for example, found that H_2S causes a greater reduction in surface tension with pressure than any other gas. The data for H_2S and for other gases suggest that the maximum lowering of surface tension corresponds to the adsorption of one close-packed monolayer of gas molecules

on the water surface and it has been found that H_2S and CO_2 form such a monolayer at about half their saturation pressure. Thus, it seems that the compatability between gas and liquid at the interface is the main parameter effecting bubble size and, consequently, gas hold-up.

3.4.3 Effect of NH_3 on Gas Hold-up

Ammonia has a dipole moment of 1.46D, and it is highly soluble in water (see Figure (3.1)) due to its high polarity. Because of the high compatability existing between ammonia and water molecules, no bubbles were observed even after the bubble column had been operated for six hours and at a gas velocity of about 4 cm/s. Later, a few, very small bubbles appeared: some of these remained almost stationary and slowly reduced in size until they disappeared; other bubbles decreased significantly in size as they ascended the length of the column. For these reasons the data obtained with NH_3 have little meaning. Generally, bubble size and bubble velocity, as based on visual observation, were very low compared with those which have been observed when using CO_2, O_2 and N_2. The formation of small and fine bubbles also indicates how NH_3 reduced the surface tension of water despite its low density compared with that of other gases.

3.4.4 Air-Kerosene and NH_3 - Kerosene Systems

In the last section we discussed how the polarity of the gas phase effected the surface tension of water, a highly polar liquid. To gain more confidence in our approach, we substituted water with kerosene (a mixture of C_{12} -C_{18} alkanes) which has a viscosity similar to that of water but is non-polar. Two sets of experiments were performed with kerosene: firstly, we used air as the gas phase, and, in the second set of experiments, we used ammonia. The results are presented in Figure (3.6).

In the air-kerosene system the compatability between air and kerosene molecules is very high because, as mentioned before, both are non-polar. Due to this compatability, the bubble size was very small (about 2 mm in diameter) and we have not previously seen so many small, uniform bubbles ascending the length of the column and forming a very stable foam at the top of the column. It is worth mentioning here that in one large scale process for producing heavy water (the Girdler-sulphide process), in which gaseous H_2S is contacted with liquid water, the formation of foam has been reported (16,17). In this process, both liquid and gas are polar, H_2S forming a stable monolayer at the interface with water; therefore, a large reduction in the surface tension of water will occur and this causes the system to form foam.

Another, very important phenomenon which was observed in the air-kerosene system was the downward movement of bubbles. This phenomenon was more evident when the air flow to the column was suddenly shut off, when many bubbles having reached the top of the column rebounded to the bottom of the column (see Figure (3.7) at almost the same velocity. Sometimes, collision between falling and rising bubbles was observed but they did not coalesce. Formation of bubble chains at very low gas velocities was another phenomenon which was observed in the air-kerosene system. The formation of bubble chains, which can result in coalescence are discussed in more detail in Section (4.5.5).

Although the NH_3-kerosene system foamed readily, it also exhibited a high degree of coalescence, and the bubbles appeared to be larger than in the air-kerosene system. As NH_3 is a highly polar gas, the compatability between NH_3 and kerosene is low, and as a consequence, the tension at the interface is high compared with that for the air-kerosene system.

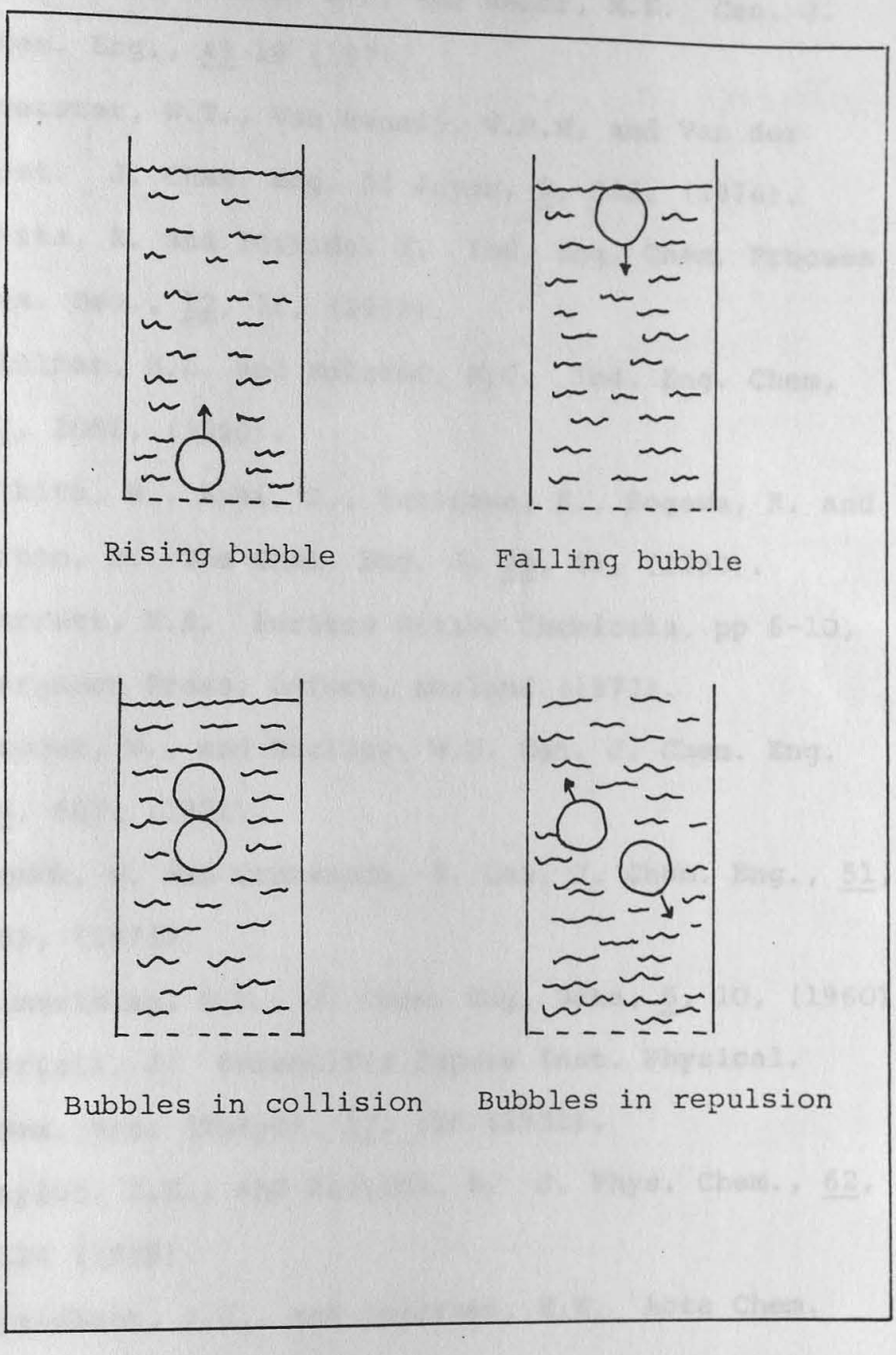

Figure 3.7 - Various stages of rising, falling, collision and repulsion of bubbles in air-kerosene system.

References

1. Bhaga, D., Pruden, B.B. and Weber, M.E. Can. J. Chem. Eng., 49 19 (1971).
2. Koetster, W.T., Van Swaaij, W.P.M. and Van der Most. J. Chem. Eng. of Japan, 9, 332, (1976).
3. Akita, K. and Yoshida, F. Ind. Eng. Chem. Process Des. Dev., 12, 76, (1973).
4. Shulman, H.L. and Molstad, M.C. Ind. Eng. Chem, 42, 1058, (1950).
5. Hikita, H., Asai, S., Tanigawa, K., Sogawa, K. and Kitao, M. The Chem. Eng. J. 20, 59, (1980).
6. Garrett, H.E. Surface Active Chemicals, pp 6-10, Pergamon Press, Oxford, England (1972).
7. Hayduk, W., and Buckley, W.D. Can. J. Chem. Eng. 49, 667, (1971).
8. Hayduk, W. and Castaneda, R. Can. J. Chem. Eng., 51, 353, (1973).
9. Himmelblau, D.M. J. Chem. Eng. Data, 5, 10, (1960).
10. Horiuti, J. Scientific Papers Inst. Physical. Chem. Res. (Tokyo), 17, 126 (1931).
11. Saylor, I.H., and Battino, R. J. Phys. Chem., 62, 1334 (1958).
12. Gjaldback, J.C., and Andersen, E.K. Acta Chem. Scand., 8 1398 (1954).
13. Hayduk, W., and Laudie, H. A.I.Ch.E.J., 19 (No.6), 1233 (1973).

14. Theoretical Basis of Inorganic Chemistry, Barnard, Alan Keith., McGraw-Hill, 1965.

15. Herrick, C.S. and Gaines, G.L. Jr. J. Phys. Chem. 77, 2703 (1973).

16. Bickerman, J.J., Foams, Springer-Verlag, New York, (1973).

17. Sagert, N.H., and Quinn, M.J. Can. Journal of Chem. Eng., 54, 392 (1976).

4 A Study of Gas-Liquid Systems with Additives in the Liquid Phase

4.1 Introduction

In chapter (2) we discussed air-water systems. However, our results were obtained for pure water only and they do not hold good for solutions. In bubble-column fermenters, the culture medium consists usually of a mixture of inorganic salts and sugars; metabolic products such as alcohols and organic acids are also frequently present in significant quantities. It is well known that the most significant difference between the air-water system and many air-aqueous solution systems is that, in the former, the bubble coalescence rate is high, whilst, in the latter, the coalescence rate is low. However, there has been little detailed analysis of this information and, consequently, the mechanisms underlying this difference in system behaviour remain only poorly understood.

Furthermore, recent interest in the production of single cell protein on various water-insoluble hydrocarbon substrates shows how important is the effect of less soluble or non-soluble organic compounds on the behaviour of air-liquid systems. Again, until recently, there has been no systematic work done on the effect of relatively insoluble or non-soluble organic compounds (such as long chain alcohols) on the behaviour of air-water systems.

Finally, little information is available about the effect of liquid viscosity on gas hold-up, and agreement among researchers is poor. Consequently, it was decided to examine the effect of this important liquid property on gas hold-up. If the liquid is highly viscous, then bubbles rise very slowly; such conditions make it possible to readily observe and photograph different stages of bubble coalescence, and it is believed that such observations can provide a better understanding of coalescence phenomena.

The above paragraphs explain briefly why the author embarked on the programme of work described in the following sections. The experimental work is preceded by a detailed review of the literature.

4.2 Literature Survey

4.2.1 General Correlations of Gas Hold-up and Liquid Physical Properties

Bridge et al. (1) observed that isoamyl alcohol, in some way, inhibited the coalescence of bubbles in aqueous solutions. The fact that isoamyl alcohol and a glycerol -water mixture exhibited foaming tends to indicate non-coalescence. Another of their observations with non-coalescing systems was the appearance of a dense bubble-bed at the top of the columns and its slow movement down to the bottom. Because of foam formation in their

runs with glycerol-water mixtures, they were not able to obtain quantitative data above a certain gas flow rate, but at higher flow rates they observed that glycerol-water systems behaved in a similar way to the iso-amyl alcohol solutions.

Marrucci et al. (2) studied the effect of ethyl alcohol on bubble size and bubble coalescence, and they found that it has a similar effect to electrolytes. They concluded that electrical repulsive forces are the factor which hinders coalescence of the bubbles.

Hughmark (3) has presented a correlation of the gas hold-up which takes into account the effect of the liquid properties based on work with the following systems; water-air, kerosene-air, light oil-air, aqueous glycerol solutions-air, $Na_2 SO_3$ solutions-air and $ZnCl_2$ solutions-air. He showed that his own data and that of other investigators on the fractional gas hold-up, ε_g, can be correlated successfully by using the term $U_{sg}\ ((1/\rho_L)(72/\tau))^{1/3}$, where U_{sg} is the superficial gas velocity and ρ_L and τ are the density and surface tension of the liquid. The final correlation was:

$$\varepsilon_g = \frac{1}{2 + (0.35/U_{sg})((\rho_L/1)(\tau/72))^{1/3}} \qquad (4.1)$$

Akita and Yoshida (4) measured the gas hold-up for various gas-liquid systems (water-air, glycol-air,

methanol-air, aqueous glycol solution-air, aqueous methanol solutions-air, water-O_2, water-He and water-CO_2) and analysed the experimental data by means of dimensional analysis. They found that gas hold-up varies with the density and viscosity of the liquid, surface tension and superficial gas velocity and can be predicted by:

$$\frac{\varepsilon_g}{(1-\varepsilon_g)^4} = C \left(\frac{d^2 \rho_L g}{\tau}\right)^{1/8} \left(\frac{d^3 \rho_L^2 g}{\mu_L^2}\right)^{1/12} \frac{U_{sg}}{(dg)^{1/2}} \qquad (4.2)$$

where C = 0.2 for pure liquids and non-electrolyte solutions and C = 0.25 for electrolyte solutions.

Akita and Yoshida (5) also measured bubble sizes by a photographic method in four systems (water, glycol, methanol and sodium sulfite solution). They found, experimentally, that the bubble sizes were independent of the properties of the system such as surface tension, liquid viscosity, and liquid and gas densities. They found that the only factors affecting the volume-surface mean diameter of initial bubbles were the orifice diameter of the gas distributor and the gas velocity through the orifice.

Hikita and Kikukawa (6) have studied the effect of liquid physical properties on gas hold-up, using air and various liquids (water, aqueous methanol solutions and aqueous sucrose solutions), and found that the liquid surface tension had a considerable effect. The

experimental data were correlated by the dimensional expression:

$$\varepsilon_g = 0.505\ U_{sg}^{0.47}\ (72/\tau)^{2/3}\ (1/\mu_L)^{0.05} \qquad (4.3)$$

Gestrich and Rahse (7) have also attempted to correlate data in the literature and have presented equation (4.4), which relates the gas hold-up to the liquid properties, the column dimensions and operating variables.

$$\varepsilon_g = 0.89\ (L/d)^{0.036(-15.7+\log K)}\ .\ (d_b/d)^{0.3}\ .$$

$$(U_{sg}^2/d_b g)^{0.025(2.6+\log K)}\ .\ K^{0.047} - 0.05 \qquad (4.4)$$

where

$$K = (\rho_L\ \tau^3/\mu_L^4 g)$$

and $d_b = 0.3$ cm.

The mean bubble diameter, d_b, usually ranging from 0.2 to 0.4 cm, has been found to have no significant effect on the gas hold-up. Therefore, the constant value of 0.3 cm can be used as the value of d_b in equation (4.4) to estimate the ε_g values.

Kumar et al. (8) have presented gas hold-up data for air and several liquids (water, 40% glycerol solution and kerosene) and found that their own data and that of previous investigators can be correlated by equation (4.5)

as a function of the dimensionless gas velocity containing the superficial gas velocity, the densities of the liquid and gas, and the surface tension of the liquid.

$$\varepsilon_g = 0.728U - 0.485\ U^2 + 0.0975\ U^3 \qquad (4.5)$$

where

$$U = U_{sg}\ (\rho_L^{\ 2}/\tau\Delta\rho g)^{1/4}$$

Botton and Cosserat (9) examined the effect of surface tension on gas hold-up by using water, water tensio-active and water-glycerol systems and found less than 10% increase in gas hold-up.

Mersman (10) has proposed a semi-theoretical correlation for the gas hold-up in terms of dimensionless groups containing the physical properties of the gas and liquid. The correlation given is as follows:

$$\frac{\varepsilon_g}{(1-\varepsilon g)^4} = 0.14\ U_{sg}\ \left(\frac{\rho_L^{\ 2}}{\tau\Delta\rho g}\right)^{1/4}\ \left(\frac{\rho_L^{\ 2}\tau^3}{\mu_L^{\ 4}\Delta\rho g}\right)^{1/24}$$

$$\left(\frac{\rho_L}{\rho_G}\right)^{5/72}\ \left(\frac{\rho_L}{\Delta\rho}\right)^{1/3} \qquad (4.6)$$

Schugerl and Lucke (11) measured the gas hold-up in a bubble column bioreactor using C_1-C_4 alcohols and they found that the type of alcohol and its concentration

influenced the hold-up: methanol produced the smallest increase in gas hold-up, n-propanol and n-butanol the highest, and ethanol produced an intermediate increase in gas hold-up.

4.2.2 The Effect of Liquid Viscosity

Although extensive theoretical and experimental studies concerning gas bubbling in low viscosity liquids are evident in the literature, there is very little information available for predicting hold-up in high viscosity liquids. Agreement amount investigators about the effect of liquid viscosity is not good. Calderbank et al. (12) found that when the liquid is viscous the clustering together of bubbles becomes more pronounced and coalescence happens, thereby leading to a reduction in hold-up. These phenomena are illustrated in Figure (4.1). In contrast Eissa et al. (13), who also studied the effect of liquid viscosity on gas hold-up (see Figure (4.2)), found that increasing liquid viscosity from 1 to about 11 cp is accompanied by increased gas hold-up, with a maximum at about 3 cp.

Rietema and Ottengraf (14) studied the effect of liquid viscosity on gas hold-up. They carried out experiments at several air flow-rates and using glycerol-water solutions of different viscosities (ranging from

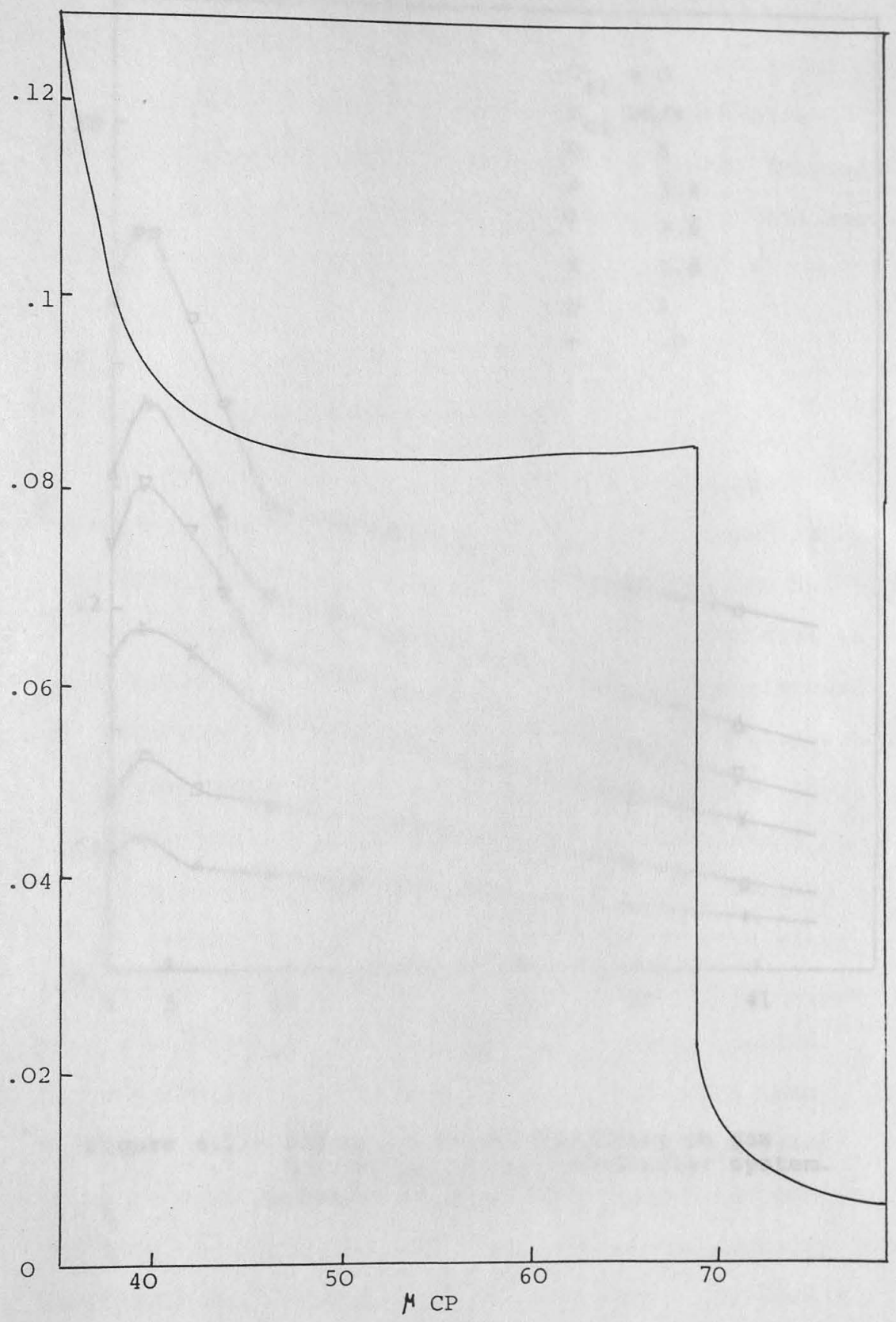

Figure 4.1 - Effect of Liquid Viscosity on Gas Hold-up in CO_2-glycerol-water system. (Calderbank et al. (12)).

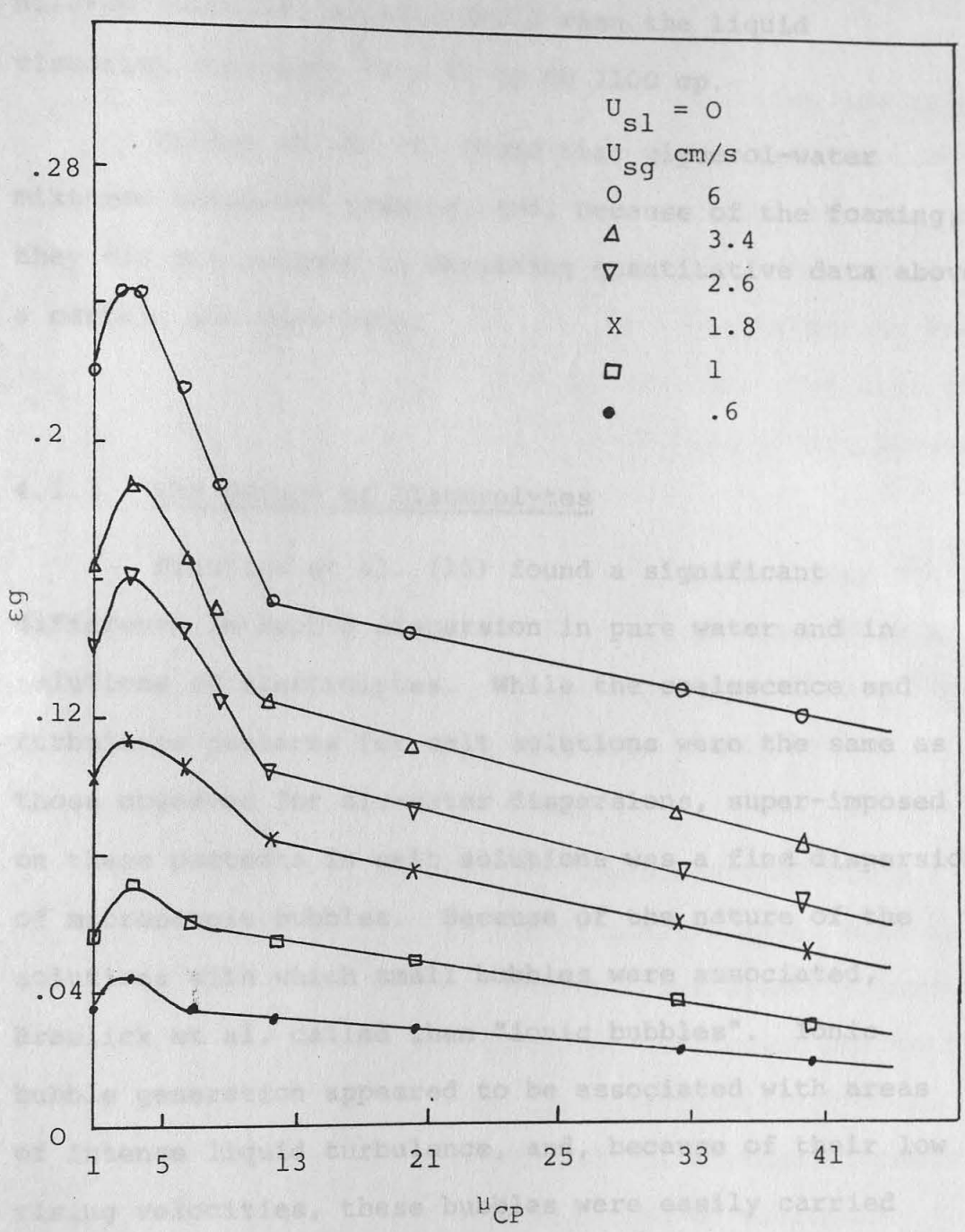

Figure 4.2 - Effect of liquid viscosity on gas hold-up in air-glycerol-water system. (Eissa et al. (13)).

97 cp to 1100 cp). Their results show that the gas hold-up increases significantly when the liquid viscosity increases from 97 cp to 1100 cp.

Bridge et al. (1) found that glycerol-water mixtures exhibited foaming, and, because of the foaming, they did not succeed in obtaining quantitative data above a certain gas flow-rate.

4.2.3 The Effect of Electrolytes

Braulick et al. (15) found a significant difference in bubble dispersion in pure water and in solutions of electrolytes. While the coalescence and turbulence patterns for salt solutions were the same as those observed for air-water dispersions, super-imposed on these patterns in salt solutions was a fine dispersion of microscopic bubbles. Because of the nature of the solutions with which small bubbles were associated, Braulick et al. called them "ionic bubbles". Ionic bubble generation appeared to be associated with areas of intense liquid turbulence, and, because of their low rising velocities, these bubbles were easily carried along with the liquid eddies and served to make them visible. It is obvious that the interfacial contact areas of such ionic bubble clouds are very large and in addition the residence times are like to be unusually long. The ionic bubble fraction cloud, therefore, provides a

mode for mass transfer in electrolyte solutions that would be absent in pure liquid systems.

Sharma and Mashelkar (16) found that the values of gas hold-up and effective interfacial area were much higher in the case of electrolyte solutions than in the case of non-electrolyte solutions. Also, the nature of the electrolyte was found to be important so far as the effective interfacial area was concerned. The true gas- and liquid-side mass transfer coefficients were, however, independent of ionic strength.

Fair et al. (17) found that electrolytes can exhibit hold-up values 20 to 30% higher than those in non-electrolytes because of the formation of very small, stable bubbles with correspondingly slower rise velocities.

Yoshida and Akita (5) suggested that the gas hold-up in aqueous solutions of electrolytes, such as sodium sulfite and sodium sulfate, was slightly larger than in non-electrolyte solutions or liquids due to the electrostatic potential at the gas-liquid interface. Marrucci et al. (2) have studied the average diameter of gas bubbles in electrolyte solutions of different concentrations, using a porous plate gas distributor of pore size 8 μm and superficial gas velocity of 0.5 cm/s. The shape of all their curves is asymptotic to a value of 0.41 mm, although the concentration at which the

asymptote is reached is different for the various electrolytes. They concluded that (i) the coalescence process is influenced by the flow rate and by the nature and concentration of the solute and (ii) the effect of the solute is mainly due to electrical repulsive forces which hinder coalescence between bubbles brought into contact by the liquid motion. The efficiency in inhibiting coalescence of the inorganic electrolytes seems to depend upon the valency and the magnitude of the derivative $d\tau/dc$ to which the surface excess is proportional.

Deckwer et al. (19) studied oxygen transfer in tall bubble columns. This study was carried out with water and aqueous solutions of NaCl and $Na_2 SO_4$ in two bubble columns of 723 cm and 440 cm height respectively. In both columns they found that the mass-transfer rates increased by about 50% for the aqueous solutions of NaCl (.17 N) and $Na_2 SO_4$ (.225 N) compared with the rates in tap water. On the basis of the findings of Marrucci et al. (2), Lessard et al. (20) and Zieminski et al. (21), the addition of electrolytes was expected to impede bubble coalescence, and owing to the smaller bubble diameter it was anticipated that the interfacial area would increase by a factor of 2 to 3 (21). On the other hand, it had been observed that the mass transfer coefficient, K_L, decreases with decreasing bubble size (22,23,24,25). Therefore, Deckwer et al. assumed that the increase of $K_L a$ could be attributed to an increase

of the interfacial area and a simultaneous decrease of K_L. In order to clarify this point Deckwer et al. (26) determined the interfacial area independently by taking photographs over approximately half the height of the bubble columns. The enlarged photographs of the gas-liquid dispersions were then analysed with a particle size analyser. It was found that the bubble size distributions were similar to those for water, and so Deckwer et al. concluded that electrolyte solutions should not be regarded as non-coalescing liquids.

Schugerl and Lucke (11) used inorganic salts to increase surface tension and found that, in high concentrations of salt solutions, the coalescence rates were greatly diminished. They also measured the bubble sauter mean diameter using a perforated plate gas distributor and they found that the addition of salts did not change the sauter mean diameter of bubbles. With a porous plate gas distributor they also found that the influence of salts on the bubble diameter was much less than that of alcohols.

4.3 Experimental Programme

Experiments to assess the effects of both soluble and non-soluble alcohols, glycol, glycerol and electrolyte solutions on gas hold-up were carried out in the two- and three-dimensional bubble columns described in

Section (2.4): the operating conditions used in the experimental programme were similar to those used in the study of the air-water system.

The experimental programme has been divided into three parts. In the first set of experiments, a study was made of the effect on gas hold-up of varying the lengths of the non-polar end of molecules having the same polar group. A range of primary alcohols with different non-polar lengths were chosen for this purpose; alcohols used were completely dry and pure. The first three alcohols (C_1-C_3) in the series are completely miscible with water; n-butanol, which is soluble to the extent of about 8%, was considered to be on the borderline for solubility; n-hexanol and n-octanol were considered to be non-soluble because of their long aliphatic chains.

The second set of experiments was planned to assess the effect of the polarity of the polar ends of molecules on gas hold-up and bubble coalescence: glycols (with two (OH) groups) and glycerol (with three (OH) groups) were used to study this effect.

Finally measurements were made with electrolyte solutions - KCl, NaCl and KI. These inorganic salts, in contrast to the alcohols, are negatively absorbed at the gas-liquid interface, and so they can be used to provide some idea of the importance of the strength of intermolecular forces in the bulk of the liquid phase.

4.4 Experimental Results

Although most of the experiments were performed for a wide range of alcohol or electrolyte compositions, the trends in the results were very consistent. Because of this the number of graphs presented has been reduced to the minimum necessary to illustrate the main effects.

The experimental programme for each column was carried out in a completely random fashion with each experiment being repeated at least two or three times. Tap water was employed as a reference system by which to compare the results using the alcohol and electrolyte solutions.

4.4.1 Effect of Soluble Alcohols

The effect of soluble alcohols (C_1-C_3) was studied by measuring gas hold-up in solutions of different concentrations of these alcohols (betwen 0-1.5%) in the two-or three-dimensional bubble columns. Figures (4.3) and (4.4) summarise the results from the two columns and Tables (1) and (2) in Appendix (C) give the detailed experimental data.

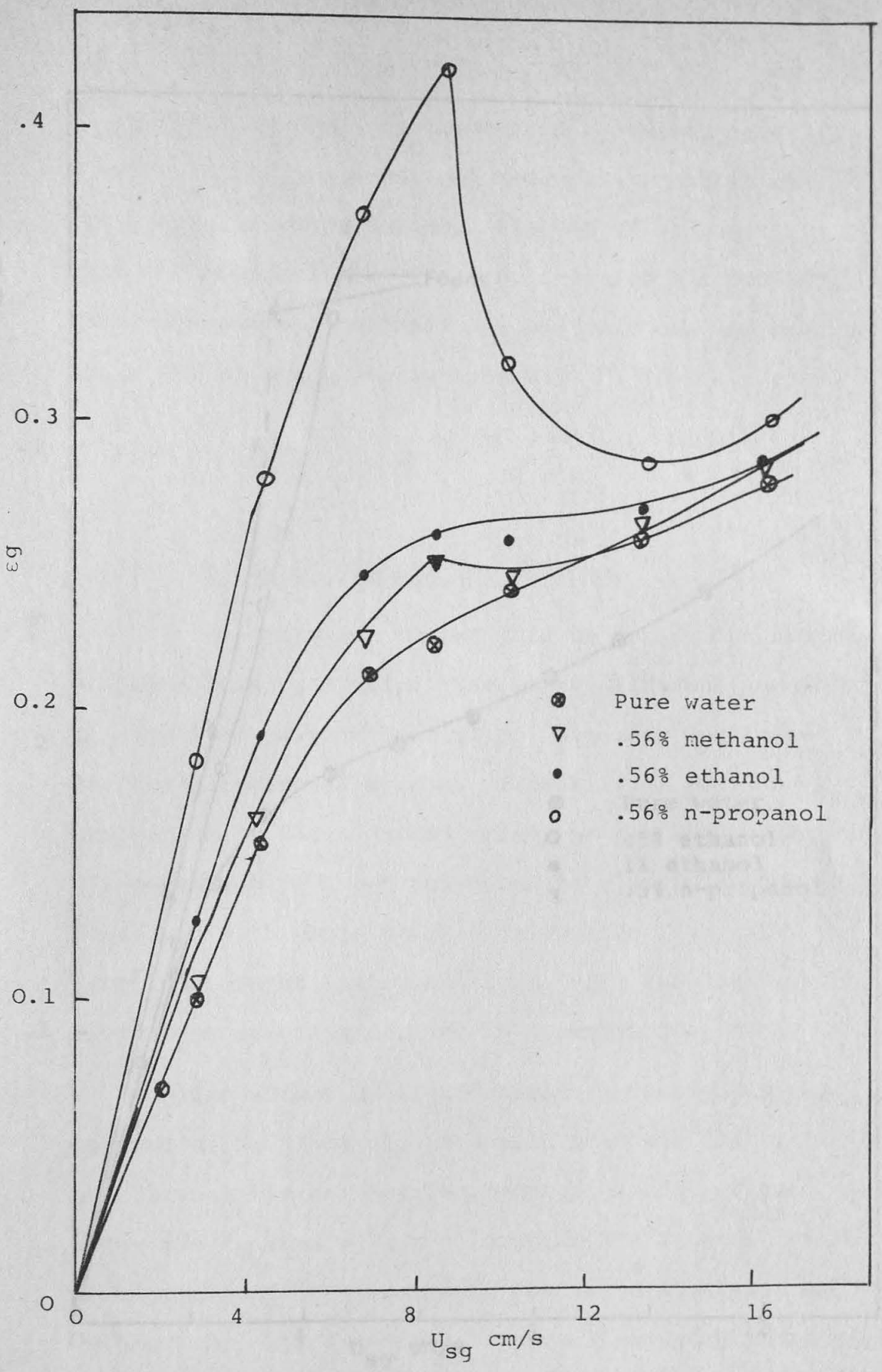

Figure 4.3 - Typical influence of soluble alcohols on gas hold-up in two-dimensional column and for $U_{sl} = 0$ -136-

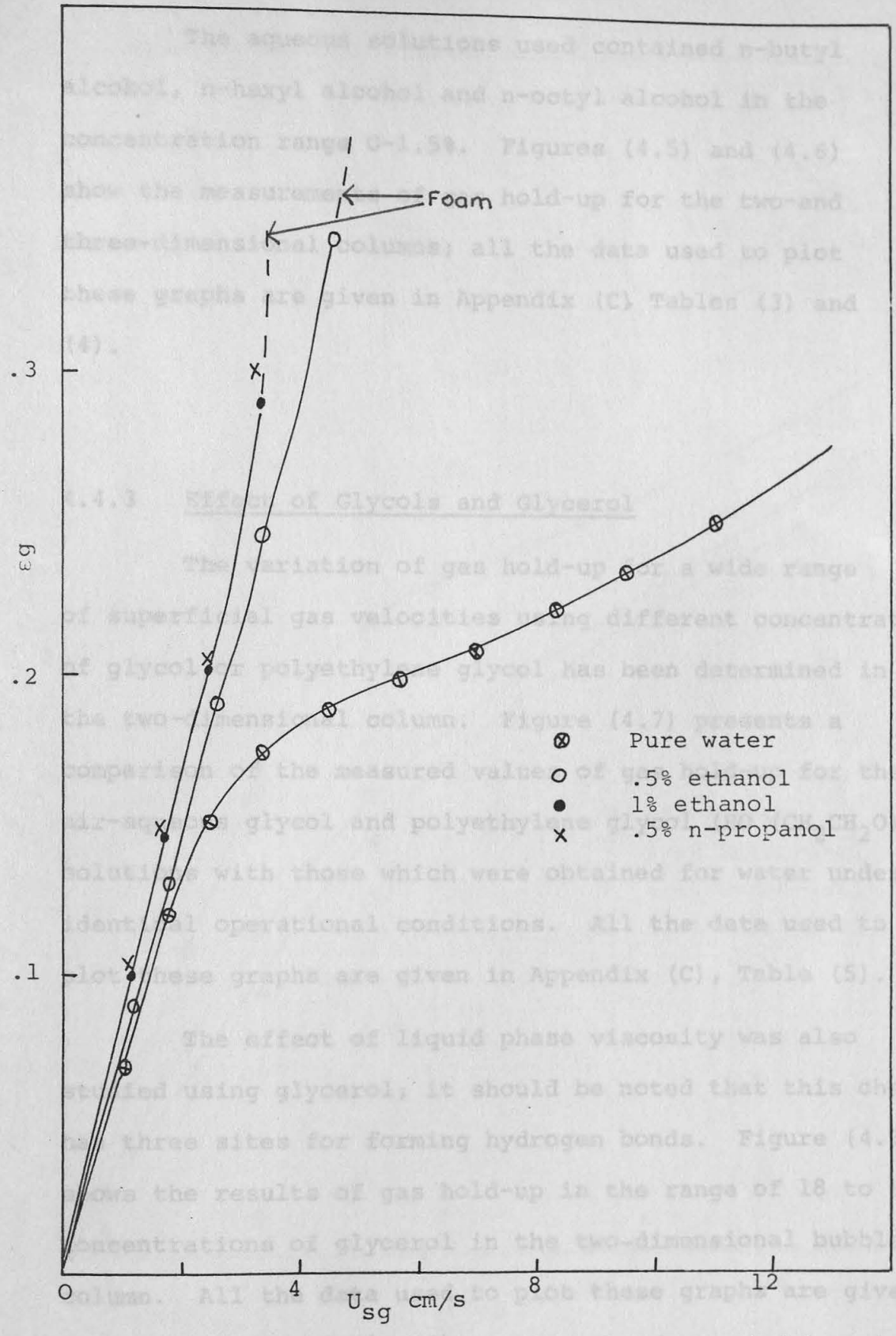

Figure 4.4 - Effect of soluble alcohols on gas hold-up in three-dimensional column and for $U_{sl} = 0$.

4.4.2 Effect of Long-chain Alcohols

The aqueous solutions used contained n-butyl alcohol, n-hexyl alcohol and n-octyl alcohol in the concentration range 0-1.5%. Figures (4.5) and (4.6) show the measurements of gas hold-up for the two-and three-dimensional columns; all the data used to plot these graphs are given in Appendix (C), Tables (3) and (4).

4.4.3 Effect of Glycols and Glycerol

The variation of gas hold-up for a wide range of superficial gas velocities using different concentrations of glycol or polyethylene glycol has been determined in the two-dimensional column. Figure (4.7) presents a comparison of the measured values of gas hold-up for the air-aqueous glycol and polyethylene glycol ($HO\ (CH_2CH_2O)_4H$) solutions with those which were obtained for water under identical operational conditions. All the data used to plot these graphs are given in Appendix (C), Table (5).

The effect of liquid phase viscosity was also studied using glycerol; it should be noted that this chemical has three sites for forming hydrogen bonds. Figure (4.8) shows the results of gas hold-up in the range of 18 to 65% concentrations of glycerol in the two-dimensional bubble column. All the data used to plot these graphs are given in Appendix (C), Table (6).

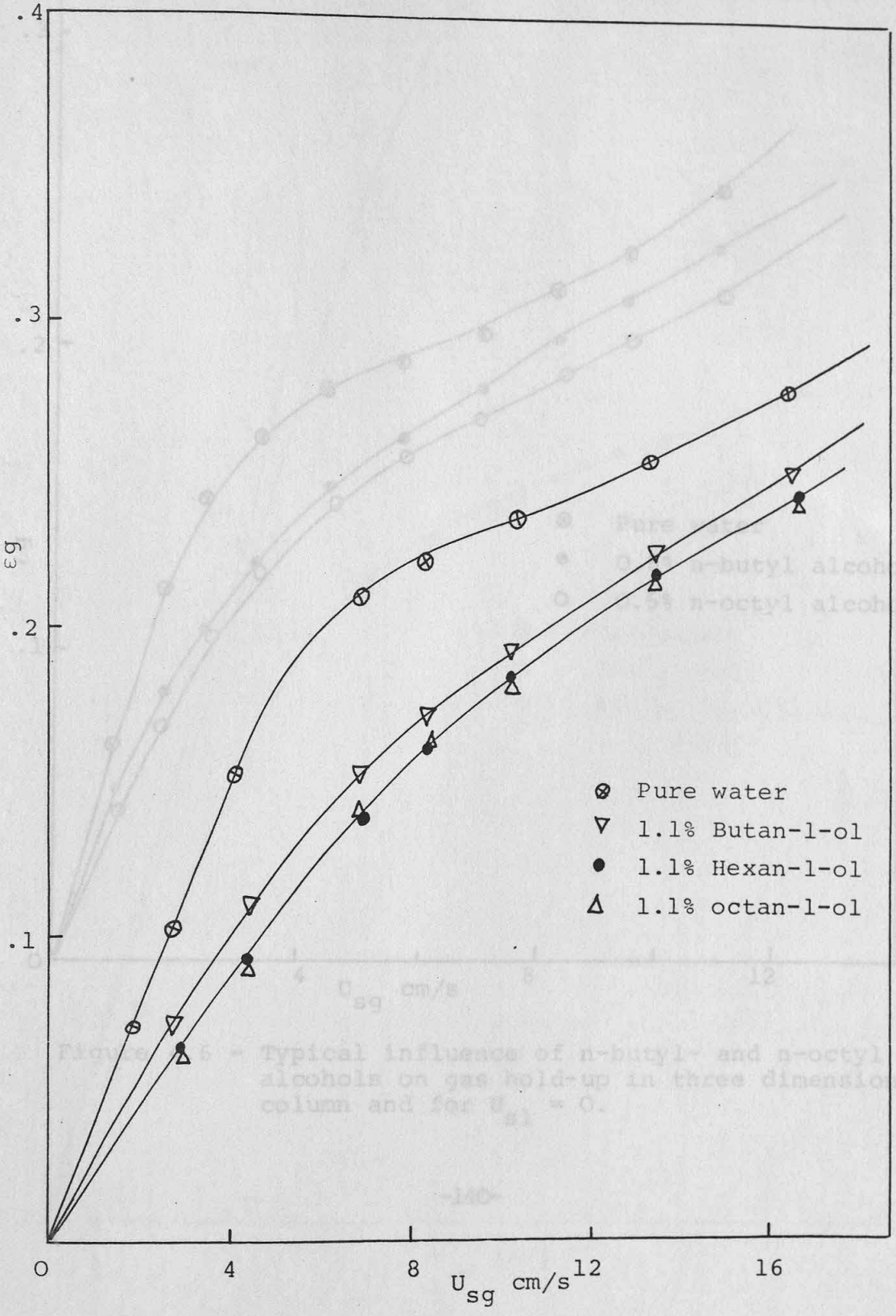

Figure 4.5 - Typical influence of long chain alcohols on gas hold-up in two-dimensional column and for $U_{sl} = 0$

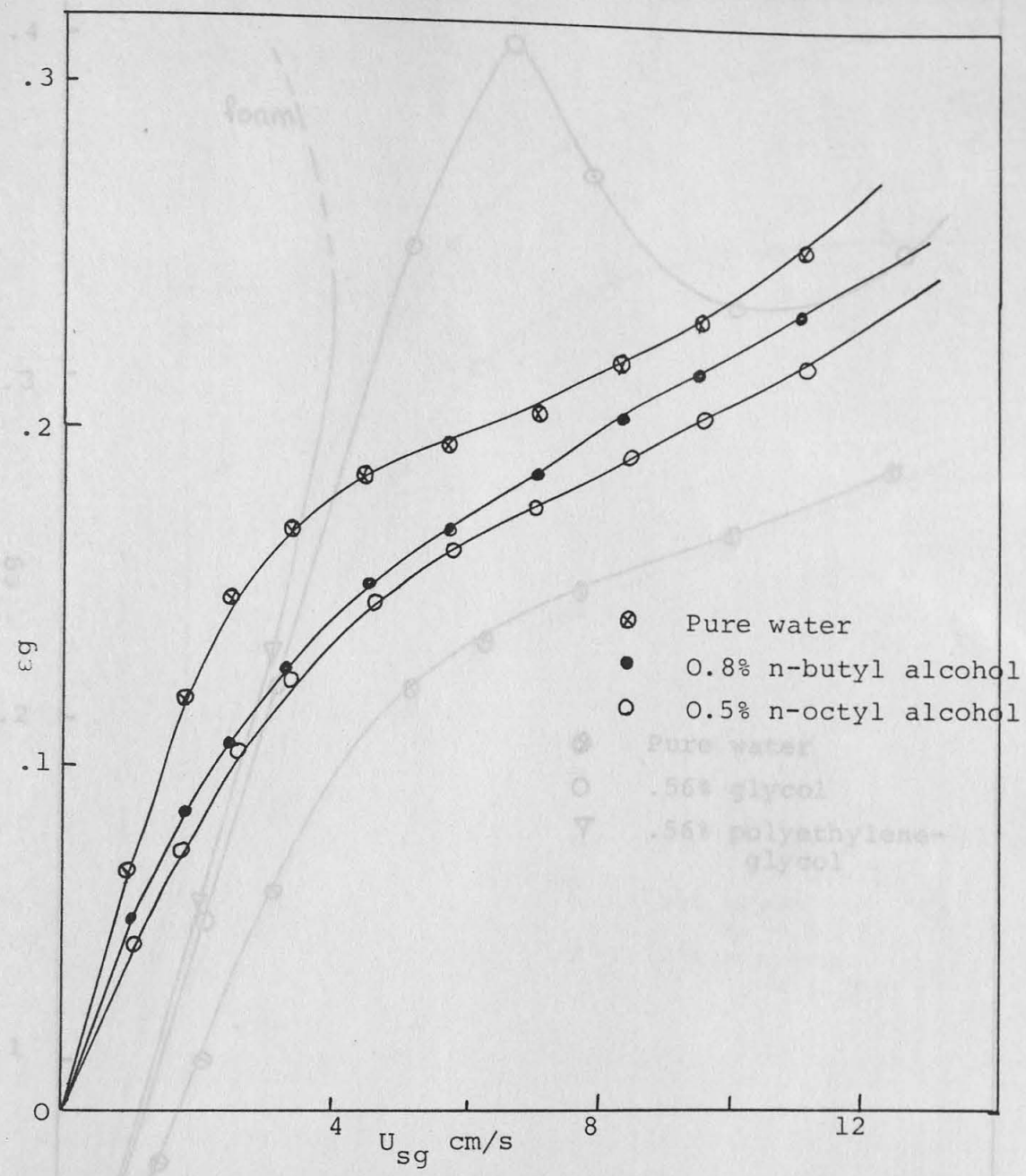

Figure 4.6 - Typical influence of n-butyl- and n-octyl alcohols on gas hold-up in three dimensional column and for $U_{sl} = 0$.

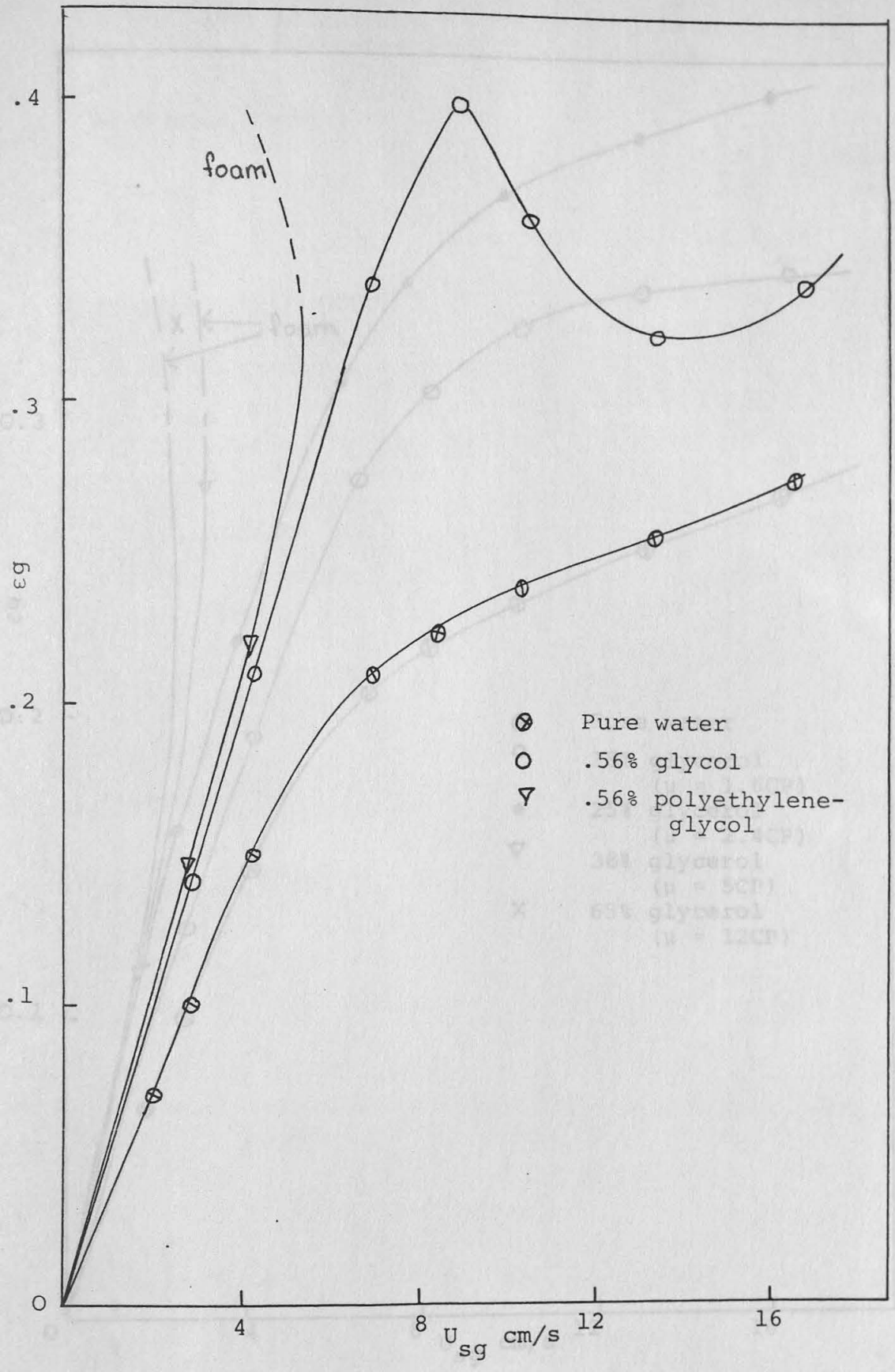

Figure 4.7 - Typical influence of glycol and polyethylene glycol on gas hold-up in two-dimensional column and for $U_{sl} = 0$

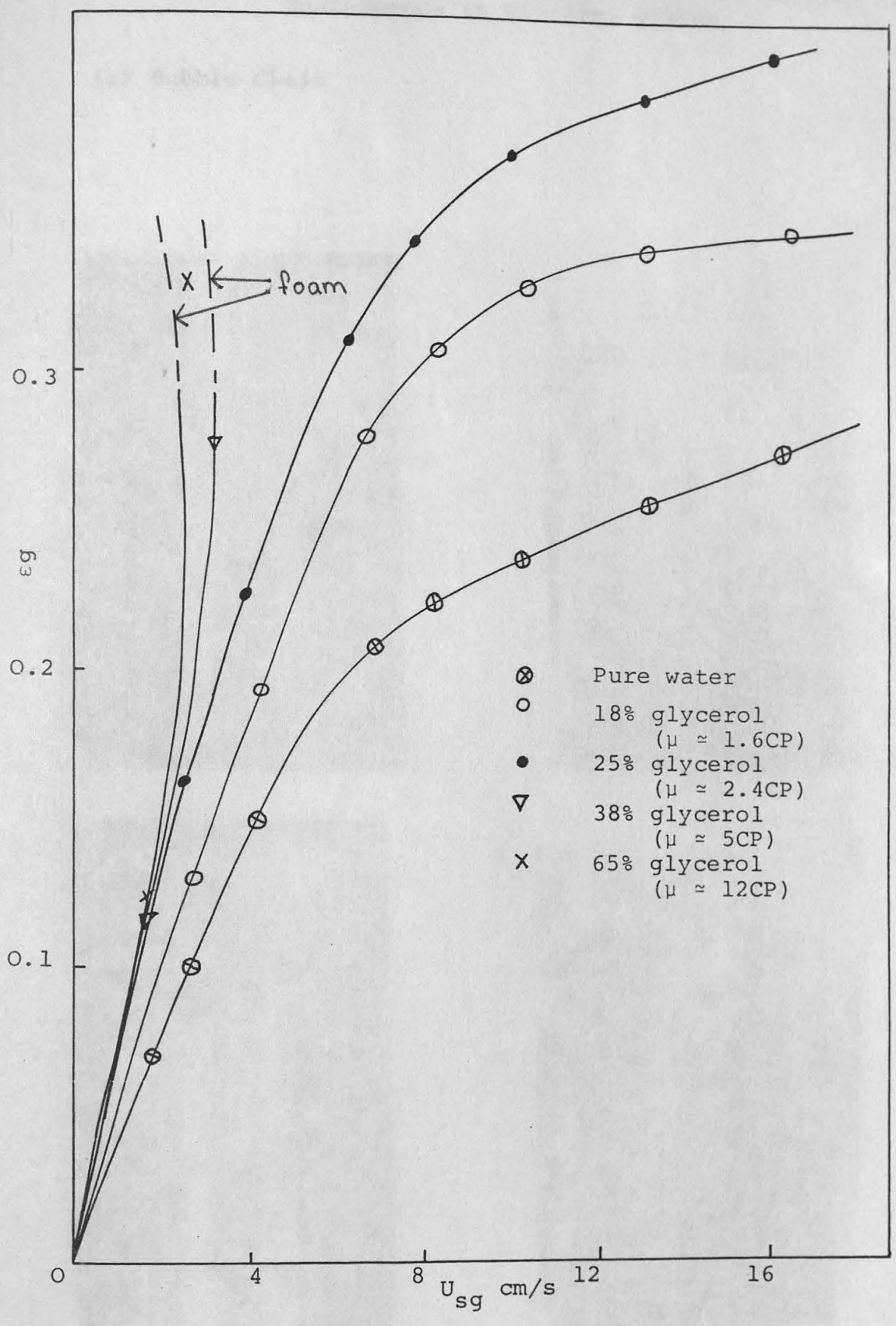

Figure 4.8 - Typical influence of glycerol (i.e. liquid viscosity) on gas hold-up in two-dimensional bubble column and for $U_{sl} = 0$.

Figure 4.9 - Illustration of Bubble Chain and Bubble Coalescence in Glycerol System

(a) Bubble Chain

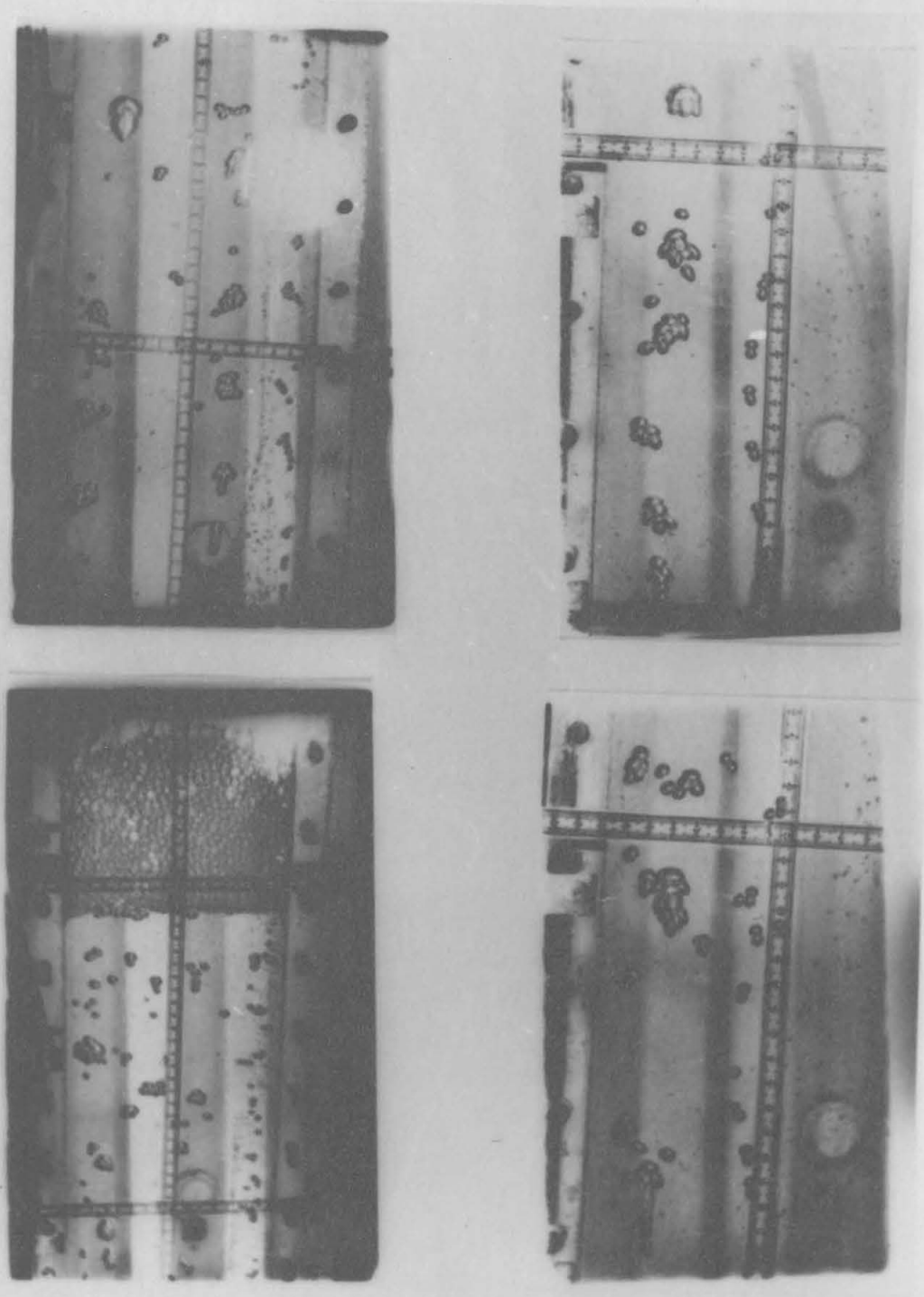

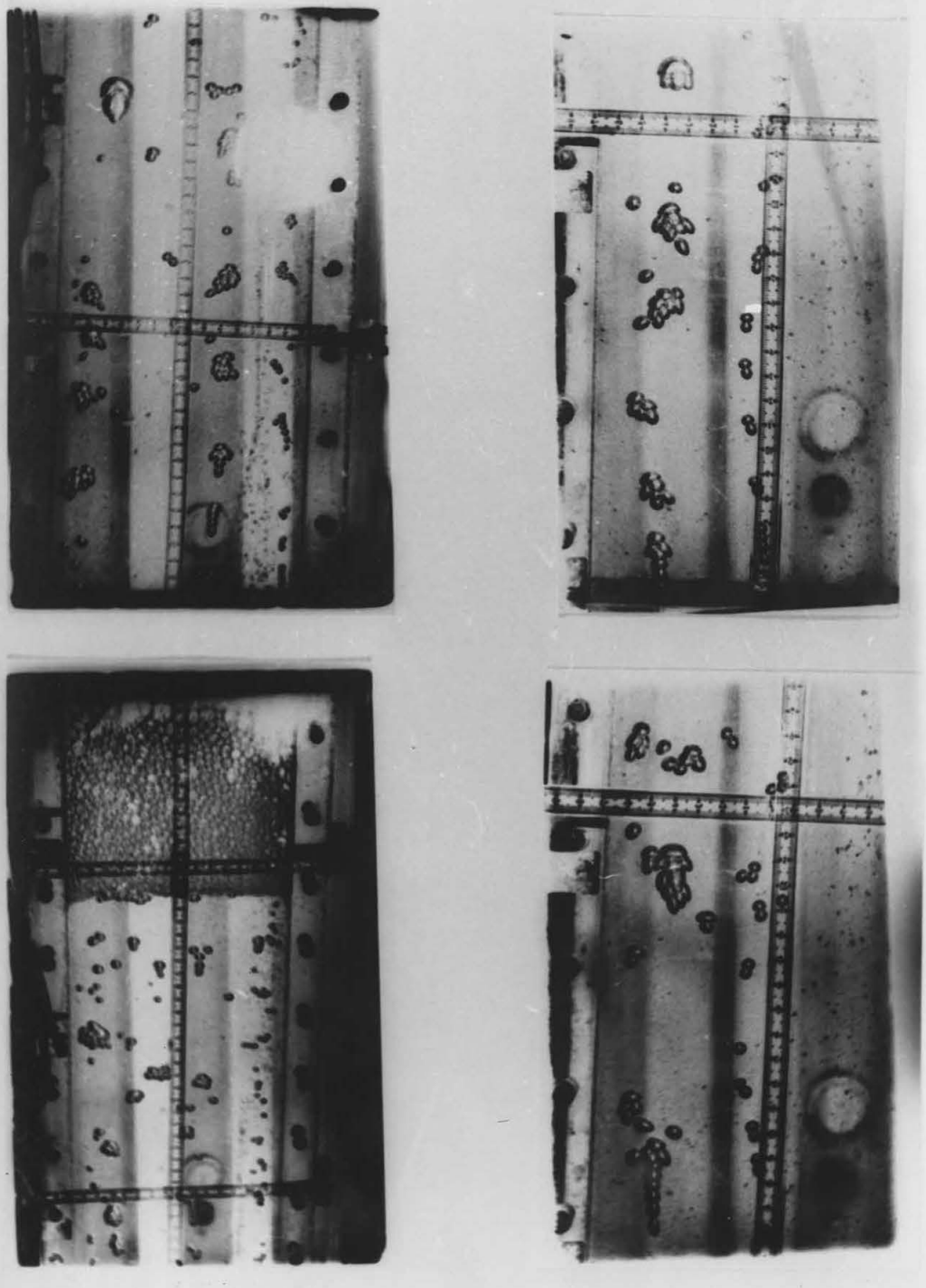

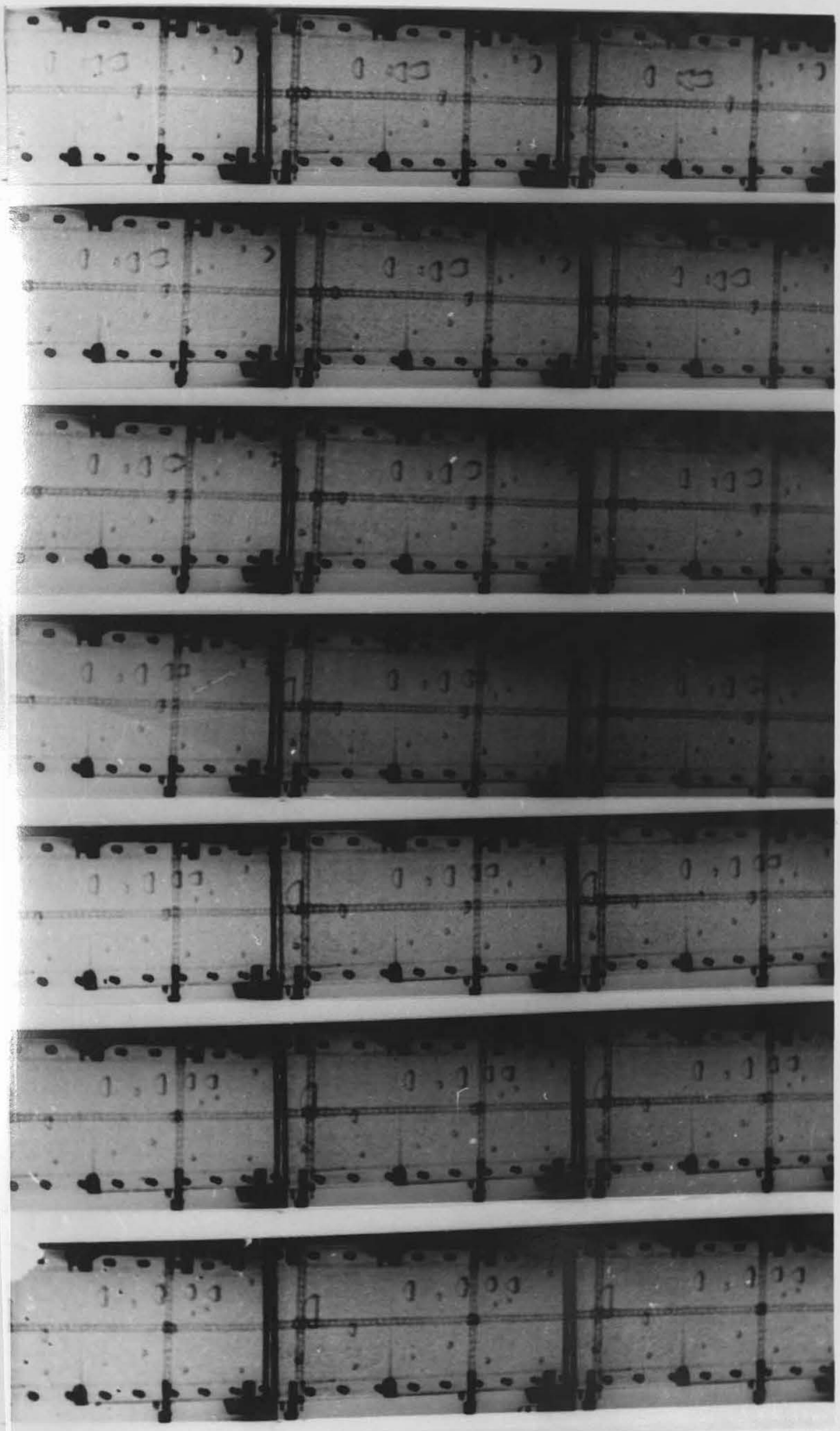

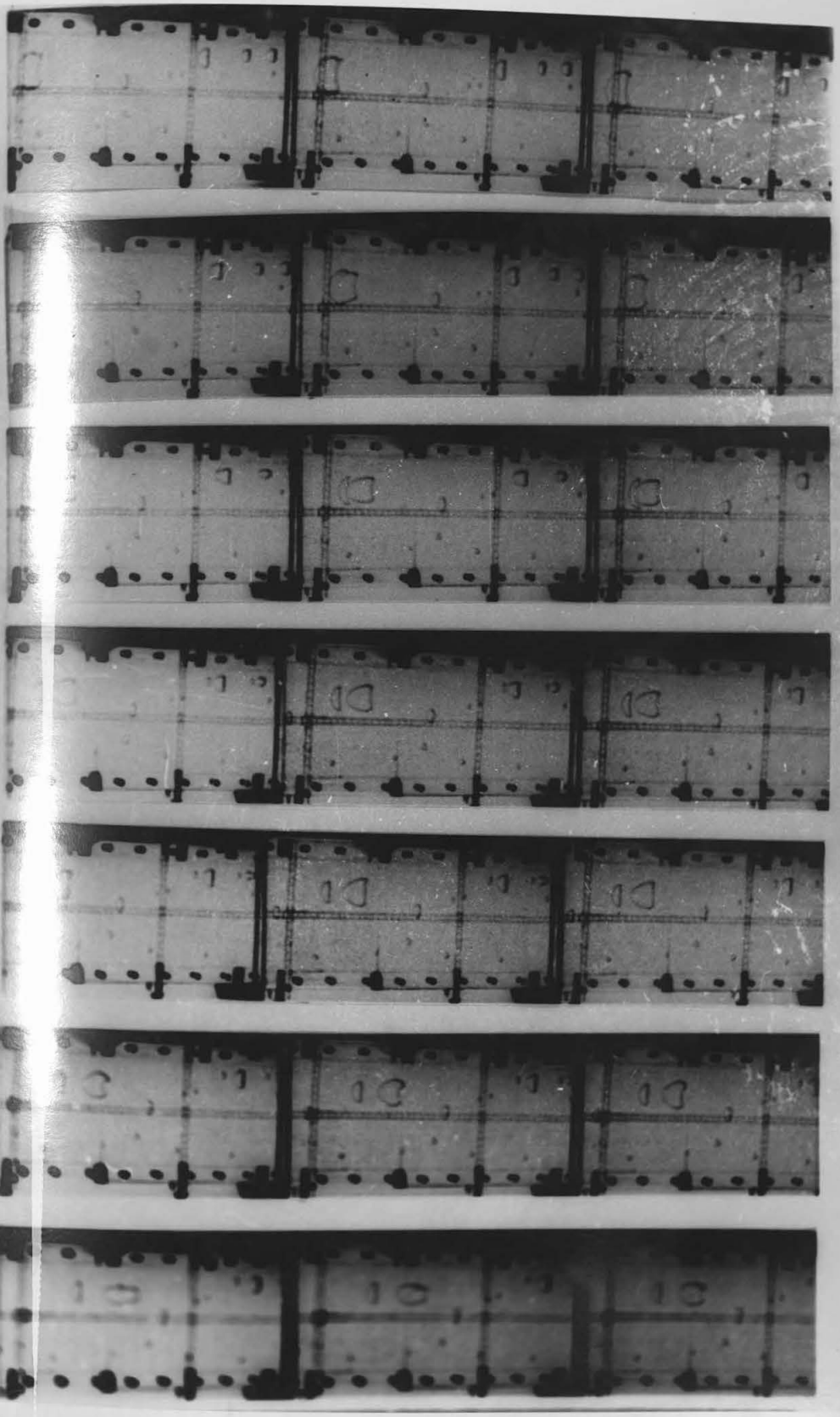

4.4.4 Effect of Electrolytes

The effect of electrolyte solutions was studied in the two-and three-dimensional bubble columns; the gas hold-up was measured at different concentrations of sodium chloride, potassium chloride, and potassium iodide over a wide range of superficial gas velocities. Figures (4.10) and (4.11) compare the values of the gas hold-up for air-water, air-potassium chloride, air-sodium chloride and air-potassium iodide solutions in the two-dimensional bubble column: Figure (4.12) shows gas hold-up in two potassium chloride solutions at different concentrations (0.05 and 0.01 g/cm^3) in the three-dimensional bubble column. Tables (7) to (9) in Appendix (C) give the detailed experimental data.

4.5 Discussion

4.5.1 Effect of Alcohols : Introductory Comments

Hydrocarbons have the physical properties that we might expect of such non-polar compounds, these being the relatively low melting and boiling points which are characteristic of substances with weak intermolecular forces; further characteristics include solubility in non-polar solvents, and insolubility in polar solvents like water. Alcohols are considerably different from hydrocarbons because of the presence of the very polar

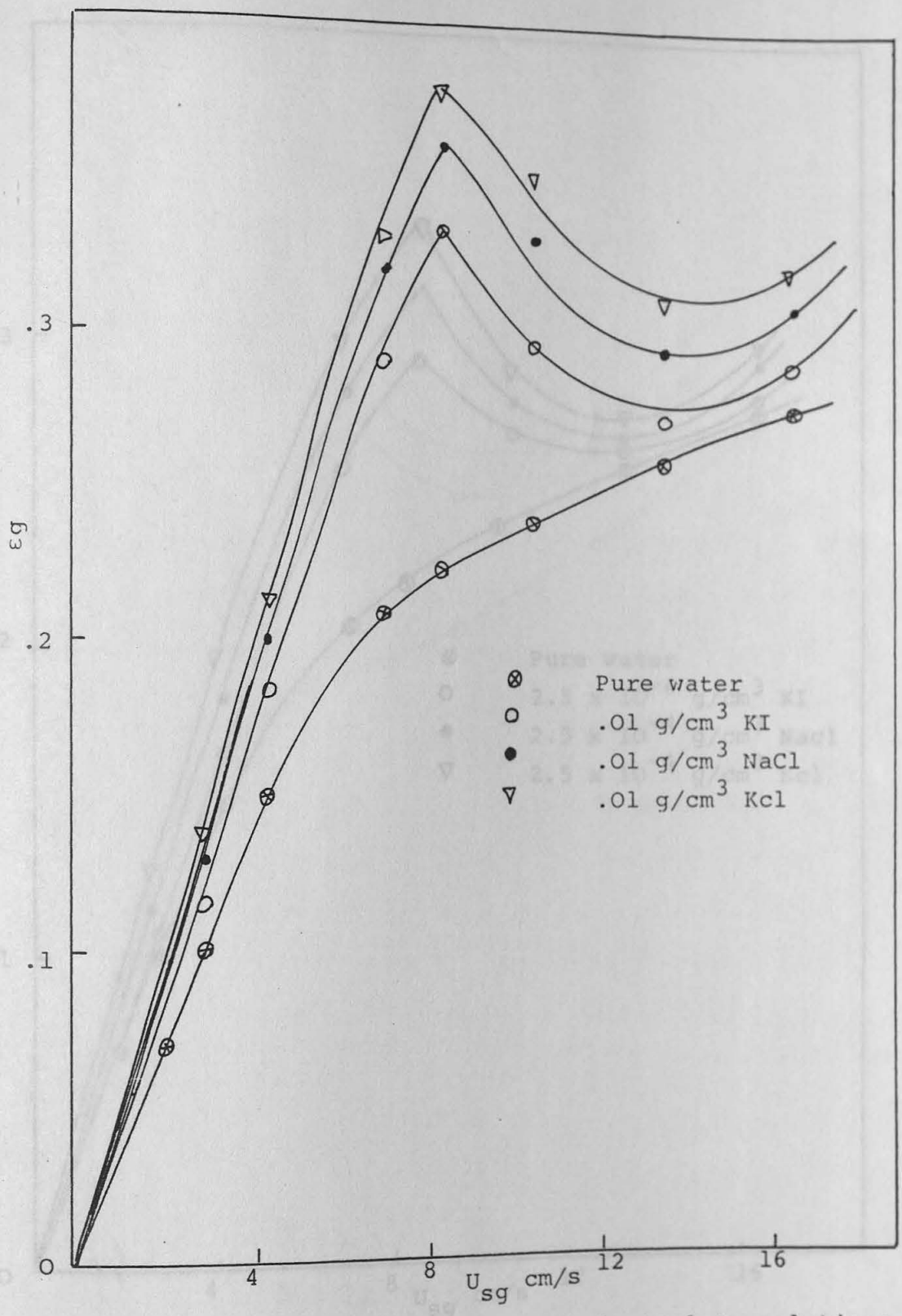

Figure 4.10 - Typical influence of electrolyte solutions on gas hold-up in two-dimensional column and for $U_{sl} = 0$.

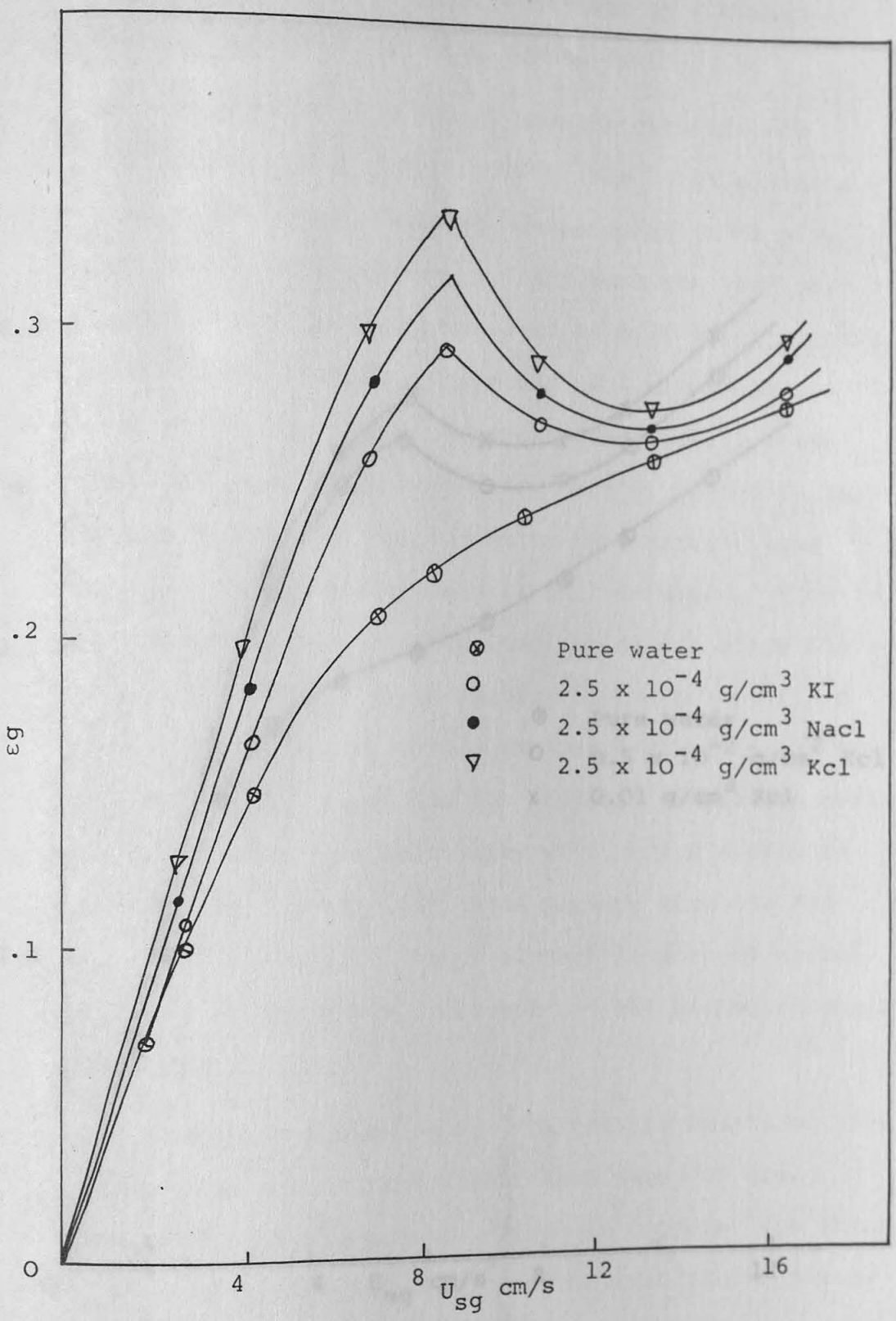

Figure 4.11 - Typical influence of electrolyte solutions on gas hold-up in two dimensional column and for $U_{sl} = 0$

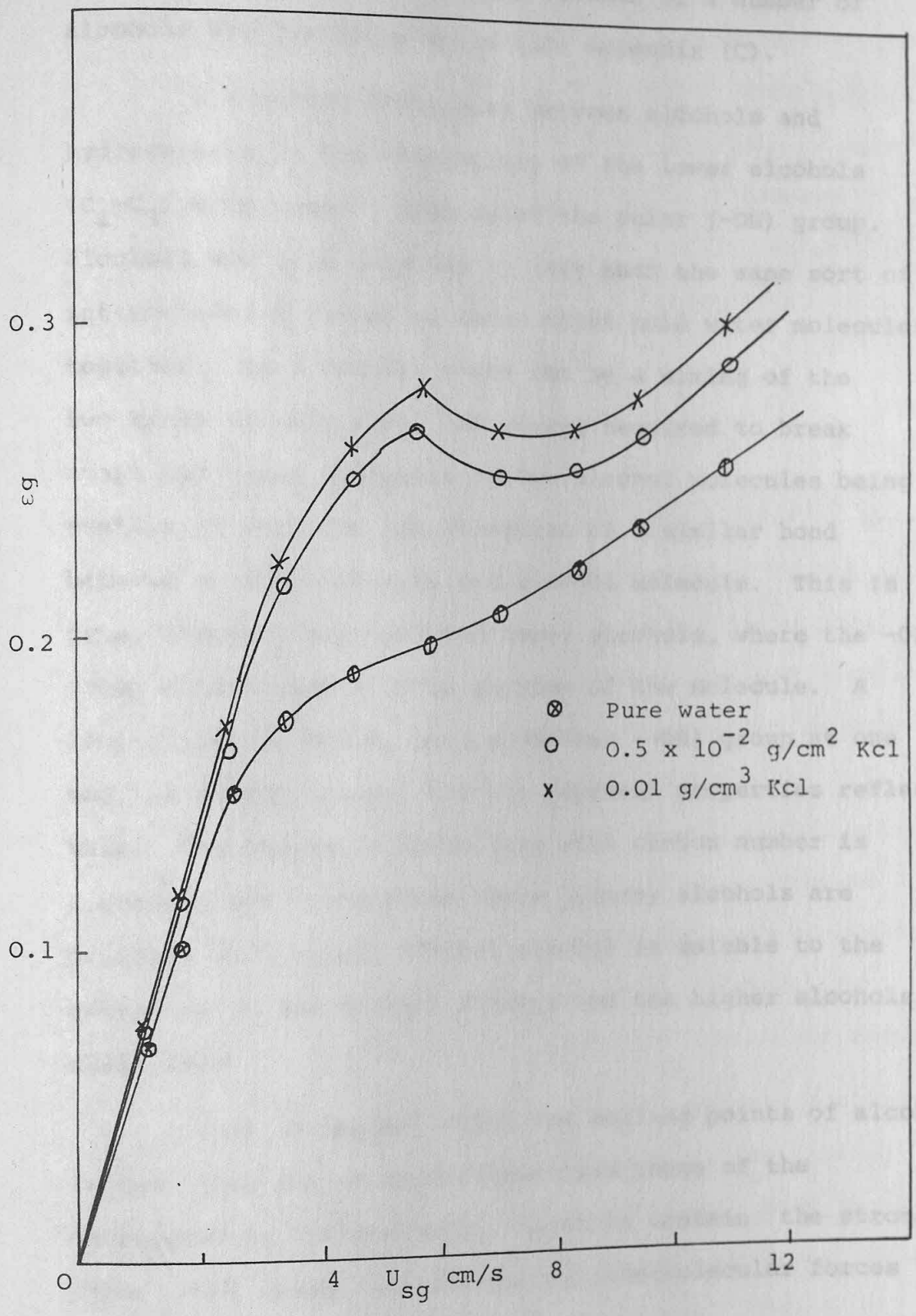

Figure 4.12 - Effect of electrolyte solutions on gas hold-up in three-dimensional column and for $U_{sl} = 0$.

(OH) group and particularly because this polar group contains hydrogen. Physical constants of a number of alcohols are listed in Table (10) Appendix (C).

A striking difference between alcohols and hydrocarbons is the miscibility of the lower alcohols (C_1-C_3) with water. Because of the polar (-OH) group, alcohols are held together by very much the same sort of intermolecular forces as those which hold water molecules together. As a result, there can be a mixing of the two kinds of molecules, the energy required to break apart two water molecules or two alcohol molecules being similar to that for the formation of a similar bond between a water molecule and alcohol molecule. This is true, however, only for the lower alcohols, where the -OH group constitutes a large portion of the molecule. A long aliphatic chain, with a smaller (-OH) group at one end, is mostly alkane, and its physical properties reflect this. The change in solubility with carbon number is a gradual one : the first three primary alcohols are miscible with water, n-butyl alcohol is soluble to the extent of 8% and n-hexyl alcohol and the higher alcohols still less.

What is unusual about the boiling points of alcohols is that they are so much higher than those of the corresponding hydrocarbons. Alcohols contain the strongly polar (-OH) group, and the strong intermolecular forces

arising from dipole-dipole attractions are overcome and boiling occurs only at higher temperatures. Consequently, like water, alcohols are associated liquids with their abnormal boiling points arising from hydrogen bonding. The solubility of the lower alcohols in water is due to the hydrogen bond that can exist between a molecule of water and a molecule of alcohol, as well as between two molecules of alcohol, or between two molecules of water.

4.5.2 The Effect of Soluble Alcohols on Gas Hold-up (C_1-C_3)

Figures (4.3) and (4.4), which were obtained using the two-and three-dimensional bubble columns respectively, show that the most important difference between pure water and solutions containing methanol, ethanol and propanol is that, in the former, the gas hold-up is low, and, in the alcohol solutions, it is high. Also a comparison of gas hold-up values for these three different systems indicates that the gas hold-up increases with gas velocity in order propanol > ethanol > methanol > water. An explanation for the above results will now be put forward.

When air is bubbled through an aqueous alcohol solution, the concentration of alcohol at the freshly formed bubble surface is low and almost the same as in the bulk solution. However, the alcohol molecules will quickly become oriented at the interface. Now, a

comparison of these three alcohols shows that there is no apparent difference between their hydrophilic groups (OH): this is due to the fact that dipole moments of these three alcohols are the same and almost identical to that of pure water (see Table (10), Appendix (C)). Consequently, the hydrogen bonds formed between water molecules and water with these three alcohols or these alcohols with themselves are almost of the same strength. However, when comparing the length of their hydrophobic groups, it is clear that there is an increase in going from methanol to propanol. Therefore, there is a greater tendency for propanol molecules to build up at the air-liquid interface; on the other hand, in the case of methanol solutions, the composition at the bulk and interface is more similar, because the length of the non-polar tail of the methanol molecules is relatively short. So alcohol solutions differ from pure water in that some water molecules are replaced by alcohols at the bulk and at the interface. Due to the similarity between these alcohols and water we can conclude that these alcohols cannot greatly change the inter-molecular forces in the bulk of the system; but at the gas-liquid interface, the non-polar end of the molecules are orientated away from the liquid and the (OH) group remains in the bulk of the liquid owing to the strong hydrogen bonds which this group can form with water. The overall effect is that the alcohol molecules (1) tend to "anchor" the bubbles to the bulk

of the liquid and (2) lower the surface tension. The degree by which the surface tension is reduced will depend on the concentration of the alcohol and the efficiency of packing of its molecules at the gas-liquid interface: it is for this reason that the lowering of surface tension of water by propanol is greater than that caused by ethanol and methanol. Expressed another way we can say that the surfaces are more easily stretched in the order:

$$CH_3CH_2CH_2OH > CH_3CH_2OH > CH_3OH > H_2O$$

and, consequently, gas hold-up is increased in the order: propanol > ethanol > methanol > water.

4.5.3 The Effect of Long-chain Alcohols on Gas Hold-up

As mentioned before, as the length of the non-polar tail of alcohols increases, so the similarity between the alcohols and alkanes increases: this is because a long, non-polar tail with a small (OH) group at one end is mostly alkane. The results of adding long chain alcohols ($C > 4$) to water is that the alcohol molecules will orient steeply to the interface, and form a surface film one molecule thick. The principal factor determining whether or not these films are stable is the strength of the bond between the alcohol and water molecule at the surface and

attraction perpendicular to the surface. In the case of shorter chain alcohols, the molecules will dissolve in water if the attraction is high or evaporate if it is low: in the case of long-chain alcohols, the water molecules cannot "pull" the alcohol molecules into the bulk of the water owing to the resistance of the long, non-polar chains to immersion and the decreasing polarity of the (OH) group as the number of carbon atoms in the non-polar chain increase; therefore, the alcohol spreads out as a monomolecular film on the surface.

Now, if the perpendicular attraction between the film molecules and the water is weak, the film tends to crumple up under small lateral compression or perhaps cannot be formed at all and remains as a compact drop (or non-wettable solid). Comparison of the polarity of butanol and higher alcohols with the polarity of water shows that the hydrogen bonds between water-water molecules are much stronger than those between water and long-chain alcohols. Therefore, the strength of the anchorage of the films formed by these alcohols at the bubble surface with the bulk liquid (i.e. water) is weak; as a consequence, the bubbles are more mobile and coalescence is not inhibited. Thus we may expect the occurrence of bubble coalescence and, as a consequence, reduction in gas hold-up to follow in the sequence:

n-butylalcohol < n-hexyl alcohol < n-octyl alcohol. Figures (4.5) and (4.6) for the two-and three-dimensional bubble columns respectively show this trend.

Finally, we should bear in mind that, by correct choice of additive, we can cause almost any liquid to foam. For example in aqueous solutions, the polarity of the polar end of a good foamer should be high in order to be able to anchor the bubbles to the bulk phase by forming strong bonds and the non-polar end should also be sufficiently long to lower the surface free energy as much as possible; soaps, whose non-polar end is a long carbon chain of 12 to 18 carbons and whose polar end ($-COO^{-}Na^{+}$) can make a very strong ionic bond with water, meet the necessary requirements.

4.5.4 The Effect of Ethylene Glycol and Polyethylene Glycol on Gas Hold-up

In the previous sections we have seen that the coalescence of bubbles occurs more readily when the polarity of an additive is less than that of water even though the non-polar end of the molecules is long enough to significantly reduce the surface tension of water at the interface. However, in order to study what happens if the polarity is greater than that of water we have chosen to use ethylene and polyethylene glycol. Ethylene glycol contains two hydroxyl groups; by comparison with ethanol we can

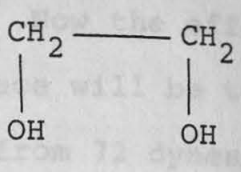

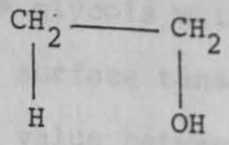

see that it is the same except for the replacement of one atom of hydrogen by the polar hydroxy group. By this substitution the polarity increases from 1.69D for ethanol to 2.2D for ethylene glycol and the surface tension increases from 23 dynes/cm for ethanol to 47.7 dynes/cm for ethylene glycol. As we might expect, because ethylene glycol has more than one site for hydrogen bonding, it boils at 197°C.

When air is bubbled through water-glycol solutions, the surface tension of a freshly formed surface is low; however it will gradually increase and reach an equilibrium value, because the constituent with the lower surface tension, the glycol, will be dragged into the bulk from the surface (due to higher attraction forces which exist between water-glycol compared to water-water molecules). Therefore, the concentration of glycol molecules at the interface will be somewhat less than in the bulk liquid phase: also, since the glycol molecules in the bulk form two strong hydrogen bonds with water molecules, the intermolecular forces will increase significantly. Therefore, there will be a greater resistance in glycol solutions to the rising of bubbles and bubble coalescence.

Now the effect of those glycols which are at the interface will be to lower the surface tension of pure water from 72 dynes/cm to some value between 72 dynes/cm and 48 dynes/cm. However, from visual observations and photographic studies there was no evidence of a significant reduction in bubble size, which means that the composition of glycol at the interfaces was negligibly small. Therefore, in glycol solutions the gas hold-up increased due to the strong inter-molecular forces and not the reduction in surface tension (except at high concentrations of glycol).

To summarise, formation of strong inter-molecular bonds in the bulk causes a reduction in bubble velocity and bubble coalescence, and, therefore higher hold-ups arise, as Figure (4.7) shows.

Polyethylene glycols can be expected to have a higher polarity and so a greater tendency for forming physical bonds; also, they have a longer non-polar part in the middle of the molecules. Therefore, they should suppress the coalescence of bubbles more than ethylene glycol, to the extent of creating foams (see Figure (4.7)).

4.5.5 The Effect of Glycerol : Another Look at Viscosity

Glycerol is an alcohol containing three hydroxy groups; as we might expect from its structure, glycerol

boils at 290°C and has a surface tension of 64 dynes/cm. Therefore, when glycerol is added to pure water it will increase the intermolecular forces in the bulk liquid phase, thereby reducing the bubble rise velocity and the tendency for bubble coalescence to occur; as a result, the gas hold-up should increase compared with that for water, as Figure (4.8) for the lower concentrations of glycerol show. However, as the concentration of glycerol increases, water molecules at the interface will be replaced with glycerol molecules. Glycerol molecules at the interface do not significantly decrease the tension of the interface, because the surface tension is similar to that of water; for this reason, the bubble sizes should not decrease, as high speed photography shows (see Figures (4.9a) and (4.9b)).

The foamability of the system at higher concentrations of glycerol deserves comment. This property can be explained by supposing that the glycerol molecules at the interface anchor the bubbles strongly to the bulk liquid phase; as a result, when bubbles reach the top of the liquid it is difficult for them to leave. The foamability of pure glycerol is shown in Figure (4.9a).

Some experiments have been performed with pure glycerol; the purpose of these experiments was to observe and photograph bubble coalescence phenomena. When the viscosity of a liquid is high, coalescence is easy to observe, as is the rise of bubbles in a chain-like

fashion through a stagnant liquid (see Figures (4.9a) and (4.9b). When the bubbles are spaced closely together, one bubble will suddenly accelerate and overtake the preceding one. This seems to be the basic mechanism for coalescence in bubble columns.

4.5.6 The Effect of Ionic Materials (KCl, NaCl and KI)

The General Effect of Electrolytes

An ionic compound forms crystals in which the structural units are ions. Solid sodium chloride, for example, is made up of positive sodium ions and negative chloride ions alternating in a very regular way. The crystal is an extremely strong rigid structure, since the electrostatic forces holding each ion in its position are powerful. These powerful "inter-ionic" forces are overcome only at very high temperatures, and it is worth noting that sodium chloride has a melting point of 810°C. The physical properties of a compound like sodium chloride are largely due to the ionic bonds.

In the liquid state, the unit of an ionic compound is again the ion. Each ion is still held strongly by a number of oppositely charged ions, and a great deal of energy is required for a pair of oppositely charged ions to break away from the liquid. Consequently, boiling

occurs only at a very high temperature, in the case of sodium chloride 1413°C. When an ionic compound dissolves, the structural units become separated from each other by solvent molecules. The energy required to break the bonds between solute particles is supplied by the formation of bonds between the solute particles and the solvent molecules. A great deal of energy is necessary to overcome the powerful electrostatic forces holding an ionic lattice and, in general, only water and a few other highly polar solvents are able to dissolve ionic compounds appreciably.

In solutions like sodium chloride, each ion is surrounded in the bulk by a cluster of water molecules as illustrated below:

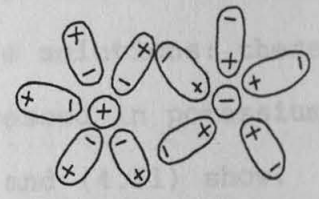

A freshly cleaved surface of an electrolyte solution will, for any given concentration, generally have a surface tension greater than that at equilibrium. As the surface ages and approaches equilibrium, solvated ions leave the surface to given way to adsorption of water molecules; therefore, the surface tension should be lower than the initial value but still greater than that of pure water. For this reason a significant reduction in bubble size is not likely to be observed.

The formation of ionic clusters in the bulk phase makes the solution highly cohesive, and so this has the effect of decreasing the bubble rise velocity and the tendency for bubbles to coalesce. The overall result is an increase in gas hold-up compared with that in air-water systems, as Figures (4.10) to (4.12) for the two-and three-dimensional bubble columns show.

The Effect of Different Anions and Cations

KI and KCl are two ionic compounds having the same cation (K^+) but different anions. The Cl^- anion is more electronegative than the I^- anion and so potassium chloride is more ionic than potassium iodide. This means that the intermolecular forces in the bulk phase of potassium chloride solutions are stronger than those in potassium iodide solutions: therefore, coalescence will be more suppressed in potassium chloride solutions, as Figures (4.10) and (4.11) show.

Furthermore, potassium chloride is a stronger electrolyte than sodium chloride, and, as a result, gas hold-up in potassium chloride solutions might be expected to be higher than that in sodium chloride solutions (see Figures (4.10) and (4.11)).

Effect of High Concentrations of Potassium Chloride

Large increases in surface tension cannot be obtained in solutions by using solutes with fields of force much greater than the solvent. Also, the rise in surface tension above that of the solvent (i.e. for water with a value of 72 dynes/cm) will be highly dependent on the strength of the particular ionic compound used and its composition. Therefore, in order to get a clear picture of what may happen when the surface tension increases significantly above that for pure water, the gas hold-up has been studied in a series of strong solutions of potassium chloride; the results of these studies in the two-and three-dimensional bubble columns are summarised in Figures (4.13) and (4.14). (Detailed information is tabulated in Appendix (C), Tables 11 and 12).

These results follow a trend exactly opposite that which has been observed in bubble columns in all previous studies. As will be seen from the figures, at low gas velocities (U_{sg} < 8 cm/s for the two dimensional column and U_{sg} < 4 cm/s for the three-dimensional column) slug flow occurs; on increasing the gas velocity above these figures a bubbly flow regime develops. When using strong potassium chloride solutions (c = 0.1 g/cm^3) in the three-dimensional bubble column with U_{sg} > 6 cm/s a heavy foam was formed from very tiny bubbles. The reason for this pheomenon may be explained as follows.

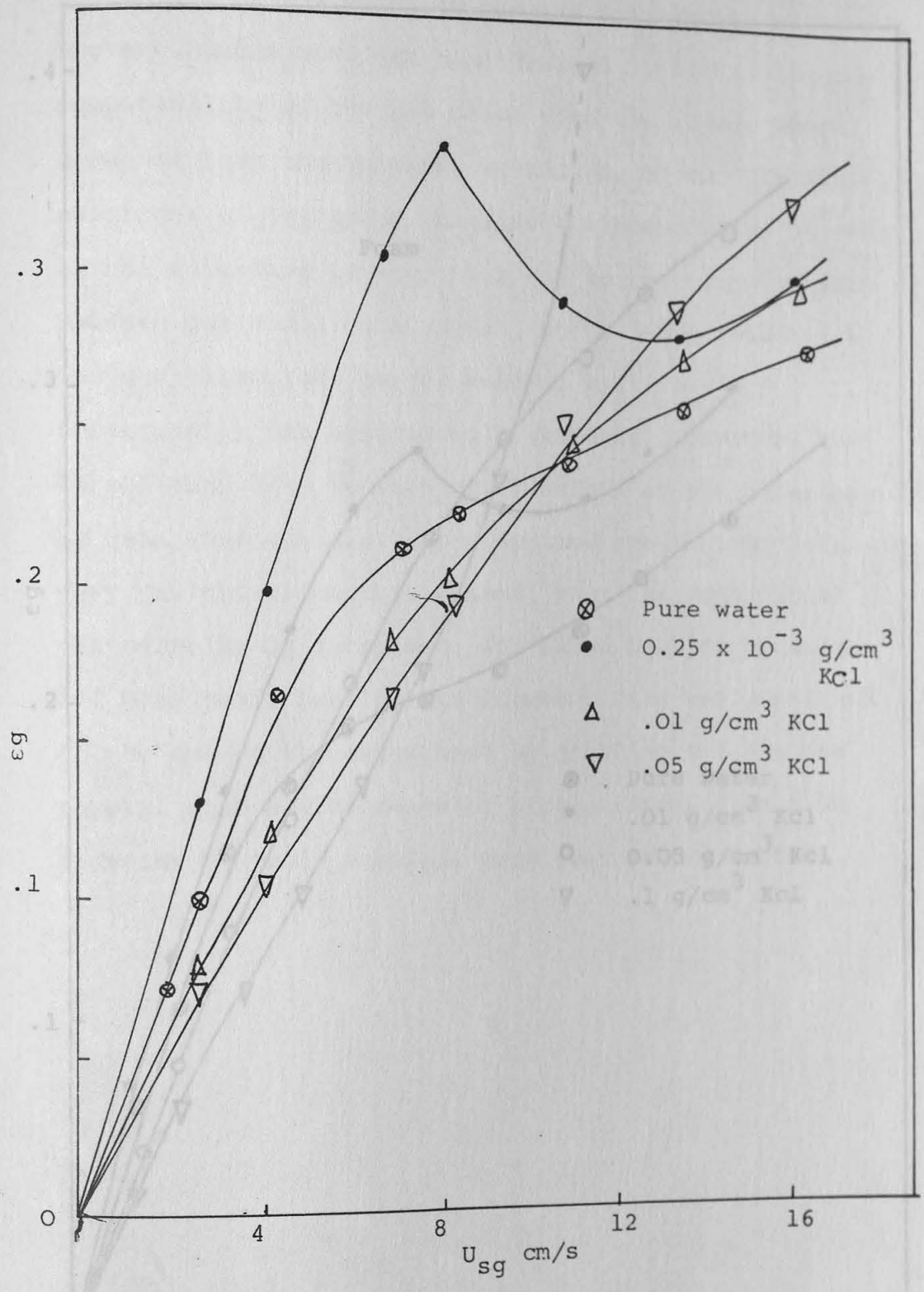

Figure 4.13 - Typical influence of high concentration of potassium chloride on gas hold-up, in two-dimensional column and for U_{sl} = 0

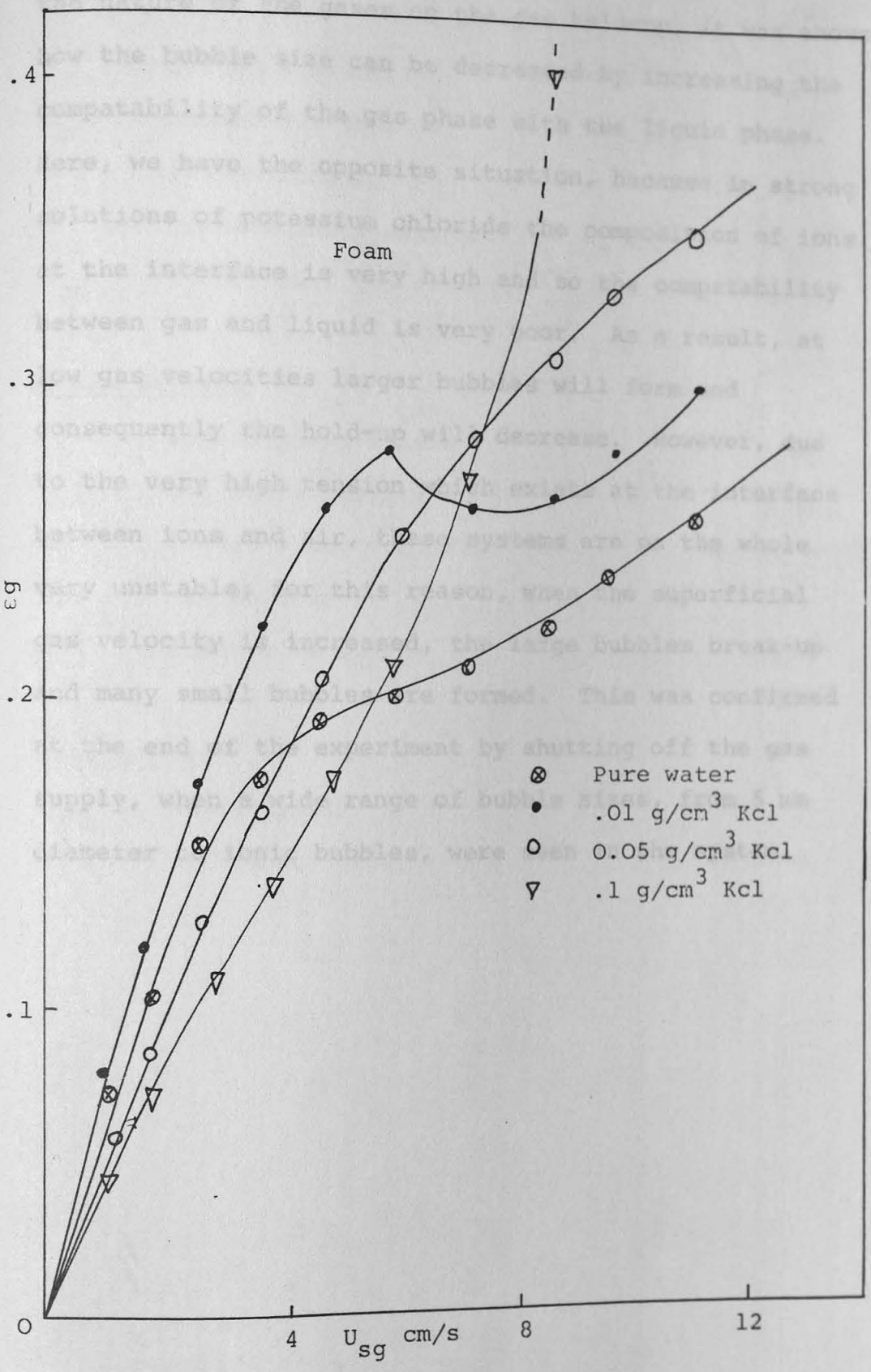

Figure 4.14 - Typical influence of high concentration of potassium chloride on gas hold-up in three dimensional column and for $U_{sl} = 0$

In Chapter 3, when we discussed the effect of the nature of the gases on the gas hold-up, it was shown how the bubble size can be decreased by increasing the compatability of the gas phase with the liquid phase. Here, we have the opposite situation, because in strong solutions of potassium chloride the composition of ions at the interface is very high and so the compatability between gas and liquid is very poor. As a result, at low gas velocities larger bubbles will form and consequently the hold-up will decrease. However, due to the very high tension which exists at the interface between ions and air, these systems are on the whole very unstable; for this reason, when the superficial gas velocity is increased, the large bubbles break-up and many small bubbles are formed. This was confirmed at the end of the experiment by shutting off the gas supply, when a wide range of bubble sizes, from 5 mm diameter to ionic bubbles, were seen in the system.

Nomenclature

		Units
d	column diameter	cm
d_b	bubble diameter	cm
L	column height	cm
g	gravitational constant	cm/s^2
U_{sg}	superficial gas velocity	cm/s

Greek Letters

ρ_L	liquid phase density	g/cm^3
ρ_G	gas phase density	g/cm^3
μ_L	liquid phase viscosity	g/cms or CP
εg	gas hold-up	-
τ	surface tension	g/s^2

Subscripts

L, l	liquid phase
G, g	gas phase

References

1. Bridge, A.G., Lapidus, L. and Elgin, J.C. A.I.Ch.E. Journal, 319, 10 (1964).
2. Marrucci, G. and Nicodemo, L. Chem. Eng. Sci, 22 (1967) 1257.
3. Hughamark, G.A., Ind. Eng. Chem. Process Des. Dev., 6 (1967), 218.
4. Akita, K. and Yoshida, F. Ind. Eng. Chem. Process Des. Dev., 12 (1973), 76.
5. Akita, K. and Yoshida, F. Ind. Eng. Chem. Process Des. Dev., 13 (1974), 84.
6. Hikita, H. and Kikukawa, Bull. Unv. Osaka Prefect, Ser. A., 22 (1973), 151.
7. Gestrich, W. and Rahse, W. Chem. Ing. Tech., 47 (1975), 8.
8. Kuma, K., Degaleesan, T.E., Laddha, G.A. and Hoelscher, H.E. Can. J. Chem. Eng., 54 (1976), 503.
9. Botton, R. and Cosserat, D. Chem. Eng. J., 16 (1978), 107.
10. Mersmann, A. Chem. Ing. Tech., 49 (1977), 679, Ger. Chem. Eng., 1 (1978), 1.
11. Schugerl, K. and Lucke, J. Advances in Biochemical Eng., 7 (1977), 1.
12. Calderbank, P.H., Moo-Young, M.B. and Bibby, R. 3rd European Symp. Chemical Reaction Engineering, Pergamon Press Ltd. (1964).

13. Eissa, S.H. and Schugerl, K. Chem. Eng. Sci., 30 (1975), 1251.

14. Rietema, K. and Ottengraf, S.P.P., Trans. Inst. Chem. Engrs, 48 (1970) T54.

15. Braulick, W.J., Fair, J.R. and Lehrer, B.J. A.I.Ch.E. Journal, 11 (1965), 73.

16. Sharma , M.M. and Mashelkar, R.A., Paper presented at Tripartite Chemical Engineering Conference, Symp. on Mass Transfer with Chemical Reaction, Montreal, September 1968.

17. Fair, J.R., Lambright, A.J. and Andersen, J.W., Ind. Engng Chem. Process Design Develop., 5 (1966), 416.

18. Yoshida, F. and Akita, K. A.I.Ch.E. Journal, 11 (1965), 9.

19. Deckwer, W.D., Burckhart R. & Zoll, G. Chem. Eng. Sci., 29 (1974), 2177.

20. Lessard, R.R. and Zieminski, S.A. Ind.Engng Chem. Fundl. 10 (1971), 260.

21. Zieminski, S.A. and Whittemore, R.C. Chem. Eng. Sci., 25 (1971), 509.

22. Calderbank, P.H. and Moo-Young, M.B. Chem. Eng. Sci., 16 (1961), 39.

23. Koetsier, W.T., Thoenes, D. and Frankena, J.F. Chem. Eng. Jl., 5 (1973), 61.

24. Koetsier, W.T. and Thoenes, D. Chem. Eng. Jl, 5 (1973), 71.

25. Robinson, C.W. and Wike, C.R. A.I.Ch.E. Journal, 20 (1974), 285.

26. Deckwer, W.D., Burckhart, R. Chem. Eng. Sci., 30 (1975), 351.

5 Three-Phase Systems - Simulation of the Behaviour of Microbial Aggregates

5.1 Introduction

Three-phase reactors have many applications in catalytic reaction engineering. There are two common modes of operation of the three-phase reactor: (1) trickle bed or packed bed operation, where the catalyst is stationary and the liquid flows as a dispersed phase, the gas being the continuous phase, and (2) slurry reactors, where the catalyst is suspended in the liquid medium by either mechanical - or gas - induced agitation. Here the liquid medium could either be a reactant or an inert medium for contacting the dissolved gases with the solids. Similarly the gaseous component could be either a reactant or an inert to provide agitation. The solid particles in most cases are catalysts or absorbents. Two types of slurry reactor operation are normally encountered - mechanically agitated slurry reactors and bubble column slurry reactors. The bubble column slurry reactor (the subject of the author's research) has a number of advantages over other three-phase reactors, such as trickle bed or packed bubble bed reactors. These are:

1. As catalyst particles of small size can be used in slurry reactors, the intra particle diffusional resistance is low in comparison to that in trickle or packed bubble bed reactors. Trickle bed reactors normally employ catalyst particle sizes at which the intra particle diffusion may be significant.

2. The external mass transfer coefficients in slurry reactors are higher than in trickle or packed beds; this leads to better utilisation of the catalyst.
3. Slurries have higher heat capacities and higher heat transfer coefficients. Due to this, temperature control of exothermic reactions is better in slurry reactors, and the formation of hot spots can be avoided. Slurry reactors are relatively safer for reactions with temperature run-away. The large liquid volume is also an advantage in maintaining isothermal conditions. The heat recovery, too, in these reactors is better.
4. In view of the difficulty of pelletizing some solids and the high cost involved in pelletizing, slurry reactors may prove to be more useful in some cases.

In spite of these advantages, the design of slurry reactors is not without problems. A major problem is that little is known about the hydrodynamics of the solid phase in such systems. In this section, we will attempt to elucidate this problem by looking at the effect of the solid phase on the performance of the bubble column, using a wide range of solids with different physical properties, i.e. wettability, density and size. At the same time, it will be possible to get some idea of the behaviour of microbial aggregates in bubble column fermenters.

5.2 Literature Survey

Gas-liquid-solid operations are of a comparatively complicated physical nature: three different phases with different physical properties are present and the flow patterns of each individual phase are complex. Three-phase fluidisation has only recently become the subject of systematic research, and the available information on this subject is indeed meagre, incomplete and mainly based on studies with air, water and glass ballotini. In the following sections published information on the behaviour of the gas and solid phases will be reviewed. Some other aspects of gas-liquid fluidisation (i.e. mixing of the liquid and solid phases) will be surveyed in Section (6.2).

5.2.1 Bubble Coalescence Studies

Several studies have been directed towards improving our understanding of the problem of bubble coalescence or disintegration in gas-liquid fluidised beds. The published papers are introduced historically to provide an indication of how ideas have been developed.

Massimila et al. (1) injected air through a single orifice into beds fluidised by tap water: orifices of 0.4 and 1.0 mm i.d. were used, the gas flowrate was

varied from 0.5 to 6.5 cm^3/s, and the solid phases were silica sand, glass ballotini and iron sand of average equivalent diameters from 0.22 to 1.09 mm. The average size of gas bubbles emerging from the bed surface was determined from photographs, and estimates of bubble coalescence were obtained by determining the size of gas bubbles emerging from beds of different heights. It was observed that bubble coalescence occurred in the lower part of the fluidised beds, whereas beyond distances of about 30-60 cm from the orifice the net rate of coalescence approached zero. The rate of coalescence was observed to decrease with increasing bed expansion. An attempt was made to interpret these results using a theoretical model of bubble flow and relatively high, effective bed viscosities.

Adlington and Thompson (2) have measured the gas-liquid interfacial area in beds of particles of from 0.3 to 3 mm diameter by oxygen absorption in a sodium sulphite solution. They found that the interfacial area decreased with decreasing bed porosity and that it was less sensitive to changes in particle size.

Lee (3) has reported measurements of average bubble diameter and gas-liquid interfacial areas for gas-liquid fluidised beds of glass beads of 6 mm diameter. The gas injection system was arranged to give fairly large bubbles at the base of the bed, and it was found that the bubble size decreased and the gas-liquid

interfacial area increased with increasing height above the gas distributor. The disintegration of bubbles occurred at a higher rate in beds of low expansion.

Ostergaard (4) measured the rate of growth of gas bubbles formed in a liquid-fluidised bed at a single orifice of 3.0 mm i.d. with gas flowrates varying from 9 to 63 cm^3/s. The experiments were carried out with tap water, air and sand particles of an average equivalent diameter of 0.64 mm. The bubble frequency at the orifice was measured by an electrical resistance probe connected to an oscilloscope, which produced a straight line at zero gas flowrates and a series of peaks at finite gas flowrates, each peak corresponding to the increase in electrical resistance resulting from the formation of bubbles. The bubble frequency of the bed surface was calculated from cine photographs. The measured bubble frequencies at the orifice did not generally deviate significantly from those measured in water with no solid particles present. Near incipient fluidisation, however, the frequencies appeared to be lower than in water. The measured rate of coalescence was markedly dependent on bed porosity, having a relatively high value near the point of incipient fluidisation and decreasing with increasing liquid velocity and bed porosity.

Sherrard (5) has carried out a large number of observations of bubble size, for varying particle size and density, bed height and bed porosity. The high rate of bubble coalescence observed in beds of small particles of relatively low density was explained by reference to the relatively high viscosity of such beds.

Ostergaard (6,7) observed that bubbles in a bed of small particles near incipient fluidisation were nearly spherical in shape or of a spherical cap shape, the included angle being larger than that observed for spherical cap bubbles in water. In contrast, bubbles in a bed of high porosity were of ellipsoidal shape or of a spherical shape, the included angle being relatively small. Therefore, Ostergaard (8) has concluded that three-phase fluidised beds may be divided into two main categories, namely beds of large particles which are capable of breaking up the gas flow into a dispersion of relatively small bubbles and beds of small particles in which the gas bubbles are considerably larger: this division is also supported by Lee et al. (9). Ostergaard has also proposed a theoretical model for bubble coalescence based on the observations of Massimila et al. "that beds of small particles are characterised by a high viscosity" and those of Calderbank et al. (10) "that the rate of gas bubble coalescence in liquids increased markedly with an increase in liquid viscosity". However, as discussed in Section (3) hold-up will

increase as liquid viscosity increases, and so Ostergaard's explanation for his results is open to question.

Rigby et al. (11) measured the size, frequency, rising velocity, and size distribution of gas bubbles within three-phase fluidised beds by means of an electro-resistivity probe. They employed water, air and four sand samples having mean diameters ranging from 0.12 to 0.775 mm. The results obtained were similar to those of Massimilla et al. Darton and Harrison (12) also employed an impedance probe to study bubble characteristics in air-water fluidised beds of 0.5 mm sand. They observed that in air-water dispersions the interfacial areas were considerably higher than those in three-phase fluidised beds at the same gas flow rate: this was because the bubbles were smaller in the air-water dispersions.

Some studies are also concerned with the mechanism of bubble break up in three-phase fluidised bed. Sherrard, Lee and Buckley (9) have developed a criterion for the disintegration of bubbles when they are penetrated by solid particles; the criterion is expressed as a critical value of Weber number. Henriksen and Ostergaard (13), in order to check the theory of Sherrard and Lee, studied the break-up of 2 cm bubbles in beds of water and methanol. Three solids were employed, namely 5 mm steel spheres and 3 and 6 mm glass spheres. A bubble

was held stationary by a downward flow of liquid and a particle was then allowed to fall through it. In no case was the bubble observed to distintegrate: they concluded that the bubbles were broken up as a result of Taylor instability (14) of their roofs. Since the minimum sized particle capable of splitting a bubble in air-water beds was shown to be about 8.5 mm it was concluded that the instability was generated by fingers of liquid projecting down through the roof of the bubble.

Kim et al. (15) also identify two distinct types of three-phase fluidisation. These may be termed "bubble coalescing" and "bubble disintegrating" situations. The former occurs when the particles are smaller than the critical size and the latter when they are larger. The addition of particles smaller than the critical size to a liquid-gas bed resulted in an increase in the mean bubble size: they called this the "bubble coalescing" type. The addition of solids larger than the critical size resulted in a reduction in bubble size, and this is the "bubble disintegrating" type. Interestingly, Kim et al. (16) have since claimed that liquid viscosity plays an important role in determining which type of fluidised bed behaviour is observed: they found from experiment that beds of gravel and 6 mm glass beads fluidised by air and low viscosity solutions exhibited

bubble disintegrating behaviour whereas bubble coalescing behaviour was observed on increasing the viscosity of the liquid fluidising medium. Kim et al. made reference to the work of Calderbank (see Section (4.55)) in support of these findings. Kim et al. (17) in their recent paper on the characteristics of bubbles in three-phase fluidised beds concluded that liquid viscosity and surface tension have little effect either on bubble size or rising velocity. Interestingly, they found that, at low viscosities in three-phase systems, the solids played a minimal role in coalescence but, at higher viscosities, the coalescence rate in gas-liquid beds decreased and in the three-phase system remained approximately constant. Also, they reported that there appeared to be no statistical difference between bubble characteristics in beds of different particle size when operated under the same experimental conditions.

5.2.2 Gas Hold-up

Some measurements of gas hold-up have been reported in the literature, and these will now be described again in date order.

Adlington and Thompson (2) reported results from experiments with (a) 3 in diameter beds of alumina

particles of from 0.3 to 2.8 mm diameter fluidised by white spirit and (b) 10 in diameter beds of sand particles of 0.3 mm diameter fluidised by water. They found that the presence of solids had little influence on gas hold-up below superficial gas velocities of about 1.5 cm/s. At higher gas velocities the presence of solids caused a decrease of gas hold-up, particularly in the denser beds prevailing at lower liquid rates.

Schugerl (18) and Afschar and Shugerl (19) have reported data on hold-up in gas-liquid fluidised beds of 0.25 mm solid particles, the liquid medium being water. It was observed that gas hold-up was considerably lower in the gas fluidised bed than in a corresponding solids-free system. Ostergaard and Gilliland (20) measured the gas hold-up in beds of sand particles of 40-60 and 60-80 mesh. The fluid media were nitrogen and water. The gas hold-up was largely independent of particle size and liquid velocity. Comparison with an equivalent gas-liquid system free of solids showed that the gas hold-up of such a system was higher than that of a gas-liquid fluidised bed.

Michelson and Ostergaard (21) measured gas hold-up in beds of 1, 3 and 6 mm glass particles in an 6 in diameter bed fluidised by tap water and air. They found that bubble break-up occurred in beds of large particles resulting in a uniform dispersion of small bubbles and thus higher hold-ups than in the corresponding

solids-free systems. The break-up regime was not encountered in beds of 1 mm particles nor in beds of 3 mm particles at low liquid flowrates; coalescence was important in beds of small particles and, therefore, gas hold-up was lower than in the corresponding solids-free systems.

Kato et al. (22) measured gas hold-up using air, water and glass spheres. Five size ranges of glass spheres with a density of 2.52 g/cm^3 were used: 63-88, 88-105, 105-125, 125-149 and 149-177 μm in diameter. They found that (a) the gas hold-up of the air-water glass sphere system was somewhat less than that of the air-water system, and (b) the larger solid particles resulted in somewhat smaller gas hold-ups.

Kumar and Roy (23) reported data on the simultaneous gas-liquid fluidisation of solids using air, water and silica and limestone as the solid phase. It was observed that the gas hold-up decreased with increasing bed height. They explained this as follows: if both the solid bed height and solids hold-up increase, the amount of liquid contained within the effective column length is reduced and this in turn reduces the gas hold-up.

Ostergaard (24) recently measured gas hold-up in three-phase fluidised beds of 9 in diameter and found that the results were in good agreement with similar hold-up data previously obtained for a column of 6 in internal diameter (see Michelson and Ostergaard (21)).

5.3 Experimental Programme

5.3.1 Experimental Equipment

Throughout the three-phase programme use was made of the same two columns used in previous work (that is to say the two-dimensional bubble column of size 1.3 cm x 1.34 cm in diameter and the three-dimensional bubble column 15.2 cm in diameter and 173 cm in height). Details of columns and the peripheral equipment can be found in Section (2.4). A suitable mesh was fitted over the column outlet in order to prevent the solid phase from being washed out and to keep the average solids concentration in the column constant.

5.3.2 Materials and Operational Conditions

Tap water was used as the liquid fluidising medium, and air was used as the gaseous phase. Solid particles of plastic material in the form of spheres, right cylinders and irregular fragments and ballotini beads of a wide range of sizes were used to simulate either microbial aggregates or inorganic catalysts: the properties of these materials are given in Appendix D. The operational conditions were almost the same as those given in Section (2.2.1), the numerical values of the gas and liquid superficial velocities remained the same as those used for two-phase systems (see Section 2.2.1).

5.3.3 Experimental Procedure

Initially, solids were introduced into the bubble column, liquid and gas were then fed in at pre-determined values. Following this, and after a steady concentration distribution of solid particles was established in the column (it was assumed that this happened when the bubble column became full of liquid and started to overflow from the take-off system), samples of fluidised suspension were withdrawn through sampling taps into measuring cylinders. The volume of each sample was then measured, and the solid particles were then separated from the liquid and allowed to settle in measuring cylinders. The settled volume of solids was than measured. The solids concentration was expressed in cm^3 of settled solids particles per cm^3 of fluidised suspension.

Gas hold-up was estimated as a function of superficial gas velocity, liquid flowrate and solids concentration. The method (detailed in Section 2.3) was to measure the displacement in the system height due to the air-flow. The difference in height was assumed to be produced by the gas hold-up in the system according to the definition that gas hold-up or volume voidage, εg, is the fraction of the mixture volume occupied by the gas bubbles.

5.4 Three-Phase Systems Containing Non-Wettable Solid Particles

5.4.1 Solid Surface Properties

Non-wetting means, as discussed in Appendix D, that the contact angle between a liquid and solid is greater than 90^{o}. It seems that, as yet, the largest contact angle to be found is 105^{o} for paraffin wax. However, the non-wettable solid particles which we used were Styrocel.

The Styrocel particles were spherical in shape and of a wide range of size and density; details are presented in Appendix D. From the molecular aspect, these particles are made of polystyrene, the basic unit being;

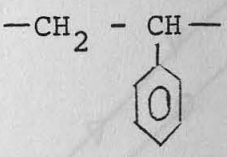

The above structure has no polar group and, consequently, it cannot form any kind of bond with highly polar liquids such as water. For this reason, it will remain unwetted in water.

5.4.2 Experimental Results

The results in Figures (5.1) to (5.6) were obtained with three-phase systems containing non-wettable

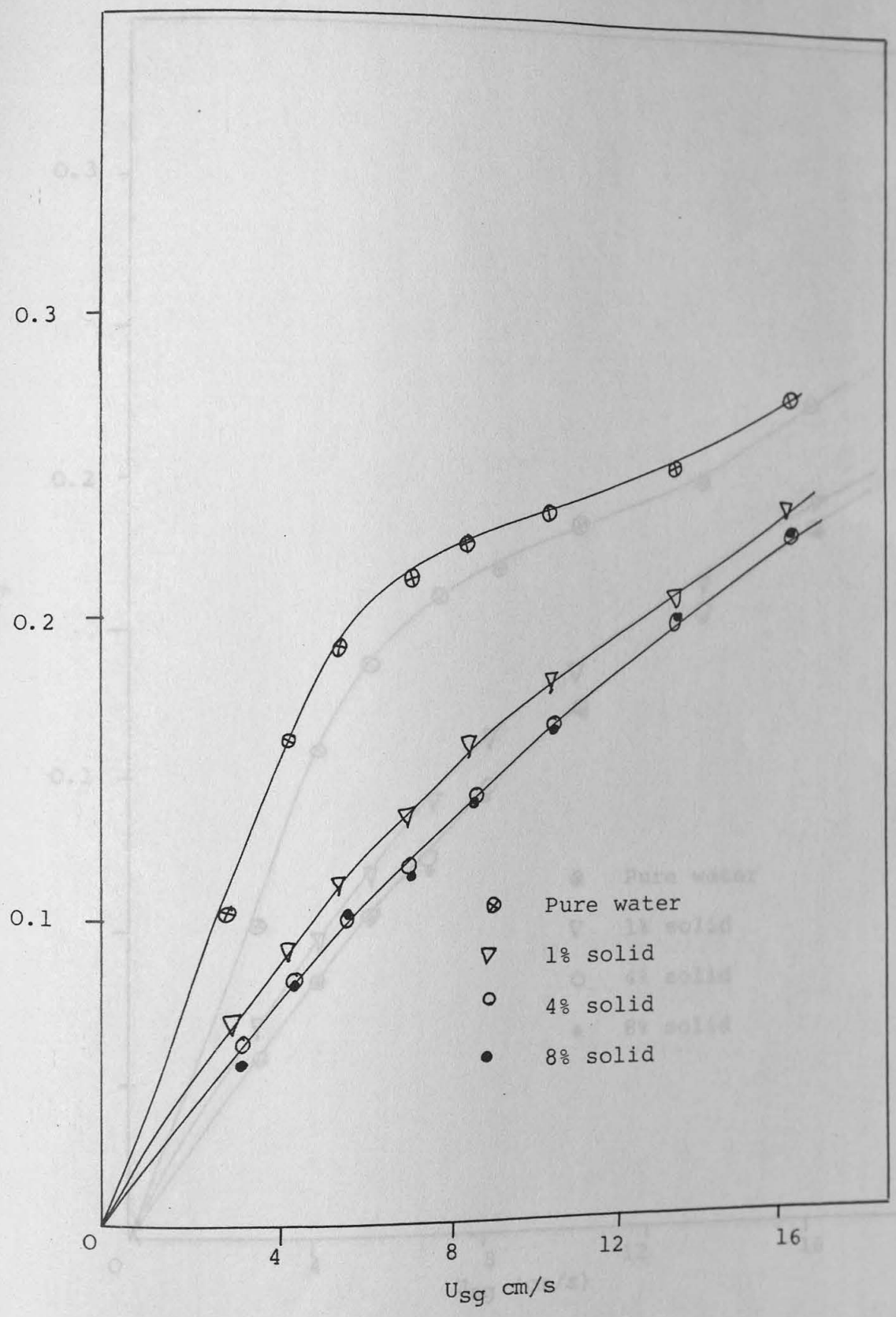

Figure 5.1 Effect of solid phase ($d=810\mu$ & $\rho=1.2$ g/cm^3) on gas hold-up in two dimensional bubble column and for $U_{s\ell}=.17$cm/s

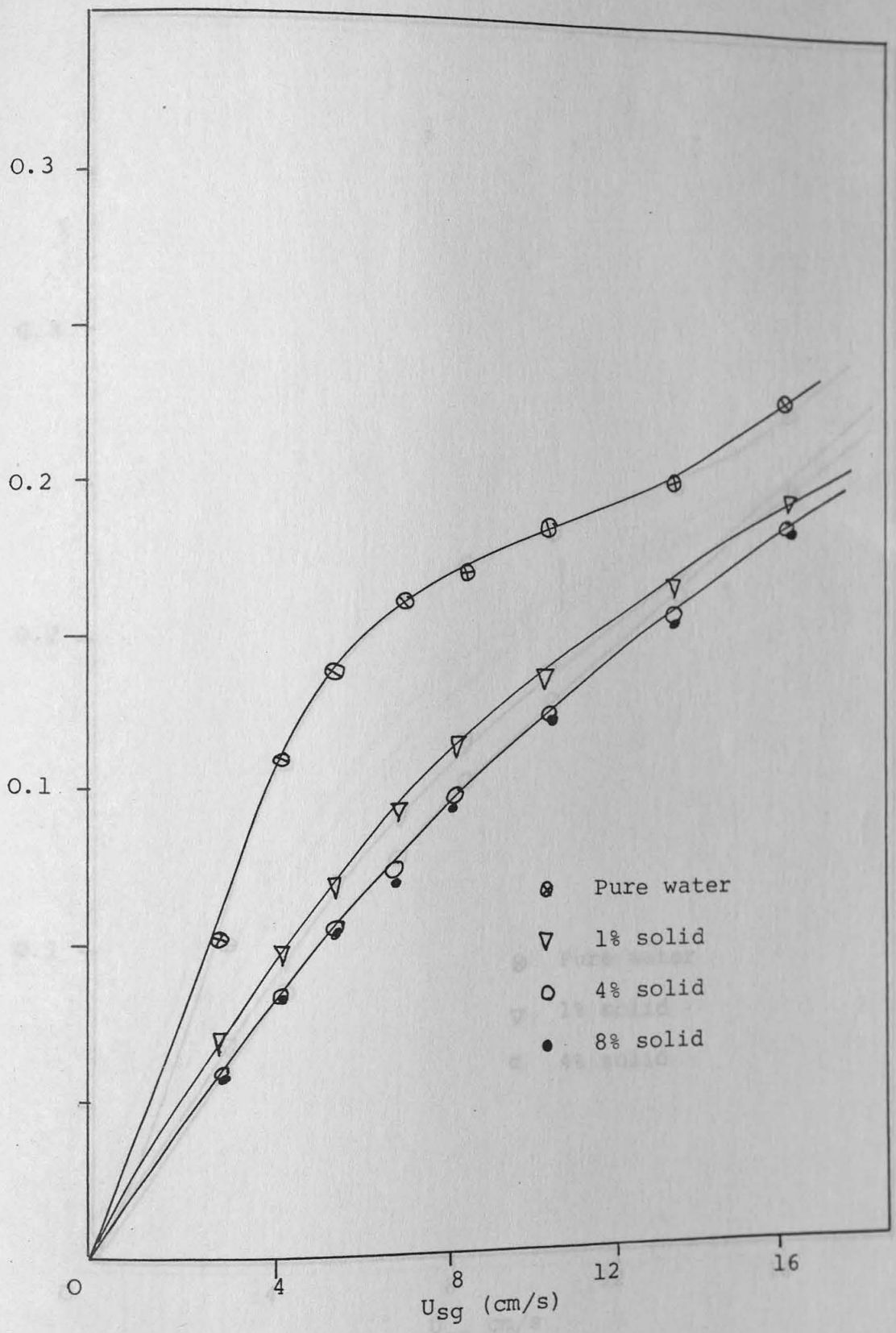

Figure 5.2 Effect of solid phase (d=1204$^{\mu}$ and ρ= 1.36 g/cm3) on gas hold-up in two dimensional column and for $U_{s\ell}$=0.17 cm/s

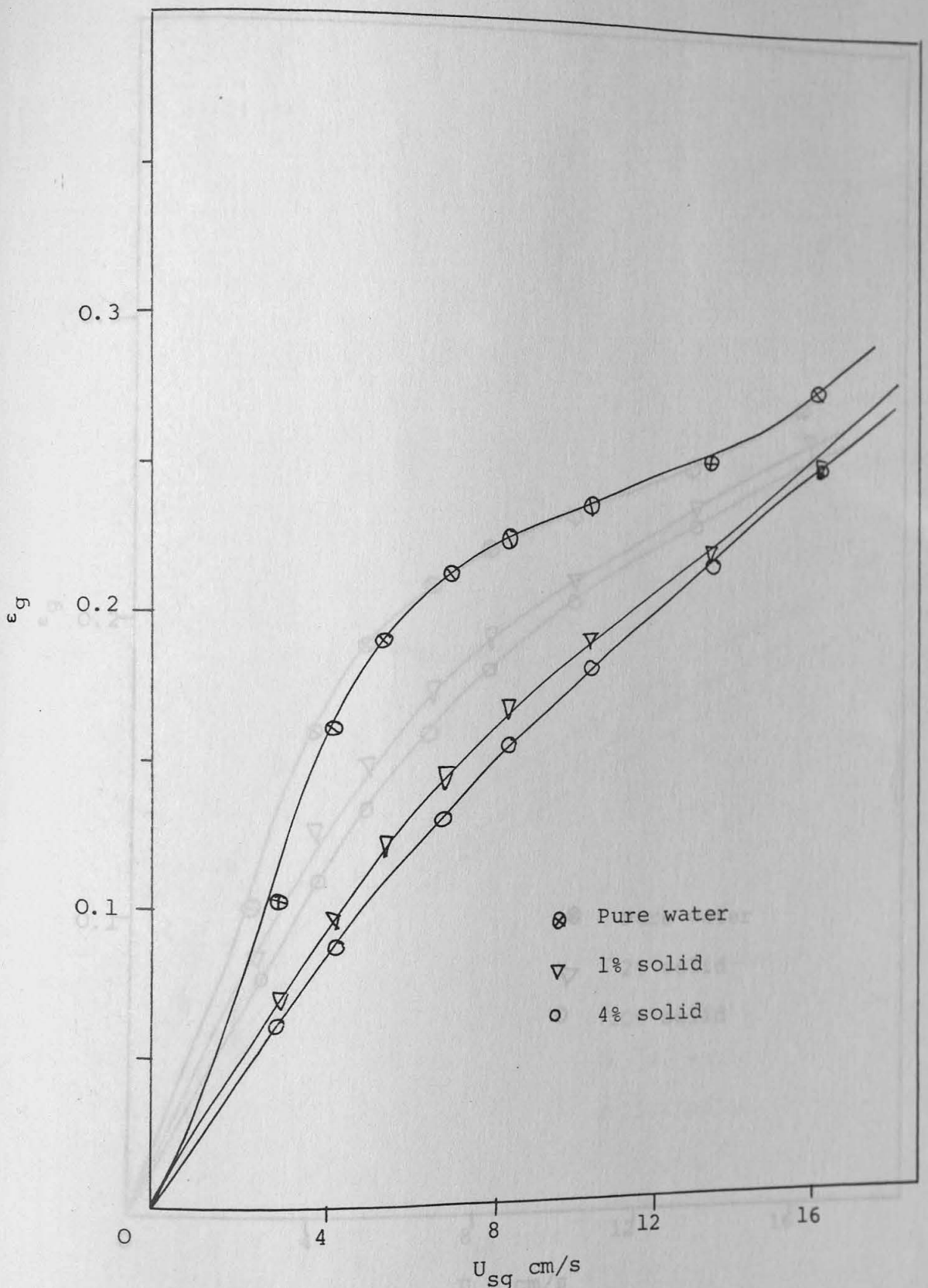

Figure 5.3 Effect of solid phase (ρ=0.85 g/cm^3 & d= 1883 μ) on gas gold-up in two dimensional column and for $U_{s\ell}$ = 0.17 cm/s

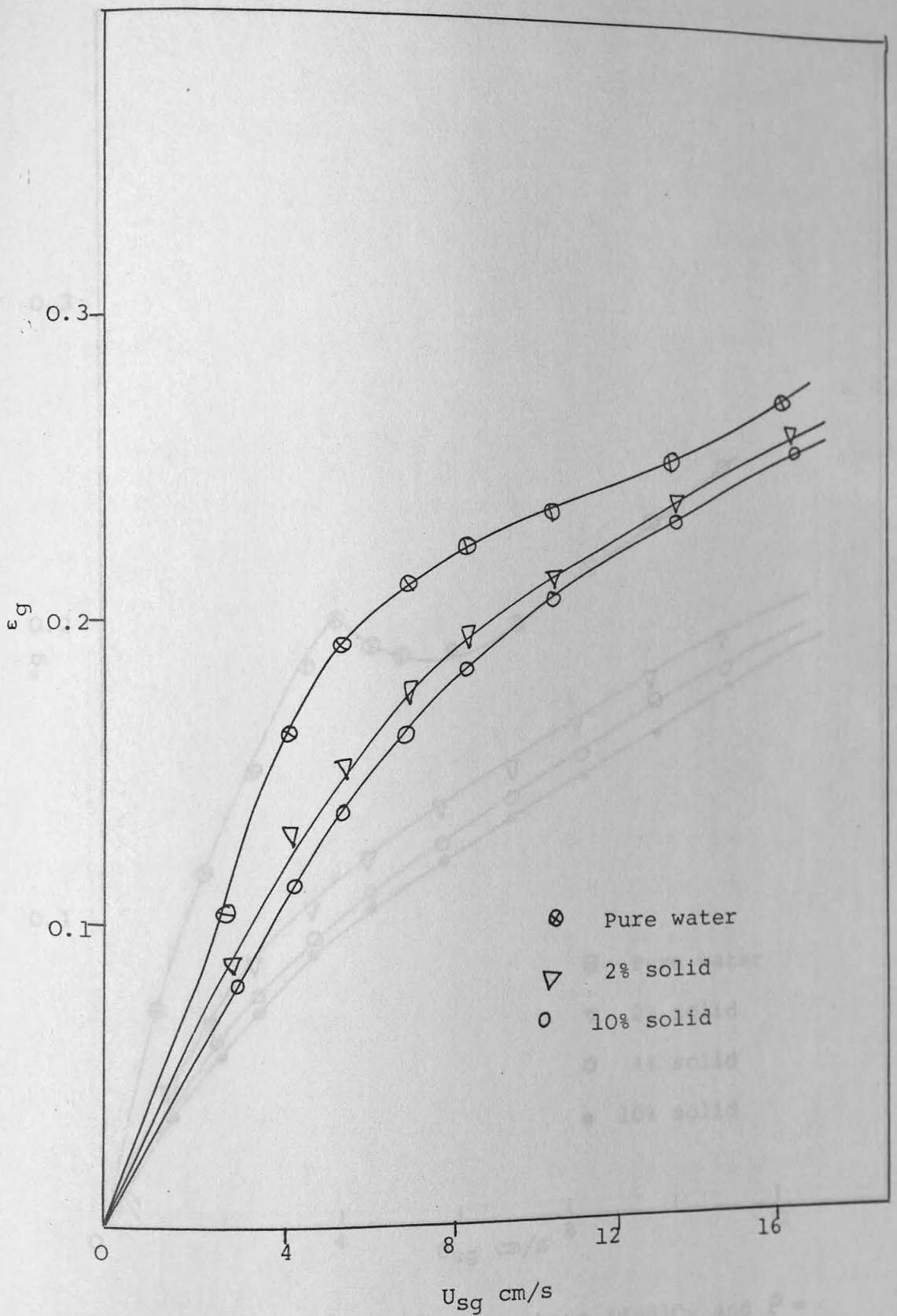

Figure 5.4 Effect of solid phase (d=1625 μand ρ = 0.45 g/cm3) on gas hold-up in two-dimensional bubble column and for $U_{s\ell}$ =0.17 cm/s.

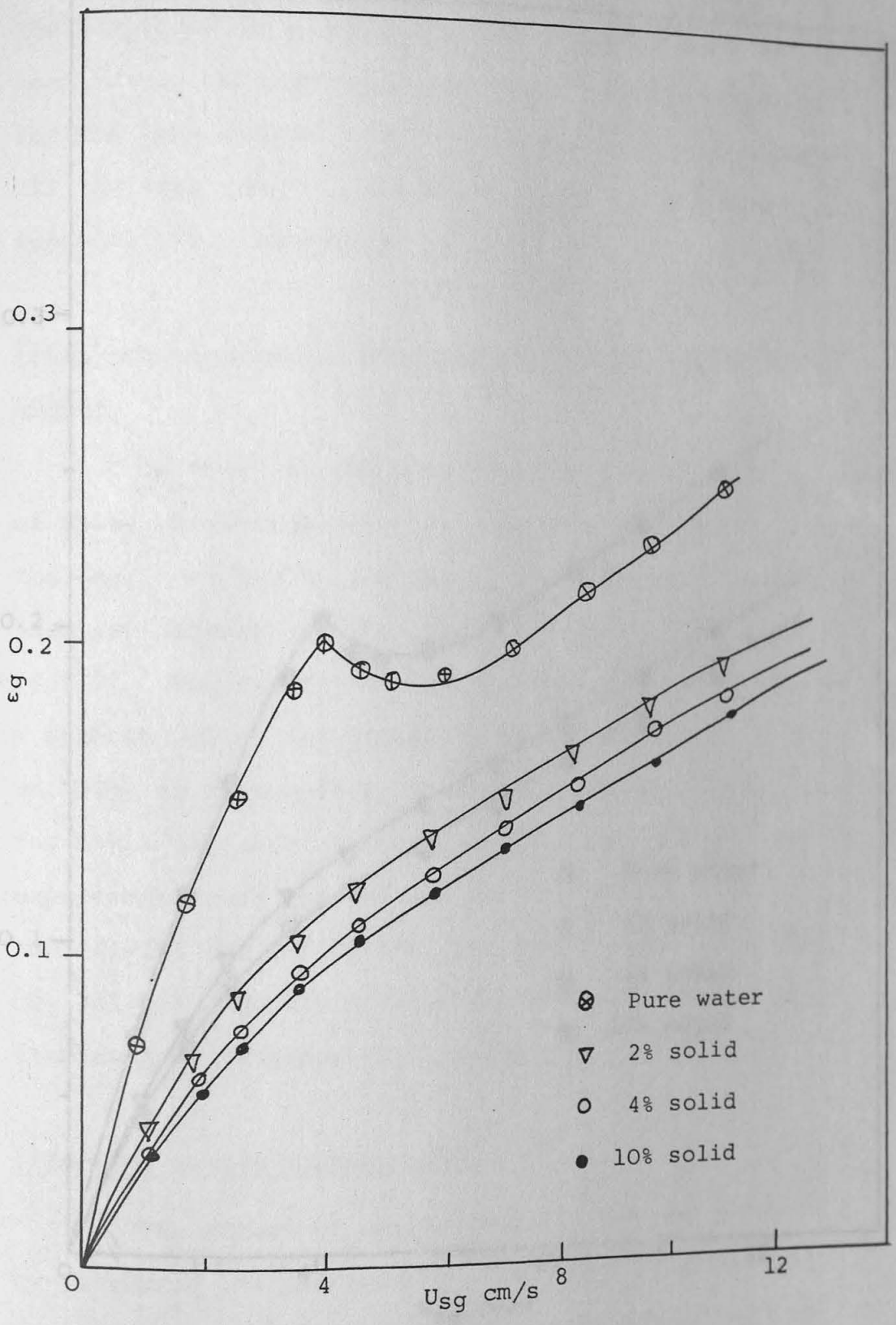

Figure 5.5 Effect of solid phase (d=810μ and ρ = 1.2 g/cm3) on gas hold-up in three dimensional column and for $U_{s\ell}$ = 0.045 cm/s.

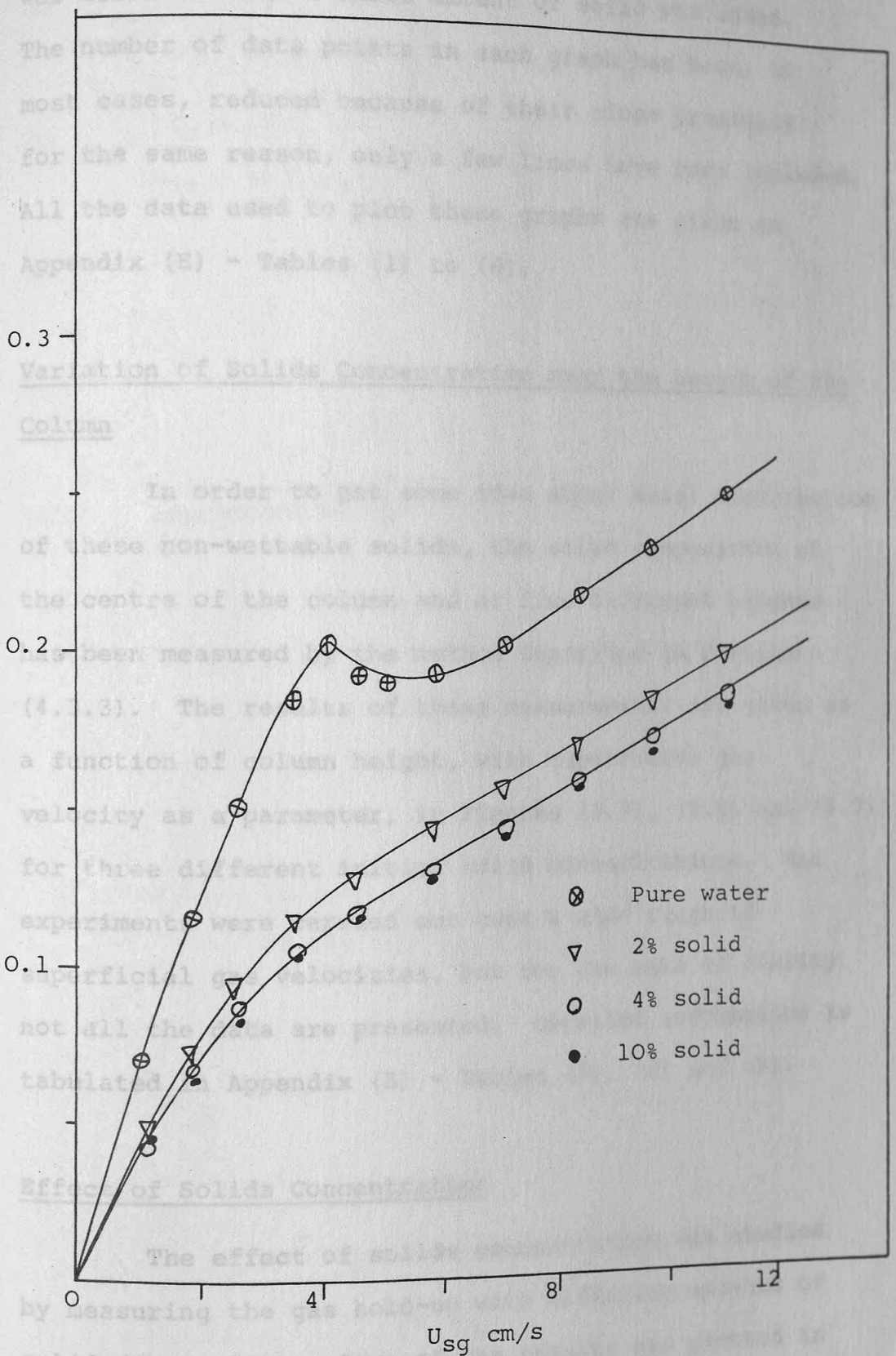

Figure 5.6 Effect of solid phase (d=1204$^{\mu}$ & ρ = 1.36 g/cm^3) on gas hold-up in three dimensional column and for $U_{s\ell}$ = 0.045 cm/s

solids (Styrocel) and show how the bubbly-flow regime was affected when a small amount of solid was added. The number of data points in each graph has been, in most cases, reduced because of their close proximity : for the same reason, only a few lines have been included. All the data used to plot these graphs are given in Appendix (E) - Tables (1) to (6).

Variation of Solids Concentration over the Length of the Column

In order to get some idea about axial distribution of these non-wettable solids, the solid composition at the centre of the column and at five different heights has been measured by the method described in Section (4.3.3). The results of these measurements are given as a function of column height, with superficial gas velocity as a parameter, in Figures (5.7), (5.8) and (5.9) for three different initial solid concentrations. The experiments were carried out over a wide range of superficial gas velocities, but for the sake of clarity not all the data are presented. Detailed information is tabulated in Appendix (E) - Tables (7), (8) and (9).

Effect of Solids Concentration

The effect of solids concentration was studied by measuring the gas hold-up with differing amounts of solid (0% to 30%). Some of the results are plotted in

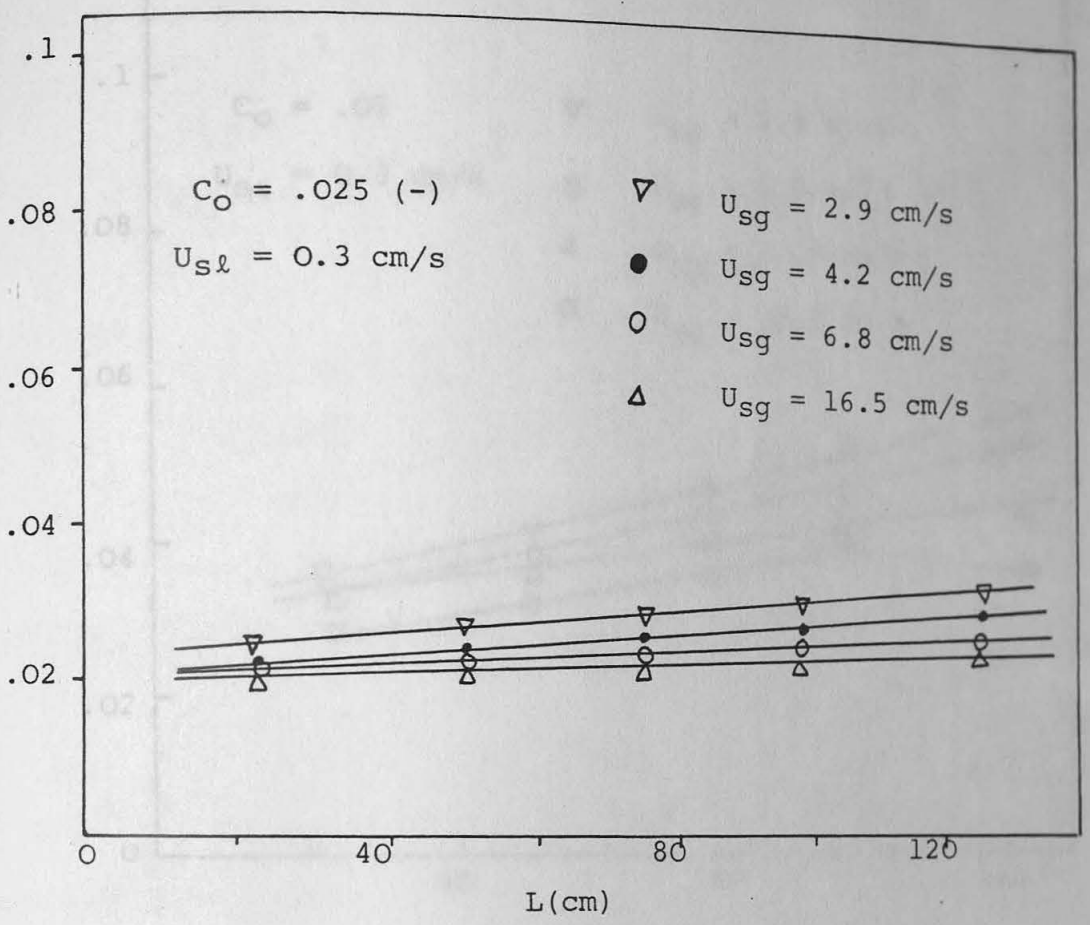

Figure 5.7 Variation of solid (styrocel, d=810$^{\mu}$ and ρ = 1.2 g/cm^3) concentrations over the length of the two dimensional column

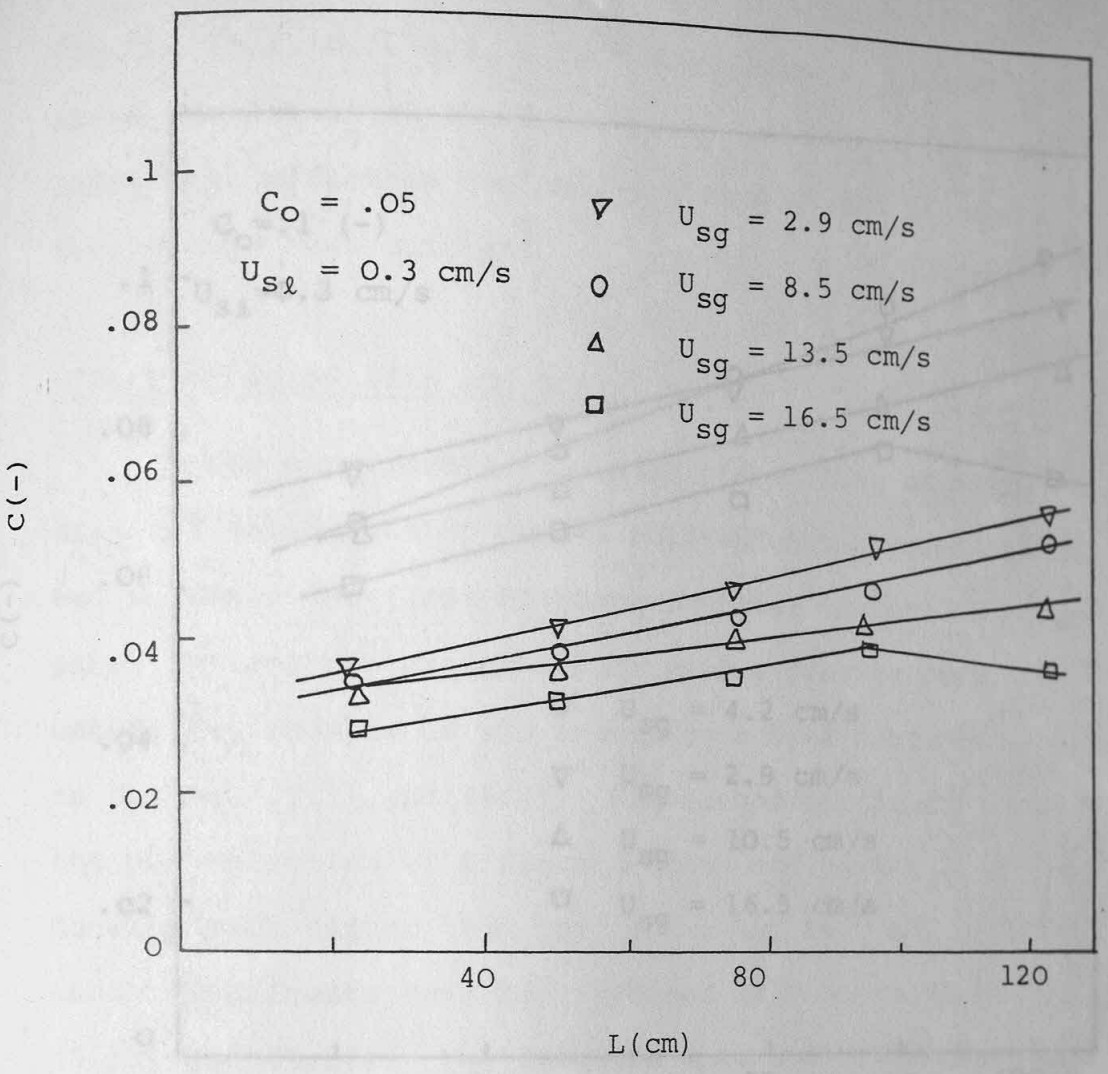

Figure 5.8 Solid (styrocel = 810$^{\mu}$ and ρ = 1.2 g/cm^3) concentrations profiles over the length of the two dimensional column

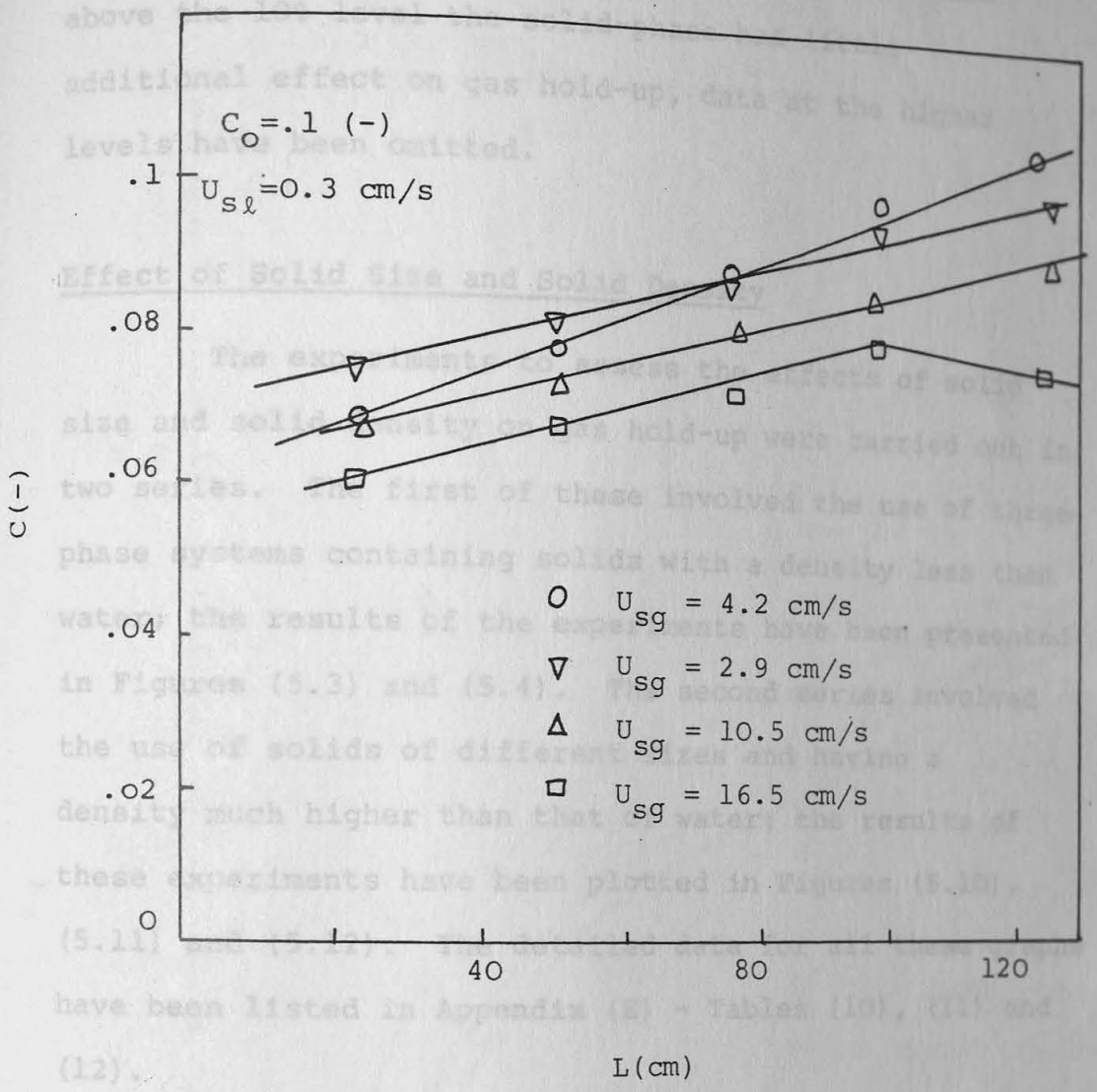

Figure 5.9 Solid (styrocel, d=810$^{\mu}$ and ρ =1.2 g/cm^3) concentrations profiles over the length of the two-dimensional bubble column

Figures (5.1, 5.2, 5.3, 5.5, 5.6). However, because above the 10% level the solid-phase had little additional effect on gas hold-up, data at the higher levels have been omitted.

Effect of Solid Size and Solid Density

The experiments to assess the effects of solid size and solid density on gas hold-up were carried out in two series. The first of these involved the use of three-phase systems containing solids with a density less than water; the results of the experiments have been presented in Figures (5.3) and (5.4). The second series involved the use of solids of different sizes and having a density much higher than that of water; the results of these experiments have been plotted in Figures (5.10), (5.11) and (5.12). The detailed data for all these graphs have been listed in Appendix (E) - Tables (10), (11) and (12).

5.4.3 Discussion

Effect of Solid Phase

Figures (5.1) to (5.6) were obtained for systems containing solids of different sizes and densities and show how the hold-up is minimized by adding small amounts of solid. Furthermore, these figures, on the whole, show that the effect of solid is more marked in the bubbly-flow regime than in the slug-flow regime. The explanation for this is as follows.

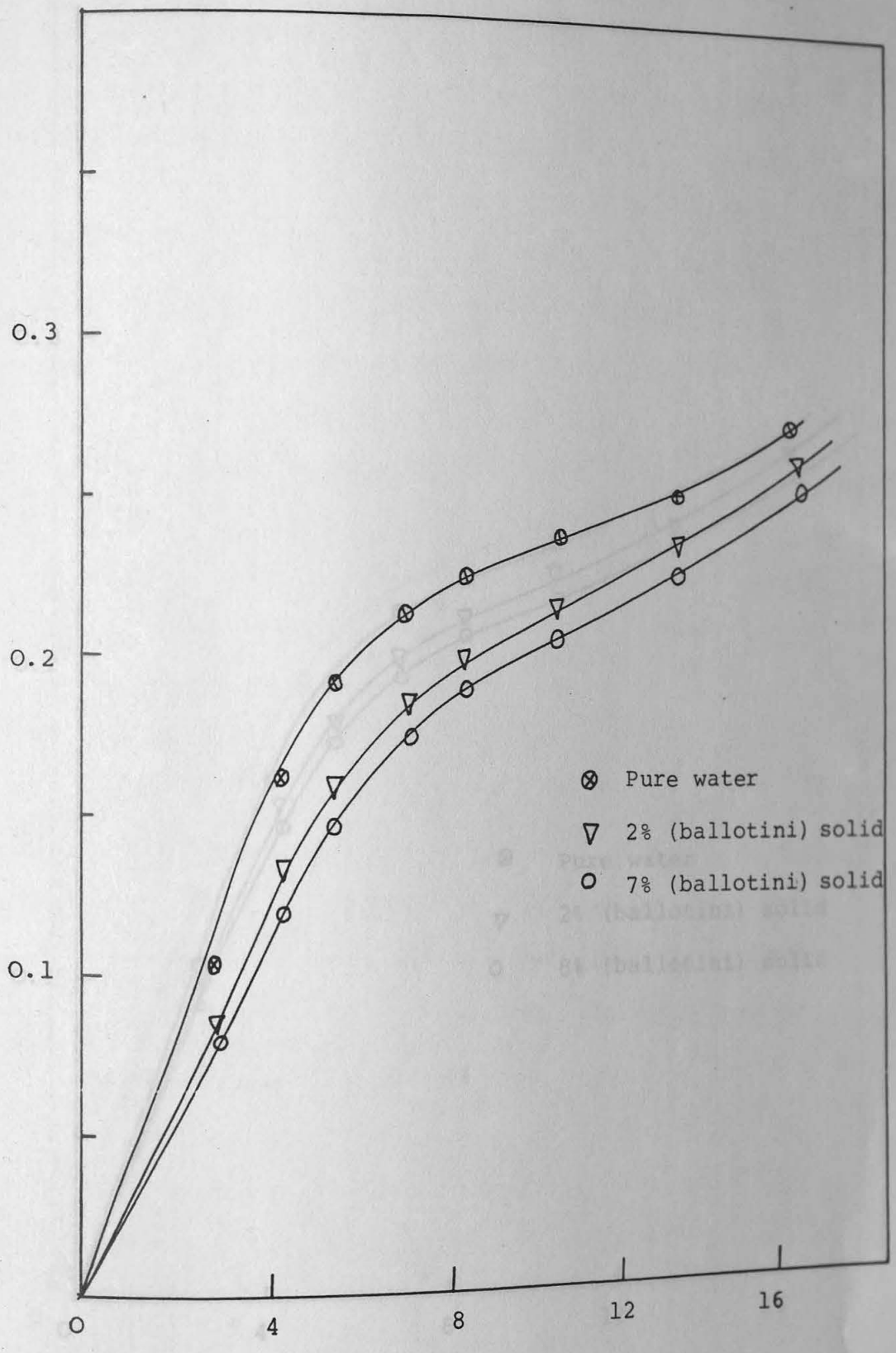

Figure 5.10 Typical influence of solid phase ($d=140\text{-}125\mu$ and $\rho = 1.71$ g/cm^3) on gas hold-up in two dimensional bubble column and for $U_{s\ell} = .17$ cm/s

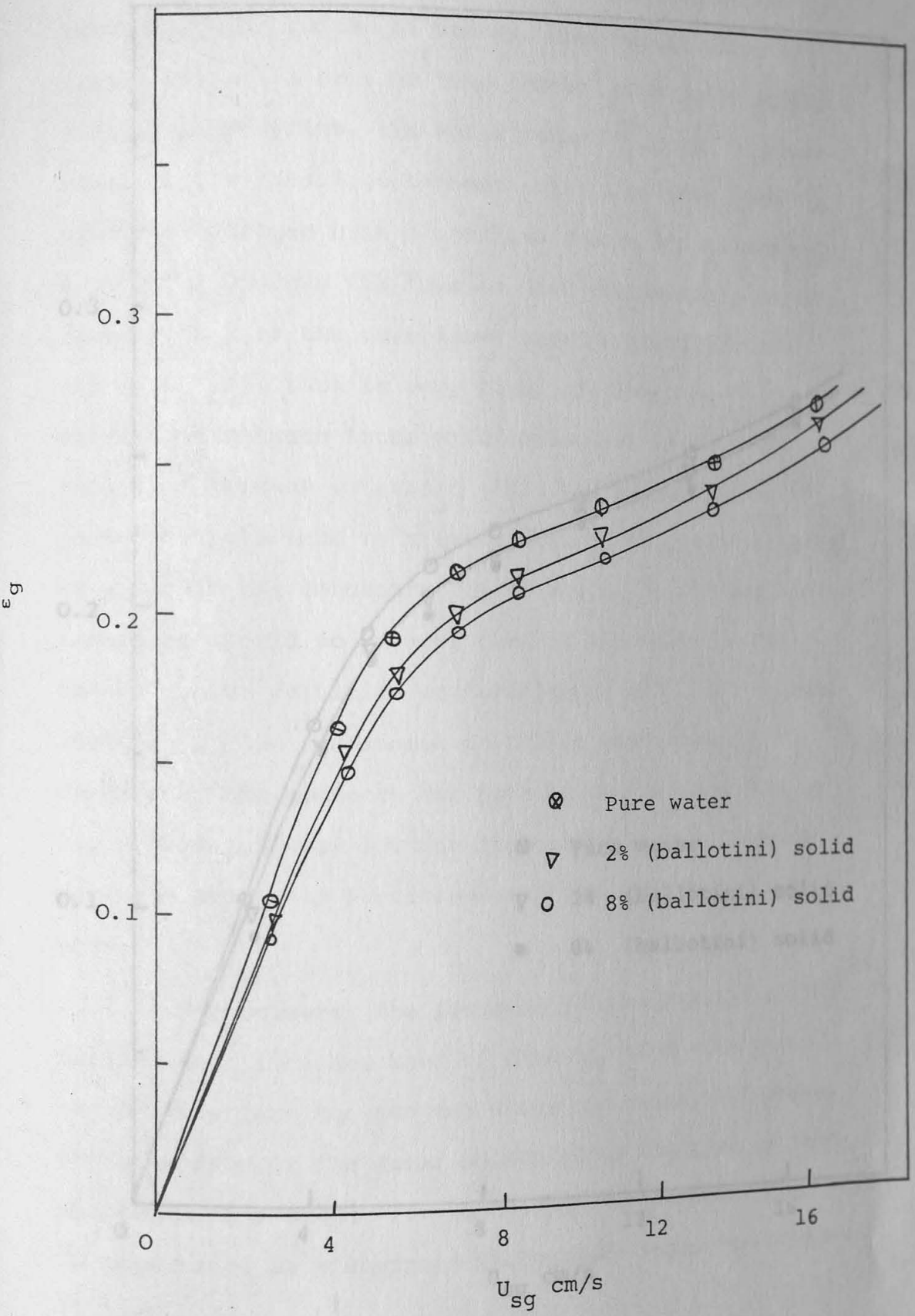

Figure 5.11 Typical influence of solid phase ($d=3000\mu$ and $\rho = 2.4$ g/cm^3) on gas hold-up in two dimensional bubble column and for $U_{s\ell} = 0.17$ cm/s

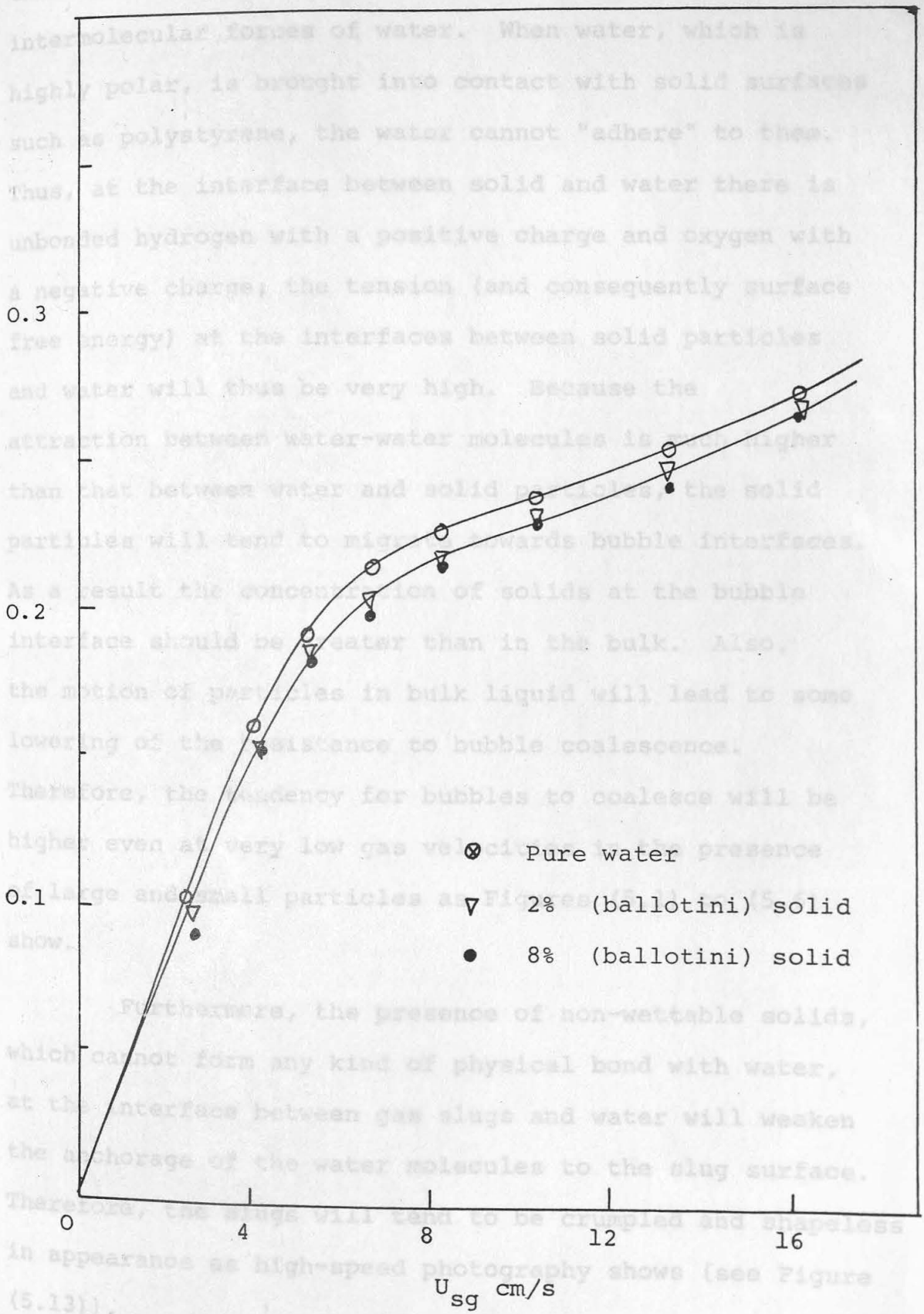

Figure 5.12 Typical influence of solid phase ($d=6000\ \mu$ and $\rho = 2.7\ g/cm^3$) on gas hold-up in two dimensional column and for $U_{s\ell} = 0.17$ cm/s

It is well known from studies of air-water systems that the coalescence of bubbles is suppressed by the intermolecular forces of water. When water, which is highly polar, is brought into contact with solid surfaces such as polystyrene, the water cannot "adhere" to them. Thus, at the interface between solid and water there is unbonded hydrogen with a positive charge and oxygen with a negative charge; the tension (and consequently surface free energy) at the interfaces between solid particles and water will thus be very high. Because the attraction between water-water molecules is much higher than that between water and solid particles, the solid particles will tend to migrate towards bubble interfaces. As a result the concentration of solids at the bubble interface should be greater than in the bulk. Also, the motion of particles in bulk liquid will lead to some lowering of the resistance to bubble coalescence. Therefore, the tendency for bubbles to coalesce will be higher even at very low gas velocities in the presence of large and small particles as Figures (5.1) to (5.6) show.

Furthermore, the presence of non-wettable solids, which cannot form any kind of physical bond with water, at the interface between gas slugs and water will weaken the anchorage of the water molecules to the slug surface. Therefore, the slugs will tend to be crumpled and shapeless in appearance as high-speed photography shows (see Figure (5.13)).

Figure 5.13 - Shape of Slugs in Three-Phase Systems Containing Non-Wettable Solids.

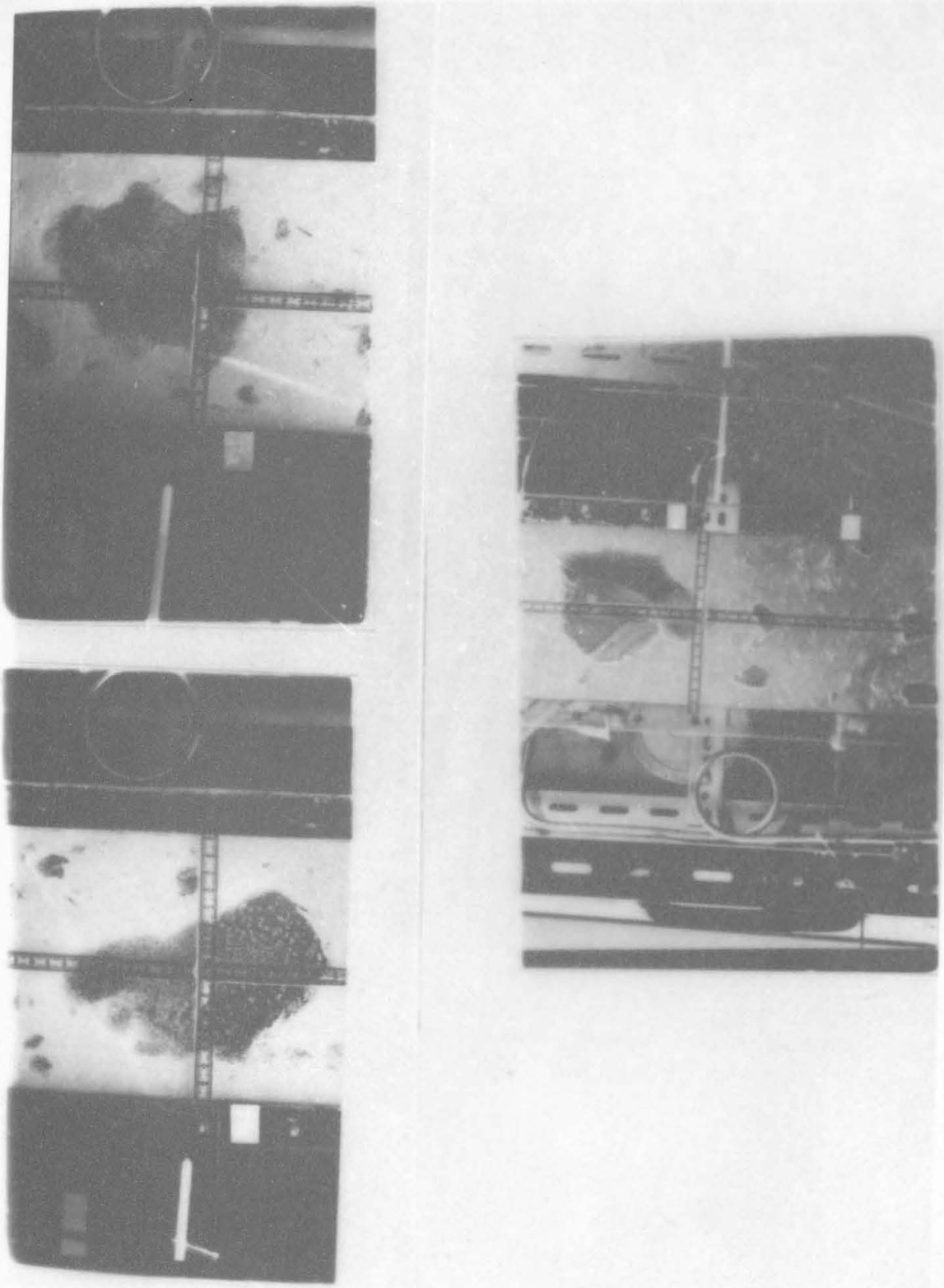

Solids Aggregation and Solids Flotation

Figures (5.7), (5.8) and (5.9), which were obtained after measuring solids concentration gradients in the axial direction in the two-dimensional bubble column, show that at lower gas velocities the solids concentration was higher in the upper sections of the column. They also show that on increasing the superficial gas velocity the solids concentration gradually decreased at the top of the column. An explanation of these phenomena will now be put forward.

The extent to which solid particles are dispersed in water depends on the balance between the adhesion of the solid particles to each other and their adhesion to water. Because the attraction between water molecules is higher than that between water and non-wettable solid, the particles will tend to stick together instead of being dispersed as single particles in water. Visual observations made after shutting off the gas, show that particles join together to form many clusters throughout the bulk of the system. Also, the low adhesion between water and solid particles causes the particles to become preferentially attached to any "ionic bubbles": such gas-solid aggregates then concentrate near the top of the column. Consequently, at lower gas velocities, the solids concentration at the top of the column is significantly higher than that at the bottom of the column. When the superficial gas velocities are high, the slugs cause more violent agitation and the particles are more uniformly dispersed (as Figures (5.7), (5.8) and (5.9) show).

Effect of Solids Concentration

As discussed before, adding a small amount of solid is enough to break the resistance between bubbles and improve the possibility of bubble coalescence even at very low gas velocities. By destroying bubbly-flow and changing it to slug flow there will be a great reduction in gas hold-up (as Figures (5.1) to (5.6) show). At higher gas velocities, the cellular or whirl-pool like flow patterns which were observed in air-water systems (see Section 2.6.3) are also completely destroyed by the solid particles; consequently, there is a reduction in gas hold-up but it is less significant compared with that at lower superficial gas velocities. When the solids concentration reaches about 5%, the slugs attain their ultimate size and almost fill the diameter of the column (as high-speed photography also proves); therefore, beyond this concentration, the reduction in gas hold-up is negligible (because slugs cannot grow any larger).

Effect of Solids Density and Size

Figures (5.1) to (5.6), which were obtained for three-phase systems containing Styrocel particles of different sizes and densities, show that the maximum reduction in gas hold-up happened on using the smallest particles of density 1.2 g/cm^3. As the particle density was decreased, compared with that of water, the

experimental results show less reduction in gas hold-up, and when the density of particles was 0.45 g/cm^3 the reduction in hold-up was minimized. Furthermore, figures (5.10), (5.11) and (5.12) which were obtained for ballotini spheres, over a wide range of particle sizes and densities show that as the density of particles increases (compared with that of water) the reduction in gas hold-up will decrease, and for particles with density of 2.7 g/cm^3 the reduction in gas hold-up is again small. These figures also show that as the particle size increases the reduction in hold-up decreases.

In general, for the particles to lower the resistance to bubble coalescence, they should, firstly be able to mix well even at low superficial gas velocities, and secondly, have some momentum. Now, when particle densities are significantly greater than that of water and at low superficial gas velocities, the bed of particles only expands by a limited amount, and so, unlike particles whose densities are similar to that of water, these heavier particles do not mix to any great extent. Consequently, heavy particles do not lower the resistance to bubble coalescence, and the reduction in gas hold-up is low, as Figures (5.11) and (5.12) show. Light particles, whose density compared with that of water is very low, will float at low superficial gas velocities, and, when the superficial gas velocity is high enough to drag them down, they have not enough momentum to break the resistance between bubbles.

Furthermore, as discussed before, the interfacial tension between non-wettable particles and water is high. Therefore, when the particle size decreases, the interfacial area between the solid particles and water will increase; as a result, the tension in a system which contains smaller, non-wettable solids is higher than that in a system which contains larger particles. Therefore, coalescence may be expected to be higher in systems containing small particles.

5.5 Three-Phase Systems Containing Wettable Solids

5.5.1 Choice of Wettable Solids

Adhesion occurs when two surfaces are joined - a commonly encountered situation. But what is adhesion and how does it arise? By considering these points it is possible to make an informed choice about the type of solid phase to be used in an experimental programme. Particular attention must be given to the cohesive bonds between the water molecules (i.e. hydrogen bonds) and the surface properties of the solid particles. The author believes that, by studying the extent of the adhesion between the solid and liquid phases and also the cohesion within the bulk of the liquid phase, it is possible to provide a better understanding of system performance. Hence, those forces which hold molecules together and are known as physical bonds will first be considered.

5.5.2 Physical Bonding

Weak attraction forces, which are known as Van der Waal's forces and result from the stray fields associated with polarized covalent bonds, are responsible for the physical properties of most organic or inorganic compounds. There are two types of such forces - those between two adjacent molecules (intermolecular Van der Waal's forces) and those associated with the same molecules (intermolecular forces). There are three categories of Van der Waal's forces - Debye forces, Keesom forces and London forces. These forces operate over molecular distances and they are attractive; however, at very small distances repulsive forces come into operation. Here we are concerned only with Keesom forces which result from the interaction of two permanent dipoles. Dipoles occur due to unequal sharing of electrol pairs in covalent bonds where displacement of electron clouds occurs. The degree of the electron displacement is reflected by the dipole moment. Many examples of permanent dipoles are available in organic and inorganic molecules. Molecules exhibiting permanent dipoles are extremely important when considering adhesion phenomena between a liquid phase and solid phase. Particular examples of dipoles are bonds formed from carbon and oxygen, carbon and nitrogen and carbon and halogen.

On the basis of the above explanation and consideration of the structure of water (which was discussed in Section 2.6), the following plastic particles, with different levels of polarity in their polar groups, were chosen for studies of the effect of wettability.

1. Nylon Particles

Nylon (or polyamide) has the following structure:

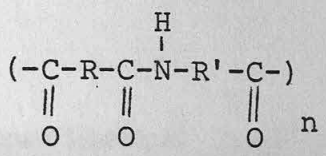

The carbonyl groups (–C=O) and amino groups (-NH) of the above structure are a good example of permanent dipoles.

2. Moviol Part

Moviol particles have the following structure:

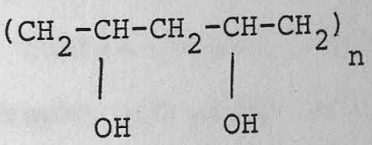

Hydroxyl groups (-OH) in a branched form give very high permanent polarity to the Moviol solids.

3. Diakon Particles

Diakon particles, like Moviol particles, have branched polar groups ($-O-\overset{O}{\overset{\|}{C}}-CH_3$), as their structure shows:

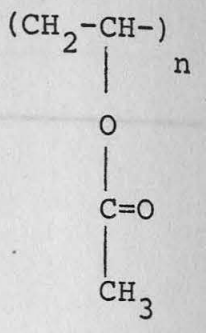

Other characteristics of the above solids (such as, shape, size and density) are given in Appendix D.

5.5.3 Experimental Results

Gas Hold-up

The influence of nylon particles on gas hold-up is presented in Figure (5.14) for a wide range of solid concentrations and superficial gas velocities in the two-dimensional bubble column. Figure (5.15) shows the same experimental results for nylon in the three-dimensional bubble column. The experimental data for these two graphs are given in Tables (13) and (14) of Appendix (E): the experimental procedure and measurements used in this part of the programme have been detailed in Section (4.3.3).

Gas hold-up is also shown as a function of superficial gas velocity for different shapes and sizes of Moviol particles in Figure (5.15) and (5.16). The detailed data which were used to plot these figures are given in Tables (14) and (15) of Appendix (E).

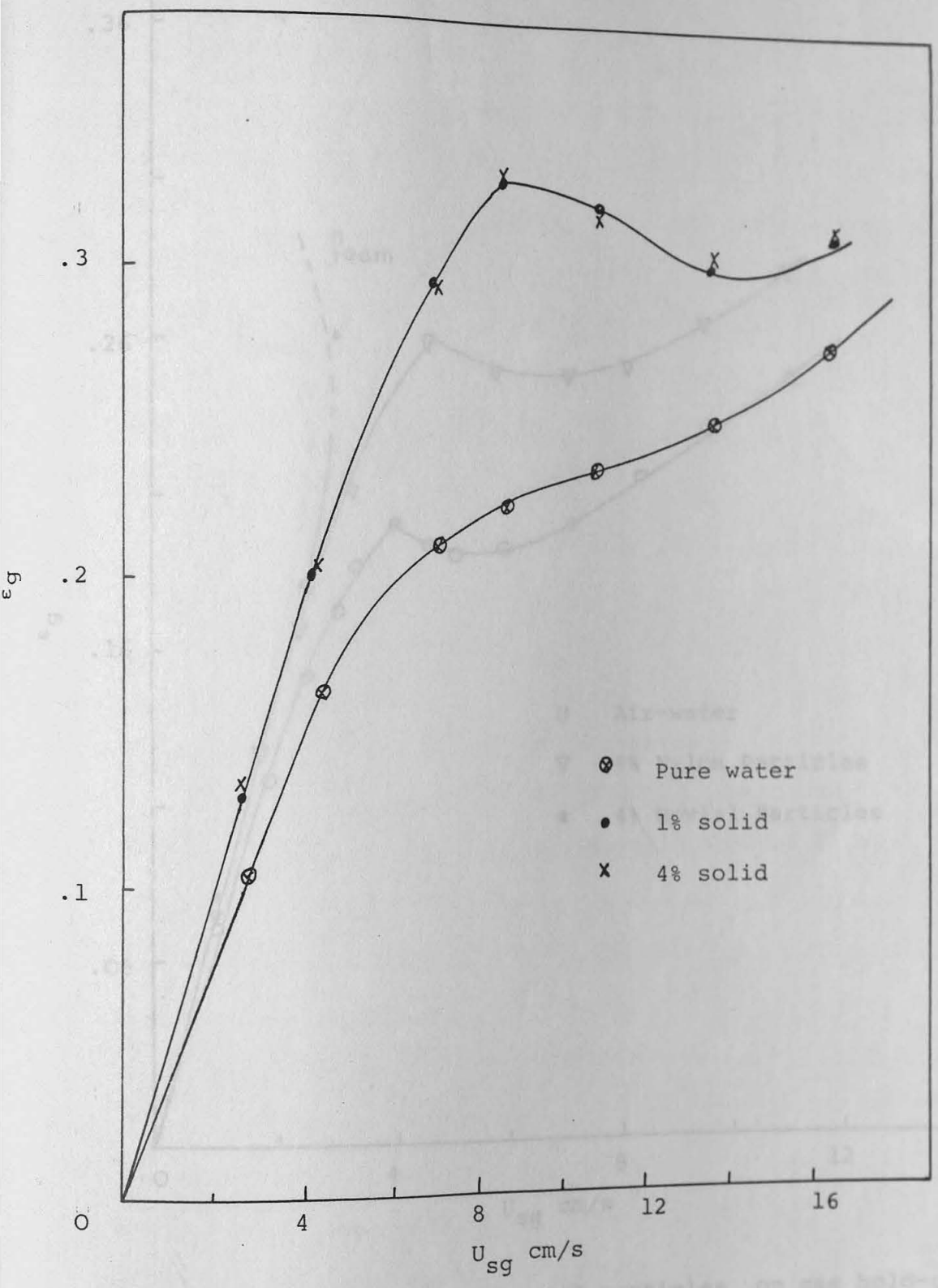

Figure 5.14 Typical influence of nylon particles (with d_{av} = 2100μ and ρ = 2.24 g/cm^3) on gas hold-up on two dimensional column and for $U_{s\ell}$ = 0.17 cm/s.

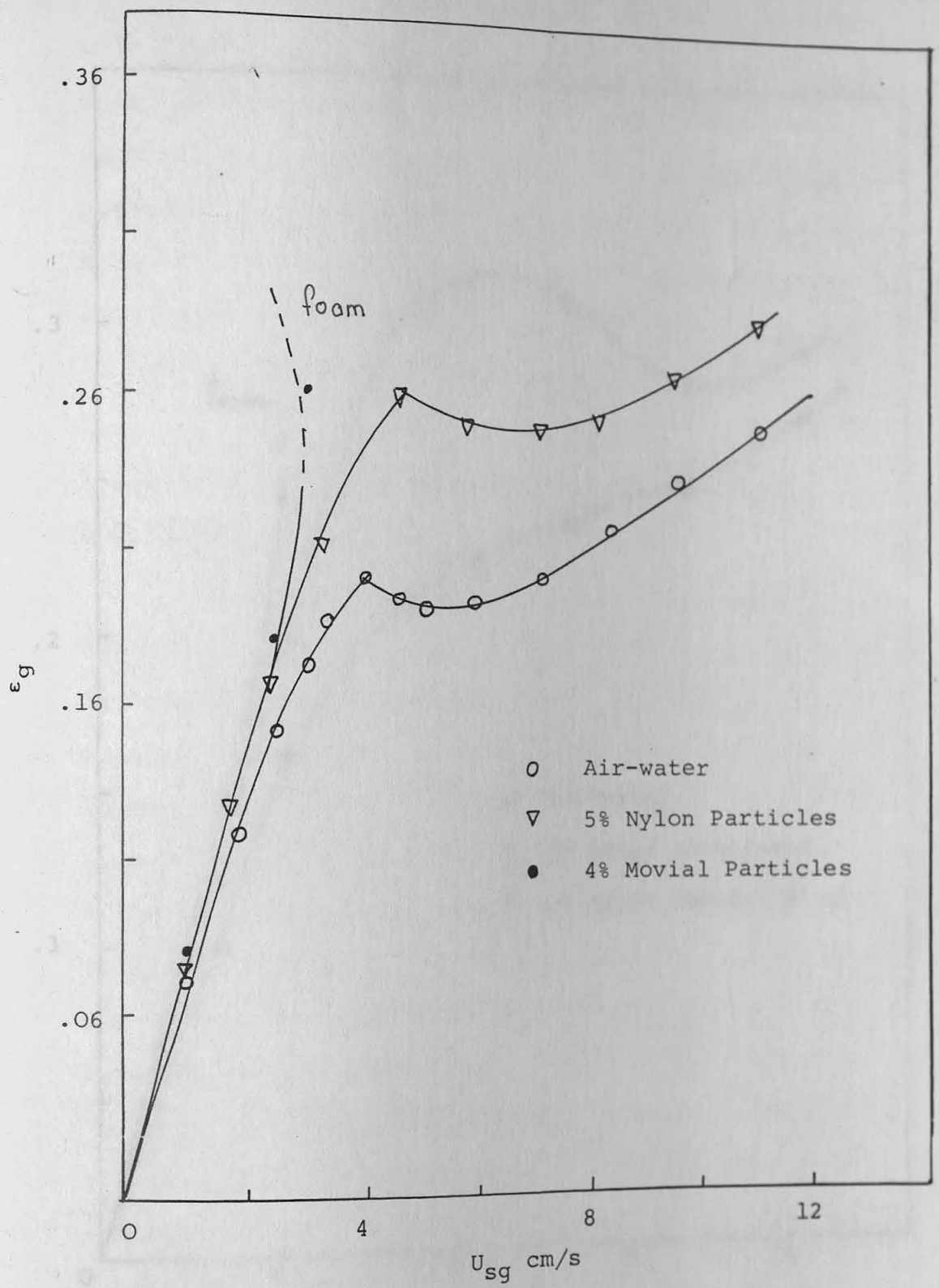

Figure 5.15 Effect of moviol particles on gas hold-up in three-dimensional column and for $U_{s\ell}$ = 0.045 cm/s

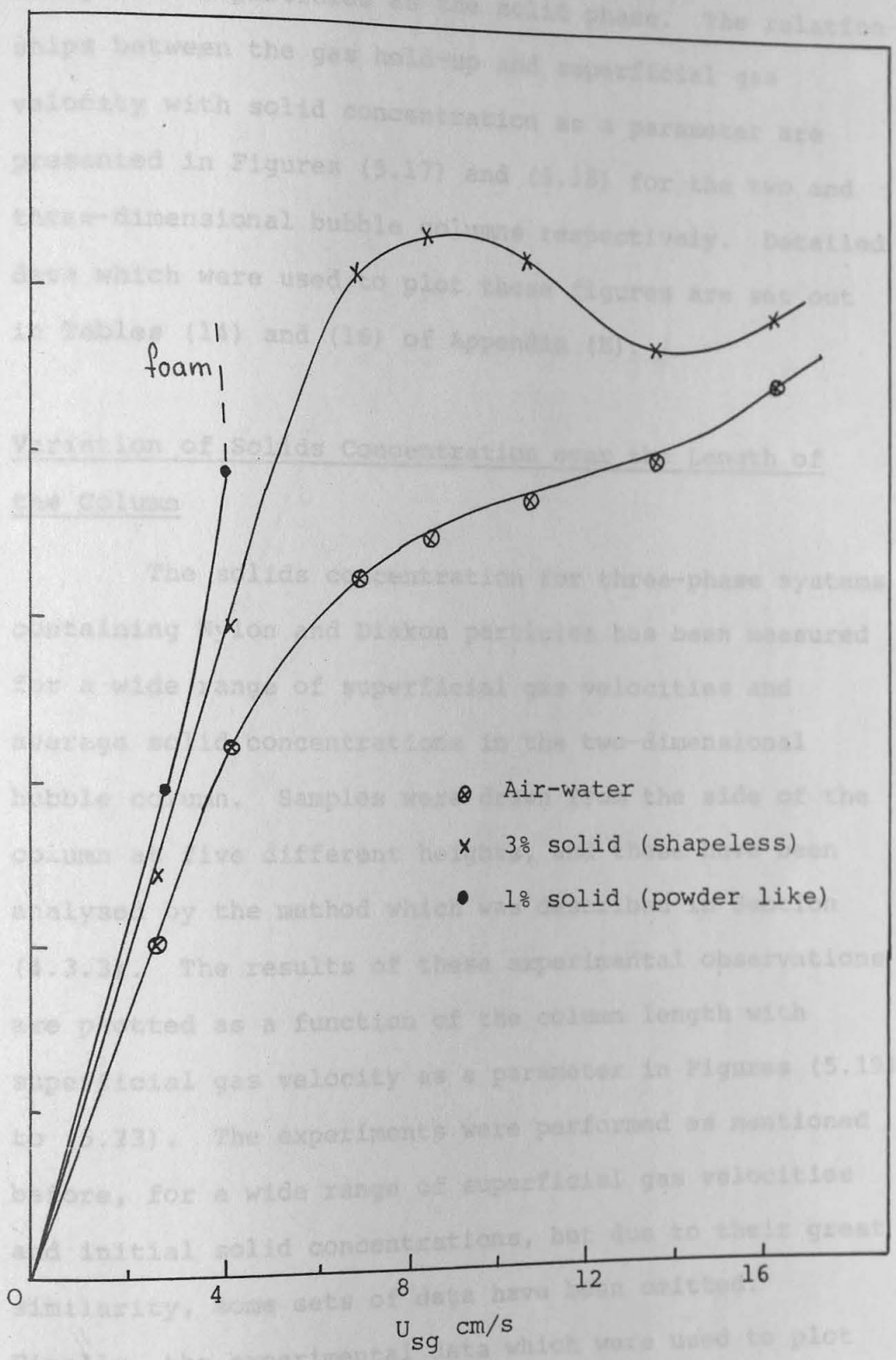

Figure 5.16 Effect of moviol particles on gas hold-up in two-dimensional column and for $U_{s\ell}$ = 0.17 cm/s

Finally, the same experiments were performed using Diakon particles as the solid phase. The relationships between the gas hold-up and superficial gas velocity with solid concentration as a parameter are presented in Figures (5.17) and (5.18) for the two and three-dimensional bubble columns respectively. Detailed data which were used to plot these figures are set out in Tables (14) and (16) of Appendix (E).

Variation of Solids Concentration over the Length of the Column

The solids concentration for three-phase systems containing Nylon and Diakon particles has been measured for a wide range of superficial gas velocities and average solid concentrations in the two-dimensional bubble column. Samples were drawn from the side of the column at five different heights, and these have been analysed by the method which was described in Section (4.3.3). The results of these experimental observations are plotted as a function of the column length with superficial gas velocity as a parameter in Figures (5.19) to (5.23). The experiments were performed as mentioned before, for a wide range of superficial gas velocities and initial solid concentrations, but due to their great similarity, some sets of data have been omitted. Finally, the experimental data which were used to plot these figures are tabulated in Tables (17 to 21) of Appendix (E).

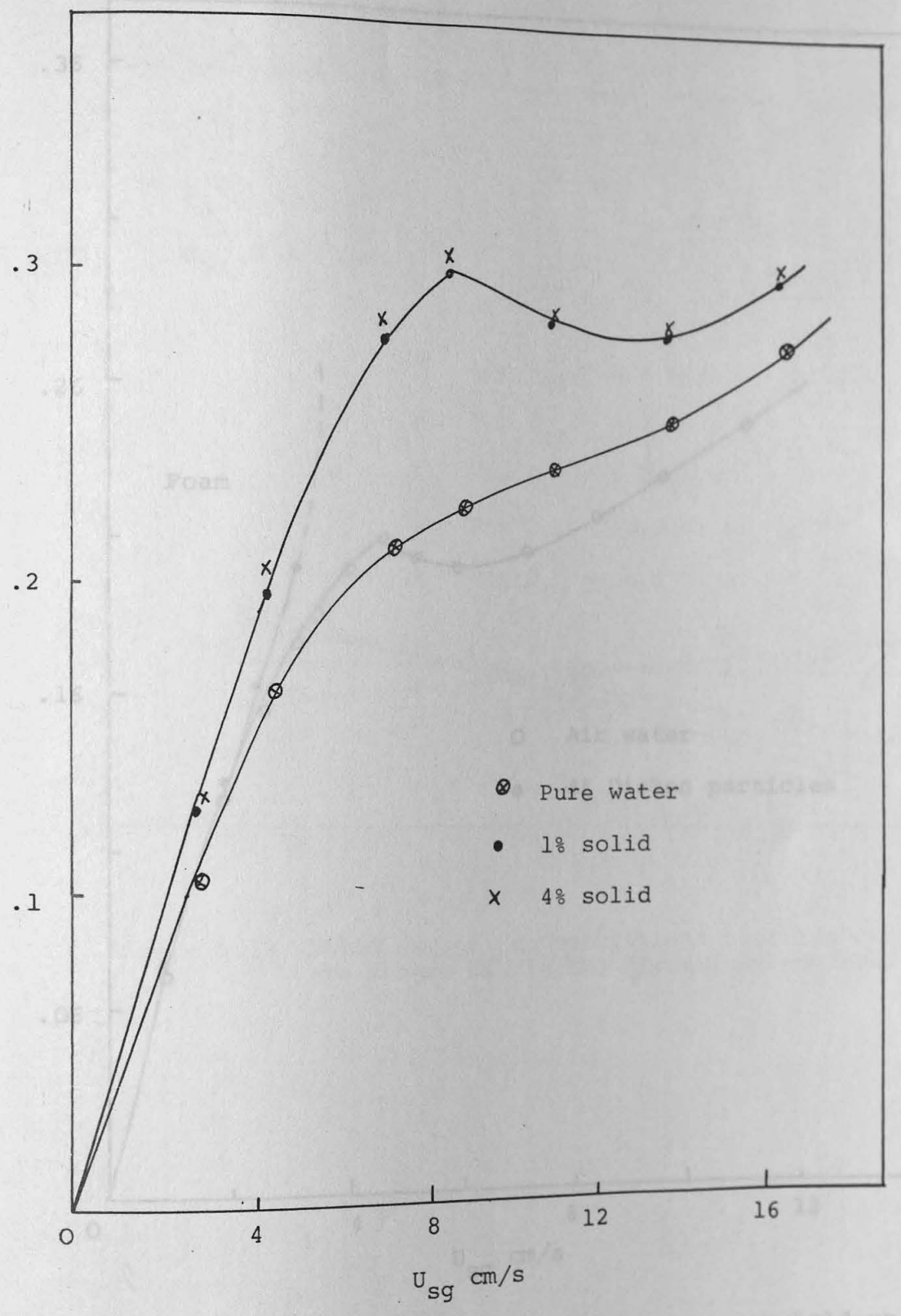

Figure 5.17. Typical influence of Diakon particles on gas hold-up in two dimensional column and for $U_{s\ell}$ =0.17 cm/s

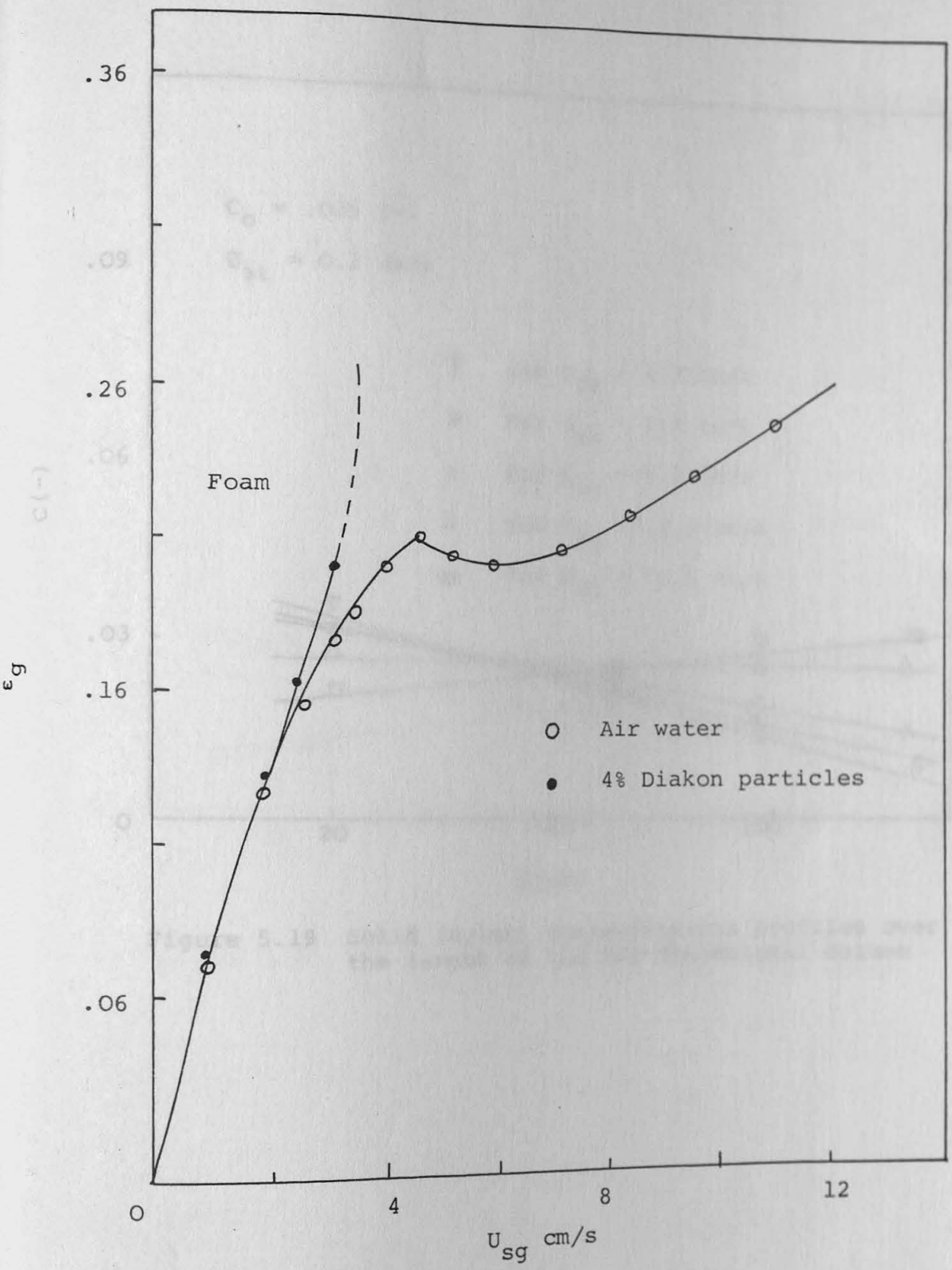

Figure 5.18 Effect of Diakon particles on gas hold-up in three dimensional column and for $U_{s\ell}$ = 0.1 cm/s

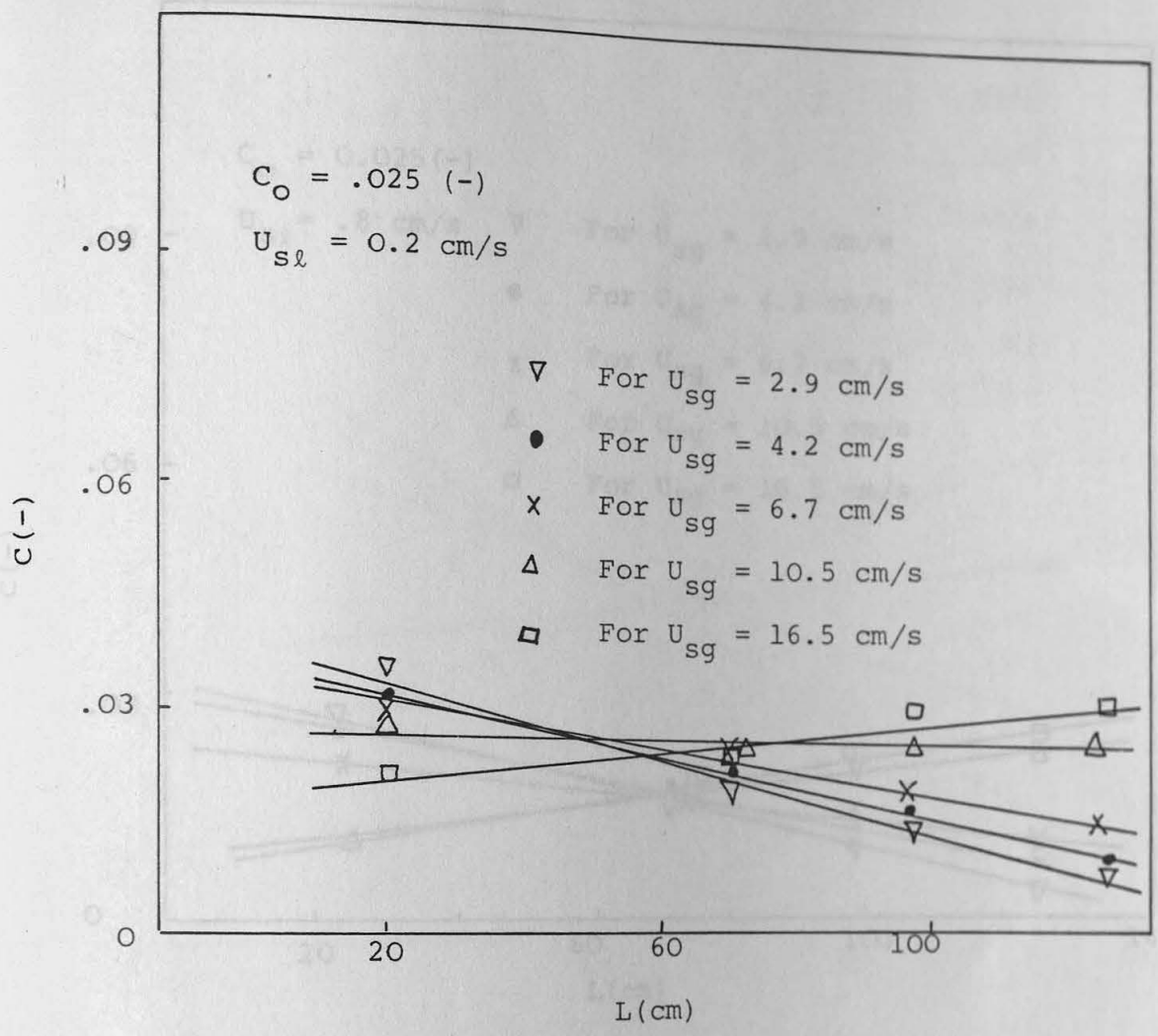

Figure 5.19 Solid (nylon) concentrations profiles over the length of the two-dimensional column

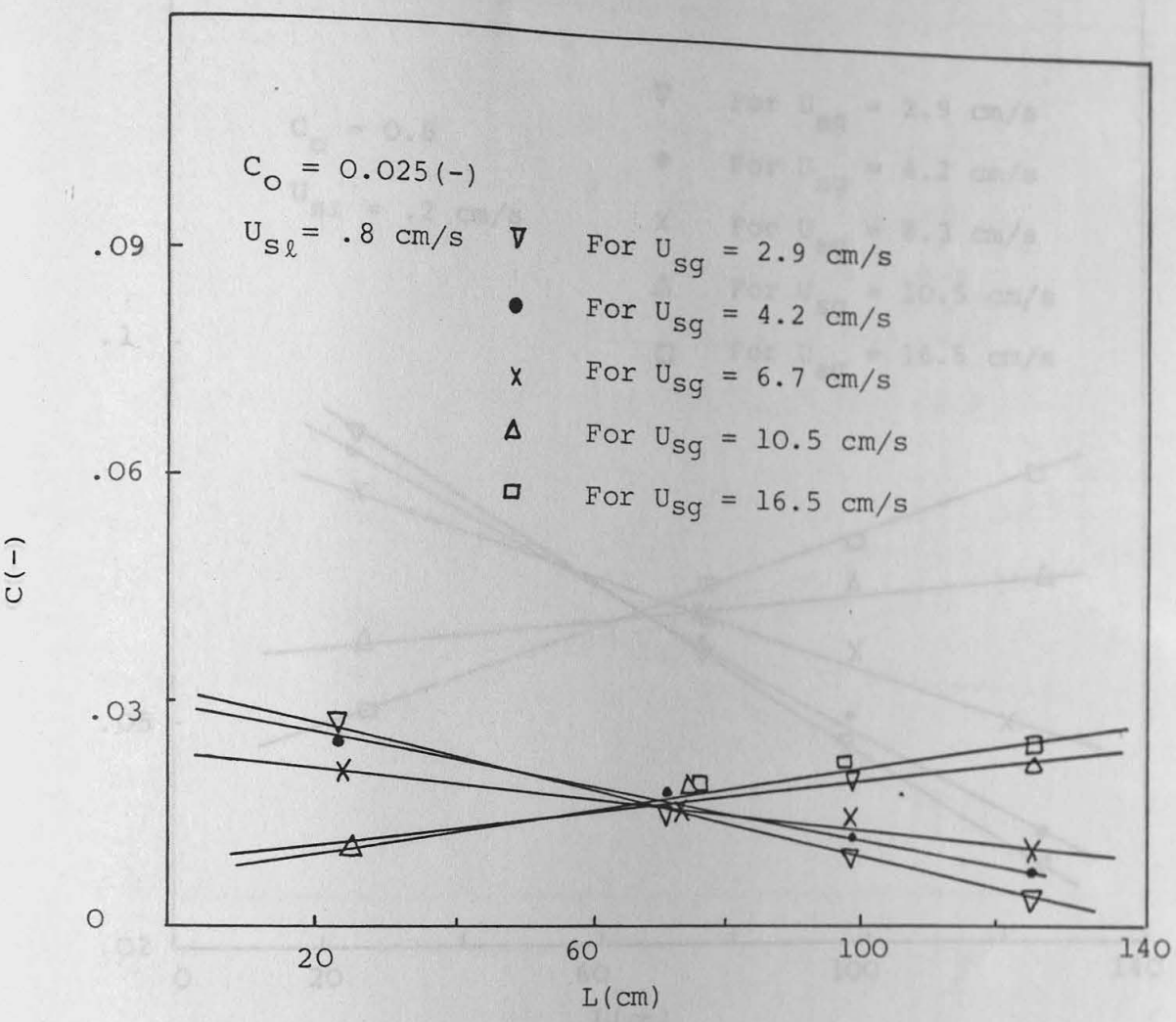

Figure 5.20 Solid (nylon) concentrations profiles over the length of the two-dimensional column

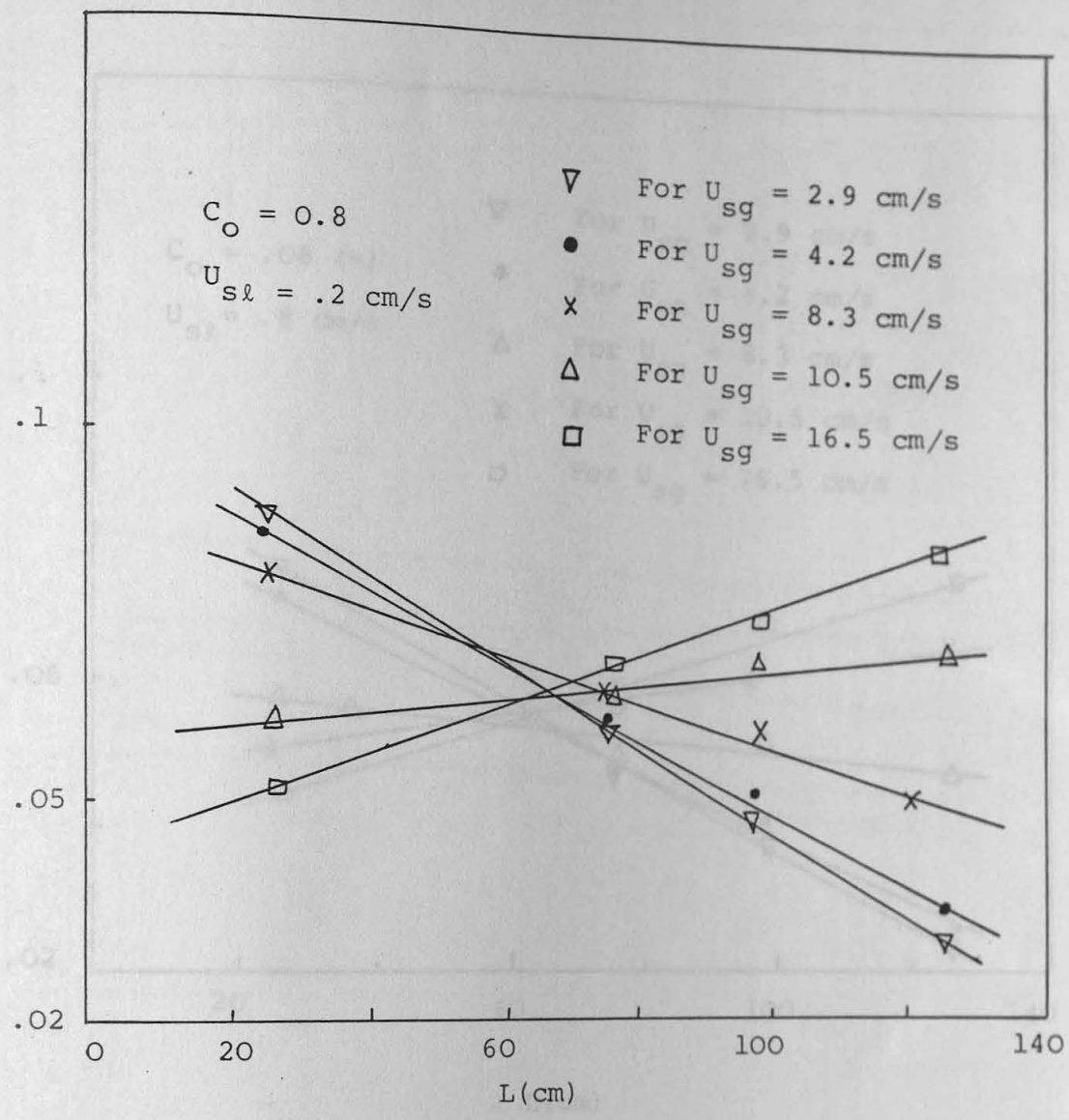

Figure 5.21 Solid (nylon) concentrations profiles over the length of the two-dimensional bubble column

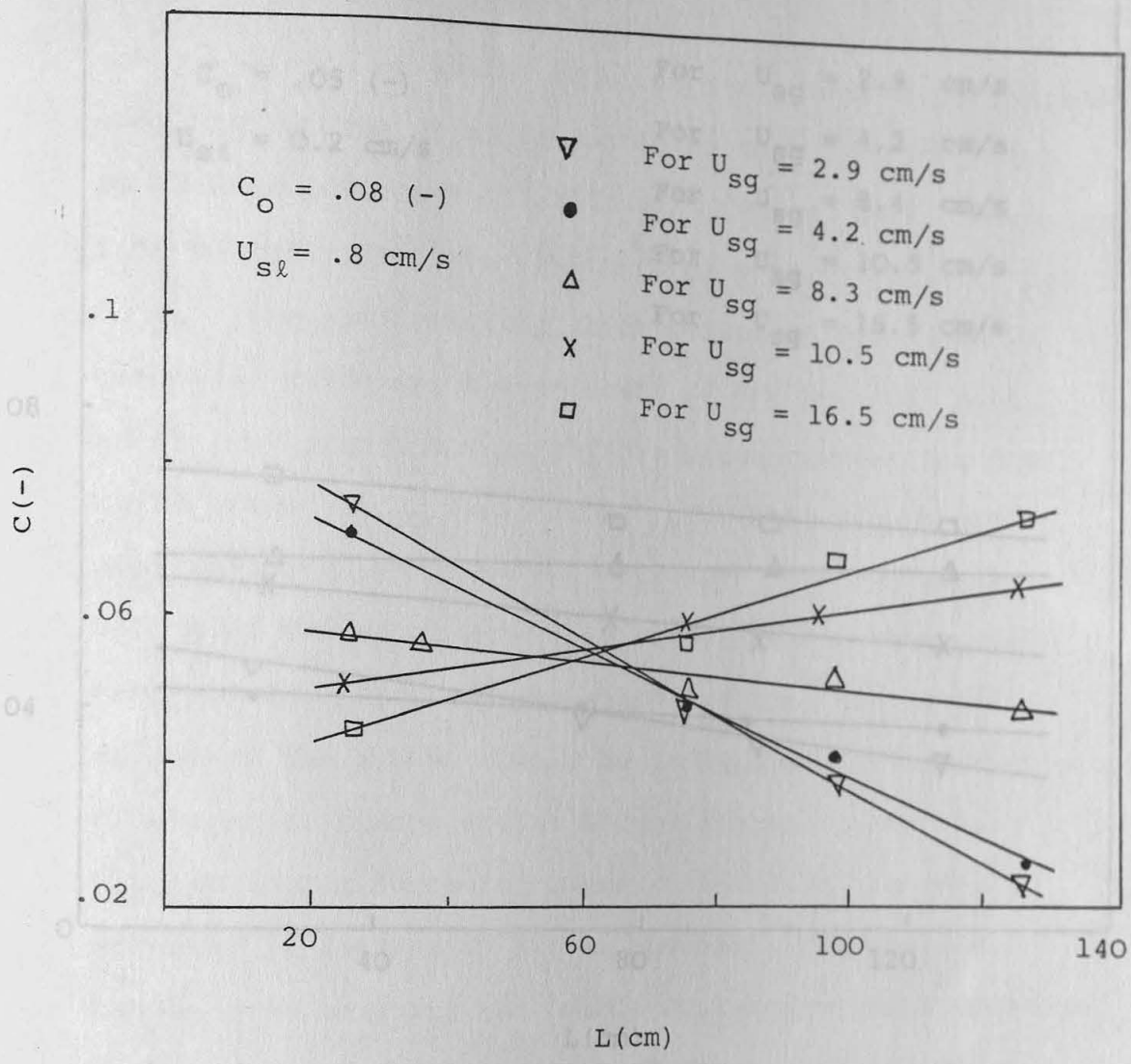

Figure 5.22 Solid (nylon) concentrations profiles over the length of the two-dimensional bubble column.

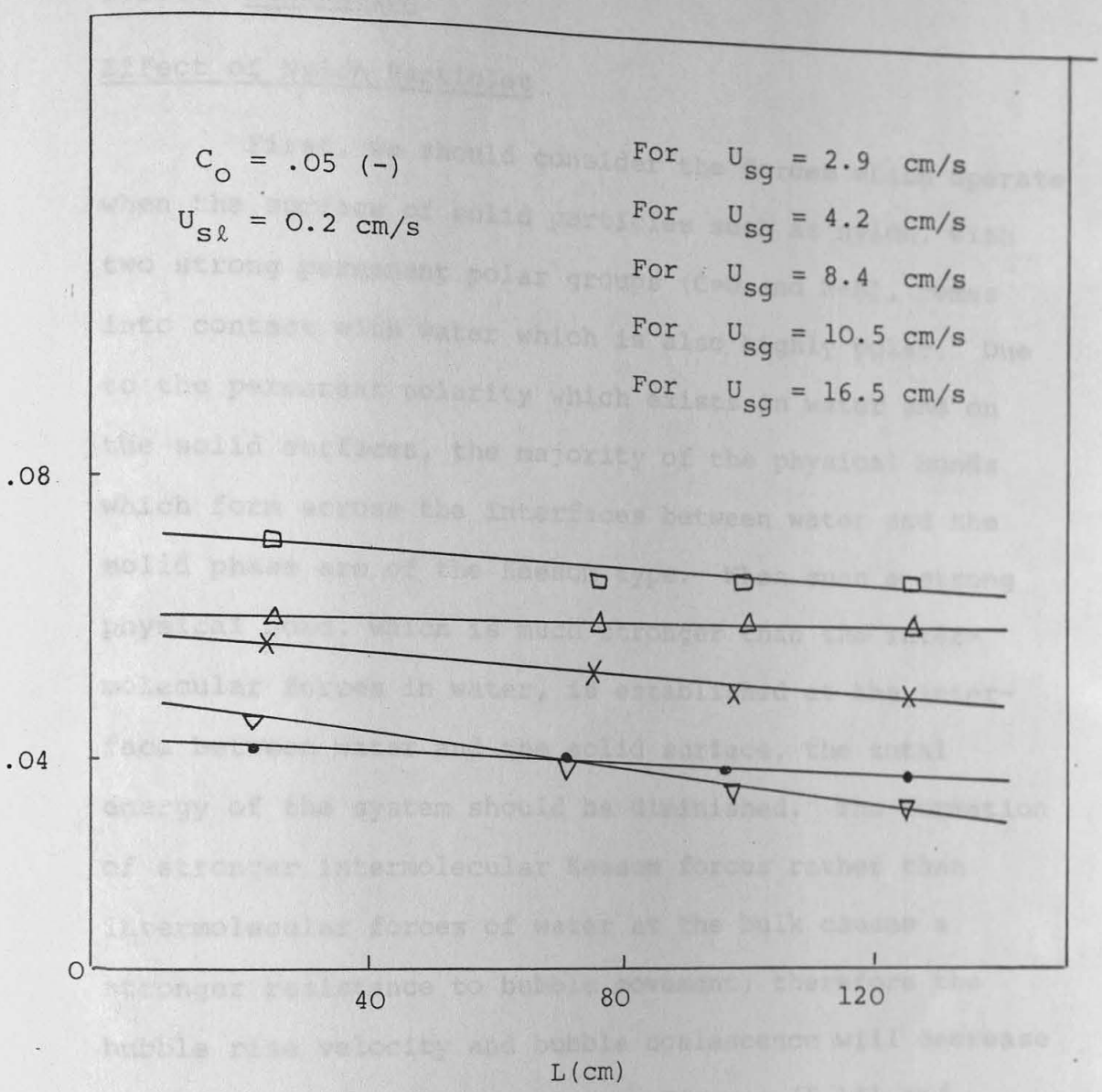

Figure 5.23 Solid (Diakon) concentrations profiles over the length of the two dimensional bubble column.

5.5.4 Discussion

Effect of Nylon Particles

First, we should consider the forces which operate when the surface of solid particles such as nylon, with two strong permanent polar groups (C=O and N-H), comes into contact with water which is also highly polar. Due to the permanent polarity which exists in water and on the solid surfaces, the majority of the physical bonds which form across the interfaces between water and the solid phase are of the Keesom type. When such a strong physical bond, which is much stronger than the intermolecular forces in water, is established at the interface between water and the solid surface, the total energy of the system should be diminished. The formation of stronger intermolecular Keesom forces rather than intermolecular forces of water at the bulk causes a stronger resistance to bubble movement; therefore the bubble rise velocity and bubble coalescence will decrease and gas hold-up will increase as Figures (5.14) and (5.15) for the two-and three-dimensional bubble columns show.

Effect of Moviol Particles

Moviol with its high hydroxyl group content in branched form on a very long hydrocarbon chain possesses both very strong hydrophilic and hydrophobic groups.

When the surface of Moviol particles is exposed to water, very strong hydrogen bonds will form between the water molecules and polar sites (i.e. OH). As a consequence, the total surface energy of the system is diminished and a system is formed with a much lower surface tension than that of water. Thus, the large reduction in the total surface energy at the interfaces causes heavy foam formation when the solid phase is powder-like and less foam, with high gas hold-up, when large particles are used, as Figures (5.15) and (5.16) show.

Effect of Diakon Particles

Diakon particles, like Moviol particles, have their polar groups ($-O-\overset{O}{\overset{\|}{C}}-CH_3$) as branches on the main hydrocarbon chain. Therefore, when they come in close contact with water, physical bonds will form. Diakon particles, due to the low surface tension they have, will reduce the surface tension of water significantly; therefore, they will not only increase gas hold-up by reducing bubble size but also, like Moviol particles, produce a foam (see Figures (5.17) and (5.18)).

Axial Distribution of the Solids Phase

Figures (5.19) to (5.23), which are based on results from the two-dimensional bubble column using Nylon as the solid phase, show that a marked axial solids

concentration profile existed. However, the extent of the profile, as these figures show, depends greatly on operational conditions and, particularly, on superficial gas velocity. The figures show that, at low superficial gas velocities (i.e. in the bubbly-flow regime), the solids concentration in the lower sections of the column was much higher than that in the upper sections of the column. Conversely, at higher gas velocities (i.e. in the slug-flow regime) the solids concentration in the upper section of the column was much higher than that at the bottom. However, for three-phase systems containing Diakon as the solid phase, the above phenomenon were not observed as Figure (5.23) shows: this figure illustrates that, on the whole, the variation of solids concentration in an axial direction was not sensitive to gas velocity as was the case when using nylon as the solid phase. The explanation for the above experimental observations is as follows.

Nylon particles because they possess two strong polar groups (-C=O and -NH) will, when added to air-water systems, be adsorbed in the bulk of the liquid. Therefore in the bubbly-flow regime, the bubbles do not have enough energy to circulate the suspension and so the solids concentration at the bottom section of the column will be higher than that in the upper section of the column. However, at higher gas velocities, the slugs that are

formed do have enough energy to circulate the liquid phase (of which the solid phase is part); therefore, the solids concentration in the upper sections of the column tends to become higher than that in the bottom sections of the column, as Figures (5.19) to (5.22) show. In contrast to nylon particles, Diakon particles tend to be adsorbed at the interface between the gas and liquid phases since they have non-polar sites for adsorbing ionic bubbles; therefore, Diakon particles will be more readily distributed over the length of the column by the gas bubbles.

The other factor to be considered is that of particle density : the Diakon particles are more buoyant because their density is similar to that of water.

References

1. Massimilla, L., Solimando, A. and Squillace, E. Brit. Chem. Eng. 6, 232, (1961).
2. Aldington, D. and Thompson, E. Proc. 3rd European Symp. Chem. React. Eng., P.203-210 Pergamon Press, Oxford (1965).
3. Lee, J.C. Proc. 3rd European Symp. Chem. React. Eng. p.211, Pergamon Press, Oxford (1965).
4. Ostergaard, K. Chem. Eng. Sci. 21 470 (1966).
5. Sherrard,A.J. Ph.D. Thesis, University Wales (1966).
6. Ostergaard, K. Chem. Eng. Sci. 20, 165 (1965).
7. Ostergaard, K. Chem. Eng. Sci. 21, 470 (1966).
8. Ostergaard, K. (1971), Fluidisation, Chap.18 (Davidson, J.F. and Harrison, D. Eds.), Academic Press, New York.
9. Lee, J.C., Sherrard, A.J. and Buckley, P.S. (1974). Proceedings of the International Symp. on Fluidisation and its Applications, pp.407, Toulouse.
10. Calderbank, P.H., Moo-Young, M.B. and Bibby, R. (1965). Proc. 3rd European Symp. Chem. React. Eng. p.91, Pergamon Press, Oxford.
11. Rigby, G.R., Van Blockland, G.P., Park, W.H. and Capes, C.E. Chem. Eng. Sci., 50, 695 (1970).
12. Darton, R.C. and Harrison, D. Some Properties of Gas Bubblesin Three-Phase Fluidised BedsSymp. on multiphase flow systems, Strathclyde, 1974.
13. Henriksen, H.K. and Ostergaard, K. Chem. Eng. Sci., 29, 626 (1974).

14. Taylor, G. Proc. Roy. Soc. (London) 1950, A201, 192.

15. Kim, S.D., Baker, C.G.J. and Bergougnou, M.A. Can. J. Chem. Eng. 50, 695 (1972).

16. Kim, S.D., Baker, C.G.J. and Bergougnou, M.A. Can. J. Chem.Eng. 53, 134 (1975).

17. Kim, S.D., Baker, C.G.J. and Bergougnou, M.A. Chem. Eng. Sci., 32, 1299 (1977).

18. Schugerl, K. Proc. International Symp. on Fluidisation, p.782, Netherlands University Press, Amsterdam (1967).

19. Afschar, A.S. and Schugerl, K. Chem. Eng. Sci., 23, 267 (1968).

20. Ostergaard, K. "Advances in Chem. Eng." 7 (1968).

21. Michelson, M.L. and Ostergaard, K. The Chemical Engineering Journal, 1, 37 (1970).

22. Kato, Y., Niskiwaki, A., Fukuda, T. and Tanaka, S. J. of Chem. Eng. of Japan, 5, 112 (1972.

23. Kumar, H. and Roy, N.K. Indian J. of Tech., 12, 421 (1974).

24. Ostergaard, K. A.I.Ch.E. Symp. Series, 74 (176), 82 (1978).

25. Young, Th.Phil. Trans. (1805), 84; Works (ed Peacock), 1, 432.

26. Dupre, A.Theorie Mecanique de la Chaleur, p.393 (1868).

6 Radial Non-Uniformity of the Solid Phase and Mixing in Three-Phase Systems

6.1 Introduction

The performance of a chemical reactor with respect to conversion and selectivity depends not only upon the intrinsic kinetics of the various chemical reactions but also on various physical rate processes such as interphase, inter-and intra-particle heat and mass transfer. The effects of these physical rate processes on reactor performance have been shown to depend upon the dynamics of the various phases involved.

The mixing of a fluid within a given phase is conventionally divided into two phenomena: "fine mixing" (i.e. micromixing) and "coarse mixing" (i.e. macromixing). In micromixing, the process is viewed in terms of the intimacy of mixing of various molecules in flow. The macromixing view is one in which the fluid is seen as independent entities and provides information on the residence time experienced by each: this component of mixing occurs solely as a result of convective diffusion.

Plug-flow and complete mixing are the two extreme cases of macromixing which can exist in a flow system. In fact, flow reactors deviate considerably from the above extreme cases of macromixing. These deviations may be the result of non-uniform velocity profiles, short circuiting, velocity fluctuations due to molecular and turbulent diffusion, reactor shape and other factors.

The study of mixing in the liquid-phase of bubble columns has been carried out by numerous investigators (some of which have been surveyed in Section (2.1.6)) by using simple air-water systems. The flow patterns and liquid circulation which are caused by upward bubble movement have been given attention in recent years, although this area has been explored more extensively in the case of gas-solid and liquid-liquid systems. However, at the present, there is a considerable amount of knowledge available on the various parameters affecting the operation of two-phase systems. On the other hand and, in spite of the extensive use made of three-phase systems containing dense particles, little consistent information concerning longitudial mixing in the solid or liquid phases has been published.

Now, as is clear from information given in previous sections, a swarm of bubbles rises uniformly within a bubble column when the superficial gas velocity is low. It is also known that on adding a small amount of non-wettable solid bubbly-flow ceases to be uniform, and this non-uniformity increases with the solids concentration. This non-uniformity of the gas in the radial direction may lead to radial non-uniformity of the solid phase, although most investigators have assumed that the solid is uniformly distributed in the radial direction. Therefore, it seems reasonable that before any study of mixing (especially in the solid phase) is

undertaken the relative magnitude of the solids concentration gradient in the radial direction should be assessed. The main objective of this section is concerned with this. Results of some mixing studies in the liquid and solid phases are also reported.

6.2 Literature Survey

Gota et al. (1) and Farkas et al. (2) have investigated the concentration distribution of solid particles in batch operations in columns ranging in diameters from 3.8 cm to 9 cm. Suganuma et al. (3) have also measured the longitudinal concentration distribution of solid particles in batch and continuous operation using columns of 6 cm, 11.8 cm and 20.1 cm diameter. They presented an empirical equation for a range of operating conditions based on the observation that there was a linear relationship between the logarithmic concentration of solid particles and axial height from the bottom of the column.

Ostergaard and Michelsen (4) studied axial mixing in the gas and liquid phases of a 21.59 cm diameter fluidised bed containing either 0.25 or 1 or 6 mm diameter glass beads. They extended their studies (5) to a 15.24 cm diameter bed using 1, 3 and 6 mm glass beads. The intensity of mixing was found to depend strongly on the

particle size and on the flow rates of the fluid phases. While beds of 1 mm beads were characterised by a high degree of mixing, 6 mm particle beds on the other hand showed negligible mixing.

Results on liquid-phase mixing of three-phase fluidised beds in a 22.8 cm diameter column have been recently reported by Ostergaard (6), glass ballotini of 1.1, 3 and 6 mm diameter being used. An increase in the axial mixing coefficients of 50-100% over those obtained in a 15.24 cm diameter bed was reported.

Kim et al. (7) used the pulse and step injection techniques to study mixing in the liquid phase of fluidised beds of 6 mm glass beads and 2.5 mm irregular gravel in a two-dimensional column (66 cm x 2.5 cm). They reported that axial mixing increased with an increase in either gas or liquid flow rates.

Vail et al. (8) employed the steady-state tracer injection technique and the diffusion type equation to study mixing in the liquid phase of 14.7 cm diameter beds of 0.87 mm sand particles. Their longitudinal mixing results were in complete agreement with those reported by Ostergaard and Michelsen (4).

Todt et al. (9) studied the axial dispersion coefficient in three-phase systems containing hollow glass beads, 125-250 μm in diameter, as the solid phase. They measured liquid-phase axial mixing by means of the pulse tracer technique using a 20% Nacl solution as tracer.

El-Temtamy et al. (10) more recently determined axial dispersion coefficients in the liquid phase of gas-liquid fluidised beds from tracer concentration measurements upstream of the injection plane using the steady-state tracer method. Water, air and glass beads of 0.45, 0.96, 2 and 3 mm diameter were used. They found that the values of the dispersion coefficients increased with increasing gas flowrate and their variation with the liquid flowrate depended on the particle size. These coefficients were found to be higher for three-phase fluidised beds than those for the corresponding two-phase, particle free systems. El-Temtamy et al. (11) also reported the measurement of dispersion in the liquid phase expressed in terms of axial and radial dispersion coefficients. These coefficients were evaluated from radial concentration profiles downstream of a point source of tracer injected continuously. They reported that the radial dispersion coefficients were one order of magnitude lower than the axial dispersion coefficients.

6.3 Experimental Programme

6.3.1 Radial Non-Uniformity of the Solid Phase

The results of the gas hold-up measurements show that in the presence of non-wettable solids the chance of coalescence of bubbles is much higher than that in the solids-free system. It was also shown that a small amount of solid in the liquid phase is sufficient to eliminate

bubbly flow and cause the formation of large bubbles which pass through almost the whole length of the column. This non-uniformity in the gas phase may cause the non-uniform distribution of solids in the radial direction. In order to determine the magnitude of the radial gradients the concentration of Styrocel particles (d=810 μ and ρ = 1.2 g/cm^3) at eight different radii were measured over a wide range of superficial gas velocities and solid concentrations. Samples were taken at the bottom (25 cm from the gas distributor), middle (90 cm from the gas distributor) and top (140 cm from the gas distributor) sections of the column.

6.3.2 Axial Solid and Liquid Phase Mixing Studies

The formation of large bubbles due to the presence of solid particles may cause more agitation of the liquid phase compared with that in simple air-water systems. The available data on dispersion or "mixing" in three-phase fluidised beds, especially those systems which contain light particles, are, however, still comparatively scarce. Therefore, it was decided to examine this important parameter to get at least some idea of the general trend of axial dispersion coefficient with respect to gas velocity.

The mixing studies could have been performed by either steady-state or unsteady state tracer techniques. Due to the simplicity of the unsteady state method, studies of mixing were performed by using this technique, and coloured particles or dyes were employed as tracers for the solid and liquid phases respectively. Mixing patterns revealed by "one shot" injection of coloured particles or dye tracers at the top of the column were carefully and frequently watched.

6.3.3 Measurement Technique

The backmixing characteristics of various phases in a multiphase reactor can be evaluated from the residence time distribution (RTD) of a tracer injected into the phase of interest. These tracer techniques usually involve the injection of a tracer at one or more locations in the system and detection of its concentration as a function of time at one or more downstream positions. Various types of tracer inputs such as step, pulse, imperfect pulse, sinusoidal and ramp have been employed by different investigators. The nature of the tracer selected usually dictates the detection system. For the liquid phase, quite often the tracers (for example potassium chloride) are such that the detection probe can be inserted directly into the reactor and continuous monitoring of the tracer concentration at any fixed position is obtained by means

of an electrical conductivity cell and a recorder. If the tracer concentration measurement requires an analytical procedure, such as titration or colorimetry, sampling of the liquid phase is required. For the solid phase a magnetic tracer is sometimes used. In general, for solid and sometimes gas phases a suitable radioactive tracer is often convenient. On the whole, the selection of the proper tracer for a given system is extremely important and the basic requirements for a satisfactory tracer experiment are as follows:

(1) the tracer should be miscible in and have physical properties similar to the fluid phase of interest;

(2) the tracer should be accurately detectable in small concentrations so that only a small quantity need be injected into the system, thus minimising disturbances in the established flow patterns;

(3) the tracer should be visible since this provides valuable qualitative information about back-mixing, and

(4) normally, the tracer should be non-reacting so that the analysis of the RTD is kept simple.

Methods for evaluating the axial dispersion coefficient from RTD data obtained from tracer techniques have been mentioned earlier (see Section 2.1.6). For the liquid or solid phase the equation:

$$\frac{C(t)}{C(\infty)} = 1+2 \sum_{n=2}^{\infty} \left(\text{Cos } \frac{n\pi}{L} x\right).\exp. \left(-\left(\frac{n\pi}{L}\right)^2 D_1.t\right)$$

can be fitted graphically.

6.4 Experimental Equipment and Procedure

Mixing studies of the liquid and solid phases and radial concentration distributions were carried out in the column of 15.2 cm diameter. Details of this column as well as the auxillary equipment are given in Section (2.4.2). The sampling systems, as described before, were 1 cm i.d. stainless steel tubes, which were inserted into the column and, because of their "push-fit", were readily movable in a radial direction.

6.4.1 Method of Measurement of Solids Concentration

Solids were initially introduced into the bubble column, and then liquid and gas were fed in at pre-determined values. After a steady concentration distribution of solid particles was established in the column, samples of the fluidised suspension were withdrawn through the sampling tubes into 250 ml measuring cylinders. The total volume of each sample was first measured, and then the solid particles were separated from the liquid and allowed to settle in measuring cylinders. The solids concentration was expressed in cm^3 of settled solid particles per cm^3 of fluidised suspension.

6.4.2 Axial Liquid Phase Mixing Measurement

The mixing studies in the liquid phase have been

pursued using the unsteady state tracer technique (for details see Section 2.4.3). A 1% methylene blue solution, prepared by dissolving methylene blue in tap water, was used as the tracer. For each experiment, after setting the appropriate gas flowrate and solids concentration for a batch of liquid, an electronic timer was switched on simultaneously with the introduction of the liquid tracer at the top of the column. Then samples were withdrawn from the sampling point (at the side of the column) placed 30 cm above the gas distributor and directed into conical flasks, the time at which the sample was taken being also recorded. Then each sample was analysed using a spectrophotometer.

6.4.3 Axial Solid Phase Mixing Measurement

When steady state conditions had been attained in the column, coloured tracer particles (Styrocel d=1204μ and ρ=1.36 g/mc^3) were introduced into the top of the column. When the coloured particles touched the surface of the liquid inside the column an electronic timer was switched on. Then samples were taken at a point 30 cm above the gas distributor using 100 ml measuring cylinders, and the time at which the samples were taken was recorded.

The samples were processed by sieving out the larger coloured particles from the non-coloured ones. After that the coloured particles were dried and their volume measured.

The experiments were carried out in a random fashion and each experiment was repeated at least twice.

6.5 Experimental Results

6.5.1 Radial Solids Concentration

The radial variations of solid concentration were measured over a wide range of superficial gas velocities and solids loading at the bottom, middle and top sections of the column. For the sake of brevity, and due to the similarity between some data sets, only the results obtained for high and low superficial gas velocities at different solids concentrations are presented here. Figures (6.1) to (6.6) show the radial non-uniformity of the solid phase when the initial average solids concentration in the column was 1%, 10% and 20% respectively at low (U_{sg} = 1 cm/s) and high U_{sg} = 6 cm/s) superficial gas velocities. The data for these graphs are presented in Tables (1), (2) and (3) of Appendix (F).

6.5.2 Axial Liquid Phase Mixing

The study of liquid-phase mixing was performed by the unsteady state method in the following systems:

(1) three-phase system with solids concentration of 0.025 (v/v);

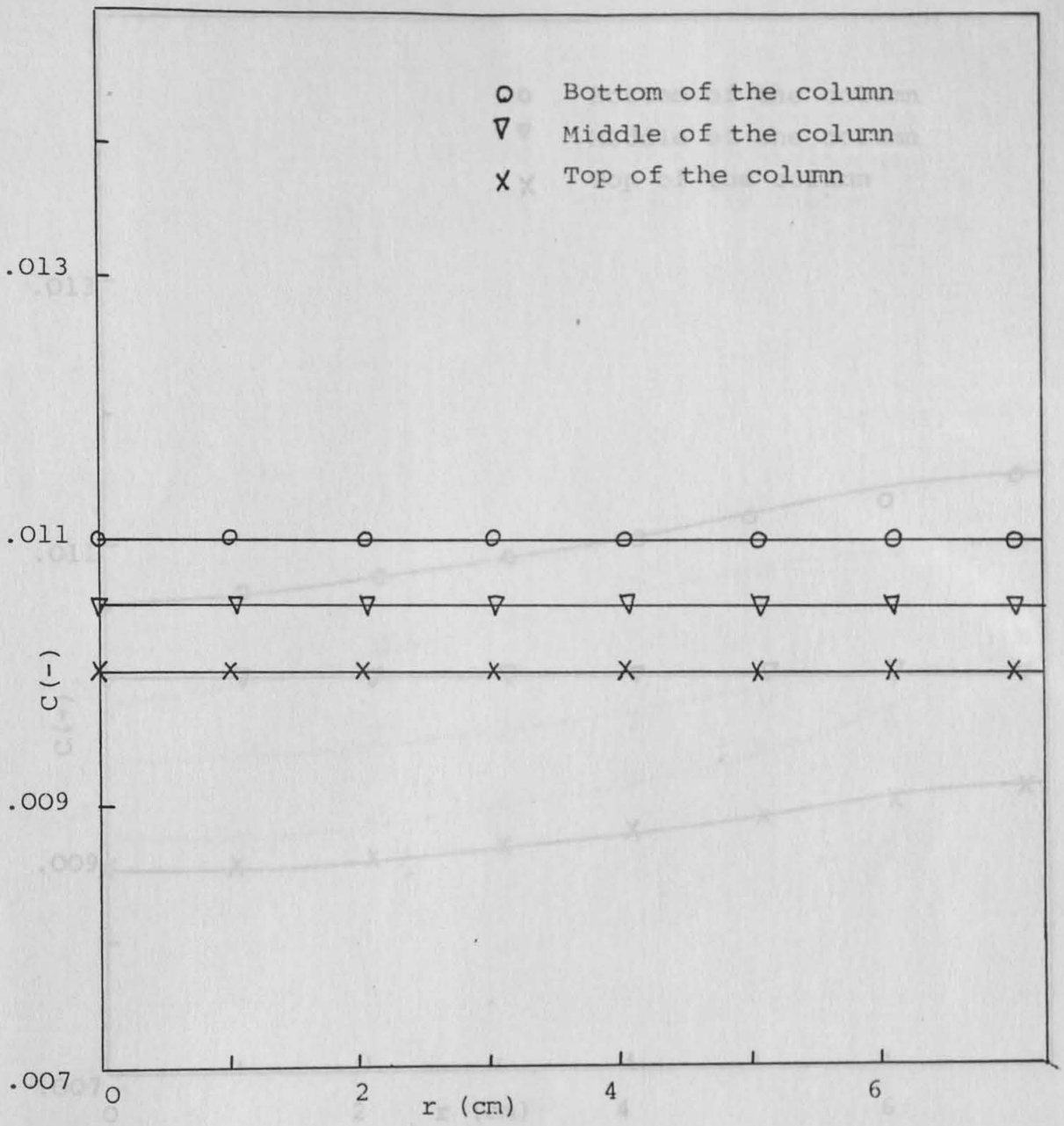

Figure 6.1 - Variation of solids concentration in radial direction for U_{sg} = 1 cm/s and C_o = 0.01 (--).

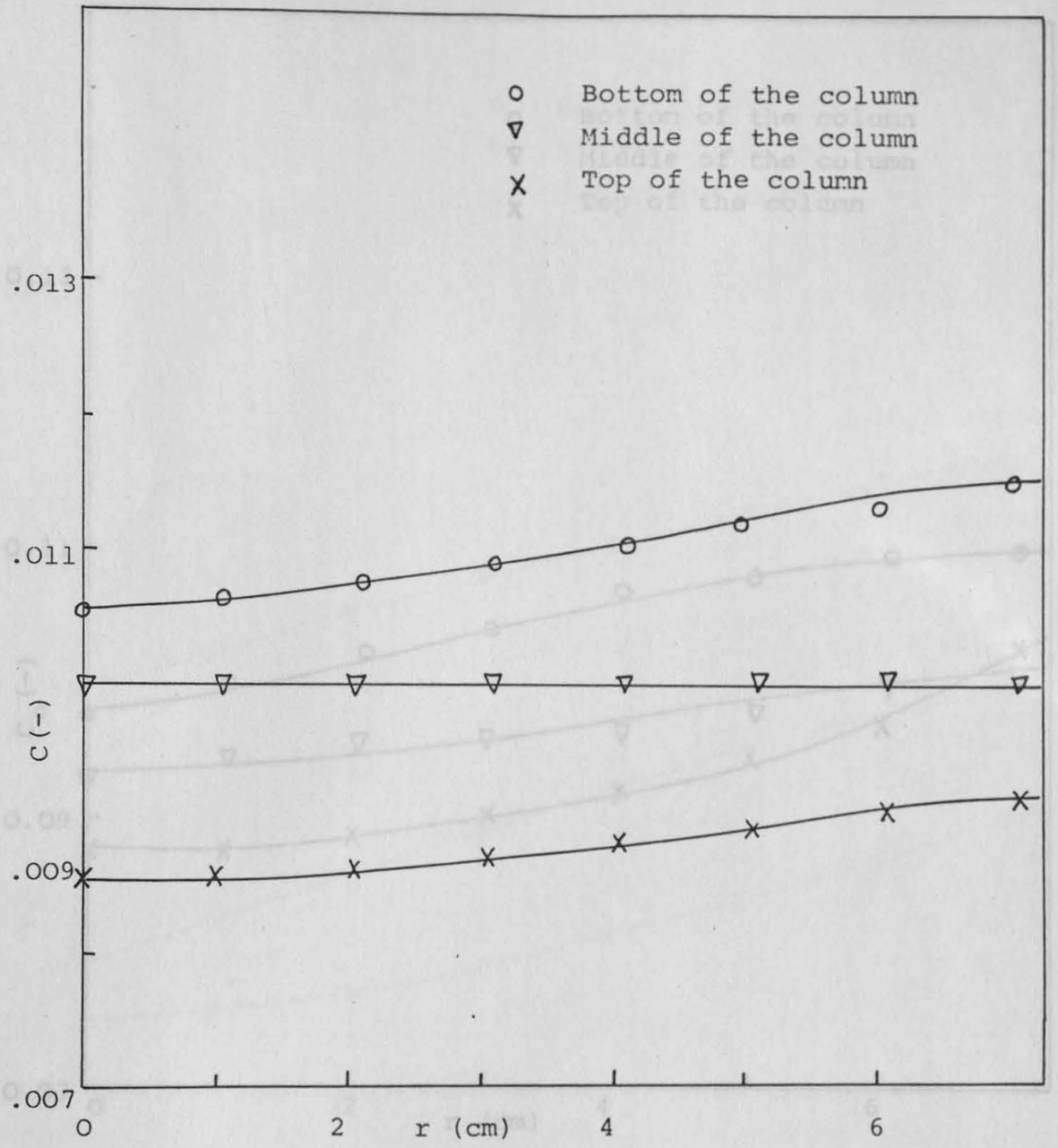

Figure 6.2 - Variation of solids concentration in radial direction for U_{sg} = 6 cm/s and C_o = 0.01 (-).

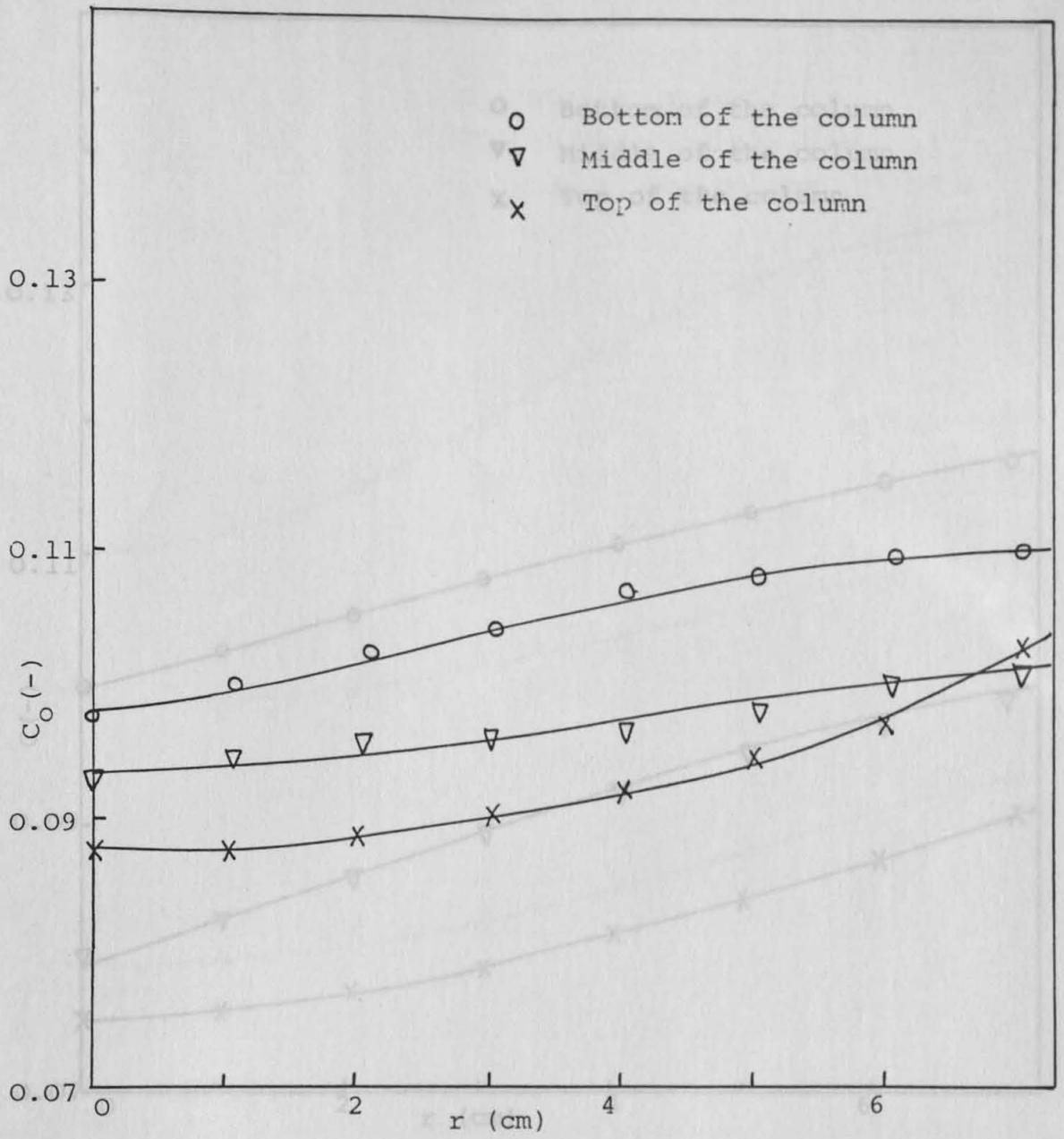

Figure 6.3 - Variation of solids concentration in radial direction for U_{sg} = 1 cm/s and C_o = .1 (-).

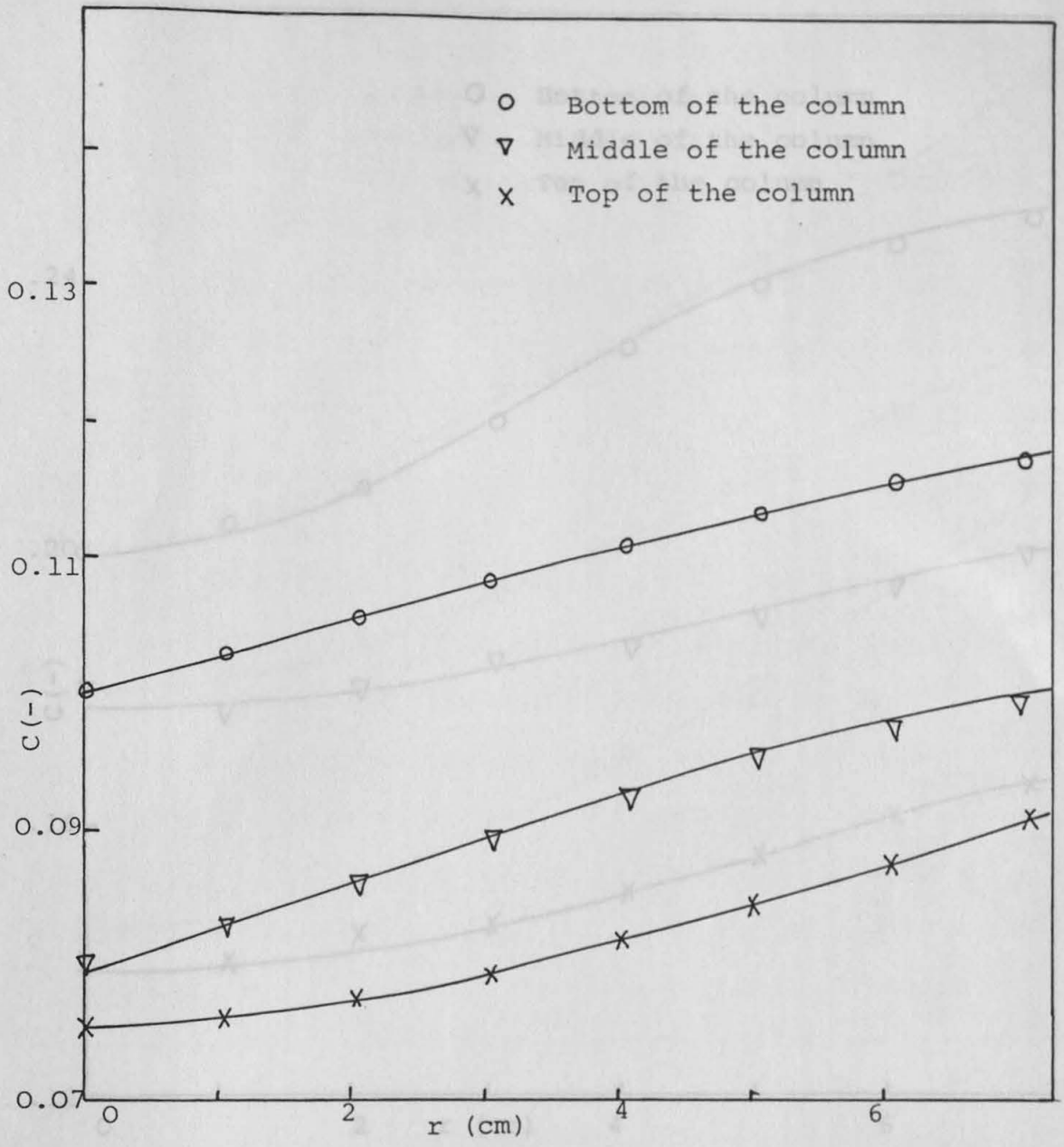

Figure 6.4 - Variation of solids concentration in radial direction for U_{sg} = 6 cm/s and C_o = .1 (-).

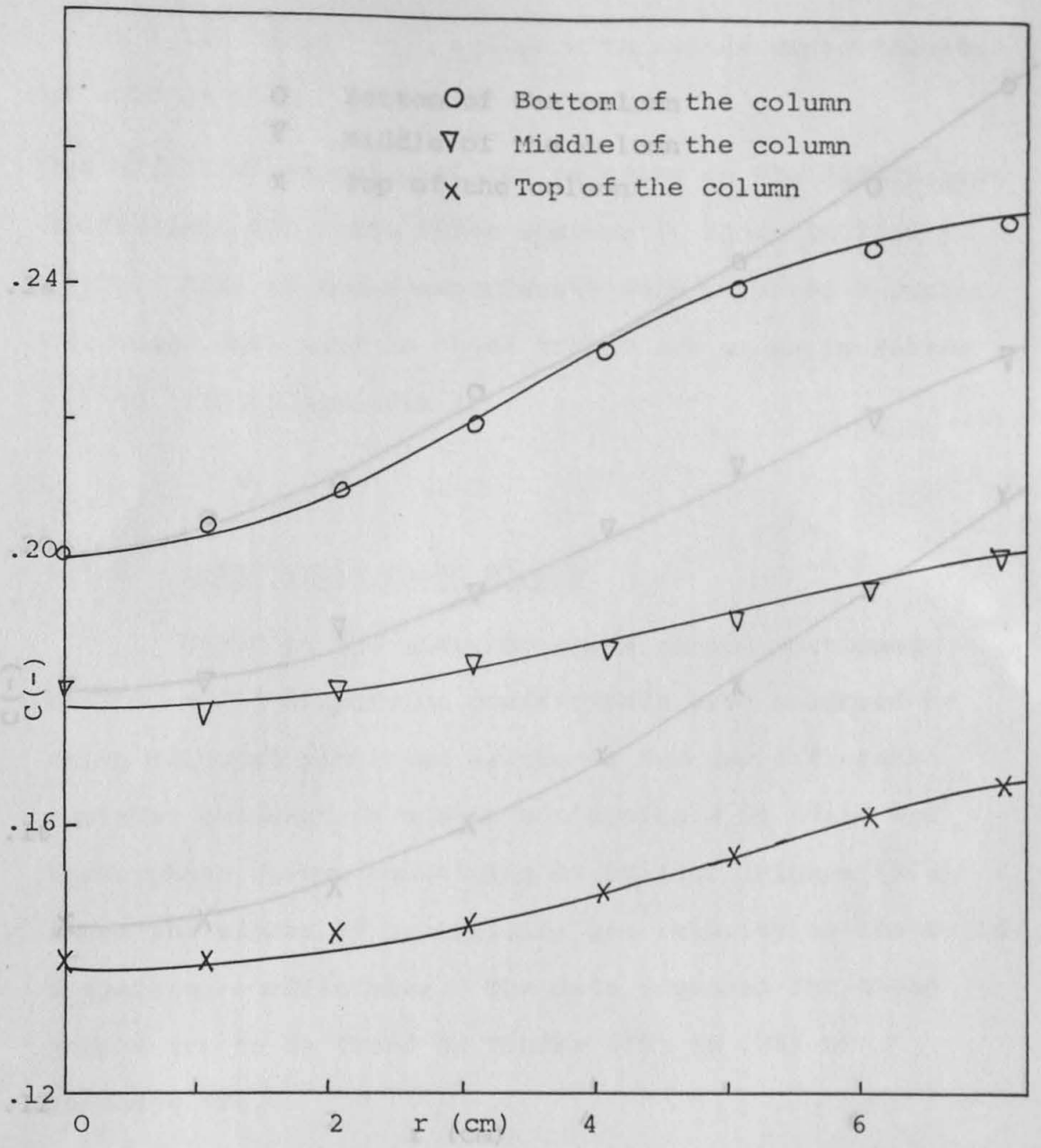

Figure 6.5 - Variation of solids concentration in radial direction for U_{sg} = 1 cm/s and C_o = 0.2 (-).

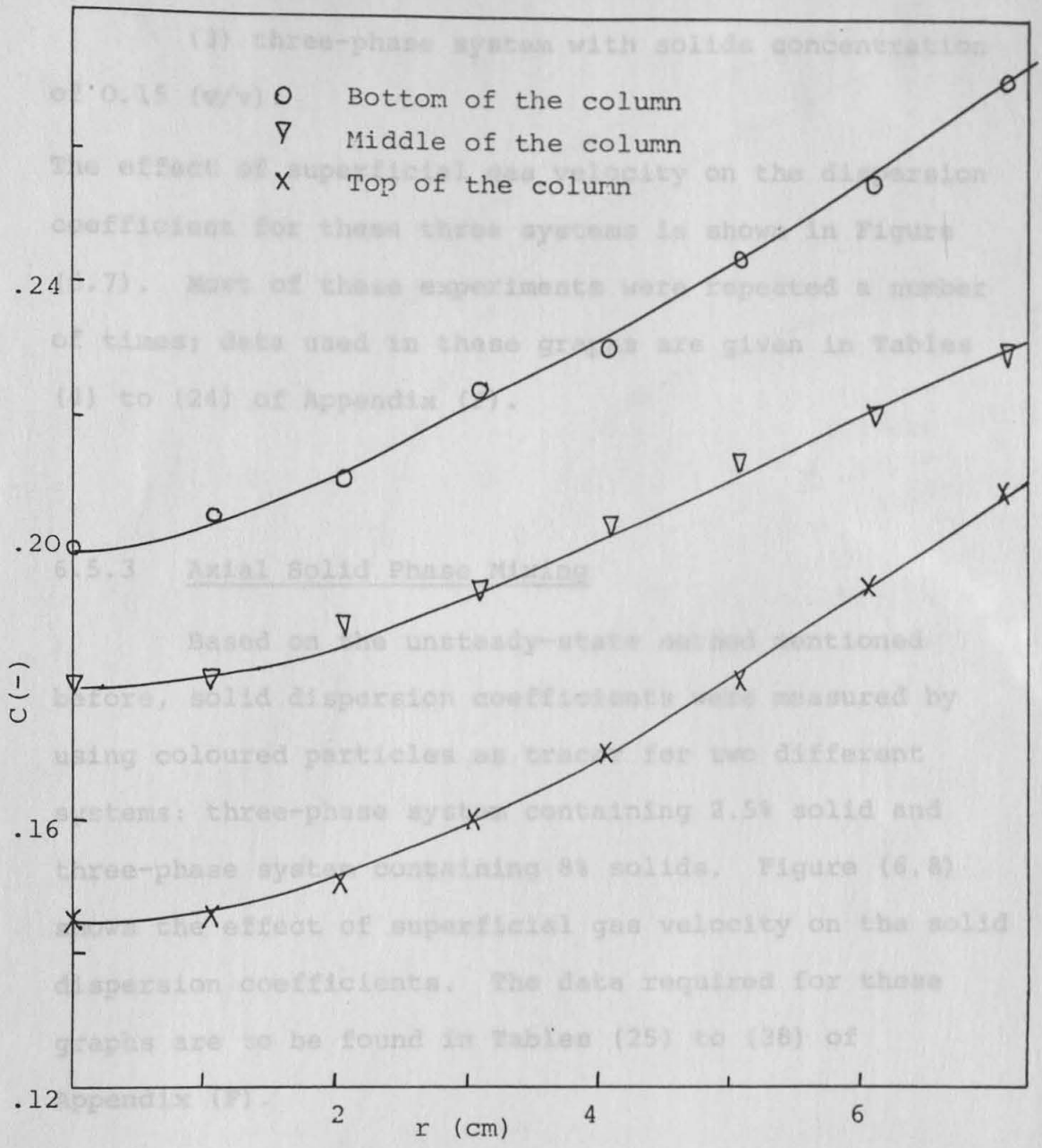

Figure 6.6 - Variation of solids concentration in radial direction for U_{sg} = 6 cm/s and C_o = 0.2(-).

(2) three-phase system with solids concentration of 0.08 (v/v);

(3) three-phase system with solids concentration of 0.15 (v/v).

The effect of superficial gas velocity on the dispersion coefficient for these three systems is shown in Figure (6.7). Most of these experiments were repeated a number of times; data used in these graphs are given in Tables (4) to (24) of Appendix (F).

6.5.3 Axial Solid Phase Mixing

Based on the unsteady-state method mentioned before, solid dispersion coefficients were measured by using coloured particles as tracer for two different systems: three-phase system containing 2.5% solid and three-phase system containing 8% solids. Figure (6.8) shows the effect of superficial gas velocity on the solid dispersion coefficients. The data required for these graphs are to be found in Tables (25) to (38) of Appendix (F).

6.6 Discussion

6.6.1 Radial Solids Distribution

As mentioned before, the radial solids distribution

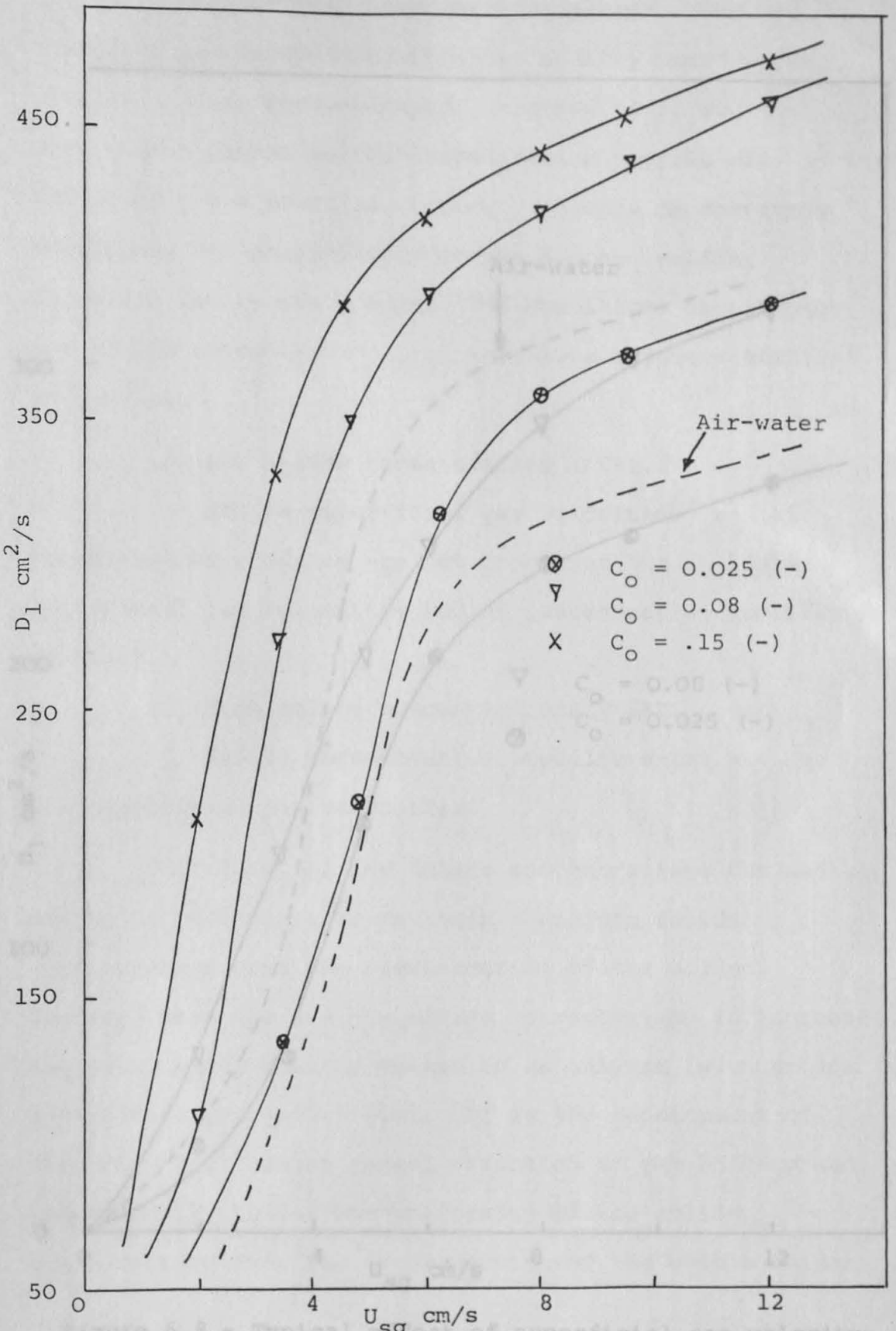

Figure 6.7 - Typical effect of superficial gas velocity on liquid dispersion coefficient for U_{sl} = 0.

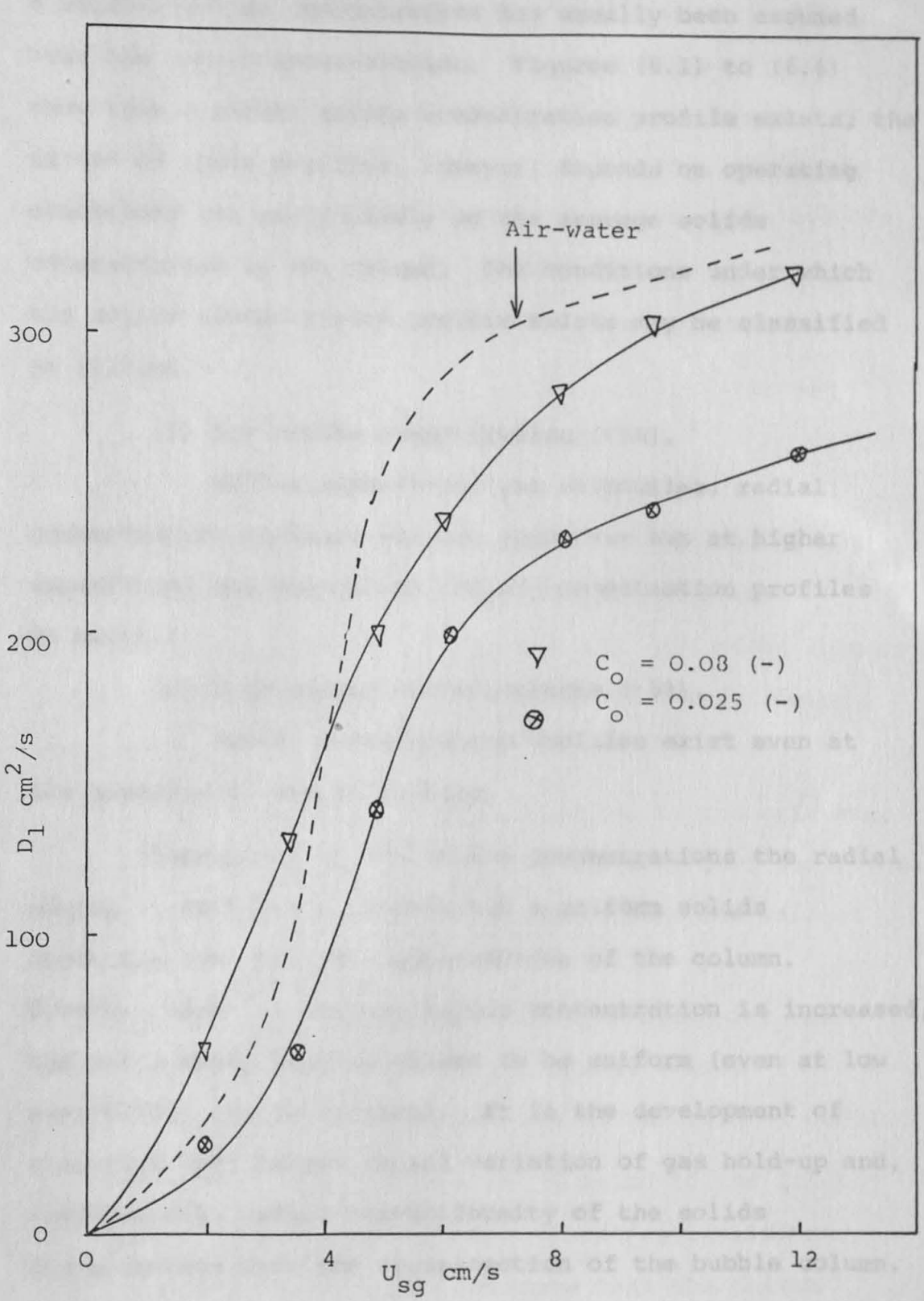

Figure 6.8 - Typical effect of superficial gas velocity on the solid phase dispersion coefficient for U_{sl} = 0.

has not until now been given much attention. Instead, a uniform solids concentration has usually been assumed over the column cross-section. Figures (6.1) to (6.6) show that a radial solids concentration profile exists; the extent of these profiles, however, depends on operating conditions and particularly on the average solids concentration in the column. The conditions under which the solids concentration profile exists may be classified as follows.

(1) Low solids concentration (<5%).

At low superficial gas velocities, radial concentration profiles are not important but at higher superficial gas velocities radial concentration profiles do exist.

(2) High solids concentrations (>5%).

Radial concentration profiles exist even at low superficial gas velocities.

Therefore, at low solids concentrations the radial mixing is sufficient to maintain a uniform solids concentration over the cross-section of the column. However, when the average solids concentration is increased, the solid phase hold-up ceases to be uniform (even at low superficial gas velocities). It is the development of slug-flow that causes radial variation of gas hold-up and, consequently, radial non-uniformity of the solids concentration over the cross-section of the bubble column.

Superficial gas velocity also has a significant effect on the radial solids concentration distribution, and these variations are increased considerably by an increase of superficial gas velocity (as illustrated in Figures (6.1) to (6.6)). The reason for this seems to be due to the increased probability of bubble coalescence and the formation of larger bubbles.

6.6.2 Axial Liquid-Phase Mixing

Introductory Comments

Liquid phase circulation (which also causes solid phase circulation) has a dominating effect on the continuous mixing of bubble columns and most investigators believe it is caused by a combination of the following phenomena:

(1) differences in densities due to the existence of a phase rich in bubbles near to the centre of the column and a phase relatively lean in bubbles near the wall of the column;

(2) downward liquid flow compensating for the liquid transported upwards in the bubble wakes;

(3) liquid displacement due to the rise of bubbles.

The contribution of each of these to the liquid circulation probably varies with operating conditions. Additionally, there is some evidence that the column

geometry (i.e. column diameter, column height and especially gas distributor design) has a significant effect on the liquid circulation in bubble columns.

Effect of U_{sg}

The superficial gas velocity has a most profound effect on the liquid dispersion coefficient, as can be seen from the curves in Figure (6.7). The experimental results show that, on the whole, the liquid dispersion coefficient increases sharply when the superficial gas velocity increases from 0 to about 6 cm/s. Beyond this range, the liquid dispersion coefficient does not significantly increase. A similar, sharp increase in gas hold-up is also apparent over this range of superficial gas velocity: this suggests that the gas bubbles are the main cause of liquid phase circulation. When the superficial gas velocity is greater than 6 cm/s the slugs reach their ultimate size; therefore, the gas hold-up does not change significantly and, as a consequence of this, the volume of liquid transported with the gas bubbles will become almost constant.

Effect of Solids Concentration

Experimental results (as illustrated in Figure 6.7) show that the solids concentration has a significant effect on the liquid dispersion coefficient. The liquid

dispersion coefficient increases as solids concentration increases from 0 to about 8% but beyond this latter value the effect is relatively small.

As discussed before, non-wettable solids increase the chance of bubble coalescence and reduce the gas hold-up. However, the effect of increasing solids concentration above about 8% on gas hold-up is negligible. Therefore during the presence of the solid phase larger bubbles and slugs will form and more liquid will be transported by the gas phase; when the solids concentration reaches about 8% the solid phase has no further effect on the bubble size. As a consequence, the liquid dispersion coefficient no longer changes significantly.

6.6.3 Axial Solids Phase Mixing

Effect of U_{sg}

In order to get an idea about the extent of back-mixing, some qualitative studies were first carried out by injecting coloured particles and dye (methylene blue) at the top of the column. It was noted that the mixing of the coloured particles (density ρ = 1.36 g/cm^3) was significantly slower than that of the methylene blue at both high and low gas velocities.

Results derived from measurements of solid phase mixing are summarised in Figure (6.8). This shows plots

of the dispersion coefficients as a function of the superficial gas velocity with solids concentration as a parameter. It is not easy to account for this difference in the degree of mixing of the two phases. It may be related to the fact that non-wettable solids are not "compatible" with the mobile liquid phase and are not readily mixed.

Finally, solids concentration has a significant effect on the solid phase dispersion coefficient due to the formation of larger bubbles at the higher solids hold-ups, as Figure (6.8) shows.

References

1. Gota, Y. and Okamoto, T. Pre-print of the 34th Annual Meeting of the Soc. of Chem. Engrs., Japan, No. C101 (1969).
2. Farkas, E.J. and Lebonde, P.F. Can. J. Chem. Eng., 47 (1969), 215.
3. Suganuma, T. and Yamanishi, T. Can. J. Chem. Eng., 30 (1966), 1136.
4. Ostergaard, K. and Michelsen, M.L. Symp. Fund. Appl. Fluidisation, Tampa, Florida, 1968, Pre-print 31D.
5. Michelsen, M.L. and Ostergaard, K. Chem. Eng. J., 1 (1970), 37.
6. Ostergaard, K. A.I.Ch.E. Symp. Series, 74, (1978), 82.
7. Kim, S.D., Baker, C.G.J. and Bergougnou, M.A. Can. J. Chem. Eng., 50 (1972), 695.
8. Vail, Y.U.K., Manoakov, N.Kh. and Manshilin, V.V., Int. Chem. Eng., 8 (1968), 293.
9. Todt, J., Lucke, J., Shugerl, K., and Renken, A. Chem. Eng. Sci., 32 (1977), 369.
10. El-Temtamy, S., El-Sharnoubi, Y. and El-Halwagi, M. The Chem. Eng. J., 18 (1979), 151.
11. El-Temtamy, S., El-Sharnoubi, Y. and El-Halwagi, M. The Chem. Eng. J., 18 (1979), 161.

7 Four-Phase Systems

7.1 Introduction

The recent interest in the production of single cell protein by growing microorganisms on various water-insoluble hydrocarbon substrates has resulted in several investigations of the nature of oxygen transfer in aerated systems with two liquid phases. The presence of a non-aqueous liquid phase has a significant effect on gas hold-up and the rate of oxygen-transfer from the gas phase to organisms.

In such systems, four phases are present - gas (usually air), an organic liquid, an aqueous solution and microorganisms. Oxygen may be transferred from the gas directly to any of the phases, and transport may also occur between the liquid phases or between cells and either of the liquids. Thus, the addition of a second liquid phase to the three phases that normally exist, doubles the number of interfaces across which mass may be transferred. Therefore, four-phase systems are much more difficult to analyse than the three-phase systems which were discussed earlier. The study of four-phase systems will form the basis for a further Ph.D. thesis; however, the author has already undertaken some systematic studies and the results are presented in this Section.

7.2 Experimental Programme

The effect of alcohols, glycol and inorganic materials on three-phase systems was investigated in the two-and three-dimensional bubble columns, which have been described in Section (2.4). Overall average gas hold-up measurements were made using the method detailed in Section (2.3).

Tap water was used as the liquid fluidising medium, air as the gaseous phase, and particles of Styrocel (ρ=1.2 g/cm^3 and d=813μ) as the solid phase. The additives used were ethanol, propanol, butanol, octanol, ethyl glycol and potassium chloride.

The operational conditions under which the experiments were carried out were similar to those used in the study of air-water systems and which were detailed in Section (2.2.1).

7.3 Experimental Results

The influence of the solid phase and its concentration on gas hold-up for methanol and ethanol systems is presented in Figures (7.1 and (7.2) for a wide range of superficial gas velocities. Figure (7.3) shows the corresponding experimental results for propanol in the three-dimensional bubble column. The experimental data for these three graphs are given in Tables (1), (2) and (3) of Appendix (G).

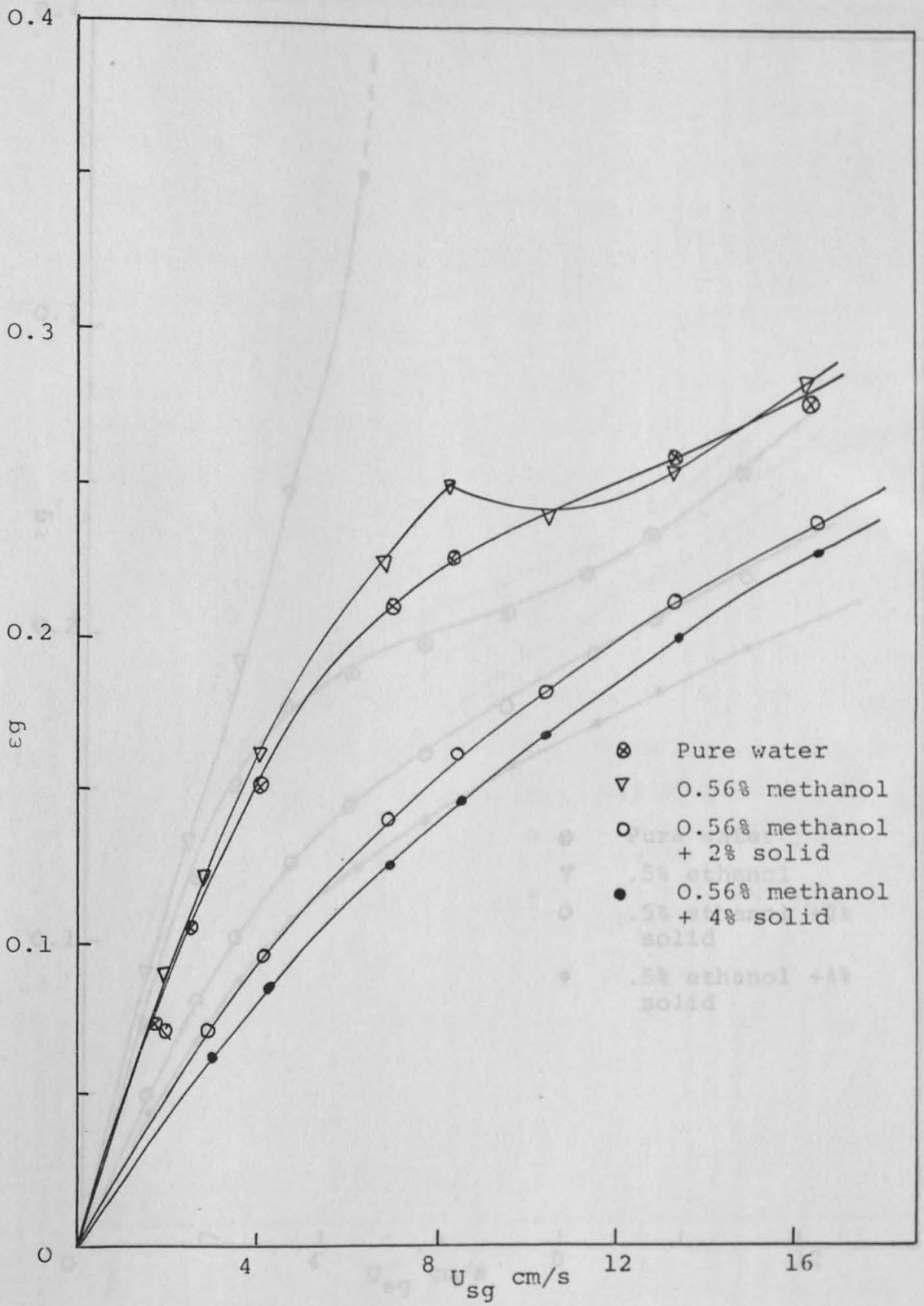

Figure 7.1 - Typical effect of solid phase on the gas hold-up for methanol system in two-dimensional bubble column and for $U_{sl} = 0$.

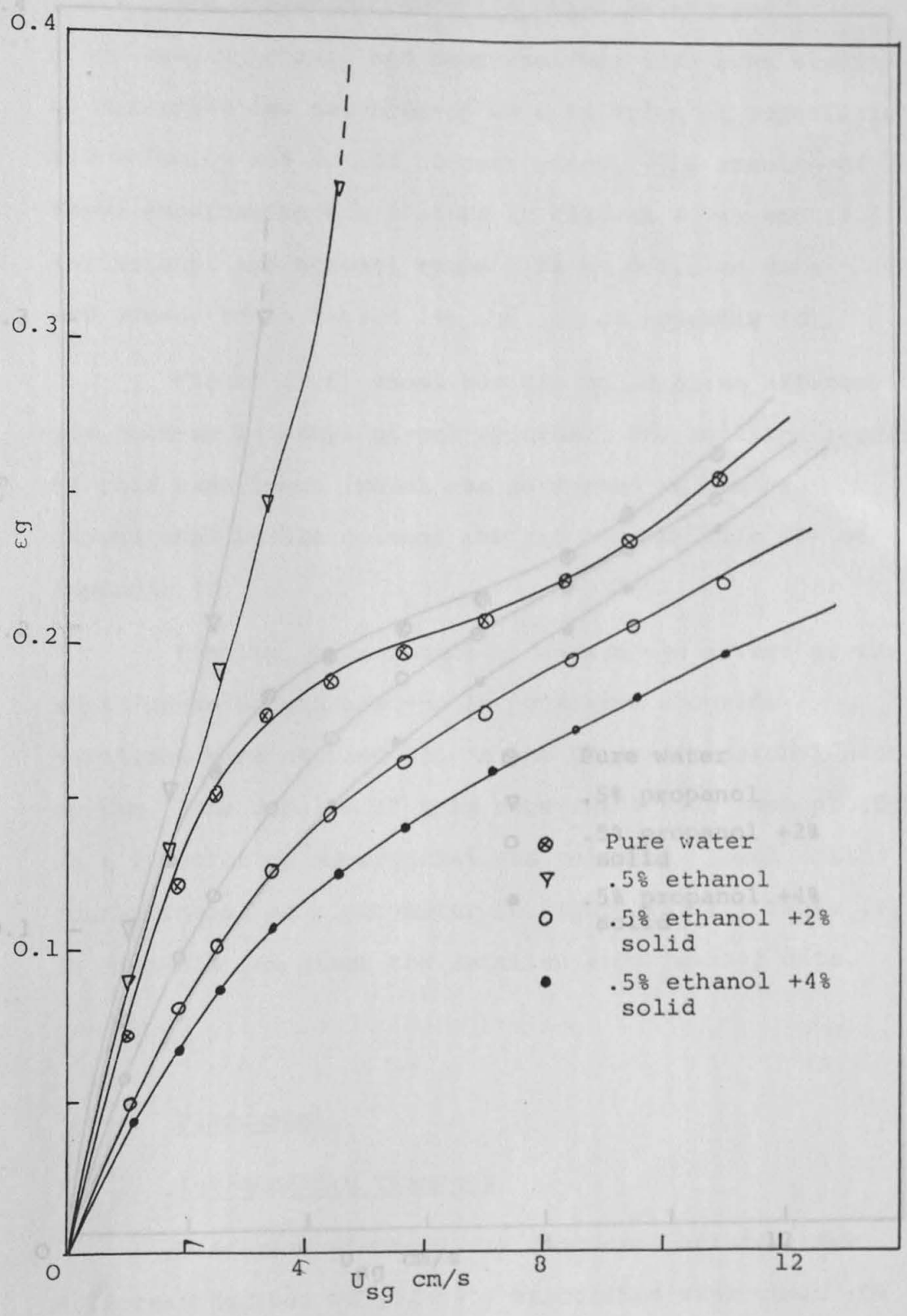

Figure 7.2 - Typical effect of solid phase on the gas hold-up for ethanol systems in three dimensional column and for $U_{sl} = 0$.

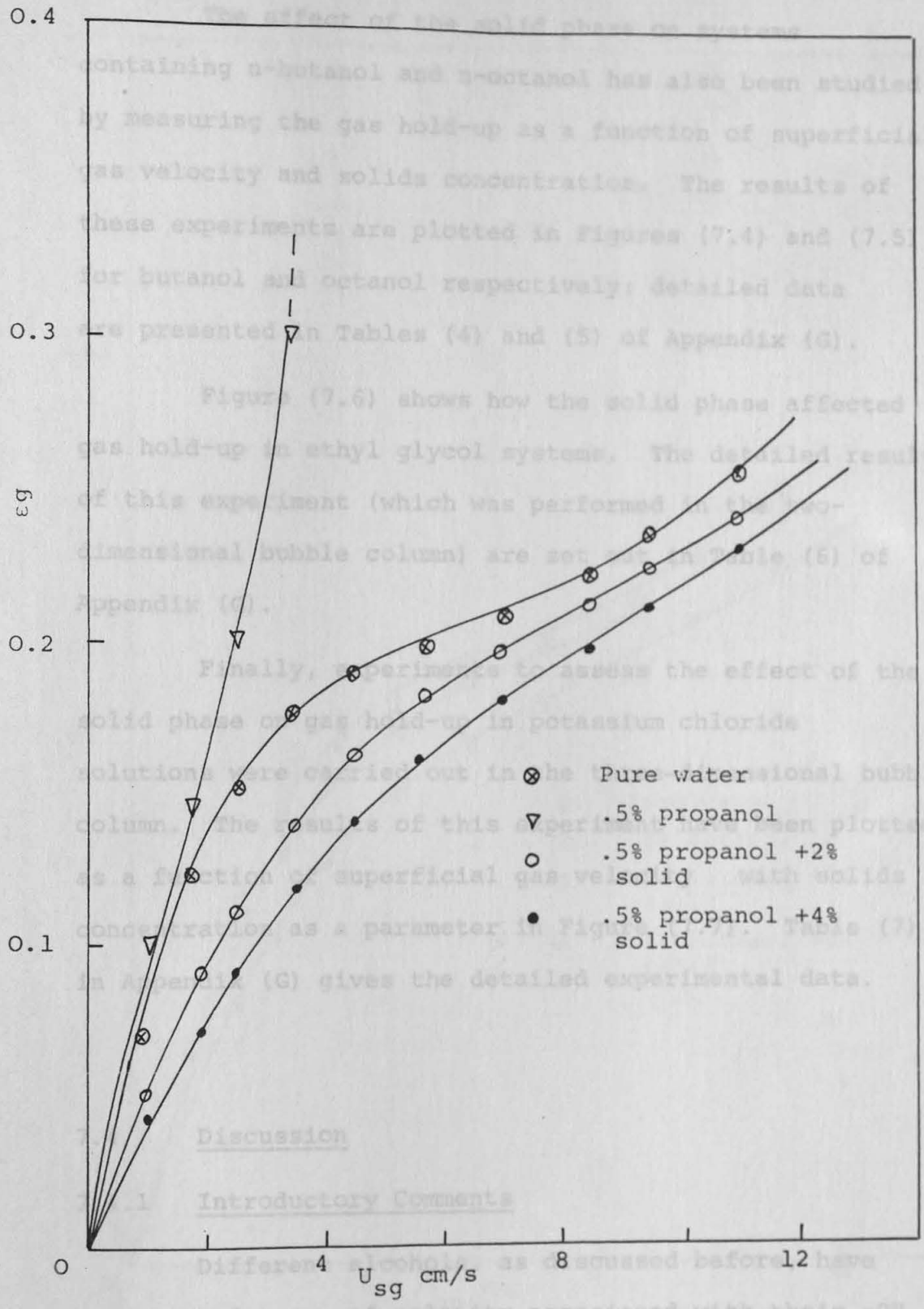

Figure 7.3 - Typical effect of solid phase on the gas hold-up for propanol system in three-dimensional bubble column and for $U_{sl} = 0$.

The effect of the solid phase on systems containing n-butanol and n-octanol has also been studied by measuring the gas hold-up as a function of superficial gas velocity and solids concentration. The results of these experiments are plotted in Figures (7.4) and (7.5) for butanol and octanol respectively: detailed data are presented in Tables (4) and (5) of Appendix (G).

Figure (7.6) shows how the solid phase affected gas hold-up in ethyl glycol systems. The detailed results of this experiment (which was performed in the two-dimensional bubble column) are set out in Table (6) of Appendix (G).

Finally, experiments to assess the effect of the solid phase on gas hold-up in potassium chloride solutions were carried out in the three-dimensional bubble column. The results of this experiment have been plotted as a function of superficial gas velocity with solids concentration as a parameter in Figure (7.7). Table (7) in Appendix (G) gives the detailed experimental data.

7.4 Discussion

7.4.1 Introductory Comments

Different alcohols, as discussed before, have different degrees of polarity associated with their -OH group. Therefore, mixing water with different alcohols

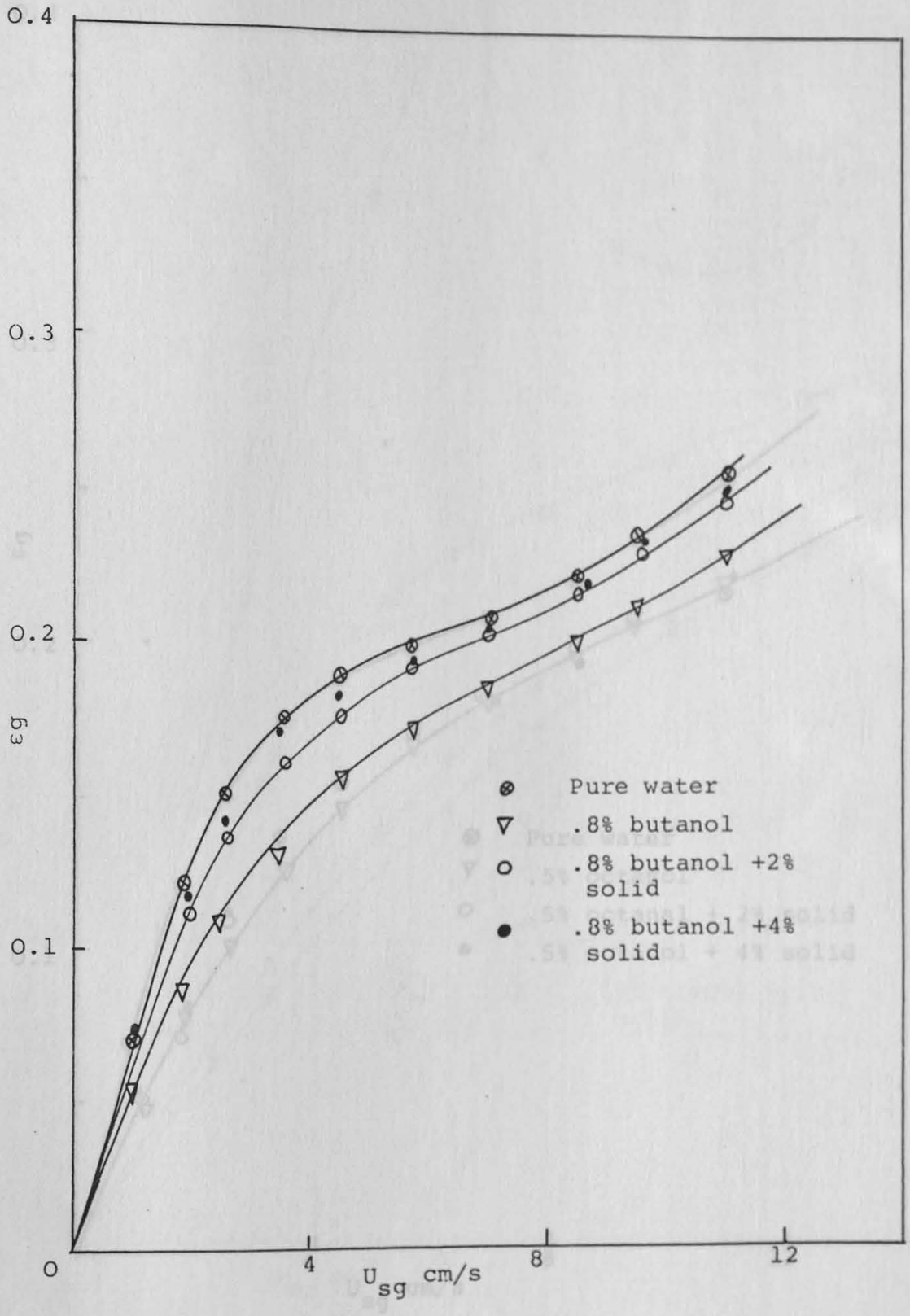

Figure 7.4 - Typical effect of solid phase on the gas hold-up for butanol system in three-dimensional column and for $U_{sl} = 0$.

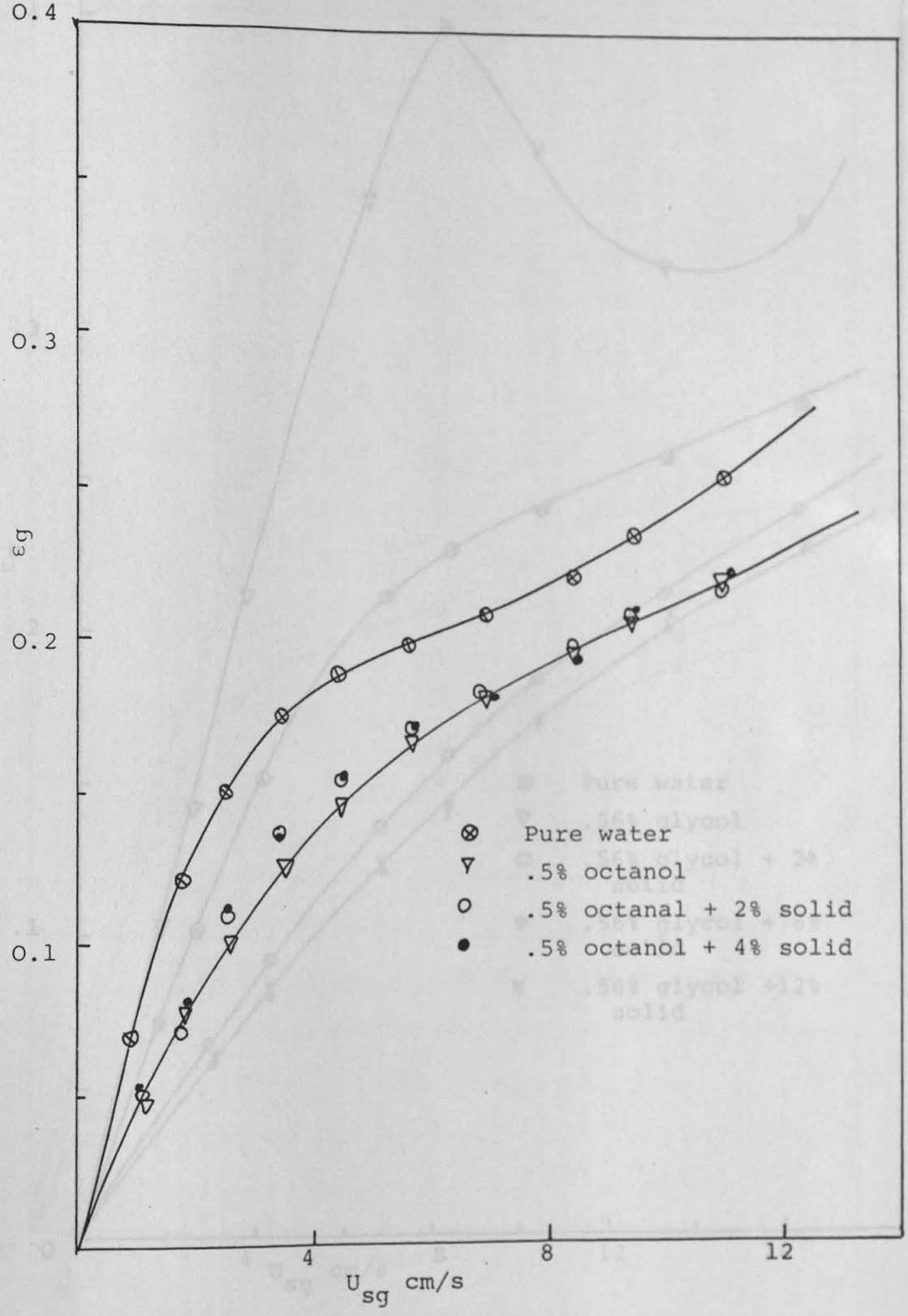

Figure 7.5 - Typical effect of solid phase on the gas hold-up for octanol system in three-dimensional column and for $U_{sl} = 0$.

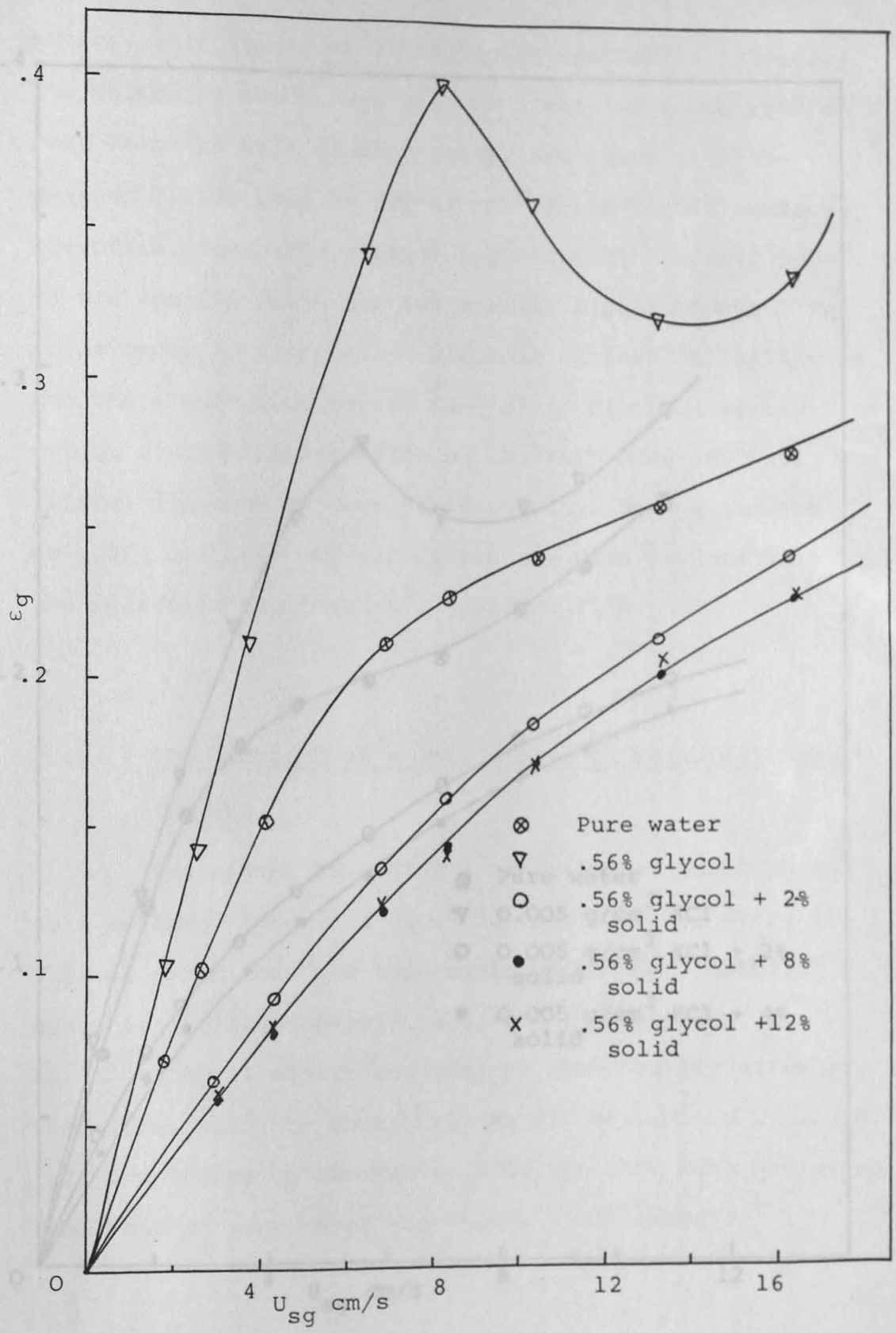

Figure 7.6 - Typical effect of solid phase on the gas hold-up for ethyl glycol system in two-dimensional column and for $U_{sl} = 0$.

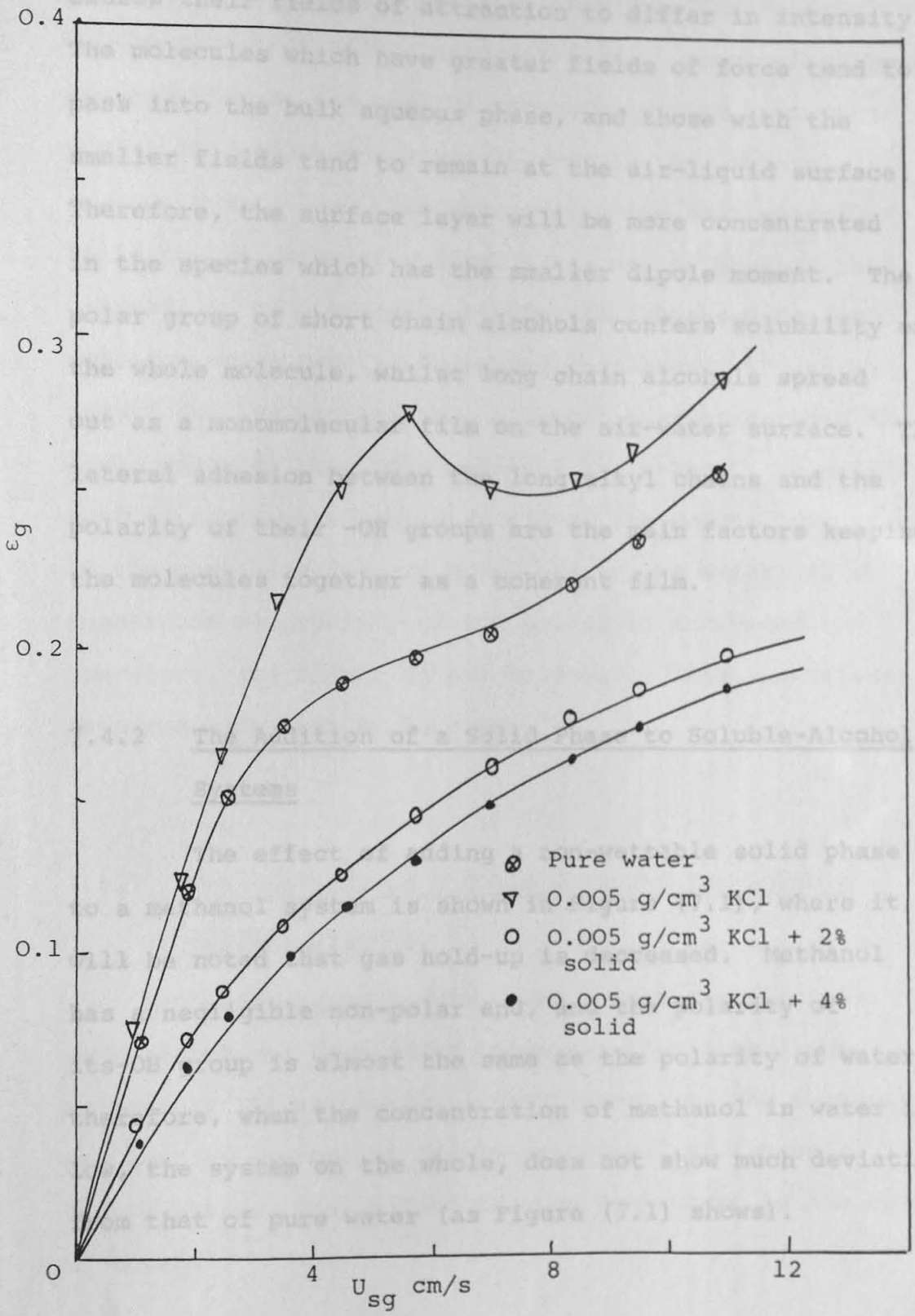

Figure 7.7 - Typical effect of solid phase on the gas hold-up for potassium chloride system in three-dimensional column and for U_{sl} = 0.

causes their fields of attraction to differ in intensity. The molecules which have greater fields of force tend to pass into the bulk aqueous phase, and those with the smaller fields tend to remain at the air-liquid surface. Therefore, the surface layer will be more concentrated in the species which has the smaller dipole moment. The polar group of short chain alcohols confers solubility on the whole molecule, whilst long chain alcohols spread out as a monomolecular film on the air-water surface. The lateral adhesion between the long alkyl chains and the polarity of their -OH groups are the main factors keeping the molecules together as a coherent film.

7.4.2 The Addition of a Solid Phase to Soluble-Alcohol Systems

The effect of adding a non-wettable solid phase to a methanol system is shown in Figure (7.1), where it will be noted that gas hold-up is decreased. Methanol has a negligible non-polar end, and the polarity of its-OH group is almost the same as the polarity of water; therefore, when the concentration of methanol in water is low, the system on the whole, does not show much deviation from that of pure water (as Figure (7.1) shows).

Figures (7.2) and (7.3) show that the importance of the effect of solids concentration on propanol systems is less than in the case of methanol systems. In other words, the reduction in gas hold-up in the propanol system is much less than when adding the same amount of solid to the methanol system. This may be because the wettability of Styrocel particles is increased by the addition of propanol. To expand this point, it can be argued that as propanol has a longer non-polar chain and lower polarity than both methanol and ethanol, it will tend to orient the non-polar end to the non-polar surface of the particles and the polar end to the water; as a result the wettability of the solids is increased. Therefore, its effect on gas hold-up is less significant compared with that of methanol.

7.4.3 The Addition of a Solid Phase to Non-Soluble Alcohol Systems

As discussed before, when long chain alcohols, such as butanol, are added to water, they form a mono-molecular film at the gas-liquid interface. As a result, gas bubbles are not so firmly "anchored" to the bulk liquid phase. This effect is more pronounced in the case of octanol.

When non-wettable, organic particles are added to these systems they tend to accumulate at the gas-liquid interfaces, as discussed before. Therefore, alchols which have long hydrocarbon chains will tend to be oriented to the solid surfaces from their hydrocarbon end, their -OH groups remaining in water. Consequently, the wettability of the solid particles will be increased, and the concentration of alcohol at the gas-liquid interface will be decreased. The net result will be that the gas hold-up will increase on increasing solids concentration, as results with butanol in Figure (7.4) show. However, because of the low level of polarity of octanol molecules, they cannot change the wettability of the solid phase to any great extent, and therefore, adding solid has almost no effect, as Figure (7.5) shows.

7.4.4 Addition of a Solid Phase to Glycol Systems

Glycol has two sites for forming physical bonds and a polarity of about 2.8D, and so it is negatively adsorbed at the gas-liquid interface. When solid particles such as Styrocel are added to the glycol system their wettability is not changed, and so bubble coalescence occurs, as Figure (7.6) shows.

7.4.5 Addition of a Solid Phase to Potassium Chloride Solutions

When the concentration of potassium chloride in water is low, it will be distributed throughout the bulk of the system. The intermolecular forces are electrostatic in nature and are much stronger than those in pure water.

When non-wettable particles are added to such systems, their wettability will tend to decrease or at least will remain the same as in water. Therefore, the solid particles will act in the same way as in water (see Figure (7.7)).

8 Single Slug Velocity Measurements

8.1 Introduction

It has been demonstrated in previous chapters that an increase in gas hold-up may happen due to either a reduction of surface tension and, consequently, bubble size or an increase in the bulk intermolecular forces which reduce the bubble rise velocity without changing the bubble size. The former situation was observed when using soluble alcohols and in three-phase systems containing either Diakon or Moviol particles; the latter situation was observed using air-water with a low concentration of salts or three-phase systems containing nylon as the solid phase. Also, in three-phase systems containing Styrocel particles as the solid phase, bubble coalescence occurred due to the weakening of the bulk intermolecular forces. In order to clarify these points, it was decided to study the velocity of a single slug in different solutions.

8.2 Experimental Programme

Experiments were carried out using the following systems.

(1) Propanol solutions. Propanol is a surfactant which has a significant effect on the surface tension of water.

(2) Potassium chloride and ethylene glycol solutions. Both these materials make the bulk of the liquid phase strongly cohesive.

(3) Styrocel, nylon and ABS (a co-polymer of polystyrene and 12% acrylonitrile) particles. Styrocel, since it lacks a polar group, weakens the intermolecular forces of water, whereas nylon particles make strong intermolecular forces with water; ABS particles occupy an intermediate position between Styrocel and nylon.

8.3 The Apparatus

A tube of approximately 400 cm length was constructed from sections of 2.5 cm diameter Q.V.F. pipe and erected in a vertical position (see Figure (8.1)). A tap at the bottom of the tube permitted the removal of the contents of the tube, which were introduced at the top. Also, a valve was fixed underneath the tube for slug production.

8.4 Procedure

The tube was filled with the desired solution to a measured volume, and air slugs of approximately 10 cm length were introduced at the bottom of the tube. The time taken for a slug to ascend a measured distance was recorded using an electronic timer. For each sample, the time for about 10 slugs was recorded and the mean rise velocity calculated.

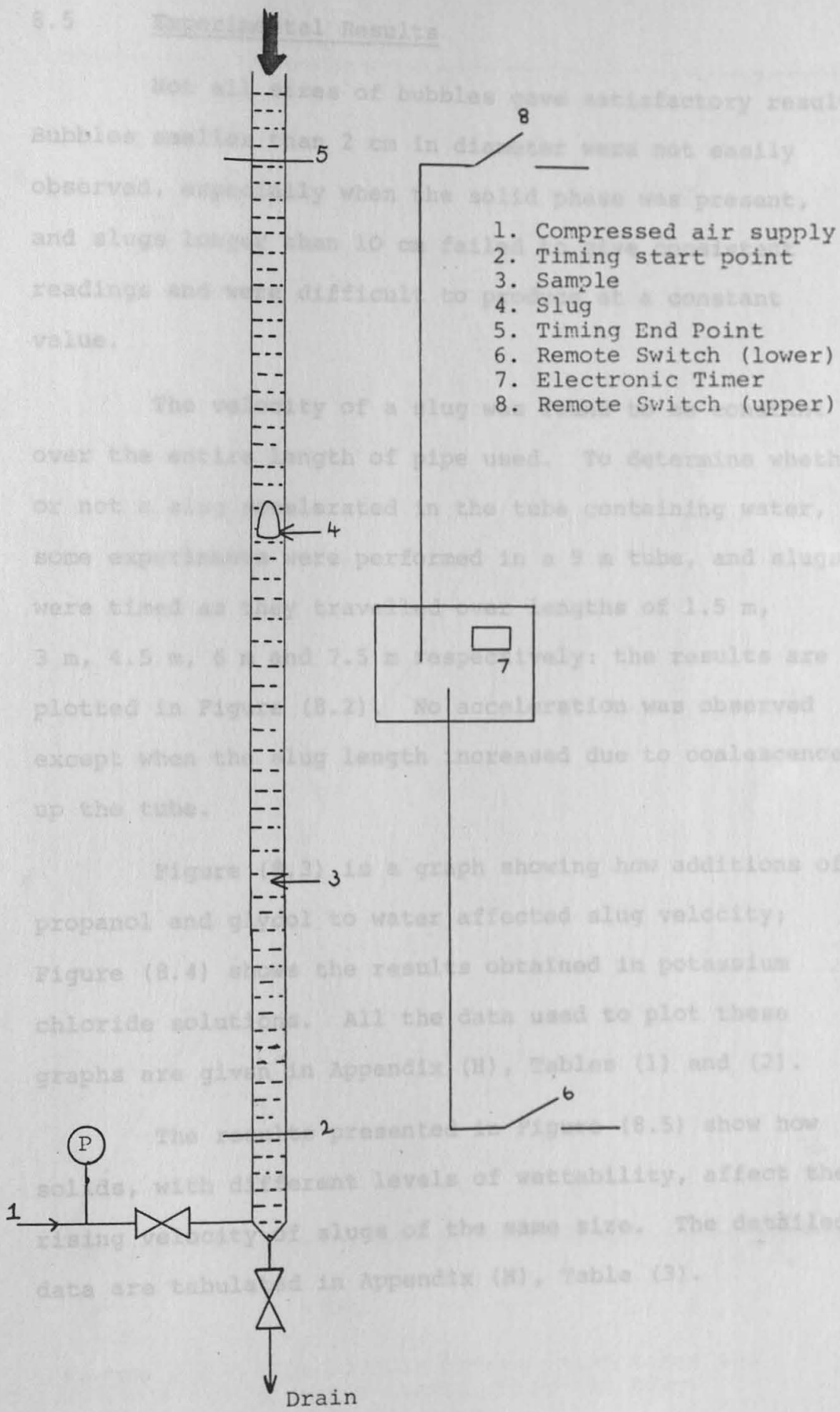

Figure 8.1 Apparatus used for slug velocity measurements

8.5 Experimental Results

Not all sizes of bubbles gave satisfactory results. Bubbles smaller than 2 cm in diameter were not easily observed, especially when the solid phase was present, and slugs longer than 10 cm failed to give consistent readings and were difficult to produce at a constant value.

The velocity of a slug was found to be constant over the entire length of pipe used. To determine whether or not a slug accelerated in the tube containing water, some experiments were performed in a 9 m tube, and slugs were timed as they travelled over lengths of 1.5 m, 3 m, 4.5 m, 6 m and 7.5 m respectively: the results are plotted in Figure (8.2). No acceleration was observed except when the slug length increased due to coalescence up the tube.

Figure (8.3) is a graph showing how additions of propanol and glycol to water affected slug velocity; Figure (8.4) shows the results obtained in potassium chloride solutions. All the data used to plot these graphs are given in Appendix (H), Tables (1) and (2).

The results presented in Figure (8.5) show how solids, with different levels of wettability, affect the rising velocity of slugs of the same size. The detailed data are tabulated in Appendix (H), Table (3).

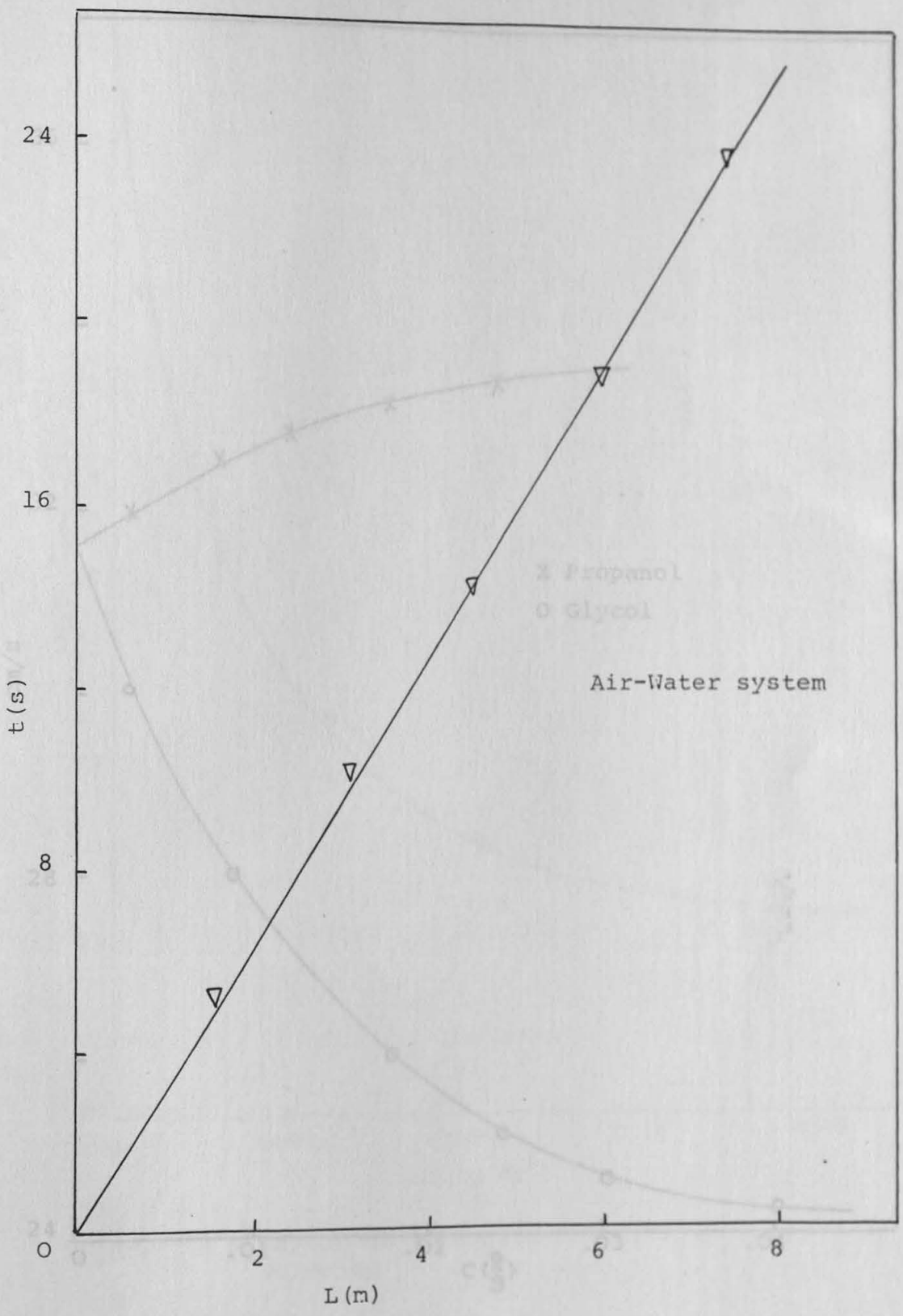

Figure 8.2 - Relationship between time taken and distance travelled by air slug.

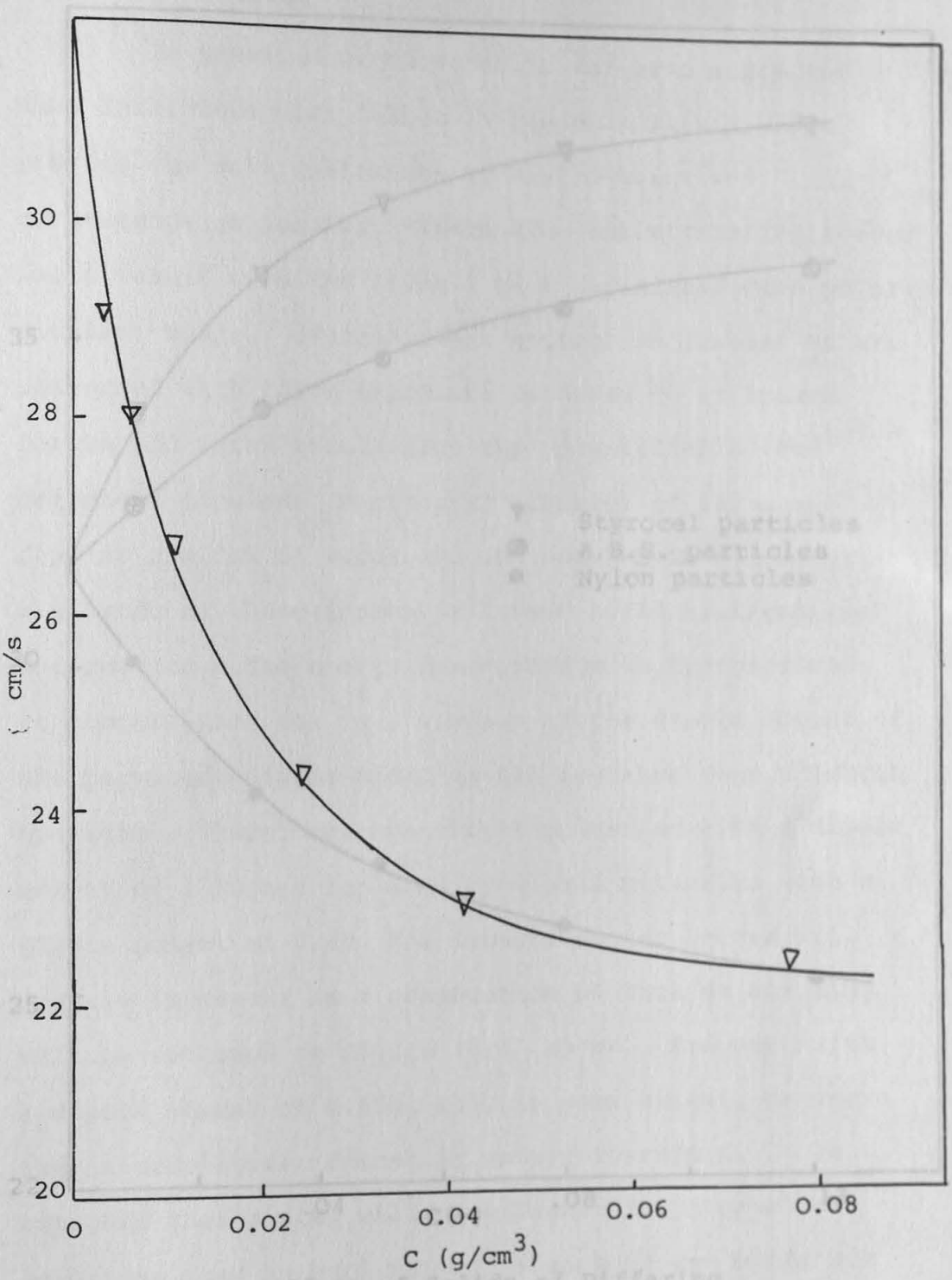

Figure 8.4 - Effect of Potassium Chloride on Slug Velocity

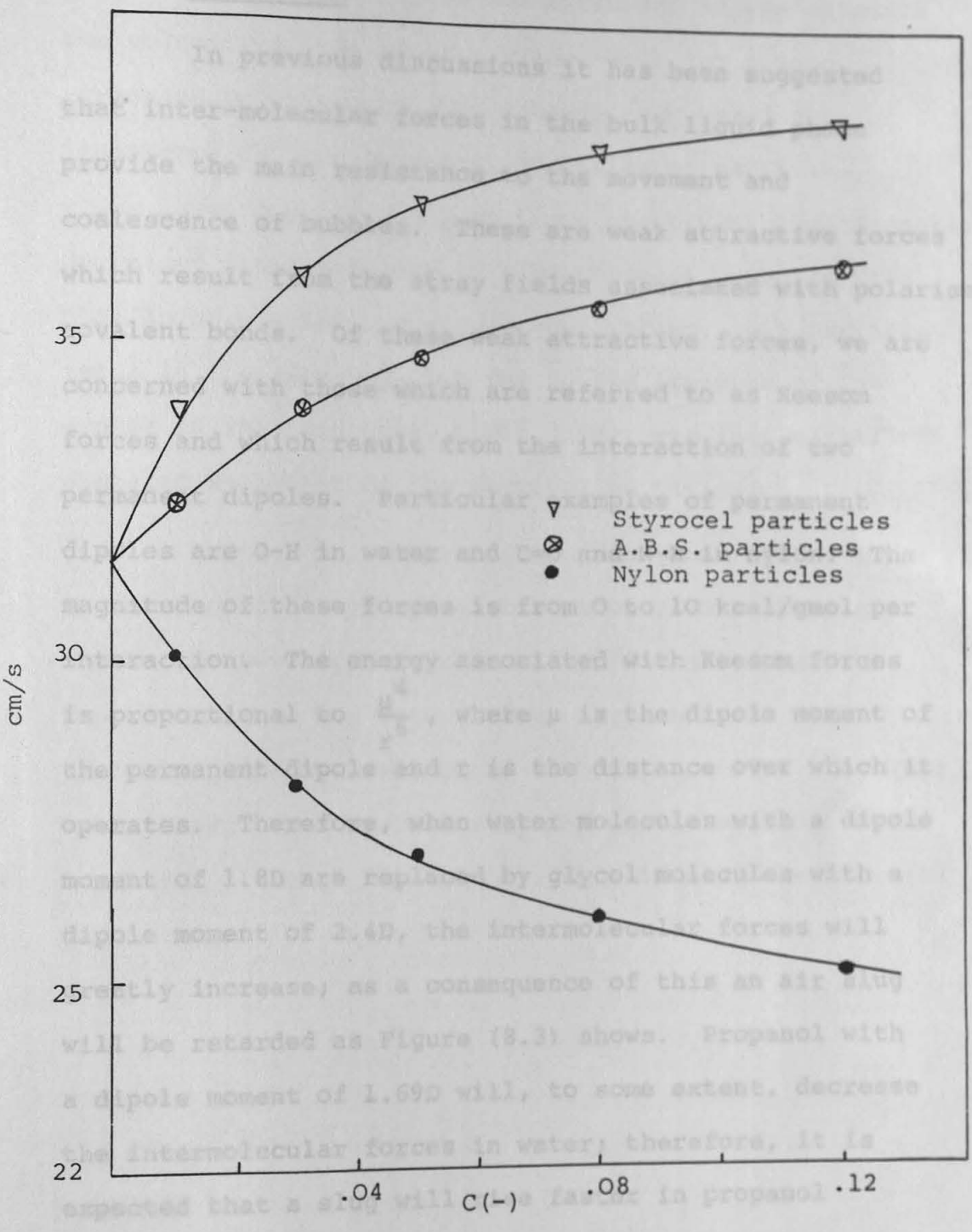

Figure 8.5 - Effect of Solids of Differing Wettabilities on Slug Velocity

8.6 Discussion

In previous discussions it has been suggested that inter-molecular forces in the bulk liquid phase provide the main resistance to the movement and coalescence of bubbles. These are weak attractive forces which result from the stray fields associated with polarised covalent bonds. Of these weak attractive forces, we are concerned with those which are referred to as Keesom forces and which result from the interaction of two permanent dipoles. Particular examples of permanent dipoles are O-H in water and C=O and N-H in nylon. The magnitude of these forces is from 0 to 10 kcal/gmol per interaction. The energy associated with Keesom forces is proportional to $\frac{\mu^4}{r^6}$, where μ is the dipole moment of the permanent dipole and r is the distance over which it operates. Therefore, when water molecules with a dipole moment of 1.8D are replaced by glycol molecules with a dipole moment of 2.4D, the intermolecular forces will greatly increase; as a consequence of this an air slug will be retarded as Figure (8.3) shows. Propanol with a dipole moment of 1.69D will, to some extent, decrease the intermolecular forces in water; therefore, it is expected that a slug will rise faster in propanol solutions than in pure water. When hydrogen bonds are partly replaced by ionic bonds in electrolyte solutions, the resistance to slug movement is increased and, consequently, slug velocity is decreased (as Figure (8.4) shows).

Figure (8.5) shows how different solids affected the velocity of the slugs. Nylon, with two strong permanent polar groups (C=O and N-H) increased the resistance to slug movement, but Styrocel particles, which have no polar group in their structure, significantly decreased the resistance to slug movement compared with that in pure water, as Figure (8.5) shows. ABS particles acted in the same way, but due to the presence of C=N groups in the structure, their effect was less significant compared with that of the Styrocel particles.

Another point worth noting is concerned with the tendency of the Styrocel particles to float: after a short time two separate phases formed - solids at the top of the tube and water below. By contrast, nylon particles remained well mixed with water whilst the slugs were rising. Not surprisingly ABS particles also tended to float, although not to the same extent as the Styrocel particles.

9 General Discussion

9.1 An Overview of the General Approach used in the Thesis

Bubble columns are frequently used for heterogeneous catalytic reactions in which physical mass transfer significantly, or completely, controls the overall rate of the process. In such situations, we are concerned with two or more phases having different physical properties and which come into close contact. At an early stage in the author's work it became clear that despite the volume of literature about bubble column reactors it was difficult to predict what would happen with specific systems. As a result, the author decided to explore to what extent the molecular approach (in contrast to the more usual continuum approach) could be applied. The molecular approach proved to be of great help when planning experimental programmes and interpreting, albeit qualitatively, the experimental data: for these reasons, it has been used throughout the thesis. The following two additional examples illustrate this approach.

(1) The Effect of Changing Solids Wettability

One of the problems which is presently manifest in three-phase systems containing non-wettable solids (see Section (5.4)) is that, usually, only a small amount of solid is sufficient to increase the possibility of bubble coalescence; this leads, in turn, to a reduction

in the interfacial area and, consequently, mass transfer rate. The degree of reduction in gas hold-up naturally depends on the "compatability" between the solid and liquid phases: therefore, the solution to this problem must lie in the direction of improving the molecular property.

In previous sections, when discussing the structure of water, it was pointed out that a molecule such as water, which has a highly significant dipole moment (1.85D), cannot form any kind of physical bond with a non-wettable solid surface such as Styrocel, which is a hydrocarbon. The consequence of this is that there is high interfacial tension between the solid and water: a reduction in the interfacial tension can only be achieved if the "compatability" between water and the solid surface is increased. One way of doing this is to reduce the attraction between water molecules and this can be readily done by increasing the temperature of the water. The results of some investigations using Styrocel as the solid phase are summarised in Figure (9.1) (detailed data for this figure are given in Table 1 of Appendix I): this figure shows how the compatability (or wettability) of the solid phase was greatly increased by increasing temperature. Furthermore, visual observations revealed that the solids sedimented very rapidly at the high temperatures but floated at the lower temperatures.

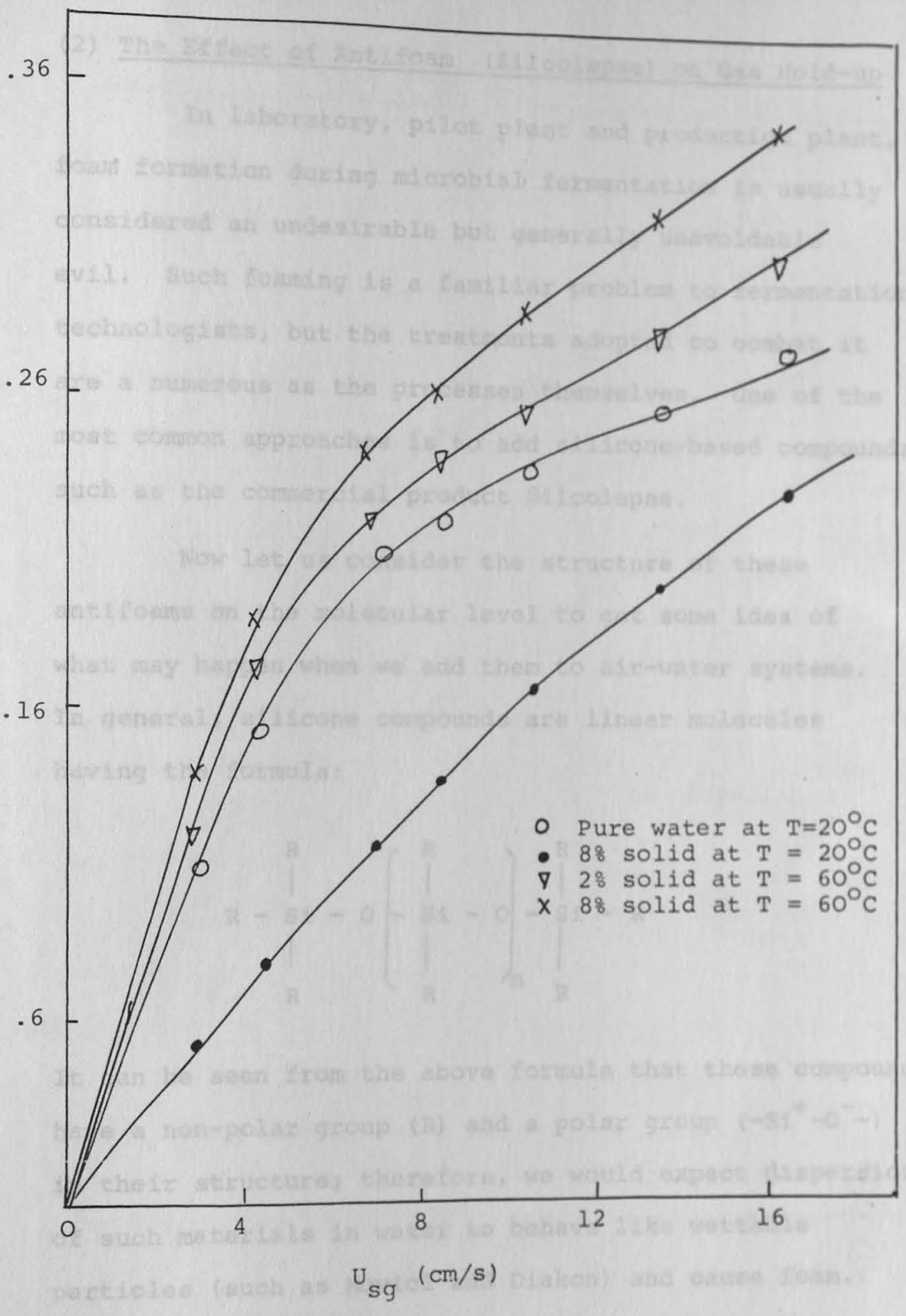

Figure 9.1 - Effect of liquid phase temperature on three-phase system containing Styrocel (d=810μ and ρ = 1.2 g/cm^3) particles as solid phase for U_{sl} = 0.

(2) The Effect of Antifoam (Silcolapse) on Gas Hold-up

In laboratory, pilot plant and production plant, foam formation during microbial fermentation is usually considered an undesirable but generally unavoidable evil. Such foaming is a familiar problem to fermentation technologists, but the treatments adopted to combat it are a numerous as the processes themselves. One of the most common approaches is to add silicone-based compounds, such as the commercial product Silcolapse.

Now let us consider the structure of these antifoams on the molecular level to get some idea of what may happen when we add them to air-water systems. In general, silicone compounds are linear molecules having the formula:

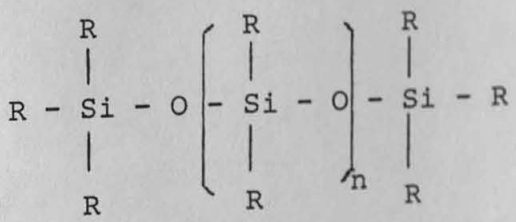

It can be seen from the above formula that these compounds have a non-polar group (R) and a polar group ($-Si^{+}-O^{-}-$) in their structure; therefore, we would expect dispersions of such materials in water to behave like wettable particles (such as Moviol and Diakon) and cause foam. The foamability of Silcolapse is illustrated in Figure (9.2) (detailed data are given in Table 2 of Appendix I).

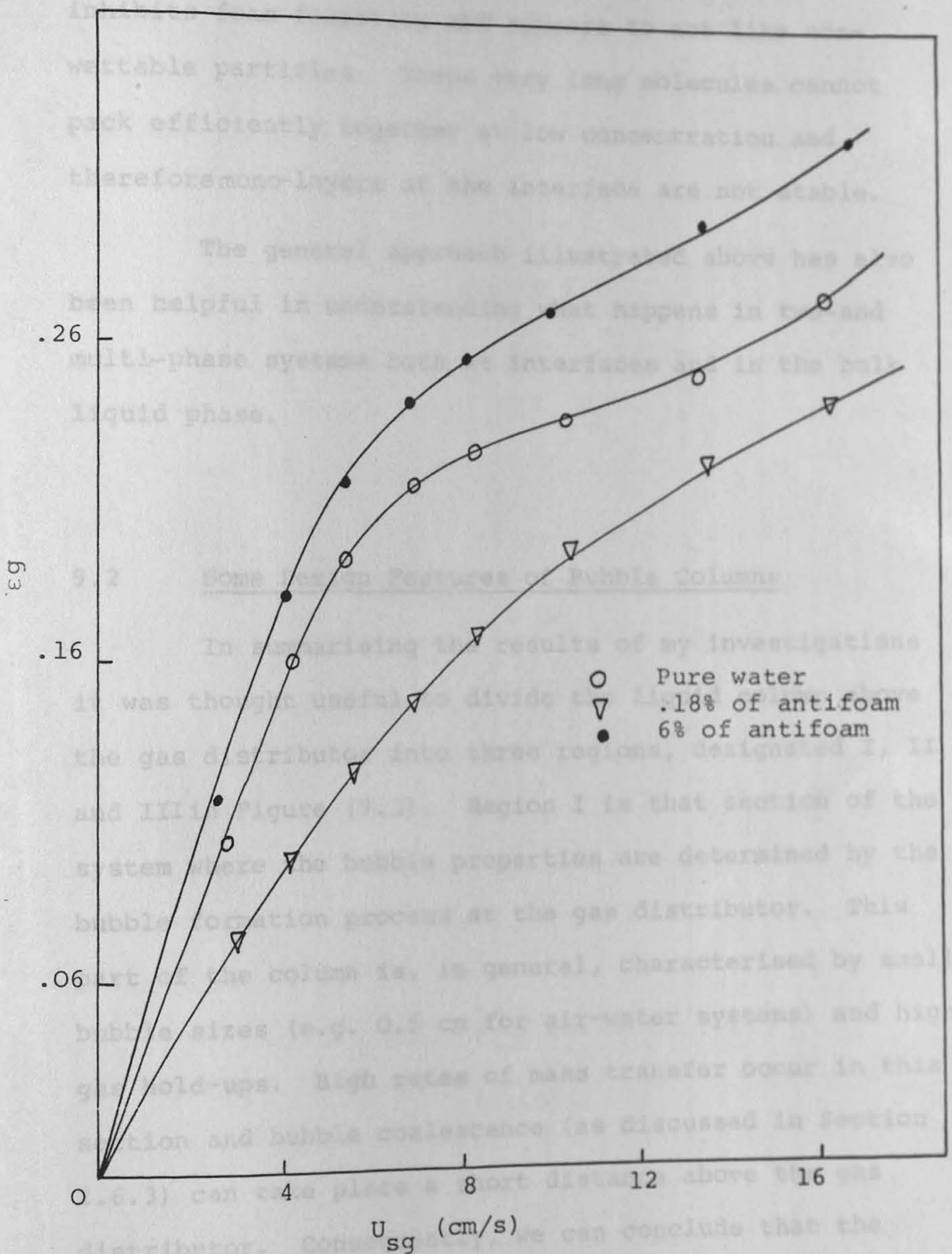

Figure 9.2 - Effect of silcolapse antifoam on gas hold up for U_{sl} = 0.17 cm/s

However, at very low concentrations Silcolapse actually inhibits foam formation and appears to act like non-wettable particles. These very long molecules cannot pack efficiently together at low concentration and, therefore mono-layers at the interface are not stable.

The general approach illustrated above has also been helpful in understanding what happens in two-and multi-phase systems both at interfaces and in the bulk liquid phase.

9.2 Some Design Features of Bubble Columns

In summarising the results of my investigations it was thought useful to divide the liquid column above the gas distributor into three regions, designated I, II and III in Figure (9.3). Region I is that section of the system where the bubble properties are determined by the bubble formation process at the gas distributor. This part of the column is, in general, characterised by small bubble sizes (e.g. 0.5 cm for air-water systems) and high gas hold-ups. High rates of mass transfer occur in this section and bubble coalescence (as discussed in Section 2.6.3) can take place a short distance above the gas distributor. Consequently, we can conclude that the performance of the column either totally or in part is determined by what happens in this region of the column.

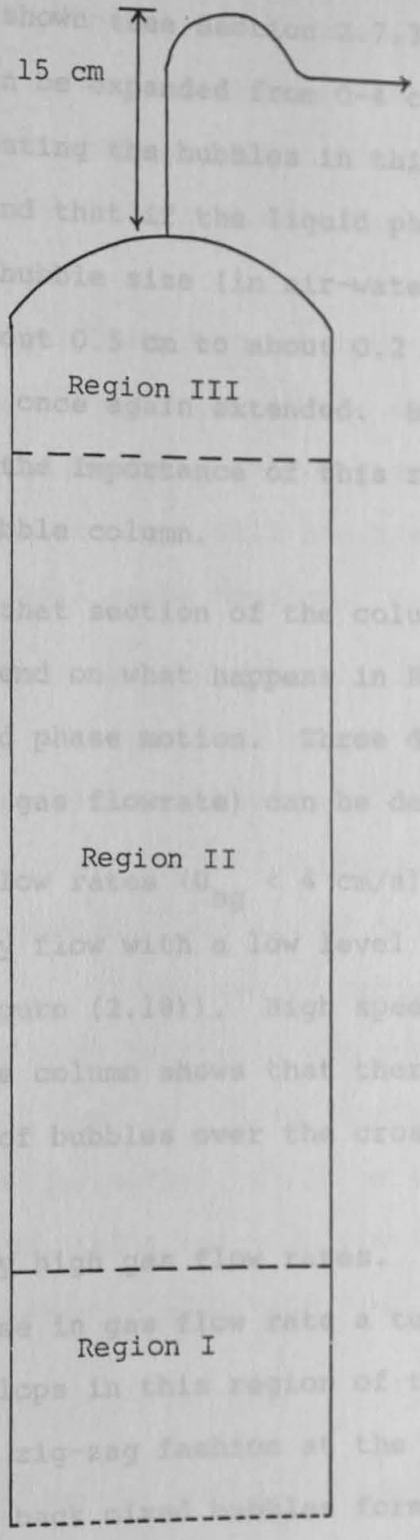

Figure 9.3 - Location of Region I, II and III in a Bubble Column

For example, we have shown (see Section 2.7.3) how the bubbly-flow regime can be expanded from 0-4 cm/s to 0-9 cm/s by redistributing the bubbles in this section. Recently, we have found that if the liquid phase is jetted into this region the bubble size (in air-water systems) will decrease from about 0.5 cm to about 0.2 cm and the bubbly-flow regime is once again extended. Both these examples demonstrate the importance of this region on the performance of the bubble column.

Region II is that section of the column where bubble properties depend on what happens in Region I and on the bulk liquid phase motion. Three distinct regimes (based on the gas flowrate) can be defined:

(1) Low gas flow rates (U_{sg} < 4 cm/s).

In this regime, bubbly flow with a low level of back-mixing occurs (see Figure (2.18)). High speed photography in this section of the column shows that there is a uniform distribution of bubbles over the cross-section of the column.

(2) Moderately high gas flow rates.

With a further increase in gas flow rate a turbulent or slug-flow regime develops in this region of the column. The slugs ascend in a zig-zag fashion at the centre of the column whilst the back mixed bubbles form circular cells at both sides of a two-dimensional column (see Figure (2.16)). This regime is characterised by very

high backmixing at the sides of the column (see Figure (2.18)) and a non-uniform distribution of bubbles over the cross-section of the column. It would appear that most mass transfer takes place in the circular cells in this part of the column.

(3) Very high gas flow rates or high energy inputs. If we further increase energy input to the system (e.g. by using very high gas flow rates, heating or vibration), observations indicate that slugs will break up and bubbly flow with high mixing will again develop.

Liquid phase backmixing in Region II of bubble columns (at moderately high gas flow rates) is a disadvantage in many practical situations. If in some way we can reduce the extent of this backmixing, overall performance will be improved. One way of doing this was mentioned in Section (2.7.2)-the use of radial baffles; however, the design of such baffles - the spacing and the diameter of the central opening - have received very little attention. Another method, which we believe can reduce liquid phase backmixing and will provide interesting results, is to use a bubble column with highly wettable walls.

Region III - Recirculation or removal of phases takes place in this section of the column, and it seems convenient to divide this region into two parts - (i) the top of the column section and (ii) the take-off section. The design of the top section seems very

important, particularly with regard to the solid phase (e.g. microbial aggregates). The main body of the column opens into a large settling zone above the tower section in bubble column fermenters. Generally, an overall aspect ratio of 10:1 with an aspect of 6:1 on the tubular section is used. Consequently, micro-organisms can settle in this upper section and return to the main body of the tower, thus maintaining a relatively high concentration within the main body of the fermenter. The design of the take-off system has previously been given little attention and the published information is confusing. According to Cova (1) and Imafuku et al. (2), in cocurrent flow, the concentration of solid particles at the top of the column is equal to that in the effluent slurry; yet, according to Suganuma et al. (3), the former is higher than the latter. We have recently carried out a preliminary study of the parameters which influence the wash-out of the solid phase in gas-liquid fluidised systems. An apparent solids residence time was defined in terms of the liquid flow, as follows:

$$\bar{t} = \frac{\text{Total volume of column (lt)}}{\text{Liquid flow rate (lt/min)}} = \text{min}$$

Dimensionless solids concentration was defined as $C_{(t)}/C_o$ where $C_{(t)}$ is the actual solids concentration at time (t) and C_o is the initial solids concentration in the column. The results obtained from solids concentrations from the take-off pipe and other sampling points over the length of the column are shown in Figures (9.4) to (9.7) (Data

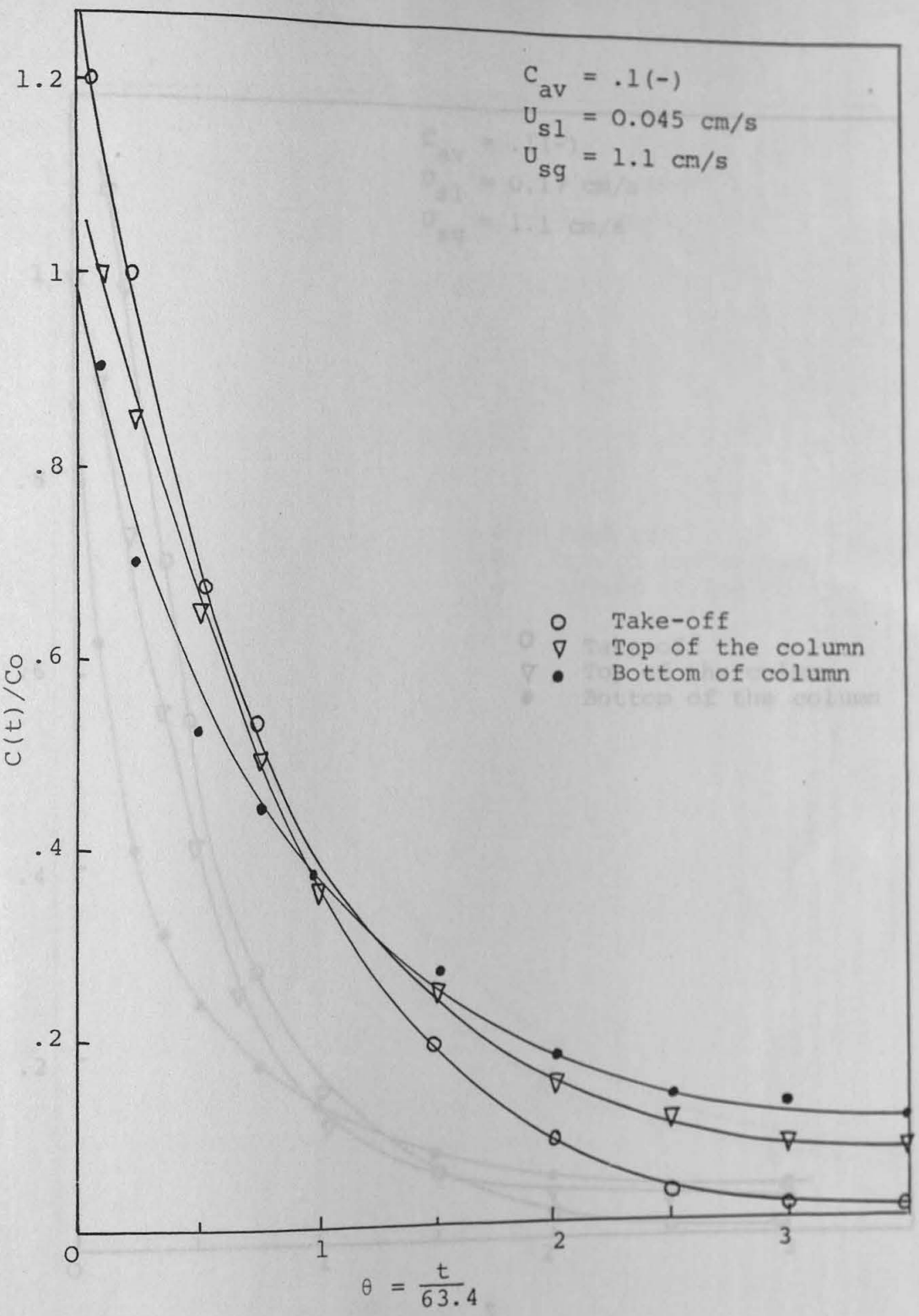

Figure 9.4 - Variation of solids concentration with time.

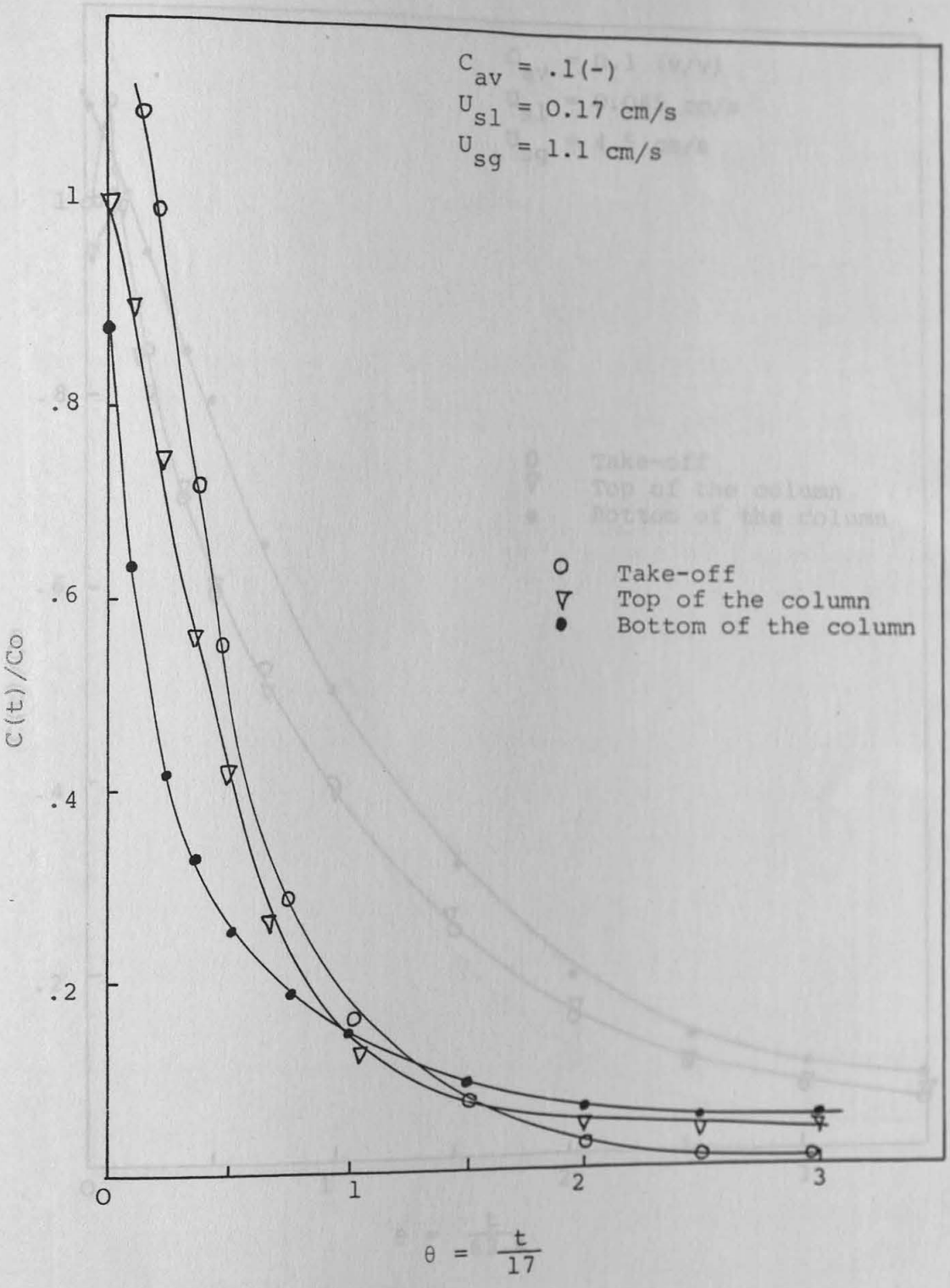

Figure 9.5 - Variation of solids concentration with time.

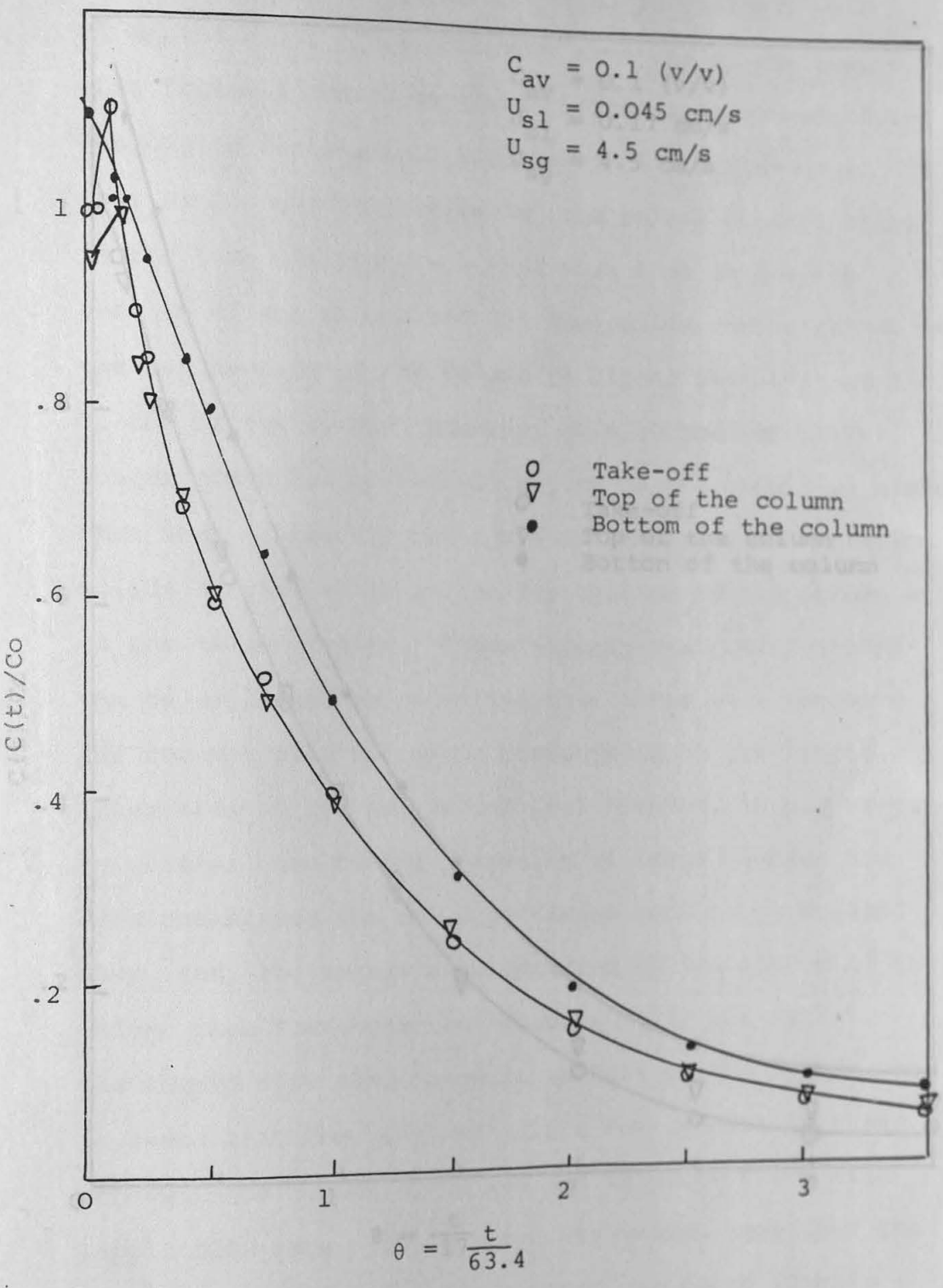

Figure 9.6 - Variation of solids concentration with time.

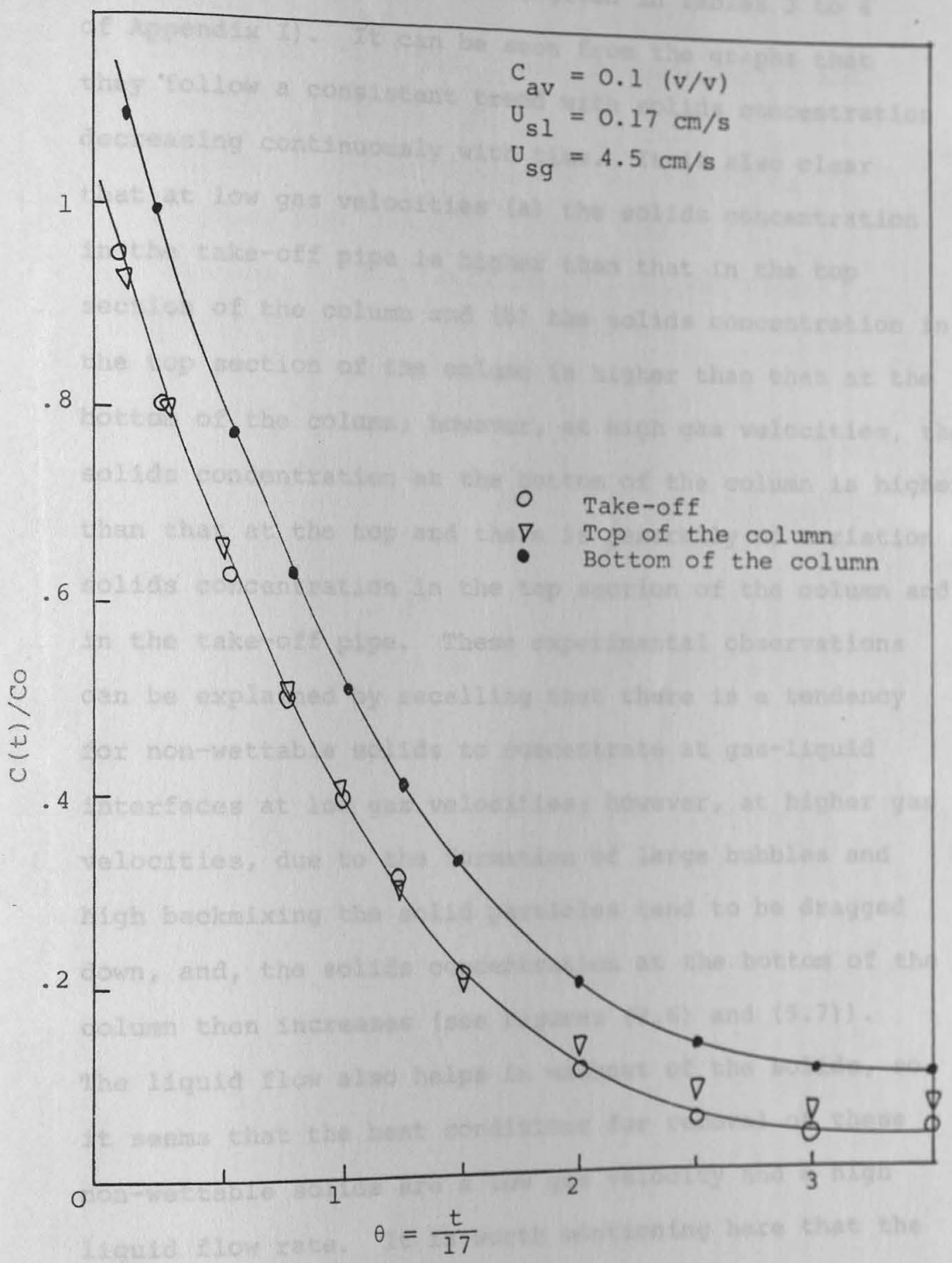

Figure 9.7 - Variation of solids concentration with time.

used to plot these graphs are given in Tables 3 to 6 of Appendix I). It can be seen from the graphs that they follow a consistent trend with solids concentration decreasing continuously with time. It is also clear that at low gas velocities (a) the solids concentration in the take-off pipe is higher than that in the top section of the column and (b) the solids concentration in the top section of the column is higher than that at the bottom of the column; however, at high gas velocities, the solids concentration at the bottom of the column is higher than that at the top and there is generally no variation in solids concentration in the top section of the column and in the take-off pipe. These experimental observations can be explained by recalling that there is a tendency for non-wettable solids to concentrate at gas-liquid interfaces at low gas velocities; however, at higher gas velocities, due to the formation of large bubbles and high backmixing the solid particles tend to be dragged down, and, the solids concentration at the bottom of the column then increases (see Figures (9.6) and (9.7)). The liquid flow also helps in washout of the solids, so it seems that the best conditions for removal of these non-wettable solids are a low gas velocity and a high liquid flow rate. It is worth mentioning here that the same experiments were also carried out using (highly wettable) nylon particles as the solid phase: the experimental results showed that there was a negligible solids concentration in the take-off system except at very high liquid flow rates.

References

1. Cova, D.R. Ind. Eng. Chem., Process Design and Develop., 5 (1966), 20.

2. Imafuku, K., Wang, T., Koide, K. and Kubota, H. J. Chem. Eng. Japan, 1 (1968), 153.

3. Suganuma, T. and Yamanishi, T. Kagaku Kogaku, 35 (1971), 912.

10 Achievements, Conclusions and Suggestions for Further Work

10.1 The Air-Water System

The following points may be concluded from the study of air-water systems:

(1) there is almost a linear increase of gas hold-up with superficial gas velocity in the bubbly flow regime;

(2) superficial liquid velocity has little effect on gas hold-up if the liquid enters the column at low velocity and has a significant effect if the liquid phase is jetted into the column;

(3) moderate agitation of the liquid will increase the possibility of bubble coalescence;

(4) the effect of energy input (i.e. heating and vibration) on gas hold-up, bubble coalescence and break-up has been analysed in terms of the chemical structure and physical properties of the phases;

(5) gas phase flow patterns have been examined visually and by high speed photography;

(6) superficial gas velocity is the most important single variable affecting liquid phase dispersion;

(7) if in some way (i.e. by the use of radial baffles) the liquid phase backmixing is decreased, the gas hold-up will increase significantly;

(8) the important effects of column height and column diameter on gas hold-up have been confirmed;

(9) the design of the gas distributor is an important factor in column performance; experiments show that it is possible to extend the bubbly flow regime up to a superficial gas velocity of about 10 cm/s and gas hold-up to about 40% by careful design of the gas distributor;

(10) the bottom end of the column has a profound effect on the performance of the system; and a careful study of the effect of the top section of the column is recommended for the future.

10.2 The Gas Phase

The following points should be noted:

(1) apart from the physical properties of the liquid, it was found that gas hold-up is also influenced by the physical properties of the gas phase;

(2) as the "compatability" between the gas and liquid phases increases, bubble size will decrease and gas hold-up will increase; when the compatability between the gas and liquid phases is poor, the converse is true;

(3) it is recommended that the effect of moderately polar gases on bubble size and gas hold-up be studied in the future.

10.3 Air-Water Systems with Various Additives

The following points are of particular significance:

(1) soluble alcohols (especially propanol) reduce the interfacial tension between the gas (air) and liquid (water) phases, thereby decreasing the bubble size and increasing the gas hold-up;

(2) as the liquid viscosity is increased from 1 to 12 cp, the gas hold-up increases; a study of the effect of liquid viscosity beyond this range, which will require a carefully designed gas distributor to maintain a constant gas flow through each orifice, is recommended in future research work;

(3) low concentrations of electrolyte increase the intermolecular forces in the bulk aqueous phase, thereby decreasing bubble rise velocity and bubble coalescence; as a result, gas hold-up increases;

(4) high concentrations of electrolyte increase the interfacial tension, resulting in increased bubble size and bubble coalescence; however, at high superficial gas velocities the slugs break-up and the bubbly flow regime develops again.

10.4 Three-Phase Systems Containing Non-Wettable Solids

The following conclusions arise from the study of three-phase systems containing non-wettable solids:

(1) the addition of small amounts of non-wettable solids to air-water systems (or air-water systems containing soluble alcohols or electrolytes) reduces the gas hold-up;

(2) the solids concentration is the main parameter in reducing the gas hold-up; however, when the solids concentration exceeds about 10% there is little further effect;

(3) gas hold-up increases as the particle size and density increases;

(4) at low solids concentrations, the concentration gradient in a radial direction is negligible, whilst at higher solids concentrations the variation is significant;

(5) compared with air-water systems, liquid phase backmixing in three-phase systems is higher, whilst that of the solid phase is less.

10.5 Three-Phase Systems Containing Wettable Solids

The key conclusions are as follows:

(1) in general, gas hold-up increases on addition of wettable solids (which have strong polar groups in their structure);

(2) solids, which have both strong polar and non-polar groups in their structure (e.g. Moviol particles), migrate to the interface between the gas and liquid phases, resulting in a reduction in the interfacial tension and foam formation;

(3) wettable solids, which have strong polar groups and relatively weak non-polar groups (e.g. Nylon) remain in the bulk liquid phase, and since they reduce bubble rise velocity and bubble coalescence, gas hold-up increases;

(4) gas hold-up increases as the particle size decreases.

10.6 Final Comment on the Basic Approach

Consideration of events at the molecular level in gas-liquid and gas-liquid-solid systems provided a sound basis for the planning of the experimental programme; we successfully used the same approach in the discussion of the experimental data. It is believed that this approach can be widely used both to integrate published work and to predict what will happen in new process systems.

APPENDIX (A)

Table 1 - Effect of Liquid-Phase Temperature on Gas Hold-up in Two Dimensional Bubble Column. $U_{sl} = 0$.

U_{sg} cm/s	20°C ε_g	28°C ε_g	35°C ε_g	70°C ε_g
2.9	.1	.095	.073	.095
4.2	.165	.13	.108	.14
6.7	.21	.175	.16	.185
8.4	.222	.2	.18	.21
10.4	.234	.22	.2	.24
13.5	.25	.243	.23	.28
16.	.275	.268	.253	.32

Table 2 - Effect of Liquid-Phase Temperature on Gas Hold-up in Three Dimensional Bubble Column. $U_{sl} = 0$ (length of the column in operation 147.2 cm)

U_{sg} cm/s	20°C ε_g	30°C ε_g	70°C ε_g
1	0.07	0.04	0.04
1.8	0.12	0.07	0.09
2.5	0.15	0.093	0.12
3.4	0.175	0.11	0.16
4.5	0.184	0.133	0.2
5.8	0.195	0.155	0.225
7	0.203	0.164	0.25
8.3	0.22	0.174	0.262
9.5	0.233	0.2	0.282
11.	0.254	0.215	0.295

Table 3 - Effect of Moderate Agitation on Gas Hold-up in Two Dimensional Column.

L_o = 134 cm

U_{sl} = 0.

No agitation		Moderate agitation
U_{sg} cm/s	ε_g	ε_g
2.9	0.093	0.1
4.2	0.143	0.165
6.7	0.19	0.21
8.4	0.21	0.222
10.5	0.225	0.234
13.5	0.24	0.255
16.5	0.255	0.275

Table 4 - Effect of Moderate Agitation on Gas Hold-up in Three Dimensional Column.

L_o = 170 cm

U_{sl} = 0.

No agitation		Moderate agitation
U_{sg} cm/s	ε_g	ε_g
1	0.07	.068
1.8	0.12	.118
2.5	0.15	.135
3.4	0.175	.156
4.5	0.184	.167
5.8	0.195	.178
7	0.204	.182

Table 5 - Gas Hold-up Data for Two Dimensional Column. Air-Water System.
L_o = 134 cm

U_{sl} = .17 cm/s		U_{sl} = .5 cm/s	U_{sl} = .8 cm/s
U_{sg} cm/s	ε_g	ε_g	ε_g
2.5	.102	.103	.104
4.2	.16	.17	.17
5.5	.19	.2	.209
7	.212	.226	.235
8.3	.222	.232	.246
10.3	.234	.244	.259
13.5	.253	.255	.245
16.5	.278	.267	.262

Table 6 - Gas Hold-up Data for the Three Dimensional Column. Air-Water System.
L_o = 173 cm

U_{sl} = 0.045		U_{sl} = .1	U_{sl} = 0.17
U_{sg} cm/s	ε_g	ε_g	ε_g
1	.07	.07	.07
1.8	.118	.127	.133
2.5	.15	.156	.165
3	.173	.178	.185
3.38	.185	.185	.195
4	.2	.198	.203
4.5	.19	.204	.205
5	.189	.2	.201
5.8	.195	.198	.195
7	.203	.208	.206
8.3	.221	.222	.217
9.5	.234	.235	.233
11	.25	.249	.247

Table 7 - Liquid Dispersion Data for Two Dimensional Column. Air-Water System

U_{sl} = 0

L_o = 134 cm

x/L = 0.83 (samples were withdrawn from side of the column)

U_{sg} = 2 cm/s

t	$C(t)/C(\infty)$	$(\frac{\pi}{L})^2 . D_l . t$	D_l
11	0.05	.5	60
12.7	.1	.55	59
14.6	.14	.6	59
16.5	.20	.65	59
18.4	.25	.75	62

Table 8

U_{sg} = 4.2 cm/s

t	$C(t)/C(\infty)$	$(\frac{\pi}{L})^2 . D_l . t$	D_l
12.5	0.28	.8	116
14	.35	.9	117
15.5	.4	1	117
17	.45	1.1	118
19	.5	1.2	115

Table 9

U_{sg} = 5.5 cm/s

t	$C(t)/C(\infty)$	$(\frac{\pi}{L})^2 . D_l . t$	D_l
11	.26	.77	127
13	.35	.9	126
14.5	.43	1.05	132
16.2	.5	1.2	135
17.8	.55	1.3	133

Table 10

U_{sg} = 7 cm/s

t	$C(t)/C(\infty)$	$(\frac{\pi}{L})^2 . D_l . t$	D_l
11	.55	1.3	215
12.7	.6	1.5	215
14.6	.7	1.7	212
16.5	.75	1.9	209
18.4	.8	2.1	207

Table 11

U_{sg} = 8.4 cm/s

t	$C(t)/C(\infty)$	$(\frac{\pi}{L})^2 . D_l . t$	D_l
2	.2	.67	609
4	.57	1.3	591
5.4	.77	1.8	606
7	.82	2.3	597
8.5	.9	2.8	599

Table 12

U_{sg} = 10.5 cm/s

t	$C(t)/C(\infty)$	$(\frac{\pi}{L})^2 . D_l . t$	D_l
1.5	.082	.52	630
2.5	.32	.86	625
3.9	.6	1.4	620
6	.78	2.05	621
8.2	.9	2.8	621

Table 13

U_{sg} = 13.5 cm/s

t	$C(t)/C(\infty)$	$(\frac{\pi}{L})^2 . D_l . t$	D_l
1.5	.1	.55	666
3	.45	1.08	654
4.5	.66	1.6	646
5.9	.8	2.1	647
7.4	.88	2.6	640

Table 14

U_{sg} = 16 cm/s

t	$C(t)/C(\infty)$	$(\frac{\pi}{L})^2 . D_l . t$	D_l
2	.22	.73	664
3.4	.55	1.3	675
4.9	.72	1.8	668
6.6	.86	2.5	680
8.1	.9	3	673

Table 15 - Liquid Dispersion Data for Three Dimensional Bubble Column

Air-water system

U_{sl} = 0

L_o = 173 cm

x/L = 0.88 (samples were taken from the side of the column)

U_{sg} = 1.8 cm/s

Time	$C(t)/C(\infty)$	$(\frac{\pi}{L})^2 . D_l . t$	D_l
28	.05	.48	50
32	.075	.55	51
36.2	.1	.6	48
39.8	.11	.65	48
44.2	.2	.75	49
46.6	.24	.8	50

Table 16

U_{sg} = 2.5 cm/s

Time	$C(t)/C(\infty)$	$(\frac{\pi}{L})^2 . D_l . t$	D_l
28.8	.1	.6	61
32.5	.11	.65	59
34.7	.15	.7	59
37.5	.21	.77	60
42	.24	.8	56

Table 17

U_{sg} = 3.5 cm/s

Time	$C(t)/C(\infty)$	$(\frac{\pi}{L})^2 . D_l . t$	D_l
26	.29	.9	102
29	.35	1	101
31.7	.37	1.05	97
35.2	.46	1.2	100
38	.5	1.3	100

Table 18

U_{sg} = 4.7 cm/s

Time	$C(t)/C(\infty)$	$(\frac{\pi}{L})^2 . D_l . t$	D_l
10.3	0.11	0.65	186
12	0.2	0.75	183
14	0.29	0.9	189
16.3	0.35	1	180
18.1	0.42	1.15	187
20.2	0.46	1.2	175

Table 19

U_{sg} = 5.8 cm/s

Time	$C(t)/C(\infty)$	$(\frac{\pi}{L})^2 . D_l . t$	D_l
10.5	0.35	1	280
12.6	0.46	1.2	280
15	0.56	1.4	274
17.2	0.65	1.6	273
19.8	0.75	1.9	282

Table 20

U_{sg} = 7 cm/s

Time	$C(t)/C(\infty)$	$(\frac{\pi}{L})^2 . D_1 . t$	D_1
10	0.35	1	294
12.1	0.46	1.2	292
14	0.6	1.5	315
15.9	0.67	1.65	305
19.1	0.77	1.95	300

Table 21

U_{sg} = 9.5 cm/s

Time	$C(t)/C(\infty)$	$(\frac{\pi}{L})^2 . D_1 . t$	D_1
7.5	0.22	0.8	314
9.4	0.35	1	312
12	0.46	1.2	294
13.8	0.56	1.4	298
16.1	0.7	1.7	310

Table 22

U_{sg} = 11 cm/s

Time	$C(t)/C(\infty)$	$(\frac{\pi}{L})^2 . D_1 . t$	D_1
7	0.2	0.75	315
9.3	0.35	1	316
12.5	0.56	1.4	329
14.7	0.65	1.6	320
17.2	0.75	1.9	325

Table 23 - Effect of Column Height on Gas Hold-up

Air-Water System

U_{sl} = 0.045 cm/s

L_o = 110 cm		L_o = 173 cm	
U_{sg} cm/s	ε_g	U_{sg} cm/s	ε_g
1.1	.074	1	.07
1.8	.13	1.8	.118
2.56	.165	2.5	.15
3.38	.208	3	.173
4.5	.233	3.38	.186
5.8	.25	4	.201
7	.246	4.5	.123
8.3	.265	5	.19
9.5	.285	5.8	.196
11	.303	7	.204
		8.3	.221
		9.5	.234
		11	.25

Table 24 - Gas Hold-up Data for Three-Dimensional Column with Two Gas Distributors 25 cm apart.

Air-Water

L_o = 173 cm

U_{sl} = 0.17 cm/s

U_{sg} cm/s	ε_g
1	.082
1.8	.14
2.5	.17
3.4	.22
4.5	.256
5	.276
5.8	.295
7	.325
8.3	.349
9.5	.36
11	.358

Appendix (B)

Table 1 : Effect of the nature of gas phase on gas hold-up, when water is the liquid phase.

$U_{sl} = 0$

$L_o = 134$ cm (two-dimensional column)

U_{sg} cm/s	ε_g Air-water	CO_2-water	N_2-water	O_2-water	NH_3-water
2	0.07	0.1	0.75	0.07	0.09
2.9	0.1	0.130	0.1	0.1	0.132
4.2	0.163	0.196	0.157	0.154	0.195
6.7	0.210	0.240	0.215	0.21	0.253
8.4	0.22	0.253	0.23	0.222	0.28
10.5	0.235	0.270	0.242	0.236	
13.5	0.255	0.287	0.57	0.253	
16.5	0.276	0.318	0.28	0.275	

Table 2 : Effect of the nature of gas phase on gas hold-up, when kerosene is the liquid phase.

U_{sl} = 0

L_o = 134 cm (two-dimensional column)

U_{sg} cm/s	ε_g Air-water	NH_3-kerosene	Air-kerosene
1	-	0.05	0.075
2	0.07	-	-
2.8	0.1	0.14	0.31
4.2	0.163	0.21	foam
6.7	0.210	foam	
8.4	0.22		
10.4	0.235		
13.4	0.255		
16.5	0.276		

Appendix C

Table 1 - Effect of Soluble Alcohols (C_1-C_3) on Gas Hold-up.

U_{sl} = 0

L_o = 134 cm (two dimensional column)

U_{sg} cm/s	ε_g Air-water	Aq.soln.of: 0.56% methanol	0.56% ethanol	0.56% propanol
2	0.07	-	-	-
2.5	0.1	0.108	0.125	0.18
4.2	0.163	0.16	0.19	0.28
6.7	0.210	0.222	0.245	0.37
8.3	0.220	0.249	0.26	0.42
10.5	0.234	0.24	0.256	0.32
13.5	0.255	0.26	0.265	0.28
16.5	0.276	0.28	0.285	0.3

Table 2 - Effect of Soluble Alcohols (C_1-C_3) on Gas Hold-up, in Three Dimensional Column.

U_{sl} = 0

L_o = 173 cm

U_{sg} cm/s	ε_g Air-water	Aq.soln.of 0.5% ethanol	1% ethanol	.5% propanol
1	.07	.09	.1	0.1
1.8	0.12	.13	.145	0.145
2.5	0.15	.19	.2	0.205
3.4	0.175	.245	.288	0.3
4.5	.185	.35	foam	foam
5.8	.195	foam		
7	.203			
8.3	.22			
9.5	.233			
11	.254			

Table 3 - Effect of Long Chain Alcohols on Gas Hold-up.

U_{sl} = 0

L_o = 134 cm (two dimensional column)

U_{sg} cm/s	ε_g Air-water	Aq.soln.of 1.1% butanol	1.1% hexanol	1.1% octanol
2	0.07	-	-	-
2.5	0.1	.07	.65	.067
4.2	.164	.11	.9	.85
6.7	.21	.153	.137	.133
8.3	.22	.17	.162	.156
10.5	.23	.192	.185	.181
13.5	.255	.225	.218	.212
16.5	.276	.25	.245	.24

Table 4 - Effect of n-Butyl and n-Octyl Alcohols on Gas Hold-up, in Three Dimensional Column.

$U_{sl} = 0$

$L_o = 173$ cm

U_{sg} cm/s	ε_g Air-water	Aq. soln. of 8% butanol	.5% octanol
1	0.07	.054	.048
1.8	0.12	0.85	.075
2.5	0.152	.104	.105
3.4	0.175	.128	.125
4.5	.185	.155	.147
5.8	.195	.170	.165
7	0.205	.185	.178
8.3	0.219	.20	.194
9.5	0.232	.215	.205
11	0.253	.232	.219

Table 5 - Effect of Ethylene Glycol and Polyethylene Glycol ($HO(CH_2CH_2O)_4H$) on Gas Hold-up

$U_{sl} = 0$

$L_o = 134$ cm (two dimensional column)

U_{sg} cm/s	ε_g Air-water	Aq. soln. of 0.56% glycol	0.56% Polyethylene Glycol
2	0.07	.1	-
2.5	0.1	.14	.142
4.2	0.163	.21	.223
6.7	0.210	.34	foam
8.4	0.220	.4	foam
10.5	0.235	.36	
13.5	0.255	.32	
16.5	0.276	.34	

Table 6 - Effect of Liquid Glycerol (i.e. liquid viscosity) on Gas Hold-up.

$U_{sl} = 0$

L_o = 134 cm (two dimensional column)

ε_g

U_{sg} cm/s	Air-water	Aq.soln.of 18% glycerol (μ=1.6CP)	25% glycerol (μ=2.4CP)	38% glycerol (μ=5CP)	65% glycerol (μ=12CP)
2	.07	-	-	.12	.13
2.5	.1	.133	.165	.28	.34
4.2	.163	.195	.227	foam	foam
6.7	.21	.28	.312	foam	foam
8.4	.22	.31	.345	foam	foam
10.5	.236	.33	.37		
13.5	.255	.34	.389		
16.5	.276	.35	.4		

Table 7 - Effect of Electrolyte Solutions on Gas Hold-up.

$U_{sl} = 0$

$L_o = 134$ cm (two dimensional bubble column)

U_{sg} cm/s	ε_g Air-water	Aq.soln.of 2.5×10^{-4} g/cm^3 KCl	2.5×10^{-4} g/cm^3 NaCl	2.5×10^{-4} g/cm^3 KI
2	0.07	-	-	-
2.5	0.1	.128	.117	.108
4.2	.16	.198	.185	.168
6.7	.21	.299	.283	.259
8.3	.222	.337	.315	.295
10.5	.236	.29	.28	.27
13.5	.258	.275	.265	.262
16.5	.276	.298	.29	.28

Table 8 - Effect of Electrolyte Solutions on Gas Hold-up

$U_{sl} = 0$

$L_o = 134$ cm (two-dimensional column)

U_{sg} cm/s	ε_g Air-water	Aq.soln.of .01 g/cm^3 KCl	.01 g/cm^3 NaCl	.01 g/cm^3 KI
2	.07	-	-	-
2.5	.1	.136	.13	.112
4.2	.162	.212	.2	.185
6.7	.21	.33	.32	.29
8.3	.222	.377	.36	.335
10.5	.237	.355	.335	.296
13.5	.256	.307	.29	.27
16.5	.276	.32	.31	.292

Table 9 - Effect of Potassium Chloride Solutions on Gas Hold-up in Three Dimensional Column.

U_{sl} = 0

L_o = 173

U_{sg} cm/s	ε_g Air-water	0.5×10^{-2} g/cm^3 KCl	0.01 g/cm^3 KCl
1	0.07	0.73	0.7
1.8	0.12	.116	.116
2.5	0.152	.165	.167
3.4	0.175	.214	.22
4.5	0.185	.249	.26
5.8	0.195	.265	.28
7	0.205	.25	.263
8.3	0.219	.255	.267
9.5	0.232	.265	.28
11	0.253	.288	.30

Table 10 - Some Physical Properties of Alcohols (C_1 - C_8)

Alcohols	Dipole moments D	Boiling points C^o	Surface tension dyne/cm	Density g/cm^3
CH_3OH	1.7	64.5	22.61	0.791
CH_3CH_2OH	1.69	78.3	22.75	0.789
$CH_3CH_2CH_2OH$	1.68	97	23.78	0.803
$CH_3(CH_2)_2CH_2OH$	1.66	118	24.6	0.809
$CH_3(CH_2)_4CH_2OH$	-	156.5	-	0.813
$CH_3(CH_2)_6CH_2OH$	-	195	32.5	0.827

Table 11 - Effect of Highly Concentrated Potassium Chloride Solutions on Gas Hold-up in Two Dimensional Column.

U_{sl} = 0

L_o = 134 cm

U_{sg} cm/s	ε_g Air-water	$.25 \times 10^{-3}$ g/cm^3 KCl	.01 g/cm^3	0.05 g/cm^3
2	0.07	-	-	-
2.5	.1	.13	.083	0.07
4.2	.162	.195	.12	.103
6.7	.21	.3	.18	.165
8.3	.222	.337	.201	.193
10.5	.237	.29	.242	.252
13.5	.256	.28	.27	.29
16.5	.276	.3	.293	.304

Table 12 - Effect of Highly Concentration Potassium Chloride Solutions on Gas Hold-up.

$U_{sl} = 0$

$L_o = 173$ (three dimensional column)

U_{sg} cm/s	ε_g Air-water	.01 g/cm^3 KCl	.05 g/cm^3 KCl	.1 g/cm^3 KCl
1	0.07	0.077	0.055	0.04
1.8	0.12	0.116	0.085	0.068
2.5	0.152	0.169	0.125	0.108
3.4	0.175	.22	0.16	0.14
4.5	0.185	.26	0.205	0.175
5.8	0.195	.28	0.25	0.21
7	0.205	.261	0.28	0.27
8.3	0.219	.265	0.308	0.4
9.5	0.232	.28	0.33	foam
11	0.253	.3	0.35	foam

Appendix D

D.1 General Properties of Solid Surfaces

The essential difference between liquids and solids is that liquids are highly mobile, whereas solids are more or less immobile and practically fixed in position. The immobility of the surface of a solid results in the atoms in a solid surface staying where they are placed when the surface is formed, and this may result in no adjacent atoms or molecules having quite the same properties.

D.2 The Contact Angle

When a liquid drop is placed on a clean solid surface, the liquid drop may either spread out as shown in Figure (D.1), forming a thin film of the dispersed phase liquid on the solid surfaces or remain "bunched up" in the form of a segment of a circle, as shown in Figure (D.2). The surface tensions of the solid and liquid and interfacial tension between them determine whether or not the liquid spreads on the solid. Liquids frequently rest on solids at a finite angle, θ; the surface tension and the contact angle may be derived from Figure (D.3) to give the relationship known as the Young Equation (25):

Figure D.1 Behaviour of a liquid drop at a wetted solid surface placed in air.

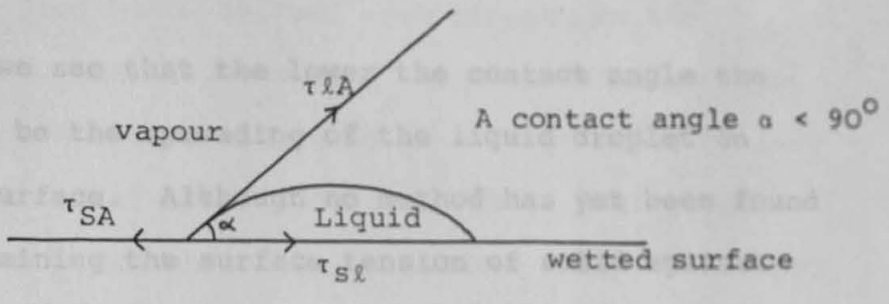

Figure D.2 Behaviour of a liquid drop at a non-wetted solid surface placed in air.

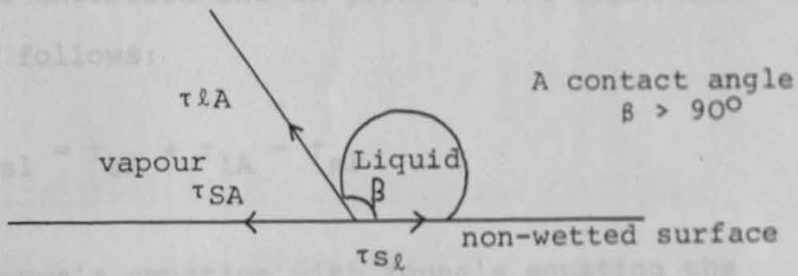

Figure D.3

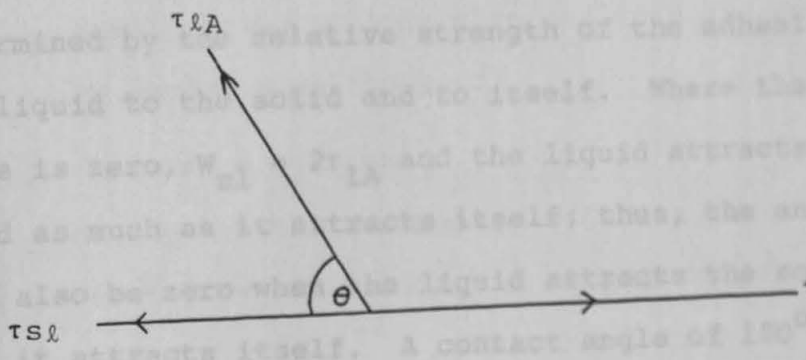

$$\tau_{sl} + \tau_{lA} \cos \theta = \tau_{sA}$$

or

$$\cos \theta = \frac{-\tau_{sl} + \tau_{sA}}{\tau_{lA}}$$

Therefore, we see that the lower the contact angle the better will be the spreading of the liquid droplet on the solid surface. Although no method has yet been found for determining the surface tension of solid against air or other liquids, the work of adhesion (W_{sl}) of a solid to a liquid can be measured easily. This is the energy required to separate one square centimetre of the solid-liquid interface and is given by the Dupre (26) equation as follows:

$$W_{sl} = \tau_{sA} + \tau_{lA} - \tau_{sl}$$

Combining Dupre's equation with Young's equation the unknown surface tension can be eliminated; therefore,

$$W_{sl} = \tau_{lA} (1 + \cos\theta)$$

The above equation shows that the contact angle is determined by the relative strength of the adhesion of the liquid to the solid and to itself. Where the contact angle is zero, $W_{sl} = 2\tau_{lA}$ and the liquid attracts the solid as much as it attracts itself; thus, the angle will also be zero when the liquid attracts the solid more than it attracts itself. A contact angle of 180^{o} would indicate no adhesion between the liquid and solid: as

there is always some adhesion, angles of 180° are not observed. The terms "wetting" and "non-wetting" of a solid by a liquid, as employed in various practical situations, tend to be defined with respect to the contact angle. Usually "wetting" means that the contact angle between a liquid and solid is zero or close to zero and that the liquid spreads over the solid easily; non-wetting" means that the angle is greater than 90° so that the liquid tends to become globular and run off the surface easily. Based on the above definition we can divide three-phase systems into two distinct types of system - those containing non-wettable solids and those containing wettable solids.

D.3 Non-wettable Solids Properties - Styrocel

Supplier : Shell Chemicals

Large particles : Styrocel Grade R351X

Small particles : Styrocel Grade R551X

D.3.1 Large particles, were relatively uniform in size. Result from particle size analysis and density, by random sampling gave:

-12 mesh + 14 mesh

Average particle diameter : 1204 μ

Density by random sampling : 1.36 g/cm^3

D.3.2 Small particles - particle size distribution was:

10% mesh No.16.

50% mesh No.18.

40% mesh No.22

Average particle size : 813 μ

Density of random sampling = 1.2 g/cm^3

D.3.3 These particles were obtained after heating small particles (D.3.2) for five hours at 100°C; they are reported thus:

Average particle size : 10 83 μ

Density of random sampling : 0.85 g/cm^3

D.3.4 These particles were obtained after heating small particles (D.3.2) for 15 hours at 100°C; they are reported as follows:

Average particle diameter : 1625 μ

Density : 0.45 g/cm^3.

D.3.5 Fractional Voidage

The method used to estimate voidage consisted of:

(i) measuring the height of a bed of dry solids in a cylinder;

(ii) filling the spaces with a known volume of water and allowing excess water to be collected and its volume measured;

(iii) calculating the fractional voidage, as follows:

$$= \frac{V_w - V_{of}}{V_s}$$

where V_w : volume of water (cm^3)

V_{of} : volume of overflowing water (cm^3)

V_s : volume occupied by packed bed of solids (cm^3)

The fractional voidage (ε) was approximately 0.5.

D.4 Ballotini Particles

These were relatively uniform in size, and the results from particle size analysis and density by random sampling, were as follows:

(1) Large particles:

$d = 6000\ \mu$

$\rho = 2.7\ g/cm^3$

(2) Medium particles:

$d = 3000\ \mu$

$\rho = 2.4\ g/cm^3$

(3) Small particles:

$d = 140\text{-}125\ \mu$

$\rho = 1.71\ g/cm^3$

D.5 Wettable Particles

D.5.1 Diakon Particles : supplier - I.C.I.

$d = 200\ \mu$

$\rho = 0.81\ g/cm^3$

D.5.2 Nylon Particles : Supplier - I.C.I.

$d_{av} = 2100\ \mu$

$\rho = 2.24\ g/cm^3$

D.5.3 Moviol Particles : Supplier - Harlow Chemical Co.

(1) Powder with $\rho = 0.8\ g/cm^3$

(2) Particles obtained by chopping up plastic sheet of thickness 0.4 mm : Particle dimensions about 2 x 2 mm.

Appendix E

Table 1 - Effect of Solid Phase (Styrocel with $d = 810\mu$ and $\rho = 1.2\ g/cm^3$) on Gas Hold-up in Two Dimensional Bubble Column

$U_{sl} = .17$ cm/s

U_{sg} cm/s	ε_g 1% solid	4% solid	8% solid	12% solid
2.9	.066	.059	.055	0.054
4.2	.089	.081	.08	0.08
5.5	.11	.1	.102	0.101
6.7	.136	.115	.114	0.114
8.4	.158	.14	.14	0.138
10.5	.18	.163	.163	.162
13.5	.207	.2	.2	0.2
16.5	.240	.23	.232	.231

Table 2 - Effect of Solid Phase (Styrocel with $d = 1204\ \mu$ and $\rho = 1.36\ g/cm^3$) on Gas Hold-up in Two Dimensional Bubble Column. $U_{sl} = .17$ cm/s

U_{sg} cm/s	ε_g 1% solid	4% solid	8% solid	12% solid
2.9	.07	0.059	0.059	0.06
4.2	.095	0.083	0.083	0.082
5.5	.118	.105	0.105	0.104
6.7	.145	.125	0.12	0.119
8.4	.165	.148	0.145	0.146
10.5	.185	.174	0.172	0.172
13.5	.214	.205	0.204	0.203
16.5	.245	.235	0.235	0.235

Table 3 - Effect of Solid Phase (Styrocel with $d = 1083\ \mu$ and $\rho = 0.85\ g/cm^3$) on Gas Hold-up in Two Dimensional Bubble Column. $U_{sl} = 0.17$ cm/s

U_{sg} cm/s	ε_g 1% solid	4% solid	8% solid
2.9	0.07	0.06	0.059
4.2	0.093	0.085	0.083
5.5	.122	.112	0.11
6.7	0.145	.128	0.127
8.4	.169	.156	0.157
10.5	.19	.18	0.18
13.5	.22	0.215	0.214
16.5	.249	0.247	0.245

Table 4 - Effect of Solid Phase (Styrocel with $d = 1625\ \mu$ and $\rho = .45\ g/cm^3$) on Gas Hold-up.

$U_{sl} = 0.17$ cm/s

U_{sg} cm/s	ε_g	
	2% solid	10% solid
2.9	0.085	0.08
4.2	0.129	0.111
5.5	0.15	.136
6.7	.179	.16
8.4	.198	.183
10.5	0.213	0.207
13.5	.239	.232
16.5	.263	.259

Table 5 - Effect of Solid Phase (Styrocel with $d = 813\ \mu$ and $\rho = 1.2\ g/cm^3$) on Gas Hold-up in Three Dimensional Bubble Column.

$U_{sl} = 0.045$ cm/s

$L_o = 173$ cm

U_{sg}	ε_g			
cm/s	2% solid	4% solid	10% solid	15% solid
1.08	0.045	.036	.036	.035
1.83	0.065	.061	.056	.056
2.56	0.085	.075	.073	.072
3.38	.105	.096	.091	.09
4.46	.118	.11	.103	.103
5.85	.137	.124	.121	.12
7	.15	.14	.133	.132
8.23	.163	.153	.148	.149
9.5	.178	.167	.16	.16
10.9	.194	.181	.176	.175

Table 6 - Effect of Solid Phase (Styrocel with $d = 1204\ \mu$ and $\rho = 1.36\ g/cm^3$) on Gas Hold-up in Three Dimensional Bubble Column.

$U_{sl} = 0.045$ cm/s

$L_o = 173$ cm

U_{sg}	ε_g			
cm/s	2% solid	4% solid	10% solid	15% solid
1.08	.05	.045	.042	.042
1.83	.072	.068	.063	.063
2.56	.092	.088	.084	.084
3.4	.114	.103	.101	.102
4.5	.125	.117	.115	.114
5.85	.14	.130	.127	.123
7	.155	.145	.141	.14
8.23	.17	.16	.157	.155
9.5	.185	.173	.168	.167
10.9	.195	.185	.183	.183

Table 7 - Variation of Solids (Styrocel, d = 810 μ and ρ = 1.2 g/cm^3) over the Length of the Column, in Two Dimensional Bubble Column.

U_{sl} = 0.3 cm/s

C_o = 0.025 (v/v)

U_{sg} cm/s	bed height cm	solids concentration (v/v) 23	50	75	95	123
2.9		.024	.026	0.028	0.03	0.033
4.2		0.022	0.024	.025	0.027	.029
6.8		0.02	0.022	0.023	0.025	0.026
16.5		0.19	0.02	0.021	0.022	0.023

Table 8 - Variation of Solids (Styrocel d = 813 μ and ρ = 1.2 g/cm^3) over the Length of the Column, in Two Dimensional Bubble Column

U_{sl} = 0.3 cm/s

C_o = 0.05 (v/v)

U_{sg}	bed height	Solids Concentration (v/v)				
cm/s	cm	23	50	75	95	123
2.9		0.0378	0.042	0.047	0.054	0.058
8.5		.035	0.038	0.043	0.047	0.054
13.5		.033	0.036	0.04	0.043	0.045
16.5		0.028	0.032	0.035	0.04	0.038

Table 9 - Variation of Solids (Styrocel d = 810 μ and $\rho = 1.2\ g/cm^3$) over the Length of the Column in Two Dimensional Bubble Column.

$U_{sl} = 0.3$ cm/s

$C_o = .1$ (v/v)

U_{sg} cm/s	bed height cm	Solids concentration (v/v) 23	5o	75	95	123
2.9		0.076	0.082	0.087	0.095	.1
4.2		.068	.077	.088	0.098	.106
10.5		.068	0.073	0.081	0.086	0.091
16.5		0.06	0.068	0.073	0.08	0.078

Table 10 - Effect of Ballotini Spheres (d=140-125 μ) on Gas Hold-up in Two Dimensional Bubble Column.

U_{sl} = .17 cm/s

U_{sg} cm/s	ε_g	
	2% solid	7% solid
2.9	0.085	0.08
4.2	.135	0.123
5.5	0.16	0.145
6.7	0.185	0.175
8.4	0.20	0.191
10.5	0.215	0.205
13.4	0.235	0.225
16.5	0.265	0.256

Table 11 - Effect of Ballotini Spheres (d=3000 μ and ρ = 2.4 g/cm^3) on Gas Hold-up in Two Dimensional Bubble Column

U_{sl} = 0.17 cm/s

U_{sg} cm/s	ε_g		
	2% solid	8% solid	10% solid
2.9	0.095	.09	0.09
4.2	0.155	0.151	0.15
5.5	0.18	0.175	0.173
6.7	0.2	0.195	0.193
8.4	0.212	0.208	0.206
10.5	0.225	0.219	0.215
13.4	0.24	0.235	0.233
16.5	0.268	0.264	0.262

Table 12 - Effect of Ballotini Spheres (d=6000 μ and $\rho = 2.7 g/cm^3$) on Gas Hold-up in Two Dimensional Bubble Column.

$U_{sg} = 0.17$ cm/s

U_{sg} cm/s	ε_g		
	2% solid	8% solid	10% solid
2.9	0.095	0.09	0.09
4.2	0.158	0.158	0.16
5.5	0.185	0.185	0.184
6.7	0.2	0.196	0.190
8.4	0.216	0.213	0.212
10.5	0.23	0.224	0.224
13.4	0.242	0.24	0.24
16.5	0.27	0.265	0.262

Table 13 - Effect of Nylon Particles (with $d_{av} = 2100\mu$ and $\rho = 2.24$ g/cm^3) on Gas Hold-up in Two Dimensional Bubble Column.
$U_{sg} = .17$ cm/s

U_{sg} cm/s	ε_g		
	1% solid	2% solid	4% solid
2.5	0.126	.126	0.126
4.2	0.197	.197	0.197
6.7	0.289	.29	0.29
8.4	.325	.326	0.326
10.5	.319	.318	0.318
13.5	.3	.303	0.303
16.5	.31	0.312	0.31

Table 14 - Effect of Nylon Particles (with d_{av} = 2100 μ and ρ = 2.24 g/cm^3) Moviol Particles (powder-like) and Diakon Particles (with d=200 μ and ρ = 0.81 g/cm^3) on Gas Hold-up in Three Dimensional Bubble Column

U_{sl} = 0.045 cm/s

L_o = 173 cm

U_{sg} cm/s	ε_g 5% Nylon	4% Moviol	4% Diakon
1.08	0.075	0.08	0.073
1.85	.125	-	0.133
2.56	.165	.18	0.16
3.38	.21	.26	.2
4.5	.258	foam	foam
5.85	.25	foam	foam
7	.251	foam	foam
8.23	.254	foam	foam
9.5	.265	foam	foam
10.9	.285	foam	foam

Table 15 - Effect of Moviol Particles on Gas Hold-up in Two Dimensional Bubble Column.

U_{sl} = 0.17 cm/s

U_{sg} cm/s	ε_g	
	1% solid (powder-like)	3% solid (shapeless)
2.9	0.148	.12
4.2	0.245	.196
6.7	foam	.303
8.4	foam	0.32
10.5	foam	0.311
13.4	foam	.282
16.5	foam	.295

Table 16 - Effect of Diakon Particles ($d = 200\ \mu$ and $\rho = 0.81\ g/cm^3$) on Gas Hold-up in Two Dimensional Bubble Column.

$U_{sl} = 0.17$ cm/s

U_{sg} cm/s	ε_g	
	1% solid	4% solid
2.9	.122	.125
4.2	.19	.2
6.7	.274	.28
8.4	.296	.301
10.5	.28	.281
13.4	.278	.278
16.5	.293	.298

Table 17 - Variation of Solids (Nylon with d_{av} = 2100μ and ρ = 2.24 g/cm^3) over the Length of the Column in Two Dimensional Bubble Column.

U_{sl} = 0.8 cm/s

C_o = 0.025 (v/v)

U_{sg} cm/s	bed height cm	Solids concentration (v/v) 23 cm	70 cm	98cm	126 cm
2.9		0.028	0.015	0.01	0.004
4.2		0.025	0.018	0.012	0.008
6.7		0.022	0.018	0.014	0.012
10.5		0.012	0.019	0.021	0.022
16.5		0.011	0.019	0.022	0.025

Table 18 - Variation of Solids (Nylon with d_{av} = 2100μ and ρ= 2.24 g/cm^3) over the Length of the Column in Two Dimensional Bubble Column

U_{sl} = 0.2 cm/s

C_o = 0.025 (v/v)

U_{sg} cm/s	bed height cm	Solids concentration (v/v) 23 cm	70 cm	98 cm	126 cm
2.9		0.035	0.018	0.014	0.008
4.2		0.033	0.02	0.015	0.01
6.7		0.03	0.023	0.019	0.013
10.5		0.025	0.025	0.027	0.027
16.5		0.02	0.025	0.03	0.031

Table 19 - Variation of Solids (Nylon with d_{av} = 2100μ and ρ = 2.24 g/cm^3) over the Length of the Column in Two Dimensional Bubble Column.

U_{sl} = .8 cm/s

C_o = 0.08 (v/v)

bed height	Solids concentration (v/v)			
U_{sg} cm/s	cm 23 cm	70 cm	98 cm	126 cm
2.9	0.075	0.046	0.036	0.023
4.2	0.071	0.047	0.04	0.026
8.3	0.055	0.049	0.052	0.048
10.5	0.05	0.52	0.06	0.068
16.5	0.045	0.055	0.068	0.075

Table 20 - Variation of Solids (Nylon with d_{av} = 2100μ and $\rho = 2.24\ g/cm^3$) over the Length of the Column in Two Dimensional Bubble Column

$U_{sl} = 0.2$ cm/s

$C_o = 0.08$ (v/v)

U_{sg} cm/s	bed height cm	Solids Concentration (v/v) 23 cm	70 cm	98 cm	126 cm
2.9		0.089	0.06	0.047	0.031
4.2		0.085	0.062	0.05	0.035
8.3		0.081	0.065	0.06	0.05
10.5		0.058	0.064	0.068	0.07
16.5		0.053	0.068	0.075	0.085

Table 21 - Variation of Solids (Diakon with d = 200 μ and $\rho = 0.81\ g/cm^3$) Concentration over the Length of the Column.

$U_{sl} = 0.2$ cm/s

$C_o = 0.05$ (v/v)

U_{sg} cm/s	bed height cm	Solids Concentration (v/v) 23 cm	70 cm	98 cm	126 cm
2.9		0.045	0.04	0.037	0.033
4.2		0.041	0.04	0.039	0.038
8.4		0.055	0.053	0.05	0.049
10.5		0.06	0.06	0.06	0.06
16.5		0.07	0.065	0.067	0.067

Appendix F

Table 1 - Variation of Solids Concentration in Radial Direction at the Bottom, Middle and Top Sections of the Three Dimensional Bubble Column.

L_o = 173 cm

C_o = 0.01 (v/v)

U_{sl} = 0

(a) at the bottom:

U_{sg} cm/s	r(cm)	Solids concentration (v/v)							
		0	1.1	2.1	3.1	4.1	5.1	6.1	7.1
1		0.011	0.011	0.011	0.011	0.011	0.011	0.011	0.011
6		0.0105	0.0106	0.0108	0.0109	0.011	0.0112	0.0113	0.0115

(b) at the middle of the column:

U_{sg} cm/s	r(cm)	Solids concentration (v/v)							
		0	1.1	2.1	3.1	4.1	5.1	6.1	7.1
1		0.01	0.01	0.01	0.01	0.01	0.01	0.01	0.01
6		0.01	0.01	0.01	0.01	0.01	0.01	0.01	0.01

(c) at the top of the column:

U_{sg} cm/s	r(cm)	Solids concentration (v/v)							
		0	1.1	2.1	3.1	4.1	5.1	6.1	7.1
1		.01	0.01	0.01	0.01	0.01	0.01	0.01	0.01
6		.0085	0.085	0.0086	0.0088	0.0089	0.0088	.009	0.092

Table 2 - Variation of Solids Concentration in Radial Direction at the Bottom, Middle and Top Sections of the Three Dimensional Bubble Column.

L_o = 173

C_o = 0.1 (v/v)

U_{sl} = 0

(a) Bottom of the column:

U_{sg} cm/s	r(cm)	Solids concentration (v/v)							
		0	1.1	2.1	3.1	4.1	5.1	6.1	7.1
1		.097	.1	.102	.104	.107	.108	.109	.11
6		.1	.103	.105	.167	.111	.113	.115	.117

(b) Middle of the column:

U_{sg} cm/s	r(cm)	Solids concentration (v/v)							
		0	1.1	2.1	3.1	4.1	5.1	6.1	7.1
1		.093	.095	.096	.097	.098	.098	.1	.102
6		.08	.083	.085	.09	.093	.095	.097	.1

(c) Top of the column:

U_{sg} cm/s	r(cm)	Solids concentration (v/v)							
		0	1.1	2.1	3.1	4.1	5.1	6.1	7.1
1		.087	.087	.088	.09	.092	.094	.097	.102
6		.075	.076	.077	.079	.081	.084	.087	.09

Table 3 - Variation of Solids Concentration in Radial Direction at the Bottom, Middle and Top Section of the Three Dimensional Bubble Column

L_o = 173

C_o = 0.2 (v/v)

U_{sl} = 0

(a) Bottom section of the column:

U_{sg} cm/s	r(cm)	Solids concentration (v/v)							
		0	1.1	2.1	3.1	4.1	5.1	6.1	7.1
1		0.2	0.205	0.21	0.22	0.23	0.24	0.246	0.27
6		0.2	0.205	0.212	0.225	0.23	0.245	0.255	0.273

(b) Middle section of the column:

U_{sg} cm/s	r(cm)	Solids concentration (v/v)							
		0	1.1	2.1	3.1	4.1	5.1	6.1	7.1
1		0.178	0.176	0.18	0.185	0.187	0.19	0.195	0.2
6		0.179	0.18	0.19	0.195	0.205	0.213	0.22	0.23

(c) Top section of the column:

U_{sg} cm/s	r(cm)	Solids concentration (v/v)							
		0	1.1	2.1	3.1	4.1	5.1	6.1	7.1
1		0.138	0.14	0.145	0.146	0.15	0.155	0.16	.165
6		0.145	0.145	0.15	0.16	0.17	0.18	0.195	0.21

Table 4 - Liquid Phase Dispersion Coefficients in Three Dimensional Bubble Column Containing 2.5% Solids at Different Gas Velocities.

U_{sl} = 0

L_o = 173 cm

U_{sg} = 2 cm/s

t(s)	$C(t)/C(\infty)$	$(\frac{\pi}{L})^2 . D_l . t$	D_l (cm^2/s)
23	0.07	0.55	70
25	0.1	0.6	70.5
27.5	0.15	0.65	75
30	0.17	0.7	68
32	0.2	0.76	70
36	0.28	0.9	74

Table 5 - U_{sg} = 3.5 cm/s

t(s)	$C(t)/C(\infty)$	$(\frac{\pi}{L})^2 . D_l . t$	D_l cm^2/s
14.5	0.16	0.7	142
17	0.22	0.8	138
18.5	0.3	0.9	143
20.5	0.35	1	143
23	0.4	1.1	141
26	0.45	1.2	136

Table 6 - U_{sg} = 4.5 cm/s

t(s)	$C(t)/C(\infty)$	$(\frac{\pi}{L})^2 . D_l . t$	D_l (cm^2/s)
12	0.3	0.9	221
14	0.4	1.1	223
17	0.5	1.3	225
19	0.56	1.4	217
22	0.67	1.65	221

Table 7 - U_{sg} = 6 cm/s

t(s)	$C(t)/C(\infty)$	$(\frac{\pi}{L})^2 . D_l . t$	D_l (cm^2/s)
8	0.25	0.85	312
10	0.4	1.1	323.5
12.5	0.56	1.4	330
15	0.65	1.6	314
18	0.78	2	327

Table 8 - U_{sg} = 8 cm/s

t(s)	$C(t)/C(\infty)$	$(\frac{\pi}{L})^2 . D_l . t$	D_l (cm^2/s)
7	0.25	0.85	357
8.5	0.37	1.05	363
10.5	0.5	1.3	364
12.5	0.6	1.5	353
16	0.78	2	368

Table 9 - U_{sg} = 9.5 cm/s

t(s)	$C(t)/C(\infty)$	$(\frac{\pi}{L})^2 . D_l . t$	D_l (cm^2/s)
6	0.2	0.75	367
8.5	0.37	1.05	363
11	0.56	1.4	374
13	0.65	1.6	362
16.5	0.8	2.1	347

Table 10 - U_{sg} = 12 cm/s

t(s)	$C(t)/C(\infty)$	$(\frac{\pi}{L})^2 . D_l . t$	D_l (cm^2/s)
6	0.22	0.8	392
8	0.37	1.05	386
10.3	0.56	1.4	400
12.5	0.7	1.7	400
18	0.85	2.4	392

Table 11 - Liquid Phase Dispersion Coefficients in Three-Dimensional Bubble Column Containing 8% solids at Different Gas Velocities.

$U_{sl} = 0$

$L_o = 173$ cm

$U_{sg} = 2.0$ cm/s

t(s)	$C(t)/C(\infty)$	$(\frac{\pi}{L})^2 . D_l . t$	D_l (cm^2/s)
20	0.2	0.75	110
23	0.25	0.85	108
26.5	0.35	1	111
29	0.4	1.1	112
31.5	0.45	1.2	114
34	0.5	1.3	112

Table 12 - $U_{sg} = 3.5$ cm/s

t(s)	$C(t)/C(\infty)$	$(\frac{\pi}{L})^2 . D_l . t$	D_l (cm^2/s)
8	0.2	0.75	276
10	0.32	0.95	279
11.5	0.4	1.1	281
13.5	0.5	1.3	284
16.5	0.65	1.6	285
19.5	0.73	1.8	271

Table 13 - U_{sg} = 4.7 cm/s

t(s)	C(t)/C(∞)	$(\frac{\pi}{L})^2 . D_l . t$	D_l (cm^2/s)
7	0.25	0.85	357
9.5	0.4	1.1	340
12	0.56	1.4	343
15	0.73	1.8	353
17.5	0.8	2.1	353
20	0.85	2.4	353

Table 14 - U_{sg} = 6 cm/s

t(s)	C(t)/C(∞)	$(\frac{\pi}{L})^2 . D_l . t$	D_l (cm^2/s)
6.5	0.25	0.85	385
9.5	0.5	1.3	402
11.5	0.6	1.5	384
14	0.73	1.8	378
17	0.84	2.3	398

Table 15 - U_{sg} = 8 cm/s

t(s)	C(t)/C(∞)	$(\frac{\pi}{L})^2 . D_l . t$	D_l (cm^2/s)
6	0.25	0.85	417
8.5	0.43	1.2	415
10.7	0.6	1.5	412
13	0.73	1.8	407
15.6	0.82	2.2	415

Table 16 - U_{sg} = 9.5 cm/s

t(s)	C(t)/C(∞)	$(\frac{\pi}{L})^2 . D_l . t$	D_l (cm^2/s)
5.5	0.25	0.85	456
7	0.37	1.05	441
9	0.5	1.3	425
10.5	0.65	1.6	448
12	0.73	1.8	441

Table 17 - U_{sg} = 12 cm/s

t(s)	C(t)/C(∞)	$(\frac{\pi}{L})^2 . D_l . t$	D_l (cm^2/s)
6	0.3	0.9	441
8	0.5	1.3	480
10	0.65	1.6	470
11.7	0.73	1.8	453
13.5	0.8	2.1	458

Table 18 - Liquid Phase Dispersion Coefficients in Three Dimensional Bubble Column Containing 15% Solids at Different Gas Velocities.

U_{sl} = 0

L_o = 173 cm

U_{sg} = 2 cm/s

t(s)	$C(t)/C(\infty)$	$(\frac{\pi}{L})^2 . D_l . t$	D_l (cm^2/s)
8	0.07	0.55	202
10	0.16	0.70	206
12.5	0.3	0.90	212
15	0.4	1.08	212
18	0.5	1.3	212

Table 19 - U_{sg} = 3.5 cm/s

t(s)	$C(t)/C(\infty)$	$(\frac{\pi}{L})^2 . D_l . t$	D_l (cm^2/s)
7	0.2	0.75	315
9.5	0.37	1.05	325
12	0.5	1.3	318
14.5	0.6	1.5	305
16	0.78	2	326

Table 20 - U_{sg} = 4.7 cm/s

t(s)	$C(t)/C(\infty)$	$(\frac{\pi}{L})^2 . D_l . t$	D_l (cm^2/s)
7	0.3	0.9	378
9	0.45	1.2	392
11.5	0.6	1.5	384
14	0.73	1.8	378
17	0.84	2.3	398

Table 21 - U_{sg} = 6 cm/s

t(s)	$C(t)/C(\infty)$	$(\frac{\pi}{L})^2 . D_l . t$	D_l (cm^2/s)
7.5	0.4	1.08	424
10	0.56	1.4	412
12	0.7	1.7	417
15	0.8	2.1	412
17.5	0.88	2.5	420

Table 22 - U_{sg} = 8 cm/s

t(s)	$C(t)/C(\infty)$	$(\frac{\pi}{L})^2 . D_l . t$	D_l (cm^2/s)
6.5	0.35	1	452
8	0.45	1.2	441
10	0.6	1.5	441
13	0.78	2	452
16	0.85	2.4	441

Table 23 - U_{sg} = 9.5 cm/s

t(s)	C(t)/C(∞)	$(\frac{\pi}{L})^2 . D_l . t$	D_l (cm^2/s)
6	0.3	0.92	451
8	0.45	1.2	441
9.5	0.6	1.5	464
11.7	0.73	1.8	452
14	0.8	2.1	441

Table 24 - U_{sg} = 12 cm/s

t(s)	C(t)/C(∞)	$(\frac{\pi}{L})^2 . D_l . t$	D_l (cm^2/s)
7	0.4	1.1	462
9.5	0.6	1.5	464
11.2	0.73	1.8	473
13	0.79	2.05	464
15	0.85	2.4	471

Table 25 - Solid Phase Dispersion Coefficients in Three Dimensional Bubble Column Containing 2.5% Solids at Different Gas Velocities

U_{sl} = 0

L_o = 173 cm

U_{sg} = 2 cm/s

t(s)	$C(t)/C(\infty)$	$(\frac{\pi}{L})^2 . D_s . t$	$D_s (cm^2/s)$
50	0.05	0.5	29.5
58	0.1	0.6	30.5
67.5	0.16	0.7	30.5
77.5	0.22	0.8	30
89	0.3	0.9	29

Table 26 - U_{sg} = 3.5 cm/s

t(s)	$C(t)/C(\infty)$	$(\frac{\pi}{L})^2 . D_s . t$	$D_s (cm^2/s)$
30	0.1	0.6	59
38.4	0.22	0.8	61
47.4	0.35	1	62
58.5	0.45	1.2	60
70	0.6	1.5	63

Table 27 - U_{sg} = 5 cm/s

t(s)	C(t)/C(∞)	$(\frac{\pi}{L})^2 . D_s . t$	$D_s (cm^2/s)$
20	0.32	0.95	140
27	0.5	1.3	142
38.5	0.73	1.8	137
47	0.82	2.2	137
57.3	0.89	2.7	138

Table 28 - U_{sg} = 6 cm/s

t(s)	C(t)/C(∞)	$(\frac{\pi}{L})^2 . D_s . t$	$D_s (cm^2/s)$
12	0.22	0.8	196
18.7	0.5	1.3	205
26	0.73	1.8	204
33.6	0.84	2.3	201
40	0.89	2.7	198

Table 29 - U_{sg} = 8 cm/s

t(s)	C(t)/C(∞)	$(\frac{\pi}{L})^2 . D_s . t$	$D_s (cm^2/s)$
9	0.16	0.7	229
15.4	0.45	1.2	229
22	0.7	1.7	227
29.6	0.84	2.3	228
36	0.9	2.8	229

Table 30 - U_{sg} = 9.5 cm/s

t(s)	$C(t)/C(\infty)$	$(\frac{\pi}{L})^2 . D_s . t$	$D_s (cm^2/s)$
8.5	0.16	0.7	242
15	0.45	1.2	235
21.3	0.7	1.7	235
28	0.84	2.3	242
34.7	0.9	2.8	237

Table 31 - U_{sg} = 12 cm/s

t(s)	$C(t)/C(\infty)$	$(\frac{\pi}{L})^2 . D_s . t$	$D_s (cm^2/s)$
7	0.1	0.61	252
14	0.45	1.2	252
20.7	0.73	1.8	256
27.6	0.85	2.4	256
34.7	0.91	3	254

Table 32 - Solid Phase Dispersion Coefficients in Three Dimensional Bubble Column Containing 8% Solids at Different Superficial Gas Velocities.

U_{sl} = 0

L_o = 173 cm

U_{sg} = 2 cm/s

t(s)	$C(t)/C(\infty)$	$(\frac{\pi}{L})^2 . D_s . t$	$D_s (cm^2/s)$
25	0.05	0.5	59
31	0.1	0.6	57
37.6	0.22	0.8	63
44.5	0.3	0.9	59
51.8	0.37	1.05	60

Table 33 - U_{sg} = 3.5 cm/s

t(s)	$C(t)/C(\infty)$	$(\frac{\pi}{L})^2 . D_s . t$	$D_s (cm^2/s)$
17	0.2	0.75	130
23	0.35	1	128
30.5	0.56	1.4	135
37.2	0.65	1.6	126
45	0.75	1.9	124

Table 34 - U_{sg} = 5 cm/s

t(s)	C(t)/C(∞)	$(\frac{\pi}{L})^2 . D_s . t$	$D_s (cm^2/s)$
10	0.16	0.7	206
16	0.37	1.05	193
22.7	0.65	1.6	207
30	0.79	2.05	201
36	0.88	2.5	204

Table 35 - U_{sg} = 6 cm/s

t(s)	C(t)/C(∞)	$(\frac{\pi}{L})^2 . D_s . t$	$D_s (cm^2/s)$
7	0.07	0.55	231
13.5	0.4	1.1	240
20	0.65	1.6	235
26.4	0.82	2.2	245
34	0.9	2.8	242

Table 36 - U_{sg} = 8 cm/s

t(s)	C(t)/C(∞)	$(\frac{\pi}{L})^2 . D_s . t$	$D_s (cm^2/s)$
7	0.16	0.7	294
13	0.45	1.2	271
19.7	0.75	1.9	283
25.8	0.88	2.5	285
33.5	0.92	3.2	281

Table 37 - U_{sg} = 9.5 cm/s

t(s)	$C(t)/C(\infty)$	$(\frac{\pi}{L})^2 . D_s . t$	$D_s (cm^2/s)$
6	0.1	0.6	294
12.2	0.5	1.3	313
18.9	0.75	1.9	296
25	0.88	2.5	294
31.2	0.92	3.2	302

Table 38 - U_{sg} = 12 cm/s

t(s)	$C(t)/C(\infty)$	$(\frac{\pi}{L})^2 . D_s . t$	$D_s (cm^2/s)$
6	0.15	0.65	319
11.8	0.5	1.3	324
18	0.78	2	327
23.8	0.87	2.6	321
29.5	0.92	3.2	319

Appendix G

Table 1 - Effect of solid (Styrocel, d=813μ and $\rho = 1.2 g/cm^3$) on Methanol Systems in Two Dimensional Bubble Column and for $U_{sl} = 0$.

U_{sg} cm/s	ε_g .56% methanol	.56% methanol + 2% solids	.56% methanol + 4% solids
2	0.09	-	-
2.9	.108	0.07	0.063
4.2	.16	0.095	0.085
6.7	.222	0.14	0.125
8.4	.249	0.16	0.147
10.4	.24	0.183	0.167
13.4	.258	0.21	0.205
16.5	.28	0.24	0.235

Table 2 - Effect of Solid (Styrocel d=813 μ and ρ =1.2g/cm^3) on Ethanol Systems in Three Dimensional Bubble Column.

U_{sl} = 0

L_o = 173

U_{sg} cm/s	ε_g 0.5% ethanol	0.5% ethanol + 2% solids	0.5% ethanol + 4% solids
1.08	0.09	0.05	.048
1.83	0.128	0.08	.064
2.5	0.19	0.1	0.085
3.4	.245	0.124	.105
4.5	0.35	0.145	.125
5.6	foam	.16	.14
7	foam	.175	.158
8.4	foam	.195	.17
9.5	foam	.206	.182
10.9	foam	.22	.195

Table 3 - Effect of solid (Styrocel d=813μ and ρ =1.2g/cm^3) on Propanol Systems in Three Dimensional Bubble Column.

U_{sl} = 0

L = 173

U_{sg} cm/s	ε_g 0.5% Propanol	0.5% Propanol + 2% solids	0.5% Propanol + 4% solids
1.08	01	0.05	0.045
1.83	.145	0.09	0.07
2.5	0.200	0.11	0.09
3.4	0.3	.14	0.12
4.5	foam	.16	0.14
5.6	foam	0.18	0.16
7	foam	0.193	0.18
8.4	foam	0.21	0.192
9.5	foam	0.225	0.21
10.9	foam	0.24	0.23

Table 4 - Effect of solid (Styrocel d=813μ and ρ =1.2g/cm^3) on Butanol System in Three Dimensional Bubble Column.

U_{sl} = 0

L = 173 cm

U_{sg} cm/s	ε_g .8% Butanol	0.8% Butanol + 2% solids	0.8% Butanol + 4% solids
1.08	0.053	0.07	0.072
1.83	0.085	.11	0.115
2.56	0.104	.135	0.14
3.38	0.128	.16	0.17
4.46	.155	.175	0.185
5.58	.17	.188	0.193
7	.185	0.2	0.202
8.23	.20	0.215	0.217
9.5	0.215	0.23	0.233
10.9	0.23	0.245	0.247

Table 5 - Effect of solid (Styrocel d=810μ and ρ=1.2g/cm^3) on Octanol Systems in Three Dimensional Bubble Column.

U_{sl} = 0

L = 173 cm

U_{sg} cm/s	ε_g 0.5% Octanol	0.5% Octanol + 2% solids	0.5% Octanol + 4% solids
1.08	0.048	.051	.053
1.83	0.075	0.074	.08
2.56	0.105	0.111	.113
3.38	.125	.142	.14
4.46	.147	.156	.155
5.58	.165	.167	.17
7	.178	.181	.18
8.23	.194	.195	.195
9.5	.205	.207	.21
10.9	.219	.217	.221

Table 6 - Effect of solid (Styrocel d=318μ and ρ =1.2g/cm^3) on Ethylene Glycol Systems in Two Dimensional Bubble Column.

U_{sl} = 0

L = 134 cm

U_{sg} cm/s	ϵ_g 0.56% Glycol	0.56% glycol + 2% solids	0.56% glycol + 8% solids	0.56% glycol + 12% solids
2	0.1	-	-	-
2.9	0.14	.066	0.059	0.059
4.2	0.21	0.925	0.81	0.081
6.7	0.34	.135	0.12	.121
8.4	0.4	0.16	0.14	.139
10.5	0.36	.182	.168	.166
13.5	0.32	0.213	0.2	0.205
16.5	0.34	0.24	.227	.228

Table 7 - Effect of solid (Styrocel d=813μ and ρ=1.2g/cm^3) on Potassium Chloride Systems in Three Dimensional Bubble Column.

U_{sl} = 0

L = 173 cm

U_{sg} cm/s	ε_g 0.5% g/cm^3 Kcl	.5% g/cm^3 Kcl + 2% solids	.5% g/cm^3 Kcl + 4% solids
1.08	.73	0.045	0.04
1.83	.122	0.07	0.065
2.56	.162	0.085	0.08
3.4	.214	.108	.1
4.5	.249	.125	.113
5.8	.265	.145	.127
7	.25	.16	.143
8.4	.255	.178	.16
9.5	.265	.185	.172
10.9	.288	.195	.185

Appendix H

Table 1 - Effect of Glycol and Propanol Concentrations on Slug Velocity.

Conc. of Propanol %	Slug Velocity cm/s	Conc. of Glycol %	Slug Velocity cm/s
.3	32	.3	30
.5	32.5	.9	28
1.2	32.7	1.8	25.95
1.8	33.2	2.4	25
2.4	3.4	3	24.5
-	-	4	24.3

Table 2 - Effect of Potassium Chloride Concentration on Slug Velocity.

KCl concentration g/cm^3	Slug velocity cm/s
.003	29.5
.006	28
0.012	26.5
0.024	24.2
0.042	23
0.077	22.4

Table 3 - Effect of Nylon (d_{av}=2100 μ and ρ = 2.24 g/cm^3) ABS (d_{av}=2300 μ and ρ = 2.34 g/cm^3) and Styrocel (d=1204 μ and ρ = 1.36 g/cm^3) on slug velocity.

Solids Conc. (-)	Slug Velocity cm/s For Nylon particles	For ABS particles	For Styrocel particles
0.01	30	32.5	34
0.03	28	34	36
0.05	27	34.6	37.5
0.08	26	35.5	38
0.12	25	36.3	38.5

Appendix I

Table 1 - Effect of Temperature on Three-Phase System with Styrocel particles (i.e. d=810 μ and $\rho = 1.2$ g/cm^3) as a solid phase.

$U_{sl} = 0$

$L_o = 134$ cm (two dimensional column)

U_{sg} cm/s	ε_g at T=60°C 2% solids	8% solids
2.9	0.12	0.14
4.2	0.175	0.19
6.7	0.219	0.244
8.4	0.24	0.262
10.5	0.255	0.285
13.5	0.282	0.314
16.5	0.307	0.343

Table 2 - Effect of Antifoam (Silcolapse 437 made by I.C.I. Ltd.) on Gas Hold-up in Two Dimensional Column.

$U_{sl} = 0$

U_{sg} cm/s	ε_g .18% antifoam	6% antifoam
2.9	0.074	0.115
4.2	0.1	0.18
5.5	0.125	0.215
6.7	0.148	0.24
8.4	0.17	0.255
10.5	0.197	0.27
13.5	0.223	0.3
16.5	0.245	0.325

Table 3 - Variation of Solids Concentration with Time

L_o = 173 cm (three dimensional column)

C_o = 0.1 (v/v)

U_{sl} = 0.045 cm/s (i.e. 0.5 It/min)

U_{sg} = 1.1 cm/s

$\theta = \frac{t}{63.4}$

θ	C/C_o take-off	C/C_o Top	C/C_o Bottom
0.125	1.2	1	0.9
0.25	1	0.85	0.7
0.5	0.67	0.65	0.52
0.75	0.53	0.5	0.43
1	0.37	0.35	0.35
1.5	0.2	0.25	0.27
2	0.09	0.15	0.17
2.5	0.03	0.12	0.14
3	0.02	0.08	0.13
3.5	0.01	0.07	0.11

Table 4 - Variation of Solids Concentration with Time

L_o = 173 cm (three dimensional column)

C_o = 0.1 (v/v)

U_{sl} = 0.045 cm/s

U_{sg} = 4.5 cm/s

$\theta = \frac{t}{63.4}$

θ	C/C_o Take-off	C/C_o Top	C/C_o Bottom
0.032	1	.95	1.1
0.126	1.1	1	1.03
0.19	.9	.87	1
0.25	.85	.8	.96
0.38	.7	.72	.85
0.5	.6	.62	.8
0.7	.52	.5	.65
1	.4	.39	.5
1.5	.25	.27	.32
2	.15	.16	.19
2.5	.1	.1	.13
3	.07	.08	.1
3.5	.06	.07	.09

Table 5 - Variation of Solids Concentration with Time

L_o = 173 cm (three dimensional column)

C_o = 0.1 (v/v)

U_{sl} = 0.17 cm/s

U_{sg} = 1.1 cm/s

$\theta = \frac{t}{17}$

θ	C/C_o Take-off	C/C_o Top	C/C_o Bottom
.04	-	1	.9
.125	1.1	.9	.63
.25	1	0.75	.42
.37	.72	0.56	.33
.5	.55	0.45	.25
.75	.28	.26	.18
1	.16	1.1	.15
1.5	0.073	0.07	0.098
2	0.02	0.04	.06
2.5	0.02	0.04	.05
3	0.02	0.04	.05

Table 6 - Variation of Solids Concentration with Time

L_o = 173 cm (three dimensional column)

C_o = 0.1 (v/v)

U_{sl} = .17 cm/s

U_{sg} = 4.5 cm/s

$\theta = \frac{t}{17}$

θ	C/C_o Take-off	C/C_o Top	C/C_o Bottom
.1	0.96	0.93	1.1
.25	0.8	0.8	1
.5	0.63	0.65	0.76
.75	0.5	0.5	0.63
1	0.4	0.4	0.5
1.25	0.31	0.3	0.41
1.5	0.21	0.2	0.34
2	0.11	0.13	0.2
2.5	0.04	0.06	0.13
3	0.035	0.05	0.1
3.5	0.035	0.045	0.1